

**Studies on the cAMP-responsive regulatory network
of *Corynebacterium glutamicum***

Inaugural dissertation

submitted to

the Faculty of Mathematics and Natural Sciences
at the Heinrich Heine University Düsseldorf

presented by

Natalie Wolf

Düsseldorf, April 2023

The thesis in hand has been conducted at the Institute of Bio- and Geosciences IBG-1: Biotechnology, Forschungszentrum Jülich GmbH, from September 2016 until March 2020 under the supervision of Prof. Dr. Michael Bott and Dr. Meike Baumgart.

Printed with the permission of the
Faculty of Mathematics and Natural Sciences of the
Heinrich Heine University Düsseldorf

Examiner: **Prof. Dr. Michael Bott**
Institute of Bio- and Geosciences, IBG-1: Biotechnology
Forschungszentrum Jülich

Co-examiner: **Prof. Dr. Georg Groth**
Institute of Biochemical Plant Physiology
Heinrich Heine University Düsseldorf

Date of oral examination: 11.08.2023

Results described in this dissertation have been published in the following original publication or are described in a manuscript that will be submitted for publication:

Wolf N., Bussmann M., Koch-Koerfges A., Katcharava N., Schulte J., Polen T., Hartl J., Vorholt J.A., Baumgart M. and Bott M. (2020). Molecular basis of growth inhibition by acetate of an adenylate cyclase-deficient mutant of *Corynebacterium glutamicum*. *Front Microbiol* 11(87). doi: 10.3389/fmicb.2020.00087

Wolf N., Lehmann L., Filipchuk A., Polen T., Bussmann M., Baumgart M. and Bott M. (2023). Comparison of *in vivo* GlxR binding in *Corynebacterium glutamicum* ATCC 13032 and the adenylate cyclase deletion mutant Δ *cyaB* using ChAP-Seq. *To be submitted*.

Table of contents

Summary	i
Zusammenfassung	ii
Abbreviations.....	iii
1 Introduction	1
1.1 The molecule 3',5'-cyclic adenosine monophosphate (cAMP).....	1
1.1.1 cAMP synthesizing and degrading enzymes.....	2
1.1.2 Physiological function of cAMP in <i>E. coli</i>	4
1.1.3 Physiological function of cAMP in <i>Mycobacterium</i> species	5
1.2 The role of cAMP in <i>Corynebacterium glutamicum</i>	7
1.2.1 GlxR – the CRP-like protein of <i>C. glutamicum</i>	8
1.2.2 CyaB – the AC of <i>C. glutamicum</i>	11
1.2.3 CpdA – the PDE of <i>C. glutamicum</i>	13
1.2.4 cAMP levels in <i>C. glutamicum</i>	15
1.3 Aims of this doctoral thesis.....	16
2 Results	18
2.1 Molecular basis of growth inhibition by acetate of an adenylate cyclase-deficient mutant of <i>Corynebacterium glutamicum</i>.....	20
2.2 Supplementary materials ‘Molecular basis of growth inhibition by acetate of an adenylate cyclase-deficient mutant of <i>Corynebacterium glutamicum</i>’	37
2.3 Comparison of <i>in vivo</i> GlxR binding in <i>Corynebacterium glutamicum</i> ATCC 13032 and the adenylate cyclase deletion mutant $\Delta cyaB$ using ChAP-Seq	44
2.4 Supplementary materials ‘Comparison of <i>in vivo</i> GlxR binding in <i>Corynebacterium glutamicum</i> ATCC 13032 and the adenylate cyclase deletion mutant $\Delta cyaB$ using ChAP-Seq’	70
3 Discussion.....	89
3.1 The role of CyaB activity in <i>C. glutamicum</i>.....	90
3.1.1 Further effects contributing to the ‘acetate effect’ of the $\Delta cyaB$ mutant	93
3.1.2 CyaB as the main adenylate cyclase in <i>C. glutamicum</i>	97
3.2 Intracellular cAMP concentration of <i>C. glutamicum</i> compared to other bacteria	99
3.3 The role of cAMP for the <i>in vivo</i> activity of GlxR	101
3.3.1 Further CRP-like proteins in <i>C. glutamicum</i>	101
3.3.2 cAMP-GlxR system important for energy metabolism in <i>C. glutamicum</i>	103
3.3.3 Closer look at suppressor mutants <i>C. glutamicum</i> $\Delta cyaB$ _sup2 and $\Delta cyaB$ _sup3....	104
3.4 Universal stress protein as putative cAMP binding protein	106
4 Literature.....	110

Summary

Cyclic adenosine monophosphate (cAMP) is one of the best studied signalling molecules. In prokaryotes, the molecule was shown to be involved in numerous processes, such as metabolism, motility, and virulence. In the Gram-positive actinobacterium *Corynebacterium glutamicum*, cAMP serves as an effector for the global transcriptional regulator GlxR, a homolog of Crp of *Escherichia coli*. Enzymes responsible for the synthesis and degradation of cAMP in *C. glutamicum* are the membrane-bound adenylate cyclase CyaB and the cytoplasmic phosphodiesterase CpdA, respectively. In this study, the consequences of decreased intracellular cAMP levels of a *cyaB* deletion mutant ($\Delta cyaB$) were investigated. The main objectives were (i) to characterize the physiological differences between the $\Delta cyaB$ mutant and the wild-type strain and (ii) to investigate the effects of a low cAMP level on GlxR-DNA interactions *in vivo*. The following results were obtained:

(i) The lack of the adenylate cyclase CyaB led to a growth defect of *C. glutamicum* when acetate was present in the medium. The acetate sensitivity of the $\Delta cyaB$ mutant could be reversed by plasmid-based *cyaB* expression or supplementation of the medium with cAMP, showing that indeed the low intracellular cAMP level in the $\Delta cyaB$ mutant was the reason for this acetate sensitivity. The acetate effect was concentration- and pH-dependent, suggesting a link to the uncoupling activity of acetate. In agreement, the $\Delta cyaB$ mutant displayed an increased sensitivity to the protonophore carbonyl cyanide *m*-chlorophenyl hydrazone (CCCP). The increased uncoupler sensitivity correlated with a lowered membrane potential of acetate-grown $\Delta cyaB$ cells compared to wild-type cells. Transcriptome analyses and RT-qPCR experiments showed that the genes encoding the cytochrome *bc*₁-aa₃ supercomplex and the F₁F₀-ATP synthase, previously shown to be activated by GlxR, had a decreased expression in the $\Delta cyaB$ mutant. Since the cytochrome *bc*₁-aa₃ supercomplex is the major provider of proton-motive force in *C. glutamicum*, decreased expression of its genes in the $\Delta cyaB$ mutant was assumed to be mainly responsible for the deficits in energy metabolism and the higher sensitivity to uncouplers. During cultivations of $\Delta cyaB$ mutant with acetate, a suppressor mutant was identified which had lost the acetate sensitivity. Genome sequence analysis revealed a single mutation in the suppressor strain causing the amino acid exchange Ala131Thr in GlxR. Introduction of this point mutation into the original $\Delta cyaB$ mutant abolished the growth defect on acetate, supporting the importance of GlxR for the phenotype of the $\Delta cyaB$ mutant and for the control of energy metabolism.

(ii) The influence of a lowered cAMP level on GlxR-DNA interaction *in vivo* was studied by ChAP-Seq experiments with the wild type and $\Delta cyaB$ mutant grown either on glucose or on glucose plus acetate. Analysis of the four data sets identified 243 GlxR peaks with an enrichment factor (EF) of ≥ 3 in at least one data set. *De novo* motif search identified the consensus sequence TGTGN₈CACA in 242 of the GlxR peaks. 141 of these peaks were also reported in previous studies, whereas 102 represent novel binding sites. Remarkably, the majority of the 243 GlxR binding sites were found to be enriched in all four data sets when using an EF ≥ 1.5 as cutoff. These results show that the strongly diminished or completely absent cAMP level in the $\Delta cyaB$ mutant reduced GlxR binding, particularly in the presence of acetate, but did not prevent it. This suggests that GlxR binding to its target sites *in vivo* is less dependent on cAMP than GlxR binding *in vitro* and that additional, yet unknown factors might be involved in the control of GlxR-binding to DNA within the cell.

Zusammenfassung

Zyklisches Adenosinmonophosphat (cAMP) ist eines der am besten untersuchten Signalmoleküle. In Prokaryonten ist das Molekül an zahlreichen Prozessen beteiligt, z. B. am Stoffwechsel, an der Motilität und an der Virulenz. Im Gram-positiven Actinobakterium *Corynebacterium glutamicum* dient cAMP als Effektor für den globalen Transkriptionsregulator GlxR, ein Homolog von Crp aus *Escherichia coli*. Die für Synthese und Abbau von cAMP verantwortlichen Enzyme sind in *C. glutamicum* die membrangebundene Adenylatzyklase CyaB bzw. die zytoplasmatische Phosphodiesterase CpdA. In dieser Studie wurden die Folgen eines verminderten intrazellulären cAMP-Spiegels einer *cyaB*-Deletionsmutante ($\Delta cyaB$) untersucht. Hauptziele waren (i) die Charakterisierung der physiologischen Unterschiede zwischen der $\Delta cyaB$ -Mutante und dem Wildtyp-Stamm und (ii) die Untersuchung der Auswirkungen eines niedrigen cAMP-Spiegels auf GlxR-DNA-Interaktionen *in vivo*. Die folgenden Ergebnisse wurden erzielt:

(i) Das Fehlen von CyaB führte zu einem Wachstumsdefekt in Gegenwart von Acetat, der durch plasmidbasierte *cyaB*-Expression oder Supplementierung des Mediums mit cAMP aufgehoben werden konnte. Der Acetat-Effekt war konzentrations- und pH-abhängig, was auf einen Zusammenhang mit der Entkoppleraktivität von Acetat hindeutete. In Übereinstimmung damit besaß die $\Delta cyaB$ -Mutante eine erhöhte Sensitivität gegenüber dem Protonophor Carbonylcyanid *m*-Chlorphenylhydrazon (CCCP) sowie bei Wachstum in Gegenwart von Acetat ein niedrigeres Membranpotential als der Wildtyp. Transkriptom- und RT-qPCR-Analysen zeigten, dass die Expression der durch GlxR aktivierten Gene für den Cytochrom-*bc₁-aa₃*-Superkomplex in der $\Delta cyaB$ -Mutante verringert war. Da der Superkomplex der Hauptlieferant der protonen-motorischen Kraft in *C. glutamicum* ist, wurde eine verringerte Expression seiner Gene als Hauptursache für die Acetat- und Entkoppler-Sensitivität der $\Delta cyaB$ -Mutante postuliert. Bei der Kultivierung der $\Delta cyaB$ -Mutante mit Acetat wurde eine Suppressor-Mutante identifiziert, die die Acetat-Empfindlichkeit verloren hatte. Die Genomsequenzanalyse ergab eine einzige Mutation in dem Suppressorstamm, die den Aminosäureaustausch Ala131Thr in GlxR verursachte. Durch Einführung dieser Punktmutation in das Genom der parentalen $\Delta cyaB$ -Mutante wurde der Wachstumsdefekt auf Acetat wiederhergestellt, was die Bedeutung von GlxR für den Phänotyp der $\Delta cyaB$ -Mutante und die Kontrolle des Energiestoffwechsels belegt.

(ii) Der Einfluss eines verringerten cAMP-Spiegels auf die GlxR-DNA-Interaktion *in vivo* wurde durch ChAP-Seq-Experimente mit dem Wildtyp und der $\Delta cyaB$ -Mutante untersucht, die entweder auf Glukose oder auf Glukose plus Acetat kultiviert wurden. Die Analyse der vier Datensätze ergab 243 GlxR-Peaks mit einem Anreicherungsfaktor (AF) von ≥ 3 in mindestens einem Datensatz. Die *de novo* Motivsuche identifizierte die Konsensussequenz TGTGN₈CACA in 242 der GlxR-Peaks. 141 dieser Peaks wurden auch in früheren Studien gefunden, während 102 Peaks neue Bindungsstellen repräsentieren. Bemerkenswert ist, dass die meisten der 243 GlxR-Bindungsstellen in allen vier Datensätzen angereichert waren, wenn ein AF $\geq 1,5$ als Grenzwert verwendet wurde. Die Ergebnisse zeigen, dass der stark verringerte oder völlig fehlende cAMP-Spiegel in der $\Delta cyaB$ -Mutante die GlxR-Bindung, insbesondere in Gegenwart von Acetat, reduzierte, aber nicht verhinderte. Dies deutet darauf hin, dass die GlxR-Bindung *in vivo* weniger cAMP-abhängig ist als die GlxR-Bindung *in vitro* und dass zusätzliche, noch unbekannte Faktoren an der Kontrolle der GlxR-Bindung an die DNA innerhalb der Zelle beteiligt sein könnten.

Abbreviations

Δ	Deletion
AC	Adenylate cyclase
AMP	Adenosine monophosphate
ATCC	American Type Culture Collection
ATP	Adenosine triphosphate
bp	Base pairs
BHI	Brain heart infusion
cAMP	Cyclic adenosine monophosphate
CCR	Carbon catabolite repression
CCCP	Carbonyl cyanide <i>m</i> -chlorophenyl hydrazone
CDW	Cell dry weight
cGMP	Cyclic guanosine monophosphate
ChAP-Seq	Chromatin affinity purification combined with DNA sequencing
CHD	Cyclase homology domain
ChIP-Seq	Chromatin immunoprecipitation combined with DNA sequencing
CRP	cAMP receptor protein
Da	Dalton
EIA	Enzyme immunoassay
ELISA	Enzyme-linked immunosorbent assay
EMSA	Electrophoretic mobility shift assay
HAMP	Histidine kinases, adenylate cyclases, methyl accepting proteins and phosphatases
ITC	Isothermal titration calorimetry
Kan ^R	Kanamycin resistant
K_d	Dissociation constant
K_m	Michaelis constant
LB	Lysogeny broth
M	Molar (mol/l)
OD ₆₀₀	Optical density at 600 nm
PDE	Phosphodiesterase
PEP	Phosphoenolpyruvate
(p)ppGpp	Guanosine pentaphosphate/tetraphosphate
PTS	Phosphotransferase system
RT-qPCR	Reverse transcription quantitative PCR
rpm	Revolutions per minute
TLS	Translational start site
TSS	Transcription start site
USP	Universal stress protein
V_{max}	Maximum initial velocity of a reaction (moles/min)
wt	Wild type
w/v	Weight per volume

Further abbreviations not included in this section are according to international standards.

1 Introduction

1.1 The molecule 3',5'-cyclic adenosine monophosphate (cAMP)

The molecule 3',5'-cyclic adenosine monophosphate, known as cyclic AMP or cAMP, was simultaneously discovered and described by two groups in 1957. One group was studying the chemical alkaline degradation of adenosine-5'-triphosphate (ATP), while the other studied the role of the hormones glucagon and epinephrine in the gluconeogenesis of the liver (Berthet et al., 1957; Cook et al., 1957; Sutherland & Rall, 1958). The discovery and characterization of cAMP was important for revealing the mechanism of action of hormones. Earl W. Sutherland and co-workers showed that in the course of signal transmission via hormones like adrenaline, cAMP serves as a second messenger within the cell (Berthet et al., 1957). In 1971, this discovery was rewarded with the Nobel Prize in Physiology or Medicine.

The hydrophilic molecule cAMP is an adenine nucleotide with a single phosphate group linked to the 3'- and 5'-hydroxyl groups of ribose. The cyclic nucleotide cAMP is synthesized from ATP with the concomitant release of pyrophosphate. The enzyme which catalyses this reaction is referred to as adenylyl cyclase or adenylylase (AC, EC 4.6.1.1) (Danchin, 1993). The degradation of cAMP is mediated by a 3',5'-cyclic-AMP phosphodiesterase (PDE, EC 3.4.1.55), which catalyses the hydrolytic cleavage of the 3'-phosphoester bond, forming 5'-adenosine monophosphate (AMP) (Richter, 2002) (Figure 1). Today, we know that cAMP occurs in all domains of life, found in animals, plants, fungi, archaea, and bacteria (Blanco et al., 2020; Botsford & Harman, 1992; D'Souza & Heitman, 2001; Kamenetsky et al., 2006). The control of the intracellular cAMP concentration is mostly described to be regulated by the activity of ACs and PDEs, meaning by the adjustment of synthesis or degradation of the cyclic nucleotide (McKnight, 1991; Sassone-Corsi, 2012). Only for few organisms (e.g. *Escherichia coli*) it has been described that the control of the intracellular cAMP levels can be mediated through the transport of cAMP across the membrane (Goldenbaum & Hall, 1979). However, a distinct cAMP transporter has not been described yet.

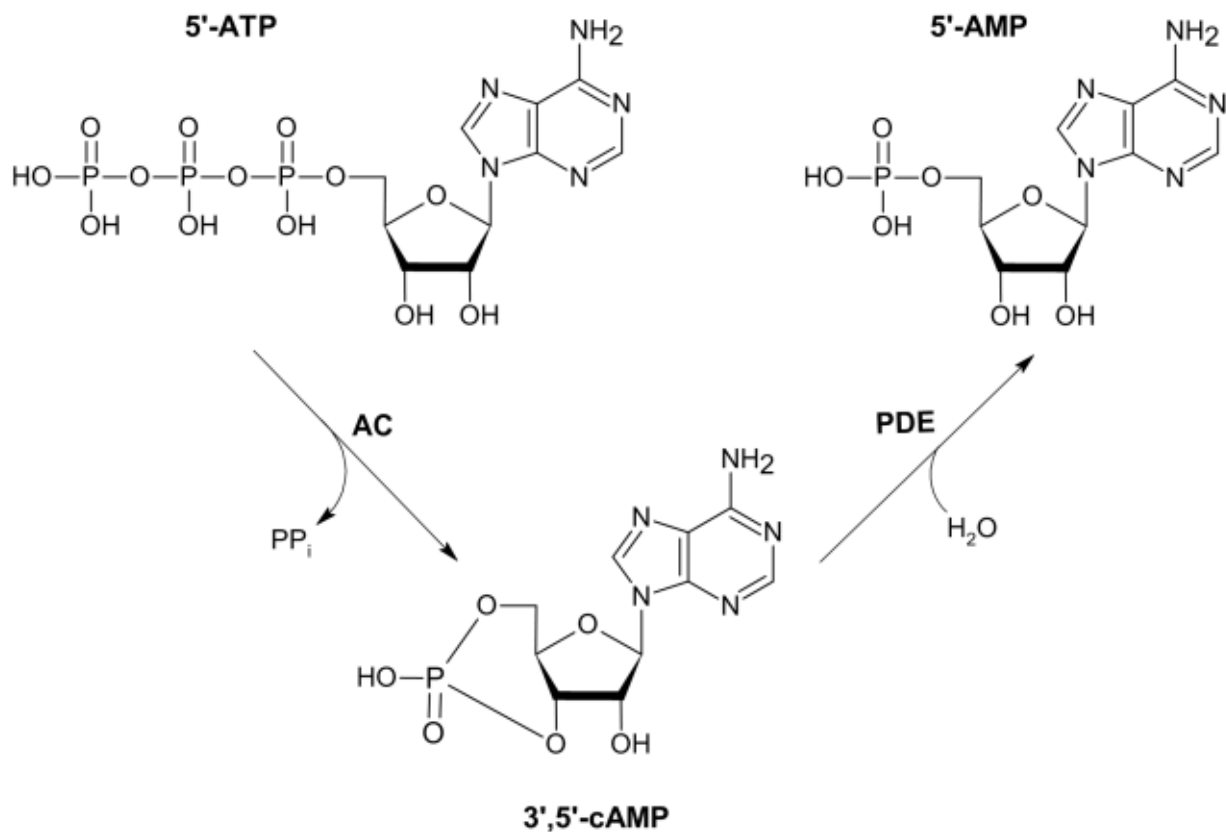


Figure 1: Biosynthesis and degradation of 3',5'-cAMP. The cyclic nucleotide cAMP is synthesized from 5'-ATP through cyclization at the 3'-OH group of the ribose moiety. Enzymes that catalyze this reaction under release of pyrophosphate (PP_i) are called adenylyl cyclases (ACs). The cAMP phosphodiesterases (PDEs) catalyze the hydrolytic cleavage of the 3'-phosphoester bond and thereby degrade 3',5'-cAMP to 5'-AMP. The molecule structures were generated with the program ACD/ChemSketch.

1.1.1 cAMP synthesizing and degrading enzymes

As mentioned above ACs are enzymes that catalyze the synthesis of cAMP from ATP. All ACs described so far are grouped into six classes based on the similarity of their amino acid sequence (Bâzu & Danchin, 1994; Danchin, 1993; Dessauer et al., 2017; Linder & Schultz, 2003). Class I ACs are found in enterobacteria, such as *E. coli*, *Salmonella typhimurium*, or *Yersinia pestis* (Saier et al., 1975). ACs of class II are found, e.g., in the Gram-negative *Bordetella pertussis* and the Gram-positive *Bacillus anthracis*. These pathogens secrete the ACs, which then are activated by the host protein calmodulin and become toxic for the host organism (Arumugham et al., 2018; Dautin et al., 2002; Weiss et al., 1984). An AC grouped into class IV was first identified in *Aeromonas hydrophila* (Sismeiro et al., 1998) and later also reported in *Y. pestis* (Gallagher et al., 2006). Not much is known about the ACs of class V and VI with only one representative found in *Prevotella ruminicola* (Cotta et al., 1998) and

Rhizobium etli (Télez-Sosa et al., 2002), respectively. In contrast, class III represents a very large group with the structurally and functionally most diverse ACs and representatives in both, eukaryotes and prokaryotes (Bassler et al., 2018). Due to the diverse forms of ACs, class III is divided into four subgroups (IIIa-III d) based on the primary sequence of the cyclase homology domain (CHD) with its catalytically active sites (Linder & Schultz, 2003). ACs of class III can be either cytosolic or integral membrane enzymes. Mammalian and bacterial ACs of class III are described to be active as homodimers (Linder & Schultz, 2003; Zhang et al., 1997). *In vitro* enzyme activity tests showed that Mn^{2+} or Mg^{2+} ions serve as cofactor in the catalytic centres, which are located at the dimer interface of the CHDs (Kasahara et al., 2001; Linder et al., 2004; Shenoy et al., 2005). The catalytic domains of ACs are often linked with regulatory domains, such as a transmembrane domain or a HAMP domain (found in histidine kinases, adenylate cyclases, methyl accepting proteins, and phosphatases) (Aravind & Ponting, 1999; Linder & Schultz, 2003). A HAMP domain is composed of two amphipathic helices connected by a short linker (Williams & Stewart, 1999); the domain connects the transmembrane domain with the catalytic domain and was shown to play a crucial role in the signal transduction of histidine kinases and ACs (Kishii et al., 2007; Tews et al., 2005). Enzyme tests with truncated ACs from *Mycobacterium tuberculosis* showed that the presence of the HAMP domain had either an inhibitory effect or a highly stimulating effect on the AC activity of the proteins Rv1319c and Rv3645, respectively (Linder et al., 2004).

Phosphodiesterases (PDEs), the enzymes that catalyse the degradation of cAMP, have been grouped in three classes based on their primary structures (Richter, 2002). The PDEs in class I harbour a conserved C-terminal catalytic domain with the motif H(X)₃H(X)₂₅₋₃₅D/E (Richter, 2002). All mammalian PDEs belong to the class I PDEs and have been grouped into 11 PDE subfamilies with preferences for cAMP, cGMP, or both cyclic nucleotides (Conti & Beavo, 2007; Francis et al., 2011; Francis et al., 2001; Omori & Kotera, 2007). A small number of class I PDEs are also found in lower eukaryotes such as yeast or amoeba (Sass et al., 1986; Thomason et al., 1999). PDEs of class II share the conserved motif H(X)HLDH and are found in lower eukaryotes and in bacteria (Callahan et al., 1995). Class III harbours mainly PDEs from bacteria, the first one being described in *E. coli* (Imamura et al., 1996). Bioinformatic approaches showed that PDEs from class III are also present in archaea and eukaryotes (Powell et al., 2014). All PDEs have in common that they are active as dimers and have two metal ions in their catalytic centre (Richter, 2002).

1.1.2 Physiological function of cAMP in *E. coli*

In 1965, cAMP in bacteria was first identified in the Gram-negative *E. coli* and since then cAMP and its physiological role was analysed in a variety of other prokaryotic organisms (Botsford & Harman, 1992). In *E. coli* the synthesis of cAMP via an AC has been intensively studied. It was shown that the glucose-specific phosphoenolpyruvate (PEP)-dependent sugar phosphotransferase system (PTS) modulates AC activity. Import of glucose into the cell through the PTS is linked to the dephosphorylation of the substrate-specific enzyme EIIA^{Glu} and in the dephosphorylated state EIIA^{Glu} does not activate AC activity, leading to a low cytoplasmic cAMP concentration. When glucose is absent in the medium, the phosphorylated form of EIIA^{Glu} increases and this form stimulates the activity of the AC, causing an increase of the cAMP level (Bettenbrock et al., 2007; Park et al., 2006). The increased concentration of the signalling molecule cAMP, in turn, influences the transcription of many genes, for example those of the *lac* operon. The respective gene products are involved in the transport and metabolism of the carbon source lactose. The activation of transcription of the *lac* operon is mediated by a cAMP-dependent transcription factor, the cAMP receptor protein (CRP). This mechanism of carbon catabolite repression (CCR) became a paradigm of cAMP-mediated signalling in bacteria (Görke & Stülke, 2008; Kolb et al., 1993). A recent study indicated that in *E. coli* cAMP signalling is responsible for coordinating the expression of catabolic proteins with that of biosynthetic and ribosomal proteins, in dependency of the metabolic demands under different environmental conditions (You et al., 2013).

CRP of *E. coli* (CRP_{Eco}) is the most intensively investigated transcriptional regulator with cAMP as the allosteric effector (Emmer et al., 1970; Gosset et al., 2004). With more than 200 promoters that are putatively under the regulatory control of the cAMP-CRP complex, CRP_{Eco} is classified as a global regulator (Gosset et al., 2004; Mendoza-Vargas et al., 2009; Robison et al., 1998; Zheng et al., 2004). It was shown that the cAMP-CRP complex binds to specific sites within a promoter sequence of a gene and activates or represses the transcription, as a result of enhanced or hindered promoter recognition by the RNA polymerase (Botsford & Harman, 1992; Kolb et al., 1993). CRP_{Eco} is active as a homodimer, each dimer binding a cAMP molecule. Analyses of CRP_{Eco} crystal structures in the presence and absence of cAMP revealed that binding of cAMP leads to notable changes in the tertiary structure and the affinity to its target DNA is significantly increased in the cAMP-CRP

complex (Passner et al., 2000; Popovych et al., 2009; Weber & Steitz, 1987).

The prediction, in which cases CRP_{Eco} tends to increase the activity of a promoter, hence, acts as an activator, is described in the 3-Class rules (Lee et al., 2012). In the Class I rule CRP_{Eco} acts as an activator if it binds upstream of the promoter elements -35 and -10 around position -61.5 relative to the transcriptional start site (TSS) (Busby & Ebright, 1997, 1999; Zheng et al., 2004). Enhanced binding of RNA polymerase to the promoter is accomplished through the interaction of CRP with the carboxyl-terminal domain of the α -subunit (α CTD) of RNA polymerase (Benoff et al., 2002). The *lac* promoter is the most prominent example for a CRP-dependent promoter of the Class I rule (de Crombrughe et al., 1984; Majors, 1975). The Class II rule of CRP_{Eco} states that activation of transcription is possible when the regulator binds around position -41.5 and the binding site overlaps with the -35 element of the promoter (Savery et al., 1998). A CRP-dependent promoter of the Class II rule is, for example, the *galP1* promoter (Attey et al., 1994). The Class III rule describes that if a promoter has two or more CRP-binding sites, the promoter tends to be activated upon cAMP-CRP binding. The Class III rule is also valid if the promoter has one or more CRP binding sites and one or more binding sites for another protein acting as activator. The promoters of *araBAD* and *malK* are prominent examples of such Class III rule promoters (Richet et al., 1991; Zhang & Schleif, 1998).

1.1.3 Physiological function of cAMP in *Mycobacterium* species

In *M. tuberculosis* and the faster growing *Mycobacterium smegmatis*, cAMP plays a role for the pathogenicity of the cells (Lowrie et al., 1979). *M. tuberculosis* possesses 16 different ACs and the intracellular cAMP concentration is considered to be 100-fold higher compared to other bacteria, such as *E. coli* (McCue et al., 2000; Shenoy & Visweswariah, 2006). Macrophages infected with *M. tuberculosis* showed an increase of cytoplasmic cAMP levels, which then led to an intoxication of the host cell. The mycobacterial origin of the cAMP was demonstrated by *M. tuberculosis* cells that were pre-labelled with ^{14}C -glycerol. Furthermore, the mycobacterial AC Rv0386 responsible for the synthesis of the majority of the radiolabelled cAMP was identified by detecting a significant drop in cAMP when using an Rv0386 deletion strain (Agarwal et al., 2009). The secretion of cAMP by *M. tuberculosis* and the resulting increase of the cAMP level in the host cell play an important role in the suppression of the host defence mechanisms inside of macrophages (Bai et al., 2011; Lowrie

et al., 1979). In contrast to the 16 described ACs, only two cAMP-degrading enzymes are known in *M. tuberculosis* (Shenoy et al., 2005; Thomson et al., 2020). And although the bacterium seems to regulate the intracellular cAMP level through excretion of cAMP, no distinct cAMP transporter protein was characterized yet.

A cAMP-dependent lysine acetyltransferase (KATmt) (Rv0998) of *M. tuberculosis* was detected, which acetylates catalytically important lysine residues of fatty acyl-CoA synthetases (FadD enzymes) (Nambi et al., 2010; Nambi et al., 2013, 2019). In a search for further cAMP-binding proteins in mycobacteria, the protein Usp (Rv1636) was identified in *M. tuberculosis* as an abundant and specific cAMP-binding protein (Banerjee et al., 2015). Binding of the Rv1636 protein to cAMP was confirmed by cAMP agarose affinity chromatography and verified by isothermal titration calorimetry (ITC). Rv1636 belongs to the family of universal stress proteins (USPs) and carries a USP domain. Members of the USP family were described to be involved in stress responses, because it was shown that their synthesis was induced upon different stress conditions, such as starvation for carbon or phosphate, entry into the stationary phase in rich medium, exposure to heat, or presence of uncouplers inhibiting oxidative phosphorylation (Vollmer & Bark, 2018). The biological function of the cAMP-binding protein Rv1636 has not yet been elucidated. However, it was proposed that cAMP-binding to USPs in mycobacteria is a mechanism for regulation of the intracellular 'free' cAMP level and therefore a regulation of the downstream effects of cAMP (Banerjee et al., 2015). In another study, it was shown that Rv1636 of *M. tuberculosis* is in the top twenty of the most abundant proteins of the organism, which also supports the hypothesis that Rv1636 acts as a cAMP reservoir (Schubert et al., 2013).

M. tuberculosis carries a cAMP receptor protein (CRP) that acts as a global transcriptional regulator with its effector cAMP (Stapleton et al., 2010). The faster growing mycobacterium *M. smegmatis* contains two CRP homologues, the major CRP1 protein Msmeg_6189 and its paralog CRP2/Msmeg_0539 (Sharma et al., 2014). Both transcriptional regulators recognize the same DNA consensus sequence, but have different binding affinities for cAMP (K_d 30 μ M for Msmeg_6189 and K_d 3 μ M for Msmeg_0539) and are probably active under different conditions in response to carbon and energy supply (Aung et al., 2015; Sharma et al., 2014). While Msmeg_0539 was shown to regulate genes involved in transport and catabolism of carbohydrates, Msmeg_6189 was found to play a dominant role for the induction of the *cydAB* operon under hypoxic conditions (Aung et al., 2014; Ko & Oh, 2020).

The *cydAB* genes encode for subunit I and II of the terminal cytochrome *bd* oxidase, which has a high affinity for O₂ and thus its activity is important under oxygen-limiting conditions (Kana et al., 2001).

Apparently, in mycobacteria, cAMP is not only involved in the regulation of gene expression via cAMP-CRP, but also serves as the effector of a cAMP-dependent lysine acetyltransferase, binds to a universal stress protein, and is an important part of host-pathogen interaction due to export of cAMP into host cells (Agarwal et al., 2009; Banerjee et al., 2015; Nambi et al., 2010; Nambi et al., 2013, 2019; Sharma et al., 2014; Stapleton et al., 2010). Thus, cAMP in prokaryotes not only serves as an effector of transcriptional regulators with generally a large regulon, but also has additional functions, which are probably only incompletely known.

1.2 The role of cAMP in *Corynebacterium glutamicum*

The Gram-positive soil bacterium *Corynebacterium glutamicum* was discovered in a screening for natural microbial glutamate producers (Kinoshita et al., 1957; Udaka, 1960). It is a facultative anaerobic bacterium with a GC-content of 53.8% and belongs to the order *Corynebacteriales* within the phylum *Actinomycetota* (Oren & Garrity, 2021). This order also comprises the important human pathogens *Corynebacterium diphtheriae*, *Mycobacterium leprae*, and *M. tuberculosis* (Gao & Gupta, 2012). The ability of *C. glutamicum* to secrete glutamate into the medium was the starting point for the development of ‘fermentative’ industrial amino acid production, which nowadays is a billion dollar business (Becker & Wittmann, 2012; Wendisch et al., 2016). Over the years, *C. glutamicum* with the generally-regarded-as-safe (GRAS) status became the most important microorganism for the large scale production of the amino acids L-glutamate and L-lysine (Eggeling & Bott, 2015; Leuchtenberger et al., 2005). After genome sequencing of the *C. glutamicum* type strain ATCC13032 by two independent laboratories (Ikeda & Nakagawa, 2003; Kalinowski et al., 2003), rational strain development by metabolic engineering, novel high-throughput screening methods employing single-cell metabolite biosensors, and adaptive laboratory evolution became important tools for *C. glutamicum* strain development (Binder et al., 2012; Eggeling et al., 2015; Inui et al., 2004; Mustafi et al., 2012; Schendzielorz et al., 2014). Since 2003, numerous *C. glutamicum* strains were created for the production of various amino

acids (Stolz et al., 2007; Vogt et al., 2014; Vogt et al., 2015) and other industrially relevant compounds such as organic acids (Litsanov, Brocker, et al., 2012; Litsanov, Kabus, et al., 2012; Okino, Noburyu, et al., 2008; Okino, Suda, et al., 2008; Wieschalka et al., 2013), alcohols (Blombach et al., 2011; Inui et al., 2004), carotenoids (Heider et al., 2014; Henke et al., 2016), or phenylpropanoids (Kallscheuer et al., 2016). The biotechnological importance of *C. glutamicum* and its close phylogenetic relationship to pathogenic bacteria fuel the ongoing interest for a deeper understanding of its metabolic and regulatory network.

1.2.1 GlxR – the CRP-like protein of *C. glutamicum*

The first time cAMP was mentioned in connection with *C. glutamicum* was in a publication that identified and characterized a CRP-like protein (Cg0350) that was named GlxR due to its involvement in the regulation of the genes of the glyoxylate pathway (Kim et al., 2004). Based on its amino acid sequence, GlxR belongs to the CRP-FNR family of transcriptional regulators and shows 27% amino acid sequence identity with CRP of *E. coli* and 78% identity with the CRP protein (Rv3676) of *M. tuberculosis* (Kim et al., 2004). Bioinformatic analysis of GlxR with the online tool PFAM (Mistry et al., 2020) showed that GlxR is composed of an N-terminal cNMP-binding domain (PF00027) and a C-terminal HTH_CRP domain (PF13545) (Figure 2). Besides GlxR, the genome of *C. glutamicum* ATCC13032 encodes two other proteins that have one or both of these domains: Cg1327 has a similar domain composition as GlxR, whereas Cg3291 only shares the HTH_CRP domain with GlxR (Figure 2). The functions of Cg1327 and Cg3291 have not yet been studied.

In 2014 the crystal structures of apo-GlxR and holo-GlxR (in complex with cAMP) were solved. Their comparison revealed that the 25 kDa protein undergoes small structural changes upon cAMP-binding, resulting in a 100-fold higher DNA-binding affinity (Townsend et al., 2014). The crystal structure of GlxR in complex with cAMP is displayed in Figure 2 and shows a homodimer with two structurally identical binding sites for cAMP in the centre of the ligand binding pocket close to the dimer interface. The K_d value measured for binding of the first cAMP molecule was 17 μM , whereas the K_d value for binding of the second cAMP molecule was 130 μM (Townsend et al., 2014). The DNA-binding helices are located in the proximity of the C-terminus. In electrophoretic mobility shift assays (EMSAs) DNA binding by GlxR only occurred in the presence of cAMP (Bussmann et al., 2009; Jungwirth et al., 2013; Kim et al., 2004; Kohl et al., 2008; Kohl & Tauch, 2009; Letek et al., 2006).

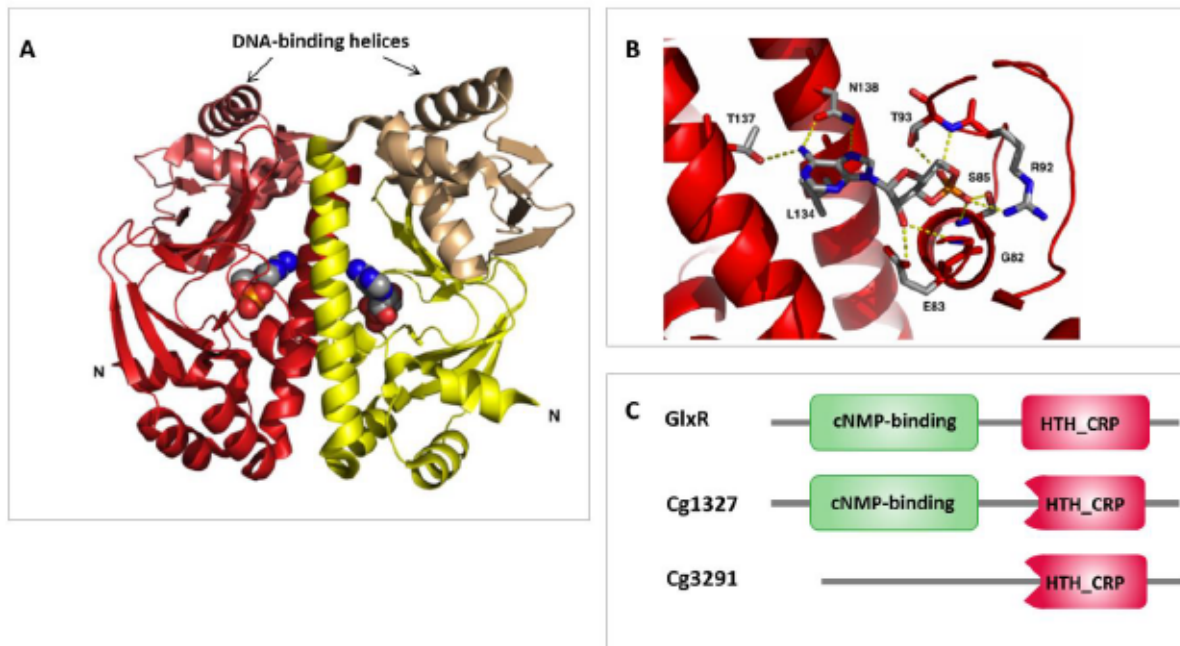


Figure 2: Structure of homodimeric GlxR in complex with cAMP and protein domains of GlxR and its paralogs. (A) Ribbon diagram of a GlxR dimer in complex with cAMP. The two protein chains are depicted in red and yellow, with the DNA-binding domains in lighter shade. Each dimer binds one cAMP molecule in the ligand-binding pocket. The ligand cAMP is shown in a ball-and-stick representation (modified after Townsend et al., 2014). (B) Close-up of one cAMP-binding site in GlxR. The figure was taken from Townsend et al., 2014. (C) Protein domains of GlxR and the related proteins Cg1327 and Cg3291. cNMP-binding domains often are composed of an eight-stranded, antiparallel beta-barrel structure and three alpha-helices. The HTH_CRP domain comprises a DNA-binding helix-turn-helix (HTH) domain.

GlxR stands for the abbreviation glyoxylate regulator, due to the initial finding that this protein represses transcription of the gene *aceB* encoding malate synthase, a key enzyme of the glyoxylate bypass (Kim et al., 2004). In the following years, more and more genes were found to be transcriptionally regulated by GlxR, such as *gntP* and *gntK* (Letek et al., 2006), the *sdhCAB* operon (Bussmann et al., 2009), *gluABCD* (Park et al., 2010), *gltA* (van Ooyen et al., 2011), *narkGHJI* (Nishimura et al., 2011), *pstSCAB* (Panhorst et al., 2011), *atpB*, *ctaCF*, and *ctaD* (Toyoda et al., 2011), or *adhA* and *ald* (Subhadra & Lee, 2013). The use of promoter fusions, quantitative RT-PCR or enzyme assays revealed that GlxR can function as an activator or a repressor. A more global approach to broaden the knowledge about the GlxR regulon was conducted by *in silico* prediction of GlxR binding sites in the genome of *C. glutamicum* ATCC13032 (Kohl & Tauch, 2009). Predictions were verified by showing *in vitro* GlxR-DNA interaction for 138 DNA regions by EMSAs. The GlxR consensus DNA-binding motif identified was 5'-TGTGANNTANNTCACA-3' and is very similar or identical

to the consensus motifs reported in other GlxR studies (Jungwirth et al., 2013; Kohl et al., 2008; Toyoda et al., 2011).

The *in vivo* DNA-binding sites of GlxR were analysed by using ChIP-Seq or ChIP-Chip. Whereas 107 DNA fragments enriched by GlxR were identified by ChIP-Seq using *C. glutamicum* ATCC13032, even 209 GlxR-binding regions could be identified by ChIP-Chip using the closely related strain *C. glutamicum* R (Jungwirth et al., 2013; Toyoda et al., 2011). Due to the large regulon, GlxR is characterized as a master regulator, with its regulatory network interconnecting different cellular functions, such as carbon metabolism and transport, nitrogen and phosphate metabolism, SOS and stress responses, respiration, sulphur homeostasis, and iron homeostasis (Kohl & Tauch, 2009). As GlxR also binds upstream of genes encoding for transcriptional regulators, such as *ramA* and *ramB*, the regulatory network of GlxR goes far beyond the direct regulation of gene transcription (Jungwirth et al., 2013). In case of *ramA*, GlxR acts as a transcriptional activator, whereas RamA and SugR function as repressors for *ramA* transcription (Toyoda et al., 2013). A prediction was made that GlxR probably could influence about 14% of the genes in *C. glutamicum* (Kohl & Tauch, 2009). A mini-review summarizing the function and regulons of transcription factors from *C. glutamicum* presented results that were gained by ChIP-based technologies and contributed to the understanding of the GlxR regulon (Toyoda & Inui, 2016). The authors emphasized that the transcriptional regulation of one gene by several transcription factors increases the possibility of multiple regulatory loops in the regulatory network of *C. glutamicum*, which requires more intensive laboratory work finding the factors that explain how the transcription of a distinct gene is balanced.

A high-throughput approach for the determination of the *in vivo* regulatory role of the transcription factor GlxR would be a comparative gene expression analysis with DNA microarrays or RNA-seq with a mutant lacking the *glxR* (*cg0350*) gene and the wild type. However, in *C. glutamicum* ATCC13032 several attempts to construct a *glxR* deletion mutant lacking the entire GlxR coding sequence failed (Bussmann, 2009; Kim et al., 2004; Letek et al., 2006). Two groups succeeded to construct *glxR* mutants that lack the *glxR* region encoding the cAMP-binding domain in strain ATCC13032 (Moon et al 2007; Park et al 2010) or nearly the complete *glxR* gene in strain R (Toyoda et al., 2009). However, due to the severe growth defects of these mutants, meaningful global gene expression experiments could not be performed. As *in vivo* data from a *glxR* deletion mutant are missing, the

regulatory role of GlxR for a particular gene is often predicted from the location of its binding site within the promoter region.

DNA affinity chromatography experiments with the *glxR* promoter region suggested that *glxR* is itself the target of several transcriptional regulators: The transcriptional regulator AtIR (Cg0146, previously known as SucR or MtlR), a regulator of the DeoR family involved in arabinol metabolism (Laslo et al., 2012; Peng et al., 2011) and the GntR-family regulator GntR3 (Cg2544) activate the transcription of *glxR* (Subhadra et al., 2015), whereas RamB (Cg0444), a transcriptional regulator of the MerR family involved in acetate metabolism, represses the transcription of *glxR* (Subhadra et al., 2015). Furthermore, *glxR* is negatively autoregulated, i.e. GlxR represses transcription of its own gene (Jungwirth et al., 2008; Subhadra et al., 2015). Although *glxR* is subject to complex transcriptional regulation, it was reported to be constitutively expressed during growth in minimal medium with glucose as carbon source (Hong et al., 2014). Furthermore, the mRNA level of *glxR* was similar when cells were cultivated with citrate or a citrate-glucose mixture as carbon source (Polen et al., 2007).

A proteome study that was searching for proteins undergoing lysine acetylation and/or lysine succinylation identified three lysine residues of GlxR in a succinylated form (K59, K155, and K212) (Mizuno et al., 2016). Furthermore, another study showed that the lysine residue K57 of GlxR was found to be covalently linked to the small prokaryotic ubiquitin-like protein Pup (Küberl et al., 2014). As *C. glutamicum* lacks a proteasome, the purpose of GlxR pupylation is not yet known and the fractions of pupylated and succinylated GlxR are unknown. Hong and co-workers reported that the subtilisin-like serine protease SprA interacts with GlxR (Hong et al., 2014). They showed that GlxR was proteolytically cleaved in the presence of purified SprA, however, this cleavage was inhibited if cAMP was present. All in all, the physiological roles of the posttranscriptional modifications of GlxR, especially of pupylation and succinylation, remain elusive and should be studied further, as the results could contribute to a deeper understanding of the activity of the transcriptional regulation of GlxR.

1.2.2 CyaB – the AC of *C. glutamicum*

The only enzyme known to date to be involved in the synthesis of cAMP in *C. glutamicum* is the membrane-bound AC CyaB (Cg0375) (Cha et al., 2020, Bussmann 2009). CyaB is

conserved in *Corynebacterium* species and is an ortholog of the AC Rv3645 of *M. tuberculosis* with 43% sequence identity (Bussmann, 2009; Shenoy et al., 2004). In the initial annotation of the *C. glutamicum* genome in 2003 (Kalinowski et al., 2003), a CyaB protein composed of 547 amino acid residues was predicted. The CyaB start codon was later changed (Pfeifer-Sancar et al., 2013), leading to a protein of 508 amino acid residues. The start codon of the latter version corresponds to the one predicted for the CyaB proteins of *Corynebacterium efficiens* and *Corynebacterium diphtheriae* (Figure 3A). Bioinformatic analysis of the CyaB amino acid sequence reveals that this cyclase consists of an N-terminal membrane-integral domain with six transmembrane helices with no signal peptide (Figure 3B) fused to a cytoplasmic HAMP domain followed by the adenylate cyclase catalytic domain (cyclase homology domain, CHD) (Mistry et al., 2020).

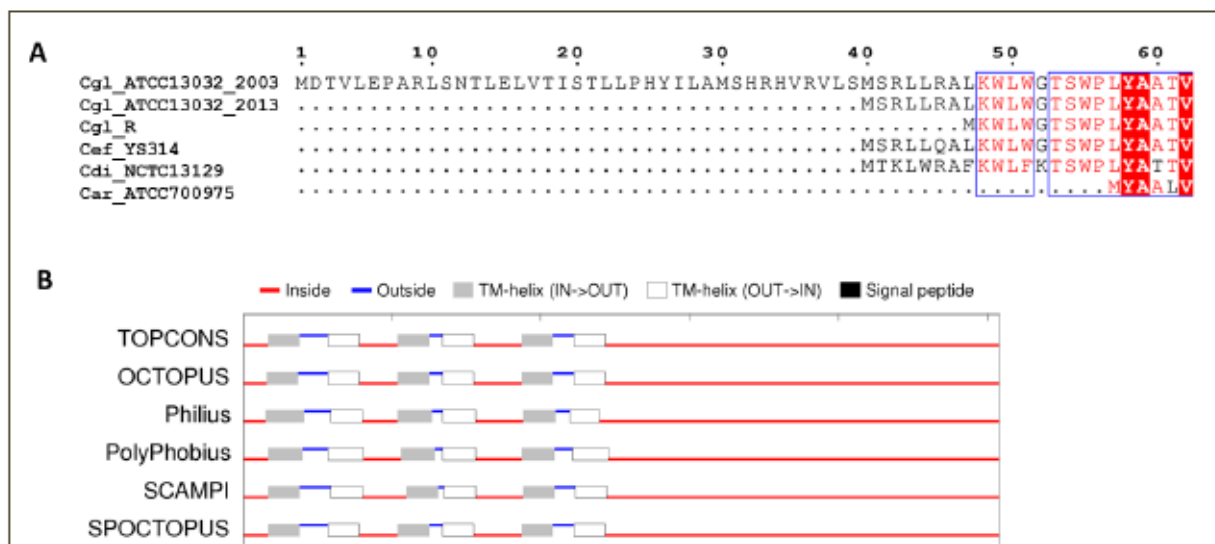


Figure 3: Alignment of the N-terminal regions of the adenylate cyclase CyaB and its homologs and predicted membrane topology of CyaB (Cg0375). (A) Amino acid sequence alignment of the N-terminal regions of CyaB from *C. glutamicum* ATCC13032 as predicted by Kalinowski et al., (2003) and by Pfeifer-Sancar et al., (2013), from *C. glutamicum* strain R (Cgl_R), from *C. efficiens* (Cef_YS314), from *C. diphtheriae* (Cdi_NCTC13129), and from *Corynebacterium aurimucosum* (Car_ATCC700975). The alignment was generated with ClustalW (Thompson et al., 1994) and further processed with ESPript 3.0 (Robert & Gouet, 2014). (B) Prediction of the membrane topology of CyaB using the webserver TOPCONS (<https://topcons.cbr.su.se/>) (Tsirigos et al., 2015). All six programs predicted a protein with six transmembrane helices. No signal peptide was detected. The input amino acid sequence of CyaB (Cg0375, 508 amino acid residues) was taken from Pfeifer-Sancar et al., 2013.

According to these predictions, CyaB in the dimeric state contains 12 transmembrane helices. This number is often found in secondary transporters (Henderson, 1993); however, a transport function of the ACs has not been recognized up to now. Furthermore, it is possible that the transmembrane domain of CyaB serves as a sensor for an extracellular or

membrane-associated stimulus. While membrane-bound mammalian ACs are known to be activated by G-proteins as a response to extracellular hormone signals (Linder & Schultz, 2003), a stimulus for bacterial membrane-bound ACs has yet to be discovered. Cultivations of *C. glutamicum* Δ *cydB* with plasmid-based expression of *cydB* showed that only plasmids coding the entire CyaB protein or an N-terminal truncated variant with a residual 13 aa transmembrane domain followed by the HAMP domain and the catalytic domain were able to abrogate the growth defect of the Δ *cydB* mutant in the presence of acetate (Katcharava, 2015). Interestingly, a plasmid-based expression of *cydB* coding for a CyaB variant which is not located in the membrane (only HAMP domain and catalytic domain) was not able to abolish the growth defect.

Although CyaB appears to be the only AC in *C. glutamicum*, the phenotype of a *cydB* deletion mutant differs strongly from that of the *glxR* mutants described above. Whereas the latter mutants showed severe growth defects, growth of *cydB*-deficient mutants was found to be comparable to the parental strain when cultivated in minimal medium with carbon sources such as glucose, gluconate, or pyruvate (Bussmann, 2009; Cha et al., 2010). Only when cultivated in the presence of acetate as carbon source, the *cydB*-deficient mutants showed a light or severe growth defect (Bussmann, 2009; Cha et al., 2010). The reasons for this phenotype were studied in the course of this doctoral thesis.

1.2.3 CpdA – the PDE of *C. glutamicum*

In *C. glutamicum* a PDE converting cAMP to AMP was described only recently (Schulte et al., 2017). This PDE, named CpdA (Cg2761), showed only 15-19% amino acid sequence identity to other known PDEs from bacteria of class II, but contained a sequence motif that is very similar to the one reported to be characteristic of class II PDEs (Richter 2002). In 2020 this CpdA together with a newly described PDE (Rv1339) of *M. tuberculosis* and the PDE Yfhl of *Bacillus subtilis* was proposed to be classified in a new PDE group called ‘atypical class II PDEs’ (Thomson et al., 2022). This atypical class II PDEs have a signature metal-binding motif (T/S)HXHXDH in common, where X is likely to be a hydrophobic or small residue (Thomson et al., 2022). Characterization of the purified corynebacterial CpdA revealed a K_m^{app} value of 2.5 ± 0.3 mM for cAMP and a $V_{\text{max}}^{\text{app}}$ of 33.6 ± 4.3 $\mu\text{mol min}^{-1} \text{mg}^{-1}$. The K_m^{app} is more than 30-fold higher compared to the class II PDEs of *Vibrio fischeri* (73 μM) (Callahan et al., 1995) or of *Myxococcus xanthus* (12 μM) (Kimura et al., 2011), but 4-fold lower than the PDE of

Arthrobacter sp. CGMCC 3584 (6.82 mM) (Schulte et al., 2017; Zheng et al., 2013). The V_{\max}^{app} value of CpdA ($33.6 \pm 4.3 \mu\text{mol min}^{-1} \text{mg}^{-1}$) is 112-fold lower compared to the V_{\max}^{app} of *V. fischeri* ($3.7 \text{ mmol min}^{-1} \text{mg}^{-1}$) but almost 500-fold higher than the V_{\max}^{app} of *M. xanthus* ($67.5 \text{ nmol min}^{-1} \text{mg}^{-1}$) (Callahan et al., 1995; Kimura et al., 2011).

A *cpdA* deletion mutant of *C. glutamicum* showed severe growth defects and reduced growth rates on all carbon sources tested, such as glucose, gluconate, acetate, citrate, or an ethanol-glucose mixture (Schulte et al., 2017). Determination of the intracellular cAMP level revealed a 2-fold higher cAMP level in the ΔcpdA mutant compared to the parental strain (50 pmol/mg protein and 27 pmol/mg protein, respectively) (Schulte et al., 2017). This result indicates that CpdA of *C. glutamicum* is a phosphodiesterase with an important role in the control of the cellular cAMP level. In agreement, transcriptome analysis comparing the ΔcpdA mutant to the parental *C. glutamicum* strain identified 247 genes with a more than 2-fold altered mRNA level in the ΔcpdA mutant. These altered gene expressions probably result from an altered activity of the transcriptional regulator GlxR due to the higher intracellular cAMP level. Indeed, many GlxR-regulated genes showed altered expression levels in the ΔcpdA mutant, including genes involved in carbon source transport and metabolism, which could explain the growth defects of the ΔcpdA mutant. For example, the ΔcpdA mutant showed more than 3-fold reduced mRNA levels of genes involved in the uptake of glucose, sucrose, and citrate (*ptsG*, *ptsI*, *ptsS*, *tctA* and *tctB*) and in the metabolism of acetate, gluconate, L-lactate, and ethanol (*pta*, *ackA*, *gntK*, *lldD*, *adhA* and *ald*). An important finding by Schulte et al. was that *cpdA* expression is transcriptionally activated by GlxR. A model shows that an intracellular increase of cAMP should lead to higher numbers of cAMP-GlxR complexes and thus a transcriptional activation of the *cpdA* expression (Figure 4). Thus, as a consequence the level of CpdA should increase, which then should lead to a lowering of the cellular cAMP level due to the higher degradation rate of cAMP by CpdA. This feedback loop is probably crucial for the regulation of the cellular cAMP level as the 2-fold increase in the level was shown to lead to severe growth defects. Further active phosphodiesterases besides CpdA have not yet been described in *C. glutamicum*.

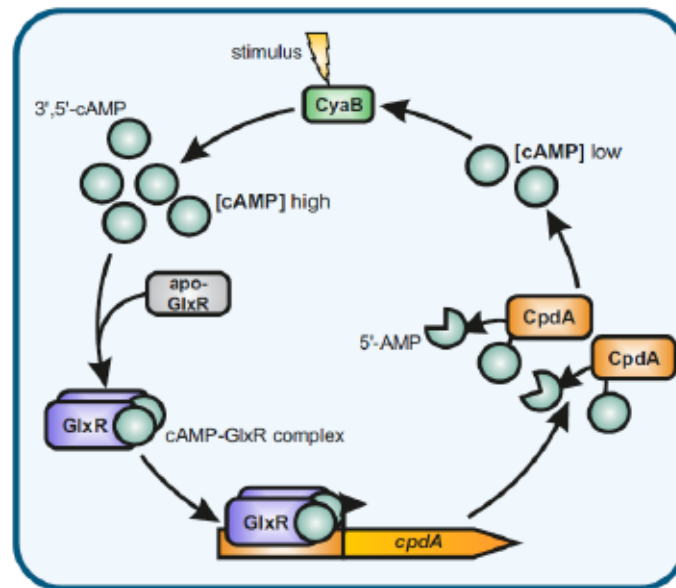


Figure 4: Prediction of a negative feedback loop formed via transcriptional activation of *cpdA* expression by the cAMP-GlxR complex (taken from Schulte et al., 2017). After activation of the adenylate cyclase (CyaB) by an unknown stimulus, the cAMP level increases. The increased cAMP concentration leads to more cAMP-GlxR complexes, which activate the expression of *cpdA* gene encoding a cAMP phosphodiesterase. Elevated CpdA activity thus lowers the intracellular cAMP level and resets the system.

1.2.4 cAMP levels in *C. glutamicum*

The intracellular cAMP concentration in *C. glutamicum* has been measured by several different groups using different strains and cultivation conditions. The first measurement was reported in the study in which GlxR was described for the first time (Kim et al., 2004). The cAMP concentration was reported to be high in the early exponential phase and low when the cells reached the stationary phase in a medium with glucose as carbon source. This finding indicated that the cAMP concentration was high when the glucose concentration was high, in contrast to the situation in *E. coli*, where the cAMP concentration is low in the presence of glucose. Several later studies showed that the intracellular cAMP level of *C. glutamicum* is higher during growth on glucose than during growth on acetate (Table 1). Additional studies determined the intracellular cAMP level in cells grown with citrate or a glucose-acetate mixture, showing that the cAMP levels on these substrates were higher than those on glucose alone (Bussmann, 2009; Cha et al., 2010; Polen et al., 2007; Schulte et al., 2017). The results of these cAMP measurements were presented in different units, which hinder a direct comparison. Therefore, in Table 1 the cAMP concentrations given in different studies were converted into cytoplasmic concentrations. The range of the reported cAMP concentrations in *C. glutamicum* was very broad and varied from $\sim 1 \mu\text{M}$ to 7.6 mM. Except

for one study (Kim et al. 2004), the cAMP concentration was typically found to be in the low μM range. As expected, the cAMP concentration was lower in mutants lacking a functional AC and higher in the mutant lacking CpdA (e.g. WT 30 ± 12 pmol/mg protein, ΔcyaB 18 ± 2 pmol/mg protein and ΔcpdA 50 ± 12 pmol/mg protein, respectively) (Bussmann, 2009; Schulte et al., 2017).

The intracellular cAMP concentration of *C. glutamicum* is controlled by the rates of synthesis and degradation, as shown by the lower cAMP level of the ΔcyaB mutants (Bussmann, 2009; Cha et al., 2010) and the higher cAMP levels in the ΔcpdA mutant (Schulte et al., 2017). Transporters catalysing cAMP export or import have not been identified. To better understand how the levels of intracellular cAMP in *C. glutamicum* are controlled, one has to study the regulation and the activity of the AC and the PDE.

1.3 Aims of this doctoral thesis

In the course of studies on cAMP-dependent regulation in *C. glutamicum*, only one gene for the cAMP synthesis was identified (*cyaB*, cg0375) (Bussmann, 2009; Cha et al., 2010). ΔcyaB mutants showed comparable growth to the wild type with glucose, but impaired growth with acetate. The reason for the negative effect of acetate on growth of the ΔcyaB mutant is unknown and one aim of this thesis was to find an explanation for this phenotype. This part involved a detailed characterization of the *C. glutamicum* strain lacking CyaB, which should help to elaborate a theory why a *C. glutamicum* strain with a low or even absent intracellular cAMP level shows a higher sensitivity towards the weak acid acetate compared to the wild type strain. The second part of this thesis aimed at an *in vivo* analysis of GlxR-DNA binding in the wild type compared to the ΔcyaB mutant under different carbon source conditions. By this approach, the effects of low intracellular cAMP levels in the ΔcyaB mutant should be elucidated, shedding light on the relevance of cAMP for DNA-binding by GlxR *in vivo*. Despite the fact that numerous previous studies investigated the regulatory hub of GlxR, many open questions remain with respect to physiological role of GlxR and the impact of cAMP. Studies with strains that harbour a high or low cAMP level should provide new insights into this topic.

Table 1: Intracellular cAMP levels of different *C. glutamicum* strains measured in different studies. The values in μM were calculated from the pmol/mg protein values. All cAMP concentrations were measured with the competitive ELISA immunoassay (Biotrak™ cAMP enzyme immunoassay (EIA) system, Cytiva, USA formerly part of GE Healthcare).

Study	Strain	Conditions	cAMP level			
			pmol/mg protein	μM^a		
Kim et al., 2004	<i>C. glutamicum</i> AS019 (spontaneous mutation of <i>C. glutamicum</i> ATCC13059)	MCGC + glucose 1%	22000 (exp ^b) 11000 (stat ^b)	7639 3819		
		MCGC + acetate 2%	5 000 (exp) 5 000 (stat)	1736 1736		
		Polen et al., 2007	<i>C. glutamicum</i> ATCC13032	CGXII + 50 mM glucose	10	4
				CGXII + 50 mM citrate	24	8
Bussmann 2009 (Doc. thesis)	<i>C. glutamicum</i> ATCC13032	CGXII + 200 mM glucose	30 ± 12 (exp)	10 ± 4		
		CGXII + glucose-acetate (100 mM each)	88 ± 22 (exp)	31 ± 8		
	<i>C. glutamicum</i> ΔcyaB	CGXII + 200 mM glucose	18 ± 2 (exp)	6 ± 1		
		CGXII + glucose-acetate (100 mM each)	9 ± 5 (exp)	3 ± 2		
Cha et al., 2010	<i>C. glutamicum</i> ATCC13032	MM + glucose 1%	448 ± 9 (exp)	156 ± 3		
		LB + acetate 1%	108 ± 3 (exp)	38 ± 1		
	<i>C. glutamicum</i> CgYA (partly deleted <i>cyaB</i> gene)	MM + glucose 1%	44 - 63	15 - 21		
		LB + acetate 1%	44 - 63	15 - 21		
Schulte et al., 2017	<i>C. glutamicum</i> ATCC13032	CGXII + glucose (200 mM)	27 ± 5	9 ± 2		
	<i>C. glutamicum</i> ΔcpdA	CGXII + glucose (200 mM)	50 ± 12	17 ± 4		
Study	Strain	Conditions	pmol/OD ₆₁₀	μM^c		
Toyoda et al., 2011	<i>C. glutamicum</i> R	nutrient rich A medium glucose 1%	~ 4 - 9 (exp) ~16 (stat)	~1.4 - 3.1 ~5.6		
		nutrient rich A medium acetate 1%	~ 4 (exp) ~ 3 (stat)	~ 1.4 ~ 1.0		
	<i>C. glutamicum</i> KT23 (strain R with deletion of <i>cyaB</i> gene)	nutrient rich A medium glucose 1%	< 0.2	< 0.1		
		nutrient rich A medium acetate 1%	< 0.2	< 0.1		

a: Intracellular cAMP concentrations have been calculated from the pmol/mg protein values under the assumption that protein represents 50% of the cell dry weight (CDW) and assuming a cell volume of 1.44 $\mu\text{l}/\text{mg}$ CDW (da Luz et al., 2017).

b: exp: concentration measured for cells in the exponential growth phase; stat: concentration measured for cells in the stationary phase.

c: Intracellular concentrations have been calculated under the assumption that OD₆₀₀ of 1 represents 0.25 mg CDW/ml (Kabus et al., 2007).

2 Results

The main topic of this thesis was the investigation of the molecular basis of the acetate sensitivity of an adenylate cyclase-lacking mutant of *C. glutamicum* and the impact of a lowered or even absent cAMP level on *in vivo*-DNA-binding of the global transcriptional regulator GlxR. The results of the first part have been published in the peer-review journal *Frontiers in Microbiology*. The results of the second part have been summarized in a manuscript to be submitted soon.

In the publication 'Molecular basis of growth inhibition by acetate of an adenylate cyclase-deficient mutant of *Corynebacterium glutamicum*' the main reason for the observed growth defect of the *cydB* deletion strain in the presence of acetate is described. The inhibitory effect of acetate was shown to be concentration-dependent and stronger when cultivated in medium with lower external pH values. These results indicate that the negative effect of acetate on the $\Delta cydB$ mutant is related to the uncoupler-like behaviour of acetate. In the protonated form the weak acid diffuses through the lipid bilayer of *C. glutamicum* into the cell, where it dissociates with release of a proton. While to a certain amount this is not problematic for the wild-type strain, the *cydB* deletion strain was shown to be more sensitive towards such uncoupler-like behaviour. Studies with CCCP confirmed that the *cydB* mutant was more sensitive towards uncouplers compared to the wild-type strain. As a possible explanation, the reduced expression of the cytochrome bc_1-aa_3 supercomplex and the F_1F_0 -ATP synthase in the $\Delta cydB$ mutant was proposed. The genes encoding these main players of energy metabolism in *C. glutamicum* were previously shown to be activated by GlxR. The low or absent cAMP level of the $\Delta cydB$ mutant causes a reduction of active GlxR and thus of the expression of genes that are activated by the cAMP-GlxR protein. Additionally, it was shown that upon deletion of *cydB*, no intracellular cAMP was detected via LC-MS/MS. Even in the double deletion mutant *C. glutamicum* $\Delta cydB\Delta cpdA$ (no functional adenylate cyclase and no phosphodiesterase catalysing cAMP degradation), no cAMP could be detected via LC-MS/MS. These data suggest that detection of cAMP via ELISA in extracts of *C. glutamicum* $\Delta cydB$ is probably an artefact and that there is presumably no second active adenylate cyclase present in this organism. Finally, a suppressor mutant of the *cydB* deletion strain was isolated, which had lost the acetate sensitivity and was shown to carry a single amino acid exchange in GlxR. The described results point out that cAMP and

GlxR play an important role in the energy metabolism of *C. glutamicum*, which may be useful also for strain engineering of this industrial workhorse.

The manuscript 'Comparison of *in vivo* GlxR binding in *Corynebacterium glutamicum* ATCC 13032 and the adenylate cyclase deletion mutant $\Delta cyaB$ using ChAP-Seq' describes the investigation of a genome-wide target profiling of GlxR in the *C. glutamicum* wild-type strain and in the adenylate cyclase-deficient mutant ($\Delta cyaB$). The method of choice for this protein-DNA interaction analysis was the so called ChAP-Seq method (chromatin affinity purification combined with DNA sequencing). The results of four data sets ($WT_{GlxR-TS}$ (glc), $\Delta cyaB_{GlxR-TS}$ (glc), $WT_{GlxR-TS}$ (glc-ac), $\Delta cyaB_{GlxR-TS}$ (glc-ac) identified 243 GlxR peaks when a cut-off of the enrichment factor (EF) ≥ 3 was used. 102 of these peaks represented novel GlxR binding sites not reported in previous studies. Many GlxR binding regions were found to be located intragenically or in a relatively large distance (>700 bp) upstream of the next transcriptional start site (TSS). Furthermore, as many GlxR binding sites were found upstream of non-coding proteins (such as asRNA, sRNA or tRNA), GlxR appears to play a more important role in the regulation of non-protein coding genetic elements than previously anticipated. The presence of acetate in the medium reduced GlxR binding, particularly in the $\Delta cyaB$ mutant. The comparison of the GlxR-DNA interaction of the wild type and the $\Delta cyaB$ mutant showed that for most DNA regions GlxR can apparently bind to DNA even without the presence of the effector cAMP, explaining why the phenotype of $\Delta cyaB$ is very moderate compared to the drastic growth defect of reported $\Delta glxR$ mutants. The observation that DNA-binding of GlxR *in vivo*, apparently occurs also in the absence of cAMP, raises the question if other, yet unknown factors, are involved in regulating *in vivo* GlxR-DNA binding.

2.1 Molecular basis of growth inhibition by acetate of an adenylate cyclase-deficient mutant of *Corynebacterium glutamicum*

Natalie Wolf¹, Michael Bussmann¹, Abigail Koch-Koerfges¹, Nino Katcharava¹, Julia Schulte¹, Tino Polen¹, Johannes Hartl², Julia A. Vorholt², Meike Baumgart¹ and Michael Bott^{1*}

¹IBG-1: Biotechnology, Institute of Bio- and Geosciences, Forschungszentrum Jülich, Jülich, Germany

²Institute of Microbiology, ETH Zürich, Zürich, Switzerland

*Corresponding author

Published in *Frontiers in Microbiology*, 11 February 2020 (doi: 10.3389/fmicb.2020.00087)

Author's contributions:

NW constructed mutants and plasmids and performed all experimental work except the one specified below for other authors. MBu constructed the $\Delta cyaB$ mutant and the plasmid pK19*mobsacB- $\Delta cyaB$* and performed the growth experiment showed in Fig. 2. AKK performed the analysis of glucose and organic acids. NK and JS performed the growth experiments with the protonophore CCCP and the determination of the membrane potential. TP supervised genome resequencing and analysed the resulting data. JH and JAV performed LC-MS/MS measurements for cAMP determination. MBa coached the experimental work and supported the design of the study. All authors contributed to the interpretation of the data. NW wrote the first draft of the manuscript and prepared the figures and tables. MBo designed the study, supervised the experimental work, and wrote the final version of the manuscript.

Overall contribution **NW: 65%**

AKK: Abigail Koch-Koerfges, JAV: Julia Anne Vorholt-Zambelli, JH: Johannes Hartl, JS: Julia Schulte, MBa: Meike Baumgart, MBo: Michael Bott, MBu: Michael Bussmann, NK: Nino Katcharava, NW: Natalie Wolf, TP: Tino Polen



Molecular Basis of Growth Inhibition by Acetate of an Adenylate Cyclase-Deficient Mutant of *Corynebacterium glutamicum*

Natalie Wolf¹, Michael Bussmann¹, Abigail Koch-Koerfges¹, Nino Katcharava¹, Julia Schulte¹, Tino Polen¹, Johannes Hart^{1,2}, Julia A. Vorholt², Meike Baumgart¹ and Michael Bott^{1*}

OPEN ACCESS

Edited by:

Häke Antelmann,
Freie Universität Berlin, Germany

Reviewed by:

Gerd M. Seibold,
Technical University of Denmark,
Denmark
Fabian M. Commichau,
Brandenburg University of Technology
Cottbus-Senftenberg, Germany
Reinhard Kraemer,
Universität zu Köln, Germany

*Correspondence:

Michael Bott
m.bott@fz-juelich.de

Specialty section:

This article was submitted to
Microbial Physiology and Metabolism,
a section of the journal
Frontiers in Microbiology

Received: 13 November 2019

Accepted: 15 January 2020

Published: 11 February 2020

Citation:

Wolf N, Bussmann M,
Koch-Koerfges A, Katcharava N,
Schulte J, Polen T, Hart J, Vorholt JA,
Baumgart M and Bott M (2020)
Molecular Basis of Growth Inhibition
by Acetate of an Adenylate
Cyclase-Deficient Mutant
of *Corynebacterium glutamicum*.
Front. Microbiol. 11:87.
doi: 10.3389/fmicb.2020.00087

¹ IBG-1: Biotechnology, Institute of Bio- and Geosciences, Forschungszentrum Jülich, Jülich, Germany, ² Institute of Microbiology, ETH Zürich, Zürich, Switzerland

In *Corynebacterium glutamicum*, cyclic adenosine monophosphate (cAMP) serves as an effector of the global transcriptional regulator GlxR. Synthesis of cAMP is catalyzed by the membrane-bound adenylate cyclase CyaB. In this study, we investigated the consequences of decreased intracellular cAMP levels in a $\Delta cyaB$ mutant. While no growth defect of the $\Delta cyaB$ strain was observed on glucose, fructose, sucrose, or gluconate alone, the addition of acetate to these growth media resulted in a severe growth inhibition, which could be reversed by plasmid-based *cyaB* expression or by supplementation of the medium with cAMP. The effect was concentration- and pH-dependent, suggesting a link to the uncoupling activity of acetate. In agreement, the $\Delta cyaB$ mutant had an increased sensitivity to the protonophore carbonyl cyanide *m*-chlorophenyl hydrazone (CCCP). The increased uncoupler sensitivity correlated with a lowered membrane potential of acetate-grown $\Delta cyaB$ cells compared to wild-type cells. A reduced membrane potential affects major cellular processes, such as ATP synthesis by F_1F_0 -ATP synthase and numerous transport processes. The impaired membrane potential of the $\Delta cyaB$ mutant could be due to a decreased expression of the cytochrome *bc*₁-aa₃ supercomplex, which is the major contributor of proton-motive force in *C. glutamicum*. Expression of the supercomplex genes was previously reported to be activated by GlxR-cAMP. A suppressor mutant of the $\Delta cyaB$ strain with improved growth on acetate was isolated, which carried a single mutation in the genome leading to an Ala131Thr exchange in GlxR. Introduction of this point mutation into the original $\Delta cyaB$ mutant restored the growth defect on acetate. This supported the importance of GlxR for the phenotype of the $\Delta cyaB$ mutant and, more generally, of the cAMP-GlxR system for the control of energy metabolism in *C. glutamicum*.

Keywords: *Corynebacterium glutamicum*, cAMP, adenylate cyclase, acetate, uncouplers, membrane potential, GlxR, cytochrome *bc*₁-aa₃ supercomplex

INTRODUCTION

The Gram-positive soil bacterium *Corynebacterium glutamicum* was identified as a natural glutamate producer in the 1950s (Kinoshita et al., 1957). Since then, various strains of this bacterium are widely used for the production of amino acids, in particular L-glutamate and L-lysine (Eggeling and Bott, 2015). For several years now, *C. glutamicum* has also been employed in commercial protein production (Freudl, 2017). In addition, strains for the synthesis of numerous other industrially relevant compounds have been developed (Schneider and Wendisch, 2011; Becker and Wittmann, 2012; Wieschalka et al., 2013). The success in rational strain development by metabolic engineering is based on detailed studies of the metabolic and regulatory network of *C. glutamicum* (Eggeling and Bott, 2005; Burkovski, 2008; Yukawa and Inui, 2013). Furthermore, efficient novel technologies for strain development involving high-throughput screening approaches with single-cell metabolite biosensors based on transcriptional regulators have been established for *C. glutamicum* (Binder et al., 2012; Mustafi et al., 2012; Schendzielorz et al., 2014; Eggeling et al., 2015).

The transcriptional regulator GlxR, a homolog of the cAMP-receptor protein Crp of *Escherichia coli*, is a global regulator of *C. glutamicum* and activates or represses more than 100 genes. Transcriptional regulation by GlxR influences various cellular functions such as central carbon metabolism, respiration, ATP synthesis, or transport processes (Toyoda et al., 2011; Jungwirth et al., 2013). *In vitro*, purified GlxR binds to DNA when complexed with 3',5'-cyclic adenosine monophosphate (cAMP) (Kim et al., 2004; Kohl et al., 2008; Bussmann et al., 2009). Crystal structures of apo- and cAMP-bound GlxR were solved and revealed conformational changes of the homodimer upon cAMP binding (Townsend et al., 2014). GlxR showed negative allosteric behavior, as binding of the first cAMP molecule ($K_{D1} = 17 \mu\text{M}$) reduced the binding affinity of the second cAMP molecule ($K_{D2} = 130 \mu\text{M}$) to the structurally identical site in the second monomer (Townsend et al., 2014). The affinity of purified GlxR to a double-stranded oligonucleotide containing a central GlxR consensus binding site increased about 100-fold upon cAMP binding from 8.3 μM to 87 nM (Townsend et al., 2014).

The intracellular cAMP level is determined by the rates of synthesis from ATP via adenylate cyclases (Shenoy et al., 2004), degradation to adenosine monophosphate (AMP) via phosphodiesterases (Richter, 2002), and possibly cAMP export and import processes. In *C. glutamicum*, a single adenylate cyclase was identified, which is encoded by the *cyaB* gene (cg0375) (Kalinowski et al., 2003). CyaB contains an N-terminal membrane-integral domain with six predicted transmembrane helices, which is linked via a HAMP domain to a class IIIId catalytic domain (CHD). The HAMP domain might function as transmitter domain, as it was found to have a strong positive stimulatory effect on the adenylate cyclase activity of Rv3645 of *Mycobacterium tuberculosis*, which has the same domain composition as CyaB of *C. glutamicum* (Linder et al., 2004). A *C. glutamicum* mutant lacking about 200 bp of the coding region of the catalytic domain of CyaB (strain CgYA) showed strongly reduced cAMP levels both in glucose minimal medium

and LB-acetate medium (Cha et al., 2010). Wild-type cAMP levels could be restored by plasmid-encoded *cyaB*, but not by supplementation of cAMP to the medium. Interestingly, this CgYA mutant had a strong growth defect in acetate and glucose-acetate minimal medium, but not in glucose or ethanol minimal medium (Cha et al., 2010). Since the activities of the glyoxylate cycle enzymes isocitrate lyase and malate synthase were even higher in the mutant than in the wild type (WT) during growth on LB-acetate, the authors speculated that the acetate uptake carrier might play a role in the growth defect of the CgYA mutant (Cha et al., 2010). Degradation of cAMP in *C. glutamicum* is catalyzed by the recently identified phosphodiesterase CpdA (Cg2761) (Schulte et al., 2017b). This enzyme belongs to the class II phosphodiesterases and deletion of the *cpdA* gene led to an increase of the intracellular cAMP concentration (Schulte et al., 2017b). The Δ *cpdA* mutant exhibited slower growth and a prolonged lag-phase on all tested carbon sources, including glucose, gluconate, citrate, acetate and ethanol (Schulte et al., 2017b). The growth defects could partially be complemented by overexpression of genes that are normally repressed by the cAMP-GlxR complex, such as *ptsI-ptsG* or *citH*, and that are involved in uptake or metabolism of the respective carbon source. This suggested that mainly the higher fraction of cAMP-bound GlxR caused by the increased cAMP level is responsible for the growth defects of the Δ *cpdA* mutant.

The major aim of our current study was to elucidate the molecular basis of the growth inhibition by acetate of a *C. glutamicum* mutant lacking the *cyaB* gene in order to understand the consequences of a reduced cAMP level. Our results suggest that the inhibitory effect of acetate is caused by its property to act as an uncoupler and that a Δ *cyaB* mutant has a reduced capability of generating membrane potential and possibly ATP by oxidative phosphorylation, which might be due to a reduced transcriptional activation of the genes encoding respiratory chain components and the *atp* operon. Support for the assumption that the growth defect of the Δ *cyaB* strain on acetate is due to a reduced activity of GlxR was obtained by the isolation of a suppressor mutant that had lost the growth defect on acetate. This mutant contained a single amino acid exchange in GlxR. In summary, we show that the cAMP level in combination with the global regulator GlxR plays an important role in the bioenergetics of *C. glutamicum*.

MATERIALS AND METHODS

Strains, Plasmids and Culture Conditions

All strains and plasmids used in this study are listed in **Table 1**. *C. glutamicum* strains were cultivated either in brain heart infusion (BHI) medium (Bacto™ BHI, BD, Heidelberg, Germany) or in CGXII minimal medium (adjusted to pH 7.0 with KOH) supplemented with 3,4-dihydroxybenzoate (30 mg l^{-1}) as iron chelator and different carbon sources (Frunzke et al., 2008) as specified in the results section. For growth experiments, 5 ml BHI medium was inoculated with a single colony and incubated at 30°C and 130 rpm for 8 h. About 400 μl of this first preculture were used for the inoculation of the second

TABLE 1 | Bacterial strains and plasmids used in this study.

Strain or plasmid	Relevant characteristics	Source or references
Strains		
<i>Escherichia coli</i> DH5 α	F ⁻ <i>thi-1 endA1 hsdR17r-m +) supE44 ΔlacU169Φ80lacZ ΔM15) recA1 gyrA96 relA1</i>	Invitrogen
<i>Escherichia coli</i> BL21(DE3)	F ⁻ <i>ompT gal dcm lon hsdSB (rB⁻ mB⁻) λ[DE3 (lacI lacUV5-T7 gene 1 ind1 sam7 nln5)]</i>	Studier and Moffatt, 1986
<i>Corynebacterium glutamicum</i> ATCC 13032	ATCC 13032, biotin-auxotrophic wild-type strain (WT)	Kinoshita et al., 1957
<i>C. glutamicum</i> Δ cyaB	ATCC 13032 with an in frame deletion of the adenylate cyclase gene <i>cyaB</i> (cg0375)	This study
<i>C. glutamicum</i> Δ cpdA	ATCC 13032 with an in frame deletion of the phosphodiesterase gene <i>cpdA</i> (cg2761)	Schulte et al., 2017b
<i>C. glutamicum</i> Δ cyaB Δ cpdA	ATCC 13032 with an in frame deletion of the gene <i>cyaB</i> and the phosphodiesterase gene <i>cpdA</i> (Δ cyaB Δ cpdA)	This study
<i>C. glutamicum</i> Δ qcr	ATCC 13032 with an in frame deletion of the <i>qcrCAB</i> genes (cg2405, cg2404, cg2403) encoding the three subunits of the cytochrome bc ₁ complex	Niebisch and Bott, 2001
<i>C. glutamicum</i> Δ cyaB _{sup1}	<i>C. glutamicum</i> Δ cyaB suppressor mutant carrying a single genomic mutation (C to T) at position 307072 in BA000036.3 leading to the amino acid exchange Ala131Thr in GlxR (cg0350)	This study
<i>C. glutamicum</i> Δ cyaB _{sup2}	<i>C. glutamicum</i> Δ cyaB suppressor mutant carrying two genomic mutations in BA000036.3, one at position 877553 (A to G) located in the intergenic region of <i>serC</i> (cg0948) and <i>gfaA</i> (cg0949) and one at position 1548741 (G to C) located in the intergenic region of <i>gpt</i> (cg1658) and cg1660	This study
<i>C. glutamicum</i> Δ cyaB _{sup3}	<i>C. glutamicum</i> Δ cyaB suppressor mutant carrying two genomic mutations in BA000036.3, one at position 307072 (C to T) leading to the amino acid exchange Ala131Thr in GlxR and one at position 2564086 (G to T) leading to a silent mutation of the Gly106 codon of ribose 5-phosphate isomerase (cg2658)	This study
<i>C. glutamicum</i> :: <i>glxR</i> _A131T	<i>C. glutamicum</i> WT in which an Ala131Thr exchange in the <i>glxR</i> coding sequence was introduced by double homologous recombination	This study
<i>C. glutamicum</i> Δ cyaB:: <i>glxR</i> _A131T	<i>C. glutamicum</i> Δ cyaB mutant in which an Ala131Thr exchange in the <i>glxR</i> coding sequence was introduced by double homologous recombination	This study
Plasmids		
pAN6	Kan ^R ; P _{lac} , lac ^R pBL1 oriV _{CG} pUC18 oriV _{EC} , <i>C. glutamicum</i> /E. coli shuttle vector, derivative of pEKEx2	Frunzke et al., 2008
pAN6-cyaB	Kan ^R ; pAN6 derivative carrying the <i>cyaB</i> gene (cg0375) including 300 bp upstream of the start codon and a 3'-terminal StrepTag-II-encoding sequence under the control of an IPTG-inducible tac promoter	This study
pAN6-glxR-Twinstrep	Kan ^R ; pAN6 derivative carrying the <i>glxR</i> gene (cg0350) including a 3'-terminal Twinstrep-tag encoding sequence before the stop codon (WSHPQFEKGGGGGGGGSAWSHPQFEK)	This study
pAN6-glxR-A131T-Twinstrep	Kan ^R ; pAN6-glxR-Twinstrep derivative with a Ala131T exchange	This study
pK19mobsacB	Kan ^R ; oriT oriV _{EC} sacB lacZ α ; vector for allelic exchange in <i>C. glutamicum</i>	Schäfer et al., 1994
pK19mobsacB- Δ cyaB	Kan ^R ; pK19mobsacB derivative containing an overlap extension PCR product covering the up- and downstream regions of <i>cyaB</i>	This study
pK19mobsacB- Δ cpdA	Kan ^R ; pK19mobsacB derivative containing an overlap extension PCR product covering the up- and downstream regions of <i>cpdA</i>	Schulte et al., 2017b
pK19mobsacB-glxR_mut	Kan ^R ; pK19mobsacB derivative containing a 800-bp PCR product covering the 3'-terminal 684 bp of <i>glxR</i> including the mutation leading to the Ala131Thr exchange and 116 bp of the downstream region	This study

preculture, which was cultivated for about 16 h at 30°C and 120 rpm in a 100 ml baffled shake flask containing 20 ml CGXII medium with 2% (w/v) glucose. For the main culture, 800 μ l CGXII medium in FlowerPlates (m2p-labs, Baesweiler, Germany) was inoculated to an optical density at 600 nm (OD₆₀₀) of 1 and cultivated in a BioLector microcultivation system (m2p-labs, Baesweiler, Germany) at 1200 rpm, 30°C and 80% humidity. Growth was followed by measuring the backscatter at 620 nm, which reflects the cell density (Kensy et al., 2009). For cultivations in 500 ml shake flasks, 50 ml CGXII medium was inoculated with the second preculture to an OD₆₀₀ of 1. The cultivations in shake flasks were performed at 30°C and 120 rpm and growth was followed by measuring OD₆₀₀. *E. coli* DH5 α was used as host for all cloning purposes and was cultivated at 37°C in LB medium (Sambrook and Russell, 2001). When required, media were supplemented with

kanamycin (25 μ g ml⁻¹ for *C. glutamicum* and 50 μ g ml⁻¹ for *E. coli*).

Construction of Plasmids and Deletion Mutants

Plasmids were constructed by standard cloning procedures (Sambrook and Russell, 2001) using the oligonucleotides listed in **Supplementary Table S1**. Deletion mutants of *C. glutamicum* were constructed by double homologous recombination as described previously (Niebisch and Bott, 2001). In brief, *C. glutamicum* ATCC 13032 was transformed with the deletion plasmid carrying the up- and downstream regions of the target gene to be deleted. After selection for the first (kanamycin resistance) and second (kanamycin sensitivity, sucrose tolerance) recombination events, Kan^S-Suc^R clones were analyzed by colony

PCR and the PCR product of clones carrying the desired deletion was further verified by sequencing.

For construction of a Δ cyaB deletion mutant, it had to be considered that the length of the coding region of *cyaB* varies in different annotations, resulting in proteins of either 347 amino acids (MRPVAA...; Cgl0311 of strain ATCC 13032) (Ikeda and Nakagawa, 2003), 547 amino acids (MDTVLE...; Cg0375 of strain ATCC 13032) (Kalinowski et al., 2003), or 501 amino acids (MKWLWG...; cgR_0397 of strain R) (Yukawa et al., 2007). RNAseq analysis of strain ATCC 13032 identified a single transcriptional start site presumably leading to a leaderless *cyaB* mRNA encoding a protein of 508 amino acids (MSRLLR...) (Pfeifer-Sancar et al., 2013). We therefore assumed the latter size to be the correct one, although additional transcriptional start sites and *CyaB* variants of other length cannot be excluded. For construction of the Δ cyaB mutant, we deleted the entire coding region except for the 5'-terminal 37 codons and the 3'-terminal 12 codons including the stop codon. After the second homologous recombination event, nine kanamycin-sensitive and sucrose-resistant clones were analyzed by colony PCR. Four clones harbored the *cyaB* deletion whereas five clones contained the wild-type fragment. Thus, the Δ cyaB deletion mutant was obtained without any difficulties.

Isolation of Δ cyaB Suppressor Mutants With Improved Growth on Acetate

The acetate-sensitive Δ cyaB strain was cultivated in CGXII medium with 150 mM potassium acetate as sole carbon source. The culture was prepared as described above. To obtain acetate-tolerant suppressor clones, cultivations were performed for at least 90 h in a BioLector. Cultures that started to grow and reached comparable backscatter values as the WT were streaked out on BHI agar plates and single colonies were inoculated again in CGXII medium with 150 mM potassium acetate. Cultures that grew better than the Δ cyaB parental strain were streaked out again on BHI agar plates. The genomic DNA of such clones was isolated and used for whole genome sequencing.

Genomic DNA Sequencing

DNA of the samples was purified with the DNeasy Blood and Tissue kit (Qiagen, Hilden, Germany) starting with the "pretreatment of Gram-positive bacteria," as described in the manufacturer's instructions. The obtained DNA was dried and resuspended in max. 100 μ l ddH₂O. For library preparation, the NEBNext Ultra II DNA Library Prep kit for Illumina (New England Biolabs GmbH, Frankfurt am Main, Germany) was used with 2 μ g genomic DNA of each sample following the manufacturer's instructions. The resulting indexed libraries were quantified using the KAPA Library Quantification kit (VWR International GmbH, Darmstadt, Germany) and normalized for pooling. Sequencing was performed on a MiSeq instrument (Illumina, San Diego, CA, United States) using paired-end sequencing with a read-length of 2 \times 150 bp. Data analysis and base calling were accomplished with the CLC Genomics workbench (Qiagen, Hilden, Germany). Reads of the parental Δ cyaB strain and the suppressor strains were mapped to the

genome sequence BA000036.3 of *C. glutamicum* ATCC 13032 (Ikeda and Nakagawa, 2003).

Determination of mRNA Levels by Reverse Transcription Quantitative PCR (RT-qPCR)

For quantifying the mRNA levels of *ctaD*, *ctaC*, and *qcrC* in *C. glutamicum* WT and the Δ cyaB mutant, RT-qPCR was performed. Cells were grown in CGXII medium containing a glucose-acetate mixture (100 mM each) and harvested at an OD₆₀₀ of 6. Cells were disrupted by the addition of QIAzol Lysis Reagent (Qiagen, Hilden, Germany) followed by bead beating with a Precellys24 device (Peqlab Biotechnologie, Erlangen, Germany). RNA was purified and concentrated with an RNeasy Mini kit (Qiagen, Hilden, Germany) including a DNase I treatment. Reverse transcription of total RNA samples to cDNA was performed using SuperscriptTM III reverse transcriptase and random primers (Invitrogen, Carlsbad, CA, United States) following the manufacturer's instructions. For the quantitative PCR, KAPA SYBR[®] FAST qPCR Master Mix (2 \times) (Roche, Basel, Switzerland) was used following the manufacturer's protocol. Primer pairs used for the reactions are listed in **Supplementary Table S1**. As reference gene, *hpt* (cg2985) was used with the oligonucleotides listed in **Supplementary Table S1**. Fluorescence measurements and analysis of the results were conducted using a qTower 2.2 and the software qPCR-soft 3.1 (Analytic Jena, Jena, Germany). RNA was isolated from three independent cultures of each strain (biological triplicates) and for each sample technical duplicates were performed.

Global Gene Expression Analysis Using DNA Microarrays

Preparation of RNA and synthesis of fluorescently labeled cDNA were carried out as described (Möker et al., 2004). Custom-made DNA microarrays for *C. glutamicum* ATCC 13032 printed with 70mer oligonucleotides were obtained from Operon (Cologne, Germany) and are based on the genome sequence entry NC_006958 (Kalinowski et al., 2003). Hybridization and stringent washing of the microarrays were performed according to the instructions of the supplier. Processed and normalized data as well as experimental details (Brazma et al., 2001) were stored in the in-house microarray database for further analysis (Polen and Wendisch, 2004). Using the DNA microarray technology, the genome-wide mRNA concentrations of *C. glutamicum* wild type were compared with those of the mutant strain *C. glutamicum* Δ cyaB. The strains were cultivated in CGXII medium with a glucose-acetate mixture (100 mM each). RNA used for the synthesis of labeled cDNA was prepared from cells in the exponential growth phase. Three independent DNA microarray experiments were performed, each starting from independent cultures.

Determination of cAMP

Cell extracts were prepared as described previously (Schulte et al., 2017b) and the cAMP concentration was measured without dilution with the direct cAMP ELISA kit (Enzo Life Sciences

GmbH, Lörrach, Germany) following the manufacturer's instructions. Amounts of cAMP were related to the protein content of the supernatant of the cell extract. The product specification of the used cAMP ELISA kit (Direct cAMP ELISA kit; Enzo, Lausen, Switzerland) reports the following cross-reactivities with nucleotides other than cAMP, which is set as 100%: AMP, 0.33%; ATP, 0.12%; cyclic GMP, GMP, GTP, cyclic UMP, CTP, all <0.001%. For determining the cross-reactivities, the nucleotides were dissolved in assay buffer to a concentration of 2000 pmol/ml, which is 10-fold higher than the highest concentration used for cAMP in the non-acetylated variant of the assay. The apparent concentrations determined for the non-cAMP nucleotides, e.g., 6.6 pmol/ml for AMP, was divided by the real AMP concentration in the assay (2000 pmol/ml) and multiplied with 100 to give the cross-reactivity in%.

Additionally, intracellular cAMP was measured by LC-MS/MS. *C. glutamicum* cells were grown to the exponential phase (OD_{600} of ~5). For the sampling, cells from a culture volume corresponding to 4 ml of OD_{600} of 1 were harvested. Sampling, quenching, metabolite extraction and measurements were performed as previously described (Müller et al., 2015; Hartl et al., 2017). Briefly, metabolite separation was achieved by reverse-phase-ion-pairing (tributylamin) liquid chromatography using a nLC-ultra (Eksigent) system. The LC was hyphenated to a QExactive Plus Orbitrap (Thermo Fisher) mass spectrometer with an electrospray ionization probe. The MS was operating in negative mode; the resolution was set to 70,000 (at m/z 200). cAMP was measured using parent reaction monitoring (PRM) with m/z 328.045 as the precursor ion and quantified with the corresponding m/z 134.0465 fragment. Fragmentation was achieved by higher energy collisional dissociations (HCDs) with a normalized collision energy (NCE) of 30.0. cAMP was identified by exact mass (m/z tolerance of 0.003 Da) as well as matching retention time and fragmentation pattern with an analytical 3',5'-cAMP standard. cAMP was quantified by peak integration using the trapezoid rule; absolute quantification was performed by external calibration. The calibration curve of reference solutions with known cAMP concentrations was fitted by linear regression. The intracellular cAMP concentrations in *Corynebacterium* were estimated assuming a correlation factor of 250 mg cell dry weight (CDW) l^{-1} at OD_{600} of 1 (Kabus et al., 2007) and a corresponding intracellular volume of 1.44 μ l per mg CDW (da Luz et al., 2016). The limit of detection (LOD) was estimated to be 14 amol l^{-1} by calculating 3.3 standard deviations of the y-intercepts divided by the slope obtained from linear regression (ICH, 2005) of reference cAMP solutions; the LOD was confirmed by visual inspection. Assuming similar dilution factors as for measured *Corynebacterium* extracts, this corresponds to an LOD of ~0.1 μ mol l^{-1} from cell extracts.

Measurement of Membrane Potential via Flow Cytometry

The membrane potential of *C. glutamicum* cells was determined by flow cytometry using the fluorescent dye 3,3'-diethyloxycarbocyanine iodide [DiOC2(3)] (Novo et al., 1999, 2000). The assay was performed according to a previously

established protocol for *C. glutamicum* (Neumeyer et al., 2013). In brief, the strains were cultivated in baffled shake flasks with 50 ml CGXII medium containing either 100 mM glucose, or 100 mM acetate, or 200 mM acetate (precultures as described for the BioLector cultivation). Measurement of the membrane potential was performed when cells had reached the mid-exponential growth phase (OD_{600} of ~5). The culture was diluted with FACSFlowTM buffer to an OD_{600} of 0.05 and cells were stained for 30 min with 30 μ M DiOC2(3) (3 mM stock solution in dimethyl sulphoxide, Sigma-Aldrich, Germany) and analyzed using a FACS Aria II and BD Diva software (BD Biosciences, Heidelberg, Germany). Green fluorescence was measured at an excitation wavelength of 488 nm and an emission wavelength of 497 nm, red fluorescence at an excitation wavelength of 488 nm and an emission wavelength of 610 nm. For each sample, 100,000 cells were measured at 2000 cells s^{-1} . The red/green fluorescence ratio was analyzed using FlowJo V.10 software and plotted as a histogram with GraphPad Prism8.

Quantitative Determinations of Carbon Sources

Glucose, gluconate and acetate concentrations in culture supernatants were determined as described (Koch-Koerfges et al., 2012) by ion-exchange chromatography using an Agilent 1100 HPLC system (Agilent Technologies, Waldbronn, Germany) equipped with a cation exchange column (Organic Acid Resin 300 \times 8 mm, CS Chromatographie Service, Langerwehe, Germany). Isocratic elution within 40 min with 100 mM H_2SO_4 and a flow rate of 0.4 ml/min at 40°C was used. Organic acids were detected using a diode array detector at 215 nm and glucose was analyzed by a refraction index (RI) detector in the same run. The quantification of organic acids and glucose was based on a calibration curve with external standards.

TMPD Enzyme Assay

N,N,N',N'-tetramethyl-*p*-phenylenediamine (TMPD) oxidase activity was measured spectrophotometrically at 562 nm in a 96-well plate with an Infinite M1000 PRO microplate reader (Tecan, Männedorf, Switzerland). TMPD was added to 100 mM Tris-HCl buffer pH 7.5 containing isolated membrane proteins to a final concentration of 200 μ M. For the calculation of the TMPD oxidation rate, an extinction coefficient of 10.5 $mM^{-1} cm^{-1}$ was used (Sakamoto et al., 2001). The autooxidation rate of TMPD was recorded using samples containing only buffer and 200 μ M TMPD and subtracted from the rates of the membranes. The cells for these measurements were cultivated at 30°C and 90 rpm in 5 l baffled shake flasks with 500 ml CGXII medium and glucose plus acetate (100 mM each) as carbon source. The cultures were harvested in the exponential growth phase at the OD_{600} of 10. The preparation of cell membranes was performed as described (Niebisch and Bott, 2003).

Electrophoretic Mobility Shift Assays (EMSAs) With Purified GlxR

EMSAs were performed to compare *in vitro* binding of the wild-type GlxR protein (GlxR_{WT}) and the variant GlxR_{A131T} to

selected DNA target sites. The gene *glxR* was amplified from genomic DNA of *C. glutamicum* WT with the oligonucleotides GlxR-twin1 and GlxR-twin2. A DNA fragment with a Twin-Strep tag-encoding sequence was amplified with the oligonucleotides GlxR-twin3 and GlxR-twin4 using a suitable plasmid with the corresponding sequence as template. Gibson assembly was performed with pAN6 cut with *NdeI* and *NheI*, the *glxR* fragment and the Twinstrep-tag fragment resulting in the plasmid pAN6-*glxR*-Twinstrep. The oligonucleotides GlxR-A131T_fw and GlxR-A131T_rv were used to introduce the mutation leading to the amino acid exchange A131T in GlxR using the QuickChange Site-Directed Mutagenesis Kit (Agilent, Waldbronn, Germany). The resulting plasmid was named pAN6-*glxR*-A131T-Twinstrep. Overproduction of GlxR_{WT} or GlxR_{A131T} was performed by cultivation of *E. coli* BL21(DE3) transformed with pAN6-*glxR*-Twinstrep or pAN6-*glxR*-A131T-Twinstrep in ZYM-5052 auto-induction medium (Studier, 2005). After harvesting and disrupting the cells, proteins were purified using Strep-Tactin XT affinity chromatography according to the protocol of the supplier (IBA Life Sciences, Göttingen, Germany). Subsequently, the proteins were further purified by size exclusion chromatography using a Superdex 200 increase column using a buffer composed of 100 mM Tris-HCl pH 7.5, 5% (v/v) glycerol, 100 mM KCl, 20 mM MgCl₂, and 1 mM EDTA.

EMSAs were performed as described previously (Bussmann et al., 2009) using the following DNA fragments: (i) a 140 bp DNA fragment upstream of *ctaD* extending from -127 to -261 upstream of the *ctaD* start codon; (ii) a 132 bp DNA fragment upstream of *ctaCF* extending from -102 to -234 upstream of the *ctaC* start codon; and (iii) a 136 bp DNA fragment covering an intragenic region of the gene *cg3153*. The first two DNA fragments contain previously described GlxR binding sites (Kohl et al., 2008; Toyoda et al., 2011). The respective DNA fragments were generated by PCR and purified with the DNA Clean & Concentrator Kit (Zymo Research, Freiburg im Breisgau, Germany).

RESULTS AND DISCUSSION

cAMP Levels in *C. glutamicum* WT and Mutants Lacking *cyaB* or *cpdA*

In order to confirm previous studies with the *C. glutamicum* mutant strain CgYA lacking approximately 200 bp coding region of the catalytic domain of the adenylate cyclase CyaB

(Cha et al., 2010), we constructed another Δ *cyaB* mutant lacking almost the entire coding region (see section “Materials and Methods”). The cAMP level of this mutant was compared with that of the WT and the Δ *cpdA* mutant lacking the cAMP phosphodiesterase (Schulte et al., 2017b) using an enzyme-linked immunosorbent assay (ELISA). The strains were grown in CGXII glucose medium to an OD₆₀₀ of about 5 (exponential growth phase). As shown in Table 2, the cAMP level of the Δ *cyaB* mutant (~20 pmol (mg protein)⁻¹) amounts to only 20% of the cAMP level of the WT (~100 pmol (mg protein)⁻¹), whereas that of the Δ *cpdA* mutant was higher (~144 pmol (mg protein)⁻¹). These results confirmed that the lack of the adenylate cyclase CyaB causes a strong decrease of the cAMP level, which is in agreement with previous results (Cha et al., 2010; Toyoda et al., 2011; Schulte et al., 2017b). It should be noted that the absolute values obtained in the ELISA measurements published in these studies differ significantly.

Bioinformatic analysis revealed only a single adenylate cyclase-encoding gene (*cyaB*) in the genome of *C. glutamicum*. Therefore, deletion of *cyaB* should result in the complete lack of the cAMP. However, both in our Δ *cyaB* mutant as well as in previously analyzed *cyaB* mutants of strain ATCC 13032 (Cha et al., 2010) and strain R (Toyoda et al., 2011), a residual cAMP level was measured by ELISA assays, raising the question for the source of this residual cAMP. The kit used in this study (Enzo Life Sciences GmbH, Lörrach, Germany) shows low cross-reactivity to AMP and ATP, which might contribute to the residual signal in the Δ *cyaB* mutant. Alternatively or additionally, *C. glutamicum* might possess another enzyme with adenylate cyclase activity besides CyaB, which contributes to the residual cAMP level in the Δ *cyaB* mutants and which is not detectable in bioinformatic searches using members of the known classes of adenylate cyclases (Shenoy et al., 2004). If a yet unknown novel enzyme with adenylate cyclase activity exists in *C. glutamicum*, a deletion of the *cpdA* gene in the Δ *cyaB* background might lead to an increase of cAMP. Therefore, we constructed a Δ *cyaB* Δ *cpdA* double mutant and determined the cAMP level by the ELISA kit. Although a small increase was detected for the double mutant, the difference to the Δ *cyaB* mutant was not significant (Table 2). In growth experiments with glucose or acetate minimal medium, the Δ *cyaB* Δ *cpdA* mutant behaved like the Δ *cyaB* mutant (Supplementary Figure S1), arguing against the existence of an alternative adenylate cyclase besides CyaB.

TABLE 2 | cAMP levels in various *C. glutamicum* strains cultivated in CGXII medium with 100 mM glucose.

<i>C. glutamicum</i> strain	Intracellular cAMP concentration ¹	
	pmol mg ⁻¹ protein (determined by ELISA)	μM (determined by LC-MS/MS)
WT	99.9 ± 31.8	0.9 ± 0.4
Δ <i>cyaB</i>	20.5 ± 4	n.d. ²
Δ <i>cpdA</i>	144.1 ± 7.9	3.4 ± 1.5
Δ <i>cyaB</i> Δ <i>cpdA</i>	30 ± 6.8	n.d.

¹Each value represents the mean value with the standard deviation of three biological replicates. ²n.d., not detectable.

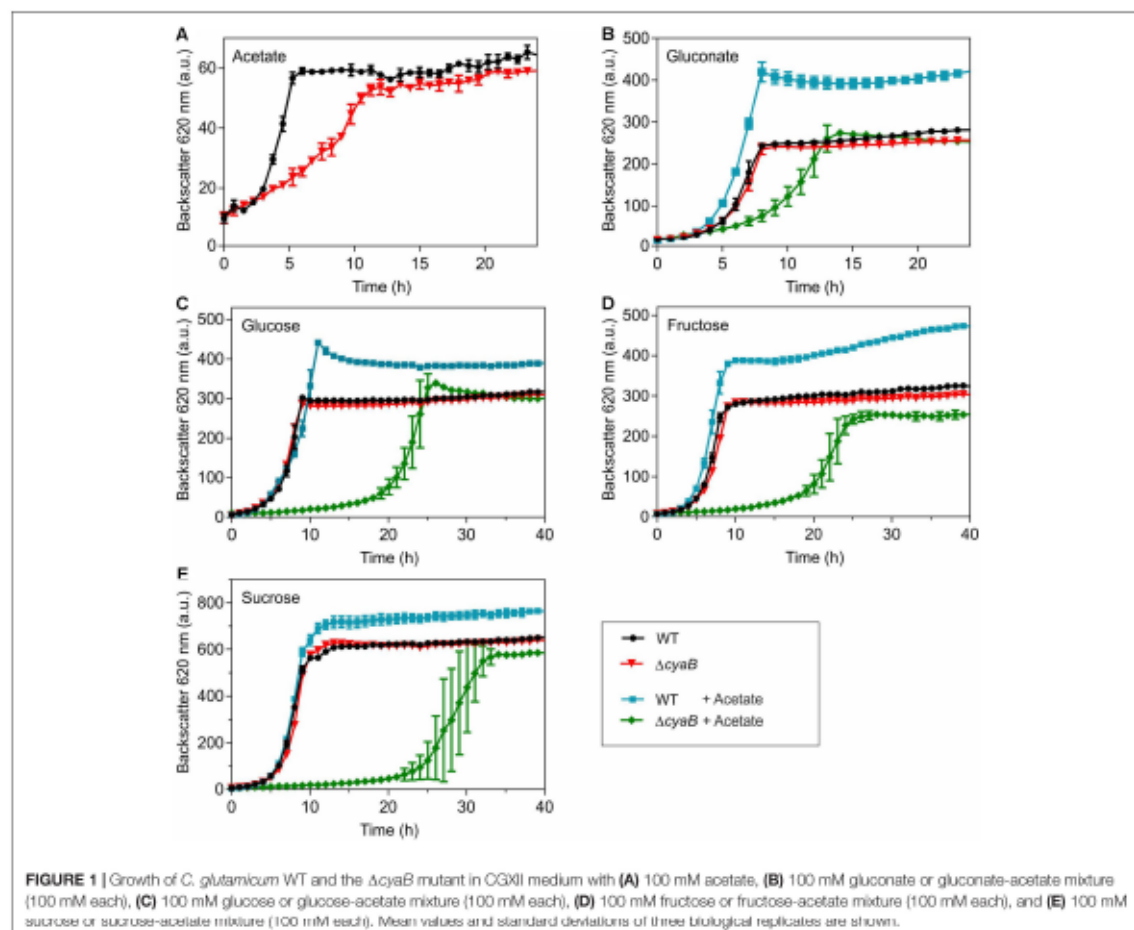
As the ELISA-based assay might be influenced by cross-reacting metabolites, LC-MS/MS was applied as an alternative method to quantify cAMP levels. With this method, we determined an absolute concentration of cAMP of $\sim 1 \mu\text{M}$ in wild-type cells, whereas a ~ 3.5 -fold higher concentration was determined in the $\Delta cpdA$ mutant. cAMP was not detected in the $\Delta cyaB$ mutant and in the $\Delta cyaB\Delta cpdA$ double mutant. These results support the possibility that the residual cAMP levels determined by the ELISA assay in the latter two mutants might be caused by cross-reactivities and suggest that CyaB is the only adenylate cyclase present in *C. glutamicum*.

Sensitivity of the $\Delta cyaB$ Mutant to Acetate

Growth of the $\Delta cyaB$ mutant and the WT with different carbon sources was compared using the BioLector cultivation system. In CGXII minimal medium containing 100 mM of either glucose, gluconate, fructose, or sucrose as carbon source, the $\Delta cyaB$

mutant grew like the WT, whereas a clear growth defect was observed for the mutant when 100 mM acetate served as carbon source (Figure 1). In media containing mixtures of gluconate and acetate, glucose and acetate, fructose and acetate, or sucrose and acetate (100 mM of each carbon source), the $\Delta cyaB$ mutant showed a strong growth defect, whereas the WT was unaffected and grew to higher cell densities (measured as higher backscatter values) (Figure 1). The data obtained with the $\Delta cyaB$ mutant for glucose, acetate, and the glucose-acetate mixture are in agreement with those described previously for the CgYA mutant, whereas the results for fructose-acetate and sucrose-acetate disagree, as growth of the CgYA mutant on these mixtures was reported not to be impaired (Cha et al., 2010). Our results indicate that acetate inhibits growth of the $\Delta cyaB$ mutant irrespective of the presence of an additional carbon source.

With respect to the inhibitory effect of acetate, ethanol is a particularly interesting carbon source, as its catabolism in *C. glutamicum* involves acetate as an intermediate. Ethanol degradation proceeds via the initial oxidation to acetaldehyde by



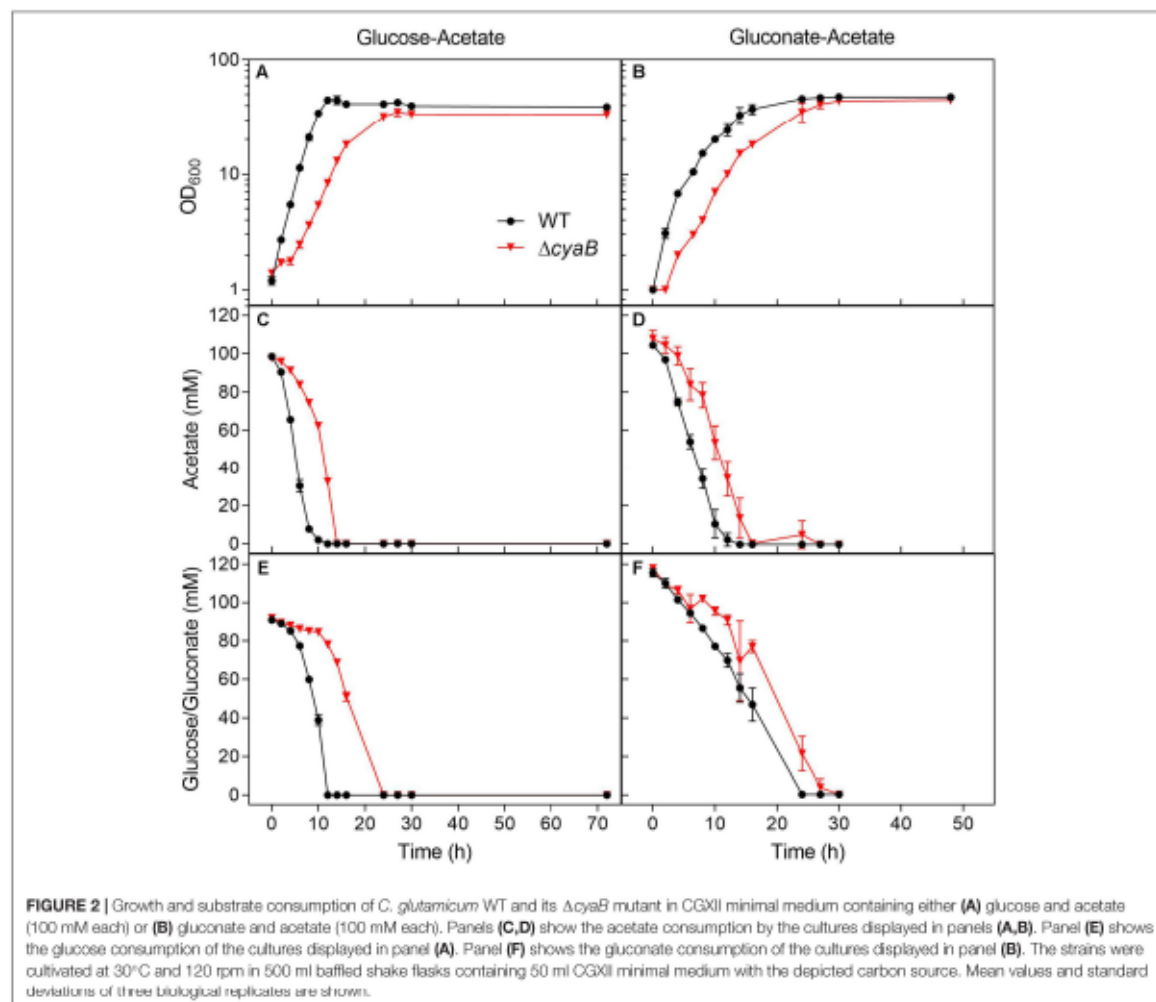
alcohol dehydrogenase followed by a second oxidation to acetate by acetaldehyde dehydrogenase (Arndt and Eikmanns, 2007; Arndt et al., 2008). Acetate is then converted via acetyl phosphate to acetyl-CoA by acetate kinase and phosphotransacetylase and acetyl-CoA is oxidized in the TCA cycle with the glyoxylate cycle serving as an anaplerotic reaction (Wendisch et al., 2000; Gerstmeir et al., 2003; Bott, 2007). As shown in **Supplementary Figure S2**, the $\Delta cyaB$ mutant grew like the WT in CGXII medium containing 150 mM ethanol as carbon source. This result is in agreement with data reported previously for the CgYA mutant (Cha et al., 2010) and shows that acetate degradation is functional in the $\Delta cyaB$ mutant.

Growth of the WT and the $\Delta cyaB$ mutant was also compared in shake flasks in order to be able to follow the consumption of the carbon sources during cultivation (**Figure 2**). The growth defect of the $\Delta cyaB$ mutant during growth on a glucose-acetate mixture (100 mM each) was confirmed and resulted in

a retarded consumption of both carbon sources compared to the WT. In CGXII medium containing a gluconate-acetate mixture, the $\Delta cyaB$ mutant also showed a growth defect and retarded consumption of gluconate and acetate compared to the WT. In contrast to glucose, fructose, and sucrose, gluconate is not taken up via the PEP-dependent phosphotransferase system (PTS), but via the secondary transporter GntP (Frunzke et al., 2008). The fact that acetate was completely consumed confirms that acetate catabolism is functional in the $\Delta cyaB$ mutant.

Abolishment of the Growth Defect of the $\Delta cyaB$ Mutant in the Presence of Acetate

The $\Delta cyaB$ mutant and the WT were transformed with the *cyaB* expression plasmid pAN6-*cyaB* or the parent vector pAN6. As shown in **Figure 3**, the growth defect of the $\Delta cyaB$ mutant in glucose-acetate medium was abolished by plasmid-based



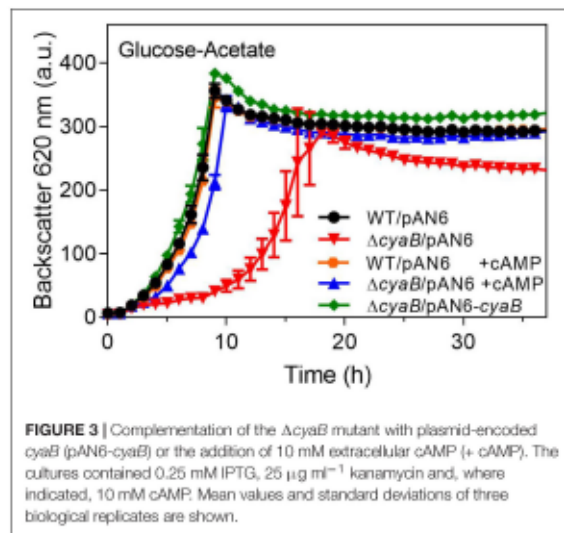


FIGURE 3 | Complementation of the $\Delta cyaB$ mutant with plasmid-encoded *cyaB* (pAN6-*cyaB*) or the addition of 10 mM extracellular cAMP (+ cAMP). The cultures contained 0.25 mM IPTG, 25 $\mu\text{g ml}^{-1}$ kanamycin and, where indicated, 10 mM cAMP. Mean values and standard deviations of three biological replicates are shown.

expression of *cyaB*, but not by the presence of the vector alone. This result confirmed that the *cyaB* deletion rather than a hypothetical secondary mutation that might have occurred during mutant construction was responsible for the acetate sensitivity. In a previous study, we showed that cAMP addition to the medium influences GlxR-based gene expression, indicating that it can enter the cell (Schulte et al., 2017a). We therefore tested the influence of cAMP addition on growth of the $\Delta cyaB$ mutant and could show that 10 mM cAMP abrogated the growth defect in the presence of acetate, confirming that it is due to a lowered cAMP level (Figure 3). In the case of the CgYA mutant, addition of cAMP to the medium could not reverse the growth inhibition (Cha et al., 2010). The reason for this discrepancy is unknown. Uptake of 3',5'-cAMP was previously reported for *E. coli* and marine bacteria, but no distinct transporter could be identified (Saier et al., 1975; Goldenbaum and Hall, 1979; Ammerman and Azam, 1982).

Concentration and pH Dependency of Growth Inhibition of the $\Delta cyaB$ Mutant by Acetate

As described above, the inhibitory effect of acetate on growth of the $\Delta cyaB$ mutant was independent of the presence of additional carbon sources. The difference when comparing growth on ethanol and growth on acetate is that during ethanol degradation acetate is only a metabolic intermediate that does not accumulate to high concentrations but is directly catabolized. In contrast, when acetate is used as carbon source, it is present in a high concentration outside of the cell. It was speculated that inhibition of acetate uptake by the secondary monocarboxylate transporter MctC (Cg0953) might play a role for the growth defect (Cha et al., 2010). However, under the conditions used in our studies (100 mM acetate, pH 7), uptake of acetate by passive diffusion is completely sufficient, as shown by the fact that growth of

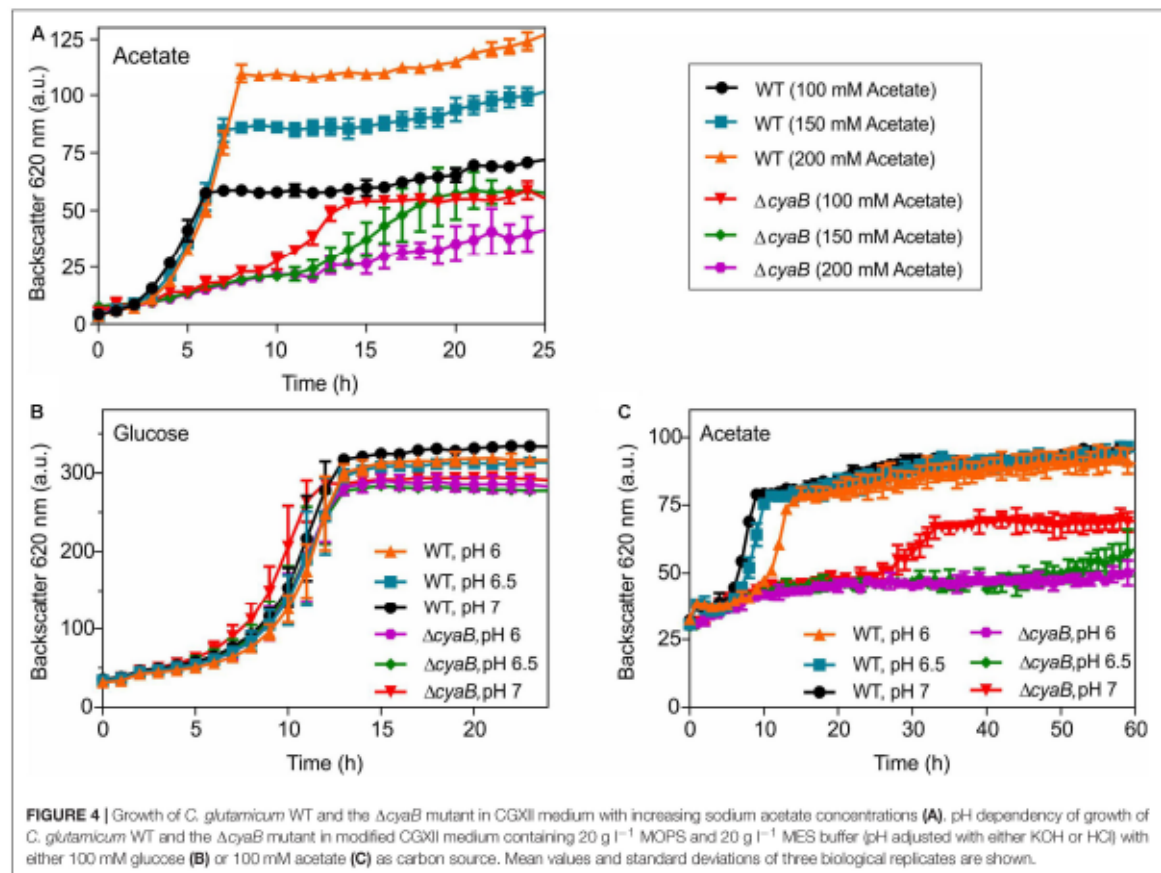
a *mctC* deletion mutant on acetate at pH 7 was unaffected (Jolkver et al., 2009).

Based on the above considerations, we assumed that the inhibitory effect of acetate on growth of the $\Delta cyaB$ mutant is due to its property to act as an uncoupler (Axe and Bailey, 1995; Pinhal et al., 2019). We tested whether the inhibitory effect of acetate is concentration- and pH-dependent. Weak acids such as acetate become more effective as proton translocator when the pH gets closer to their pK_a (4.76 in the case of acetic acid). In a first set of experiments, the WT and the $\Delta cyaB$ mutant were grown in CGXII medium containing 100 mM, 150 mM, or 200 mM acetate. In the case of the WT, increased acetate concentrations led to increased cell densities, but did not affect the growth rate strongly. In contrast, growth inhibition of the $\Delta cyaB$ mutant clearly correlated with increasing acetate concentrations (Figure 4A). The dose-dependent negative impact of acetate on growth of the $\Delta cyaB$ mutant was also observed in cultivations in CGXII medium with 100 mM glucose and either 50 mM or 100 mM acetate (Supplementary Figure S3). Furthermore, the inhibitory effect of acetate was observed independent of whether sodium acetate or potassium acetate were used for preparation of the media, showing that this effect is not caused by the cation (data not shown). For testing the pH dependency of growth inhibition by acetate, the MOPS buffer of the standard CGXII medium was substituted by a mixture of 20 g l⁻¹ MOPS (pK_a 7.20) and 20 g l⁻¹ MES (pK_a 6.15) and pH values of 6.0, 6.5, and 7.0 were adjusted by addition of KOH or HCl. Besides media with 100 mM acetate, also media with 100 mM glucose were used at the indicated pH values. As shown in Figure 4B, growth of the WT and the $\Delta cyaB$ mutant in glucose medium was comparable and hardly affected by the initial pH value. In contrast, growth of the mutant in acetate medium was strongly affected by the pH, showing almost no growth at pH 6.5 and pH 6.0 (Figure 4C). In summary, the inhibitory effect of acetate on growth of the $\Delta cyaB$ mutant was both concentration- and pH-dependent, supporting our assumption that it is due to the uncoupling properties of acetate.

Uncoupler Sensitivity and Membrane Potential of WT and the $\Delta cyaB$ Mutant

The results described above suggested that the $\Delta cyaB$ mutant is more sensitive to uncouplers than the WT. To further confirm this assumption, the influence of the protonophore carbonyl cyanide *m*-chlorophenyl hydrazone (CCCP) (Heytler and Prichard, 1962) on growth in CGXII medium with glucose was tested (Figures 5A,B). The $\Delta cyaB$ mutant was more sensitive to CCCP than the WT. In the presence of 5 μM CCCP, the mutant was stronger inhibited than the WT. In the presence of 10 μM CCCP, the mutant was not able to grow any more, while the WT showed residual growth. At 15 μM CCCP, neither strain was able to grow.

The increased sensitivity to acetate and CCCP of the $\Delta cyaB$ mutant compared to the WT might be due to a reduced capability of the mutant to build up pmf, which is composed of the membrane potential $\Delta\psi$ and the pH gradient ΔpH (Nicholls and Ferguson, 2002). At pH 7, the



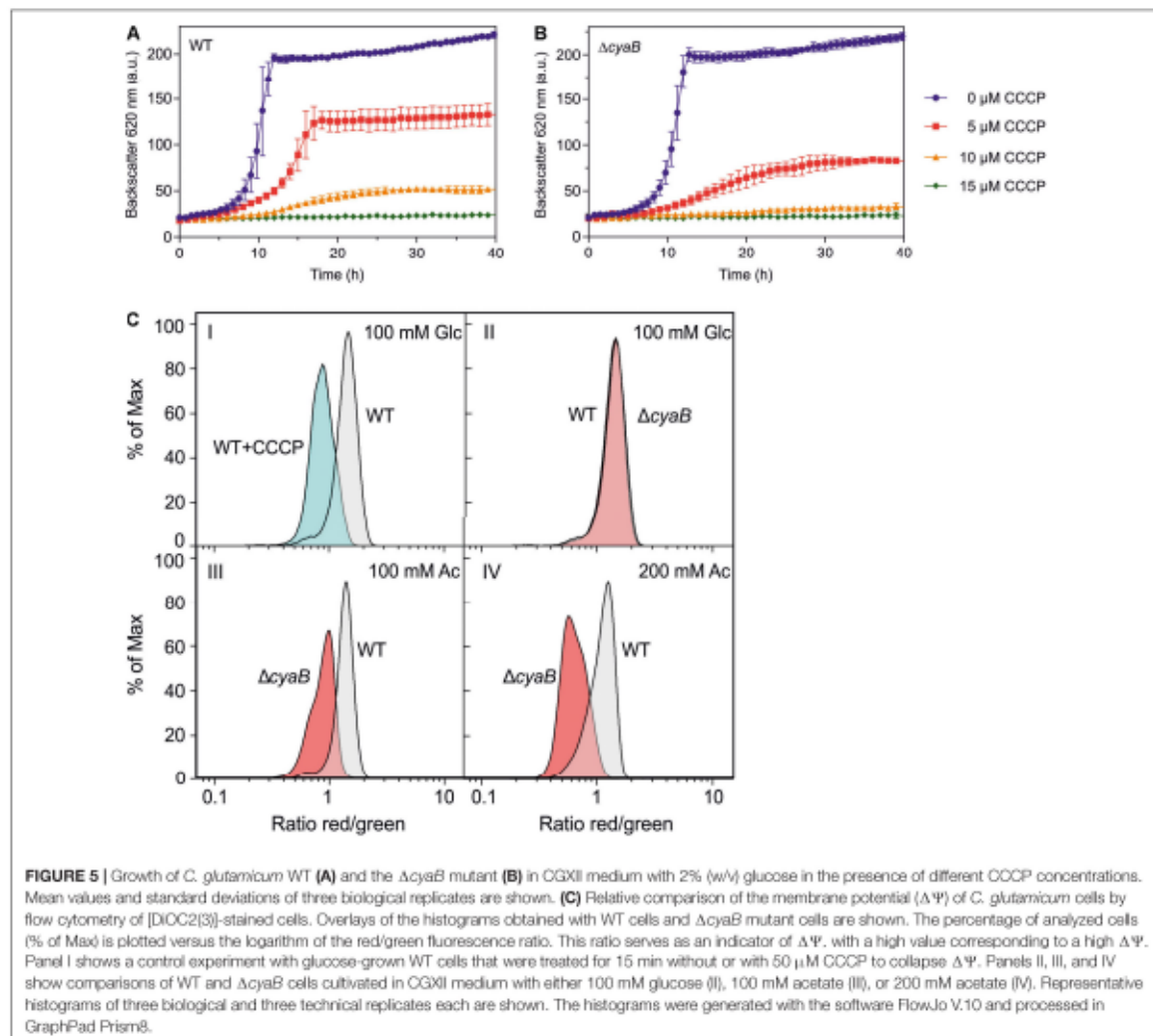
pmf of *C. glutamicum* WT is about 200 mV and formed almost exclusively by the membrane potential of 180 mV (Follmann et al., 2009; Koch-Koerfiges et al., 2012). We compared $\Delta\psi$ of the WT and the Δ cyaB mutant using the dye 3,3'-diethyloxycarbocyanine iodide [DiOC₂(3)], which exhibits green fluorescence in all stained bacteria and shifts toward red emission due to self-association of dye molecules in dependency of $\Delta\psi$. Higher $\Delta\psi$ correlates with increased red fluorescence and the ratio of red/green fluorescence gives a relative measure of the membrane potential (Novo et al., 1999, 2000). This method does not give absolute values for the membrane potential but is useful for relative comparison of the membrane potential of different strains.

Using a previously established protocol (Neumeyer et al., 2013) we first confirmed that treatment of wild-type cells grown in CGXII glucose medium with $50 \mu\text{M}$ CCCP led to the expected decrease of the red/green fluorescence ratio indicating a collapsed or strongly reduced $\Delta\psi$ (Figure 5C, panel I). When cells of the WT and the Δ cyaB mutant cultivated in glucose medium to the exponential growth phase were analyzed, no significant differences of the red/green ratio was observed, indicating that both strains had a comparably high $\Delta\psi$ (Figure 5C, panel

II). The histograms differed, however, when the strains were cultivated in CGXII medium with 100 mM acetate as carbon source. In this case, the mean fluorescence ratio of wild-type cells was almost unaltered, whereas that of the Δ cyaB mutant was strongly decreased (Figure 5C, panel III). This shift of the red/green ratio indicates that the membrane potential of the Δ cyaB mutant is reduced compared to the membrane potential of the WT. For wild-type cells cultivated with 200 mM acetate, the mean fluorescence ratio was reduced compared to cells grown with glucose or 100 mM acetate, in line with the concentration-dependent uncoupling effect of acetate, but the ratio of the Δ cyaB mutant was much stronger affected (Figure 5C, panel IV). These results indicate that acetate affects $\Delta\psi$ of the Δ cyaB mutant much more strongly than $\Delta\psi$ of the WT.

Role of the Cytochrome *bc*₁-aa₃ Supercomplex for Acetate Sensitivity

The results described above suggest that the cAMP deficiency of the Δ cyaB mutant causes a reduced ability to maintain a high membrane potential in the presence of the uncoupler



acetate. In *C. glutamicum* cultivated under oxic conditions, pmf is generated by the cytochrome bc_1-aa_3 supercomplex ($6 H^+/2 e^-$) and by cytochrome bd oxidase ($2 H^+/2 e^-$) (Bott and Niebisch, 2003; Niebisch and Bott, 2003; Kabashima et al., 2009). We previously showed that $\Delta\psi$ is reduced in a Δqcr mutant lacking a functional supercomplex, whereas it is comparable to the WT in a $\Delta cydAB$ mutant lacking cytochrome bd oxidase (Koch-Koerfges et al., 2013). Therefore, a link between the cAMP level and the activity of the respiratory supercomplex might exist.

The transcriptional regulator GlxR is the only protein currently known in *C. glutamicum* whose activity is controlled by the cAMP level. In the presence of cAMP, purified GlxR was shown to bind to double-stranded 40-mer oligonucleotides covering predicted GlxR-binding sites in the promoter regions

of the *ctaCF* operon, the *ctaE-qcrCAB* operon, and the *ctaD* gene, which encode the subunits of the cytochrome bc_1-aa_3 supercomplex (Kohl et al., 2008). In glucose-grown cells of strain R, chromatin affinity chromatography followed by DNA chip analysis of the enriched DNA fragments (ChIP-chip) confirmed that Strep-tagged GlxR binds *in vivo* to these proposed binding sites (Toyoda et al., 2011). Mutation of the GlxR-binding sites in the *ctaC* and *ctaD* promoter regions of genomically integrated single-copy transcriptional fusions reduced expression of the reporter gene *lacZ* in yeast extract-containing medium with either glucose or acetate by about 15 – 40% (Toyoda et al., 2011). These results indicated that GlxR acts as a transcriptional activator of the genes encoding the cytochrome bc_1-aa_3 supercomplex. The reduced cAMP level in the $\Delta cyaB$ mutant might thus

cause a reduced expression of the genes for the *bc₁-aa₃* supercomplex leading to a reduced capacity to build up membrane potential and to counteract the uncoupling activity of acetate. A transcriptome comparison of the Δ *cyaB* mutant with the WT revealed reduced expression of all genes encoding the supercomplex (Supplementary Table S2). Additionally, we also performed qRT-PCR of *ctaC*, *ctaD*, and *qcrC* and the resulting data also showed decreased expression of these genes in the Δ *cyaB* mutant (Supplementary Table S2).

To test for differences of cytochrome *aa₃* oxidase activity in the Δ *cyaB* mutant and the WT, the TMPD oxidase activity of membrane fractions of the two strains grown in CGXII medium with glucose-acetate was determined. TMPD is supposed to donate electrons to cytochrome *c₁*. The TMPD oxidase activity of the Δ *cyaB* mutant was 35% reduced (280 ± 11 nmol TMPD oxidized min^{-1} (mg membrane protein) $^{-1}$) compared to the WT (433 ± 22 nmol TMPD oxidized min^{-1} (mg membrane protein) $^{-1}$), supporting the assumption that a reduced activity of the *bc₁-aa₃* supercomplex contributes to the uncoupler sensitivity of the mutant during growth on acetate.

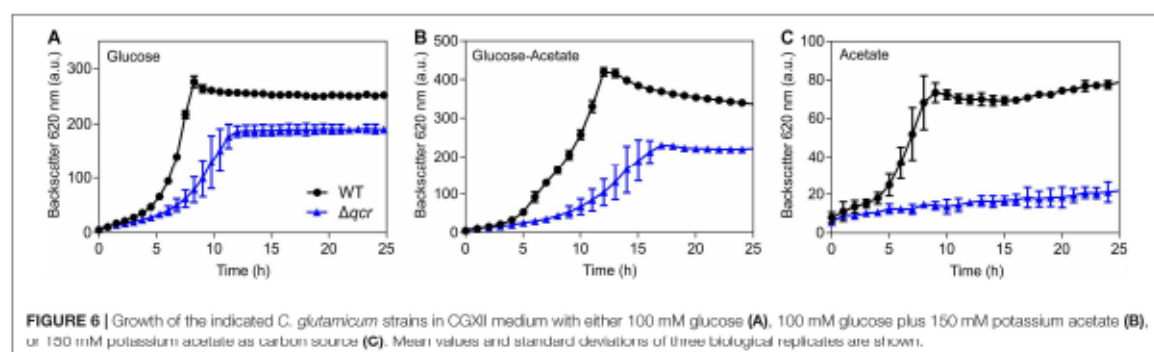
To further support the relevance of the cytochrome *bc₁-aa₃* supercomplex for the acetate sensitivity of the Δ *cyaB* mutant, growth of the WT and the Δ *qcr* mutant was compared in CGXII medium with glucose, glucose plus acetate, or acetate (Figure 6). Already in glucose medium the Δ *qcr* mutant showed a growth defect, as known from previous studies (Niebis and Bott, 2001). In medium with glucose and acetate, the growth defect of the Δ *qcr* mutant became more severe, whereas in minimal medium with acetate as sole carbon source the Δ *qcr* mutant showed no growth. These results support the assumption that the cytochrome *bc₁-aa₃* branch of the respiratory chain is crucial for growth on acetate.

Growth on acetate does not allow net ATP synthesis by substrate level phosphorylation and is strictly dependent on oxidative phosphorylation by F_1F_0 -ATP synthase (Koch-Koerfges et al., 2012). Interestingly, also the expression of the *atpBEFHAGDC* operon (cg1362-cg1369) encoding the eight subunits of F_1F_0 -ATP synthase was shown to be activated by GlxR (Toyoda et al., 2011) and therefore might be lowered in the Δ *cyaB* mutant. The transcriptome comparison supported this assumption with about two-fold lowered mRNA levels of the *atp*

genes in the Δ *cyaB* mutant. Consequently, the growth defect of the mutant on acetate is most likely additionally caused by a reduced ATP synthesis via oxidative phosphorylation, caused by reduced synthesis of the *bc₁-aa₃* supercomplex and F_1F_0 -ATP synthase.

Isolation of Suppressor Mutants of the Δ *cyaB* Strain With Improved Growth on Acetate

To get further insights into the molecular basis of the acetate sensitivity of the Δ *cyaB* mutant, we isolated Δ *cyaB* suppressor mutants that show improved growth on acetate. As shown in Supplementary Figure S4A, three independent cultures started to grow after about 80 h of incubation in acetate minimal medium. After plating on BHI agar plates, single colonies were picked from each of the three cultures and tested again for growth on acetate. As shown in Supplementary Figure S4B, two of the suppressor mutants, named Δ *cyaB*_sup1 and Δ *cyaB*_sup3, grew almost like the WT, whereas the third one, Δ *cyaB*_sup2, showed slower growth than the other two mutants. Genomic DNA of the three suppressor mutants was isolated and sequenced with average coverages of 82, 81, and 106 for Δ *cyaB*_sup1, Δ *cyaB*_sup2, and Δ *cyaB*_sup3, respectively. For strain Δ *cyaB*_sup1, a single point mutation was identified compared to the parent Δ *cyaB* mutant at position 307072 (numbering according to BA000036.3), which is located in the *glxR* gene and leads to an Ala131Thr exchange. The frequency of the mutation in the Δ *cyaB*_sup1 mutant was 100%. Interestingly, the same mutation was also identified in strain Δ *cyaB*_sup3, which additionally carried a second point mutation at position 2564086 (frequency 97.0%) leading to a silent mutation in codon 106 (Gly) of the ribose 5-phosphate isomerase gene *rpi* (cg2658). The suppressor mutant Δ *cyaB*_sup2 did not carry a mutation in *glxR*, but two point mutations in intergenic regions, one between promoters P1 and P2 of *gltA* (cg0949; citrate synthase) (van Ooyen et al., 2011) at position 877553 (A to G, frequency 100%) and the other one 39 bp upstream of the start codon of cg1660, encoding a putative manganese efflux pump (position 1548741, G to C, frequency 100%). The position of the point mutation in the *gltA* promoter does not overlap with known regulator binding sites for RamA and GlxR (van Ooyen et al., 2011)



and therefore the effect of this mutation cannot be predicted. Similarly, the effect of the second mutation upstream of cg1660 cannot be deduced as neither the promoter nor the regulation of this gene is known.

The finding that two of the three independently obtained suppressor mutants carried the same mutation (A131T) in GlxR supports the crucial role of this regulator for the acetate sensitivity of the Δ cyaB mutant. To confirm that this mutation can rescue the acetate sensitivity of the Δ cyaB strain, it was introduced by site-directed mutagenesis into the genome of the Δ cyaB mutant and for comparison into the WT. The resulting strains Δ cyaB::glxR_A131T and WT::glxR_A131T showed comparable growth in minimal medium with glucose compared to the parental strains Δ cyaB and the WT (Supplementary Figure S4C). Importantly, the Δ cyaB::glxR_A131T strain showed wild-type like growth in acetate minimal medium, confirming the phenotype of strain Δ cyaB_sup1 (Supplementary Figure S4D).

The alanine residue at position 131 of GlxR is highly conserved in homologs from other *Corynebacterium* species and *Mycobacterium tuberculosis* as well as in CRP of *E. coli* (Supplementary Figure S4E). Ala131 is located in the central α -helix of GlxR, which forms the dimer interface, and is positioned close to important cAMP-binding residues (Townsend et al., 2014) (Supplementary Figures S4E,G). Overlays of the crystal structures of apo- and holo-GlxR and of models with the Ala131T exchange are shown in Supplementary Figures S4F,G. The mutation apparently does not lead to large structural changes, making it difficult to predict the functional consequences of the amino acid exchange. Due to the vicinity of residue 131 to the cAMP-binding site, the A131T exchange might have altered the influence of cAMP on DNA-binding. We therefore tested whether purified GlxR-A131T still requires cAMP for binding to DNA targets in electrophoretic mobility shift assays. As shown in Supplementary Figure S5, binding of GlxR-A131T to DNA fragments covering the GlxR-binding sites in front of *ctaD* and *ctaC* was still dependent on cAMP. However, the *in vivo* situation is probably different. ChIP-Chip experiments with a *cyaB*-deletion strain of *C. glutamicum* R clearly showed GlxR-binding to target sites despite the lack of CyaB, although with decreased affinity (Toyoda et al., 2011).

The most intensively studied homolog of GlxR is CRP of *E. coli*. Many studies were performed in which *E. coli* Δ cya strains were used to select for mutants that regained the ability to grow on carbon sources such as lactose, maltose, or xylose requiring activation of gene expression by CRP. These studies have recently been summarized (Frendorf et al., 2019) and led the authors to conclude that adaptive mutations occur predominantly in the cAMP binding site, the D- α -helix, and in the RNA polymerase activating domains AR1 and AR2, which likely affect ligand binding, ligand-induced allosteric transitions, or the productive interaction with the core RNA polymerase, respectively. In these studies, no mutation was found in CRP residue A121, which corresponds to A131 of GlxR. However, it has to be considered that although the 3-dimensional fold of GlxR and CRP is very similar, the structural changes observed for GlxR upon cAMP binding are quite distinct from those observed for CRP (Townsend et al., 2014). It was concluded that

the mechanisms of allosteric binding and activation of DNA-binding differ considerably in the CRP/FNR family without dramatic structural changes and that the same 3-dimensional fold is finetuned using small structural changes coupled with changes in dynamic behavior to achieve the optimal combination of allostery and DNA recognition (Townsend et al., 2014). This situation makes a prediction of the effects of the A131T mutation in GlxR based on studies of *E. coli* CRP virtually impossible.

CONCLUSION

The aim of this study was to elucidate the consequences of a reduced cAMP level in *C. glutamicum* caused by the lack of the adenylate cyclase CyaB and in particular the inhibitory effect of acetate on growth of the Δ cyaB mutant. Our results strongly suggest that this effect is mainly caused by the uncoupling activity of acetate, as it is concentration- and pH-dependent and occurs also in the presence of an additional carbon source such as glucose, fructose, sucrose, or gluconate. Evidence was obtained that the Δ cyaB mutant has a lower $\Delta\psi$ on acetate than the WT, suggesting a reduced capability to build up pmf. As the growth defect of the Δ cyaB mutant could be rescued by supplementation of the medium with cAMP, a link between the major second messenger cAMP and the ability to pmf generation was proposed. The major contributor to pmf in *C. glutamicum* is the cytochrome *bc₁-aa₃* supercomplex and there is evidence from previous studies that expression of the genes encoding the supercomplex is activated by the cAMP-dependent transcriptional regulator GlxR. We observed reduced expression of the supercomplex genes and a reduced TMPD oxidase activity in the Δ cyaB mutant, supporting the idea that a decreased supercomplex activity contributes to the acetate sensitivity of the Δ cyaB mutant. Also the F_1F_0 -ATP synthase genes are known to be transcriptionally activated by GlxR and showed reduced expression in the Δ cyaB mutant, additionally contributing to the energetic deficiencies of the strain. We could rescue the growth defect of the Δ cyaB mutant on acetate by a single point mutation (A131T) in GlxR, confirming the key role of GlxR for the phenotype of the Δ cyaB mutant. Additional studies are required to elucidate the functional consequences of this amino acid exchange *in vivo*. In summary, our results disclosed that cAMP in concert with GlxR plays a key role in the control of energy metabolism in *C. glutamicum*.

DATA AVAILABILITY STATEMENT

This manuscript contains previously unpublished data. The DNA microarray data are available in the GEO database with accession number GSE140408. The genome sequencing data (bam files) are available in the ENA database via accession number PRJEB36438.

AUTHOR CONTRIBUTIONS

NW and MBu constructed mutants and plasmids and performed all experimental work except the one specified below for

other authors. AK-K performed the analysis of glucose and organic acids. NK and JS performed the growth experiments with the protonophore CCCP and the determination of the membrane potential. TP supervised the genome resequencing and analyzed the resulting data. JH and JV performed the LC-MS/MS measurements for cAMP determination. MBa coached the experimental work and supported the design of the study. All authors contributed to the interpretation of the data. NW wrote the first draft of the manuscript and prepared the figures and tables. MBo designed the study, supervised the experimental work, and wrote the final version of the manuscript.

REFERENCES

- Ammerman, J. W., and Azam, F. (1982). Uptake of cyclic AMP by natural populations of marine bacteria. *Appl. Environ. Microbiol.* 43, 869–876. doi: 10.1128/aem.43.4.869-876.1982
- Arndt, A., Auchter, M., Ishige, T., Wendisch, V. F., and Eikmanns, B. J. (2008). Ethanol catabolism in *Corynebacterium glutamicum*. *J. Mol. Microbiol. Biotechnol.* 15, 222–233. doi: 10.1159/000107370
- Arndt, A., and Eikmanns, B. J. (2007). The alcohol dehydrogenase gene *adhA* in *Corynebacterium glutamicum* is subject to carbon catabolite repression. *J. Bacteriol.* 189, 7408–7416. doi: 10.1128/JB.00791-07
- Axe, D. D., and Bailey, J. E. (1995). Transport of lactate and acetate through the energized cytoplasmic membrane of *Escherichia coli*. *Biotechnol. Bioeng.* 47, 8–19. doi: 10.1002/bit.260470103
- Becker, J., and Wittmann, C. (2012). Bio-based production of chemicals, materials and fuels - *Corynebacterium glutamicum* as versatile cell factory. *Curr. Opin. Biotechnol.* 23, 631–640. doi: 10.1016/j.copbio.2011.11.012
- Binder, S., Schendzielorz, G., Stäbler, N., Krumbach, K., Hoffmann, K., Bott, M., et al. (2012). A high-throughput approach to identify genomic variants of bacterial metabolite producers at the single-cell level. *Genome Biol.* 13:R40. doi: 10.1186/Gb-2012-13-5-R40
- Bott, M. (2007). Offering surprises: TCA cycle regulation in *Corynebacterium glutamicum*. *Trends Microbiol.* 15, 417–425. doi: 10.1016/j.tim.2007.08.004
- Bott, M., and Niebisch, A. (2003). The respiratory chain of *Corynebacterium glutamicum*. *J. Biotechnol.* 104, 129–153. doi: 10.1016/s0168-1656(03)00144-5
- Brazma, A., Hingamp, P., Quackenbush, J., Sherlock, G., Spellman, P., Stoeckert, C., et al. (2001). Minimum information about a microarray experiment (MIAME)-toward standards for microarray data. *Nat. Genet.* 29, 365–371. doi: 10.1038/ng1201-365
- Burkovski, A. (ed.) (2008). *Corynebacteria: Genomics and Molecular Biology*. Norfolk: Caister Academic Press.
- Bussmann, M., Emer, D., Hasenbein, S., Degraf, S., Eikmanns, B. J., and Bott, M. (2009). Transcriptional control of the succinate dehydrogenase operon *sdhCAB* of *Corynebacterium glutamicum* by the cAMP-dependent regulator GlxR and the LuxR-type regulator RamA. *J. Biotechnol.* 143, 173–182. doi: 10.1016/j.jbiotec.2009.06.025
- Cha, P. H., Park, S. Y., Moon, M. W., Subhadra, B., Oh, T. K., Kim, E., et al. (2010). Characterization of an adenylate cyclase gene (*cydB*) deletion mutant of *Corynebacterium glutamicum* ATCC 13032. *Appl. Microbiol. Biotechnol.* 85, 1061–1068. doi: 10.1007/s00253-009-2066-9
- da Luz, J. A., Hans, E., Frank, D., and Zeng, A.-P. (2016). Analysis of intracellular metabolites of *Corynebacterium glutamicum* at high cell density with automated sampling and filtration and assessment of engineered enzymes for effective L-lysine production. *Eng. Life Sci.* 17, 512–522. doi: 10.1002/elsc.2016.00163
- Eggeling, L., and Bott, M. (eds) (2005). *Handbook of Corynebacterium glutamicum*. Boca Raton, FL: CRC Press.
- Eggeling, L., and Bott, M. (2015). A giant market and a powerful metabolism: L-lysine provided by *Corynebacterium glutamicum*. *Appl. Microbiol. Biotechnol.* 99, 3387–3394. doi: 10.1007/s00253-015-6508-2
- Eggeling, L., Bott, M., and Marienhagen, J. (2015). Novel screening methods-biosensors. *Curr. Opin. Biotechnol.* 35, 30–36. doi: 10.1016/j.copbio.2014.12.021
- Follmann, M., Ochrombel, I., Krämer, R., Trötschel, C., Poetsch, A., Rückert, C., et al. (2009). Functional genomics of pH homeostasis in *Corynebacterium glutamicum* revealed novel links between pH response, oxidative stress, iron homeostasis and methionine synthesis. *BMC Genomics* 10:621. doi: 10.1186/1471-2164-10-621
- Frendorf, P. O., Lauritsen, I., Sekowska, A., Danchin, A., and Norholm, M. H. H. (2019). Mutations in the global transcription factor CRP/CAP: insights from experimental evolution and deep sequencing. *Comput. Struct. Biotechnol. J.* 17, 730–736. doi: 10.1016/j.csbj.2019.05.009
- Freudl, R. (2017). Beyond amino acids: use of the *Corynebacterium glutamicum* cell factory for the secretion of heterologous proteins. *J. Biotechnol.* 258, 101–109. doi: 10.1016/j.jbiotec.2017.02.023
- Frunzke, J., Engels, V., Hasenbein, S., Gägens, C., and Bott, M. (2008). Co-ordinated regulation of gluconate catabolism and glucose uptake in *Corynebacterium glutamicum* by two functionally equivalent transcriptional regulators, GntR1 and GntR2. *Mol. Microbiol.* 67, 305–322. doi: 10.1111/j.1365-2958.2007.06020.x
- Gerstmeir, R., Wendisch, V. F., Schnicke, S., Ruan, H., Farwick, M., Reinscheid, D., et al. (2003). Acetate metabolism and its regulation in *Corynebacterium glutamicum*. *J. Biotechnol.* 104, 99–122. doi: 10.1016/s0168-1656(03)00167-6
- Goldenbaum, P. E., and Hall, G. A. (1979). Transport of cyclic adenosine 3',5'-monophosphate across *Escherichia coli* vesicle membranes. *J. Bacteriol.* 140, 459–467. doi: 10.1128/jb.140.2.459-467.1979
- Hardt, J., Klefer, P., Meyer, F., and Vorholt, J. A. (2017). Longevity of major coenzymes allows minimal *de novo* synthesis in microorganisms. *Nat. Microbiol.* 2:17073. doi: 10.1038/nmicrobiol.2017.73
- Heytler, P. G., and Prichard, W. W. (1962). A new class of uncoupling agents - carbonyl cyanide phenylhydrazones. *Biochem. Biophys. Res. Commun.* 7, 272–275. doi: 10.1016/0006-291x(62)90189-4
- ICH. (2005). "Harmonised Tripartite Guideline, validation of analytical procedures: text and methodology Q2 (R1)", in *International Conference on Harmonisation of Technical Requirements for Registration of Pharmaceuticals for Human Use*, (Geneva).
- Ikedo, M., and Nakagawa, S. (2003). The *Corynebacterium glutamicum* genome: features and impacts on biotechnological processes. *Appl. Microbiol. Biotechnol.* 62, 99–109. doi: 10.1007/s00253-003-1328-1
- Jolkver, E., Emer, D., Ballan, S., Krämer, R., Eikmanns, B. J., and Marin, K. (2009). Identification and characterization of a bacterial transport system for the uptake of pyruvate, propionate, and acetate in *Corynebacterium glutamicum*. *J. Bacteriol.* 191, 940–948. doi: 10.1128/JB.01155-08
- Jungwirth, B., Sala, C., Kohl, T. A., Uplekar, S., Baumbach, J., Cole, S. T., et al. (2013). High-resolution detection of DNA binding sites of the global transcriptional regulator GlxR in *Corynebacterium glutamicum*. *Microbiology* 159, 12–22. doi: 10.1099/mic.0.062059-0
- Kabashima, Y., Kishikawa, J., Kurokawa, T., and Sakamoto, I. (2009). Correlation between proton translocation and growth: genetic analysis of the respiratory chain of *Corynebacterium glutamicum*. *J. Biochem.* 146, 845–855. doi: 10.1093/jb/mvp140
- Kabus, A., Niebisch, A., and Bott, M. (2007). Role of cytochrome *bd* oxidase from *Corynebacterium glutamicum* in growth and lysine production. *Appl. Environ. Microbiol.* 73, 861–868. doi: 10.1128/aem.01818-06
- Kalinowski, J., Bathe, B., Bartels, D., Bischoff, N., Bott, M., Burkovski, A., et al. (2003). The complete *Corynebacterium glutamicum* ATCC 13032 genome

- sequence and its impact on the production of L-aspartate-derived amino acids and vitamins. *J. Biotechnol.* 104, 5–25. doi: 10.1016/s0168-1656(03)00154-8
- Kensy, F., Zang, E., Faulhammer, C., Tan, R. K., and Büchs, J. (2009). Validation of a high-throughput fermentation system based on online monitoring of biomass and fluorescence in continuously shaken microtiter plates. *Microb. Cell Fact.* 8:31. doi: 10.1186/1475-2859-8-31
- Kim, H. J., Kim, T. H., Kim, Y., and Lee, H. S. (2004). Identification and characterization of *glxR*, a gene involved in regulation of glyoxylate bypass in *Corynebacterium glutamicum*. *J. Bacteriol.* 186, 3453–3460. doi: 10.1128/jb.186.11.3453-3460.2004
- Kinoshita, S., Uda, S., and Shimono, M. (1957). Studies on amino acid fermentation. Part I. Production of L-glutamic acid by various microorganisms. *J. Gen. Appl. Microbiol.* 3, 193–205.
- Koch-Koerfiges, A., Kabus, A., Ochrombel, I., Marin, K., and Bott, M. (2012). Physiology and global gene expression of a *Corynebacterium glutamicum* ΔF_1F_0 -ATP synthase mutant devoid of oxidative phosphorylation. *Biochim. Biophys. Acta* 1817, 370–380. doi: 10.1016/j.bbabi.2011.10.006
- Koch-Koerfiges, A., Pletzner, N., Platzner, L., Oldiges, M., and Bott, M. (2013). Conversion of *Corynebacterium glutamicum* from an aerobic respiring to an aerobic fermenting bacterium by inactivation of the respiratory chain. *Biochim. Biophys. Acta* 1827, 699–708. doi: 10.1016/j.bbabi.2013.02.004
- Kohl, T. A., Baumbach, J., Jungwirth, B., Pühler, A., and Tauch, A. (2008). The GlxR regulon of the amino acid producer *Corynebacterium glutamicum*: *In silico* and *in vitro* detection of DNA binding sites of a global transcription regulator. *J. Biotechnol.* 135, 340–350. doi: 10.1016/j.jbiotec.2008.05.011
- Linder, J. U., Hammer, A., and Schultz, J. E. (2004). The effect of HAMP domains on class IIIb adenylyl cyclases from *Mycobacterium tuberculosis*. *Eur. J. Biochem.* 271, 2446–2451. doi: 10.1111/j.1432-1033.2004.04172.x
- Möker, N., Brocker, M., Schaffer, S., Krämer, R., Morbach, S., and Bott, M. (2004). Deletion of the genes encoding the MtrA-MtrB two-component system of *Corynebacterium glutamicum* has a strong influence on cell morphology, antibiotics susceptibility and expression of genes involved in osmoprotection. *Mol. Microbiol.* 54, 420–438. doi: 10.1111/j.1365-2958.2004.04249.x
- Müller, J. E., Meyer, F., Litsanov, B., Kiefer, P., and Vorholt, J. A. (2015). Core pathways operating during methylotrophy of *Bacillus methanolicus* MGA3 and induction of a bacillitriol-dependent detoxification pathway upon formaldehyde stress. *Mol. Microbiol.* 98, 1089–1100. doi: 10.1111/mmi.13200
- Mustafi, N., Grünberger, A., Kohlheyer, D., Bott, M., and Frunzke, J. (2012). The development and application of a single-cell biosensor for the detection of L-methionine and branched-chain amino acids. *Metab. Eng.* 14, 449–457. doi: 10.1016/j.ymben.2012.02.002
- Neumeyer, A., Höbschmann, T., Müller, S., and Frunzke, J. (2013). Monitoring of population dynamics of *Corynebacterium glutamicum* by multiparameter flow cytometry. *Microb. Biotechnol.* 6, 157–167. doi: 10.1111/1751-7915.12018
- Nicholls, D. G., and Ferguson, S. J. (2002). *Bioenergetics 3*. London: Academic Press.
- Niebsch, A., and Bott, M. (2001). Molecular analysis of the cytochrome *bc₁-aa₃* branch of the *Corynebacterium glutamicum* respiratory chain containing an unusual diheme cytochrome *c₁*. *Arch. Microbiol.* 175, 282–294. doi: 10.1007/s002030100262
- Niebsch, A., and Bott, M. (2003). Purification of a cytochrome *bc₁-aa₃* supercomplex with quinol oxidase activity from *Corynebacterium glutamicum* - Identification of a fourth subunit of cytochrome *aa₃* oxidase and mutational analysis of diheme cytochrome *c₁*. *J. Biol. Chem.* 278, 4339–4346. doi: 10.1074/jbc.m210499200
- Novo, D., Perlmutter, N. G., Hunt, R. H., and Shapiro, H. M. (1999). Accurate flow cytometric membrane potential measurement in bacteria using diethyloxycarbonyl cyanine and a ratiometric technique. *Cytometry* 35, 55–63. doi: 10.1002/(sici)1097-0320(19990101)35:1<55::aid-cyto8>3.0.co;2-2
- Novo, D. J., Perlmutter, N. G., Hunt, R. H., and Shapiro, H. M. (2000). Multiparameter flow cytometric analysis of antibiotic effects on membrane potential, membrane permeability, and bacterial counts of *Staphylococcus aureus* and *Micrococcus luteus*. *Antimicrob. Agents Chemother.* 44, 827–834. doi: 10.1128/aac.44.4.827-834.2000
- Pfeifer-Sancar, K., Mentz, A., Rückert, C., and Kalinowski, J. (2013). Comprehensive analysis of the *Corynebacterium glutamicum* transcriptome using an improved RNAseq technique. *BMC Genomics* 14:888. doi: 10.1186/1471-2164-14-888
- Pinhal, S., Ropers, D., Geiselmann, J., and de Jong, H. (2019). Acetate metabolism and the inhibition of bacterial growth by acetate. *J. Bacteriol.* 201:e00147-19. doi: 10.1128/JB.00147-19
- Polen, T., and Wendisch, V. F. (2004). Genomewide expression analysis in amino acid-producing bacteria using DNA microarrays. *Appl. Biochem. Biotechnol.* 118, 215–232. doi: 10.1385/abab:118:1-3:215
- Richter, W. (2002). 3',5'-Cyclic nucleotide phosphodiesterases class III: members, structure, and catalytic mechanism. *Proteins* 46, 278–286. doi: 10.1002/prot.10049
- Saier, M. H. Jr., Feucht, B. U., and McCaman, M. T. (1975). Regulation of intracellular adenosine cyclic 3',5'-monophosphate levels in *Escherichia coli* and *Salmonella typhimurium*. Evidence for energy-dependent excretion of the cyclic nucleotide. *J. Biol. Chem.* 250, 7593–7601.
- Sakamoto, J., Shibata, T., Mine, T., Miyahara, R., Torigoe, T., Noguchi, S., et al. (2001). Cytochrome *c* oxidase contains an extra charged amino acid cluster in a new type of respiratory chain in the amino-acid-producing Gram-positive bacterium *Corynebacterium glutamicum*. *Microbiology* 147, 2865–2871. doi: 10.1099/002221287-147-10-2865
- Sambrook, J., and Russell, D. (2001). *Molecular Cloning. A Laboratory Manual*. Cold Spring Harbor, NY: Cold Spring Harbor Laboratory Press.
- Schäfer, A., Tauch, A., Jäger, W., Kalinowski, J., Thierbach, G., and Pühler, A. (1994). Small mobilizable multipurpose cloning vectors derived from the *Escherichia coli* plasmids pK18 and pK19 - Selection of defined deletions in the chromosome of *Corynebacterium glutamicum*. *Gene* 145, 69–73. doi: 10.1016/0378-1119(94)90324-7
- Schwendler, G., Dippong, M., Grünberger, A., Kohlheyer, D., Yoshida, A., Binder, S., et al. (2014). Taking control over control: use of product sensing in single cells to remove flux control at key enzymes in biosynthesis pathways. *ACS Synth. Biol.* 3, 21–29. doi: 10.1021/sb400059y
- Schneider, J., and Wendisch, V. F. (2011). Biotechnological production of polyamines by bacteria: recent achievements and future perspectives. *Appl. Microbiol. Biotechnol.* 91, 17–30. doi: 10.1007/s00253-011-3252-0
- Schulte, J., Baumgart, M., and Bott, M. (2017a). Development of a single-cell GlxR-based cAMP biosensor for *Corynebacterium glutamicum*. *J. Biotechnol.* 258, 33–40. doi: 10.1016/j.jbiotec.2017.07.004
- Schulte, J., Baumgart, M., and Bott, M. (2017b). Identification of the cAMP phosphodiesterase CpdA as novel key player in cAMP-dependent regulation in *Corynebacterium glutamicum*. *Mol. Microbiol.* 103, 534–552. doi: 10.1111/mmi.13574
- Shenoy, A. R., Sivakumar, K., Krupa, A., Srinivasan, N., and Visweswariah, S. S. (2004). A survey of nucleotide cyclases in Actinobacteria: unique domain organization and expansion of the class III cyclase family in *Mycobacterium tuberculosis*. *Comp. Funct. Genomics* 5, 17–38. doi: 10.1002/cfg.349
- Studier, F. W. (2005). Protein production by auto-induction in high density shaking cultures. *Protein Expr. Purif.* 41, 207–234. doi: 10.1016/j.pep.2005.01.016
- Studier, F. W., and Moffatt, B. A. (1986). Use of bacteriophage T7 RNA polymerase to direct selective high-level expression of cloned genes. *J. Mol. Biol.* 189, 113–130. doi: 10.1016/0022-2836(86)90385-2
- Townsend, P. D., Jungwirth, B., Pojer, F., Bussmann, M., Money, V. A., Cole, S. T., et al. (2014). The crystal structures of apo and cAMP-bound GlxR from *Corynebacterium glutamicum* reveal structural and dynamic changes upon cAMP binding in CRP/FNR family transcription factors. *PLoS One* 9:e113265. doi: 10.1371/journal.pone.0113265
- Toyoda, K., Teramoto, H., Inui, M., and Yukawa, H. (2011). Genome-wide identification of *in vivo* binding sites of GlxR, a cyclic AMP receptor protein-type regulator in *Corynebacterium glutamicum*. *J. Bacteriol.* 193, 4123–4133. doi: 10.1128/JB.00304-11
- van Ooyen, J., Emer, D., Bussmann, M., Bott, M., Eikmanns, B. J., and Eggeling, L. (2011). Citrate synthase in *Corynebacterium glutamicum* is encoded by two *gltA* transcripts which are controlled by RamA, RamB, and GlxR. *J. Biotechnol.* 154, 140–148. doi: 10.1016/j.jbiotec.2010.07.004
- Wendisch, V. F., De Graaf, A. A., Sahn, H., and Eikmanns, B. J. (2000). Quantitative determination of metabolic fluxes during coutilization of two carbon sources: comparative analyses with *Corynebacterium glutamicum*

- during growth on acetate and/or glucose. *J. Bacteriol.* 182, 3088–3096. doi: 10.1128/jb.182.11.3088-3096.2000
- Wieschalka, S., Blombach, B., Bott, M., and Eikmanns, B. J. (2013). Bio-based production of organic acids with *Corynebacterium glutamicum*. *Microb. Biotechnol.* 6, 87–102. doi: 10.1111/1751-7915.12013
- Yukawa, H., and Inui, M. (eds) (2013). *Corynebacterium glutamicum: Biology and Biotechnology*. Heidelberg: Springer.
- Yukawa, H., Omumasaba, C. A., Nonaka, H., Kos, P., Okai, N., Suzuki, N., et al. (2007). Comparative analysis of the *Corynebacterium glutamicum* group and complete genome sequence of strain R. *Microbiology* 153, 1042–1058. doi: 10.1099/mic.0.2006/003657-0
- Conflict of Interest:** The authors declare that the research was conducted in the absence of any commercial or financial relationships that could be construed as a potential conflict of interest.
- Copyright © 2020 Wolf, Bussmann, Koch-Koerfjes, Katcharava, Schulte, Polen, Hartl, Vorholt, Baumgart and Bott. This is an open-access article distributed under the terms of the Creative Commons Attribution License (CC BY). The use, distribution or reproduction in other forums is permitted, provided the original author(s) and the copyright owner(s) are credited and that the original publication in this journal is cited, in accordance with accepted academic practice. No use, distribution or reproduction is permitted which does not comply with these terms.

2.2 Supplementary materials 'Molecular basis of growth inhibition by acetate of an adenylate cyclase-deficient mutant of *Corynebacterium glutamicum*'



Supplementary Material

1 Supplementary Tables

TABLE S1. Oligonucleotides used in this study

Oligonucleotide	Sequence (5' → 3') and properties ¹
Construction of deletion plasmid pK19mobsacB-cyaB and PCR analysis of the resulting mutants	
dcl0375_1_HindIII-fw	ATTAAAGCTTCGGGGTGGCTGCCCTCCCATG
dcl0375_2-rv	CGTTTAGGTTTAGTGGCTGGGCAACAGCATTACTGCGAGCGCACC
dcl0375_3-fw	CCCAGCCACTAAACCTCCCGCGGGCTATTCGGCCGACGTTG
dcl0375_4_XbaI-rv	ATTATCTAGACAATCACGCCCGGTACATCGC
cg0375_deltaest-fw	CAATTGCTGCGGGACGATGTG
cg0375_deltaest-rv	GATCACTGCCTAAAGGTGCG
PCR analysis of <i>C. glutamicum</i> ΔcyaBΔcpdA	
cg2761_deltaest-fw	GCACAGTGGGAACCATTAAC
cg2761_deltaest-rv	GTGGTCGTGATGTACTTCC
Construction of plasmid pAN6-cyaB and sequencing of the insert	
pAN6-cyaB-Pst-fw	AAAAC <u>TGCAGATAGACA</u> AATTGCTGCCGGG
pAN6-cyaB-NheI-rv	AAAAG <u>CTAGCGGACCTATCCGCCAAC</u> CTC
pAN6_seq_fw	TTACGCCAAGCTTGCATG
pAN6_seq_rv	GTAAAACGACGGCCAGTG
Construction of WT::<i>glxR</i>_A131T and ΔcyaB::<i>glxR</i>_A131T mutant and PCR analysis of the mutation	
cg0350_mut_A131T_fw	CCTGCAGGTCGACTCTAGAGTTCGTTACTCAGGGCTCAGGAAGCTTC
cg0350_mut_A131T_rv	GTAAAACGACGGCCAGTGAATTGTGGAAGGTGTACAGGAGATCCTGTG
cg0350_PCR_fw	TGACCCGCTTTACATCATCACCTC
cg0350_PCR_rv	CCTGGTCATACCCGTGATTCTGTGTG
cg0350_mut_control	TCGAGCGCGACGTGCCAAATGC
RT-qPCR analysis	
RT-ctaD-fw1	TGAACAGCTGGTTGAAGTGC
RT-ctaD-rv1	TCCTTCAGCTTCTTCTCCTCG
RT-ctaC-fw1	GCATTACCCCTGAAGCAGTG
RT-ctaC-rv1	ATGGCGGTGAGGAATAGACC
RT-gcrC-fw1	CTGCCACAACCTCACTGGTC
RT-gcrC-rv1	TAGGCATGTTCTGAGGACCG
RT_hpt_fw	ATGTTCCAGCCAACCCATAC
RT_hpt_rv	TCTTCGCCGTCTTTGAAGTGC
Construction of plasmids pAN6-<i>glxR</i>-Twinstrep and pAN6-<i>glxR</i>_A131T-Twinstrep	
GlxR-twin1	GCCTGCAGAAAGGAGATAACAGTGGAAAGGTGTACAGGAG
GlxR-twin2	TCGAGCGCGACGTGCCAAATGC
GlxR-twin3	GGCACGTCCGGCTCGATGGAGTCACTTCAATTTCG
GlxR-twin4	AAACGACGGCCAGTGAATTTATTTTCGAAGTCCGGGGTG
GlxR-A131T_fw	TCCTGCGGTTCTGACTCGTCTGCTGCGTCCG
GlxR-A131T_rv	GCGACGCAGACGACGAGTCAGAACGCCGACGGA
DNA fragments for EMSAs	
EMSA_ctaC_fw	GGTGGAAATATCTTCGTGGGTTTCG
EMSA_ctaC_rv	GTTGATGGTCTGTGACGTGG
EMSA_ctaD_fw	CTGTAICCCCTTTTCATGC
EMSA_ctaD_rv	CTTCTGGCGAAATGTCCG
EMSA_neg_fw	AGCTGCTGCGTTCAGGTGTC
EMSA_neg_rv	TAGTGGCGGTGGATCAGG

¹Restriction sites are underlined

Supplementary Material

TABLE S2. mRNA ratios ($\Delta cyaB$ /WT) of the genes encoding F₁F₀-ATP synthase and the cytochrome *bc*₁-*aa*₃ supercomplex.¹

Locus tag	Gene	Function	mRNA ratio $\Delta cyaB$ /WT	
			DNA microarrays ²	qRT-PCR ³
cg1362	<i>atpB</i>	ATP synthase subunit A	0.51	n.d. ⁴
cg1363	<i>atpE</i>	ATP synthase subunit C	0.51 ⁵	n.d.
cg1364	<i>atpF</i>	ATP synthase subunit B	0.53	n.d.
cg1365	<i>atpH</i>	ATP synthase subunit δ	0.55	n.d.
cg1366	<i>atpA</i>	ATP synthase subunit α	0.41	n.d.
cg1367	<i>atpG</i>	ATP synthase subunit γ	0.40	n.d.
cg1368	<i>atpD</i>	ATP synthase subunit β	0.43	n.d.
cg1369	<i>atpC</i>	ATP synthase subunit ϵ	0.83	n.d.
cg2406	<i>ctaE</i>	cytochrome <i>aa</i> ₃ oxidase subunit 3	0.67	n.d.
cg2409	<i>ctaC</i>	cytochrome <i>aa</i> ₃ oxidase subunit 2	0.63	0.20
cg2408	<i>ctaF</i>	cytochrome <i>aa</i> ₃ oxidase subunit 4	0.31	n.d.
cg2780	<i>ctaD</i>	cytochrome <i>aa</i> ₃ oxidase subunit 1	0.69	0.32
cg2405	<i>qcrC</i>	cytochrome <i>c</i> ₁	0.74	0.30
cg2404	<i>qcrA</i>	Rieske iron-sulfur protein	0.64	n.d.
cg2403	<i>qcrB</i>	cytochrome <i>b</i>	0.64	n.d.

¹Cells of the $\Delta cyaB$ mutant and the WT were grown in CGXII medium with glucose plus acetate (100 mM each).

²mRNA ratios represent mean values of at least two DNA microarray analyses starting from independent cultures.

³qRT-PCR results represent mean values of three biological replicates and two technical replicates each

⁴n.d., not determined

⁵except for cg1363, the p-values for all other genes were ≤ 0.05

2 Supplementary Figures

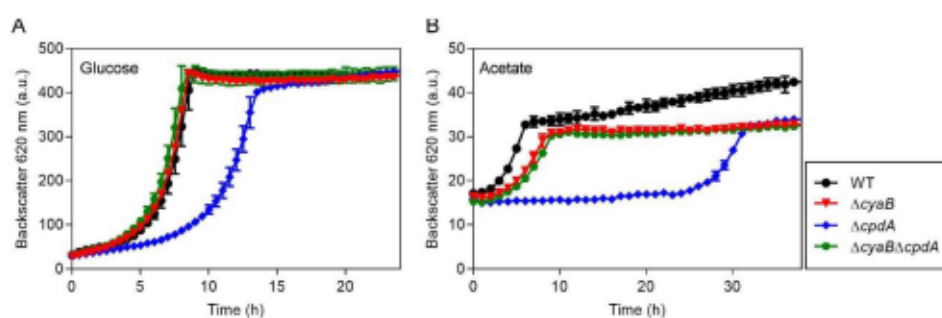


FIGURE S1. Growth of *C. glutamicum* WT and the mutant strains $\Delta cyaB$, $\Delta cpdA$, and $\Delta cyaB\Delta cpdA$ in CGXII medium with 2% (w/v) glucose (A) or 100 mM sodium acetate (B). Mean values and standard deviations of three biological replicates are shown.

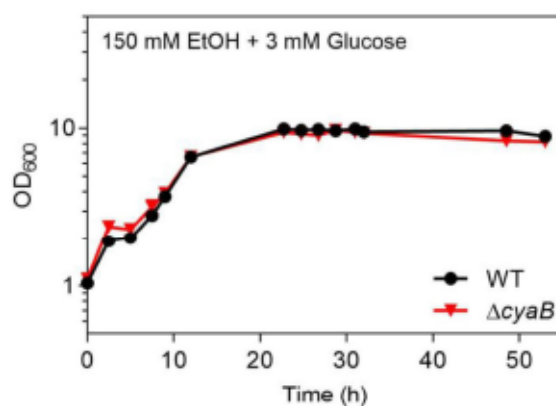


FIGURE S2. Growth of *C. glutamicum* WT and the $\Delta cyaB$ mutant in CGXII minimal medium with 150 mM ethanol and 3 mM glucose. Cultivation was performed in baffled shake flasks that were incubated at 30 °C and 120 rpm at 85% humidity. Mean values and standard deviations of three biological replicates are shown.

Supplementary Material

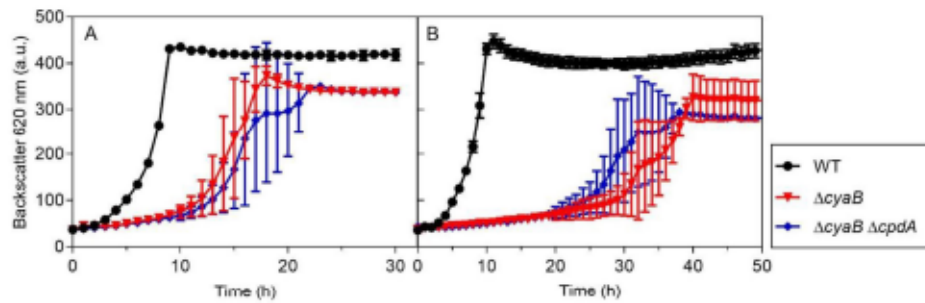
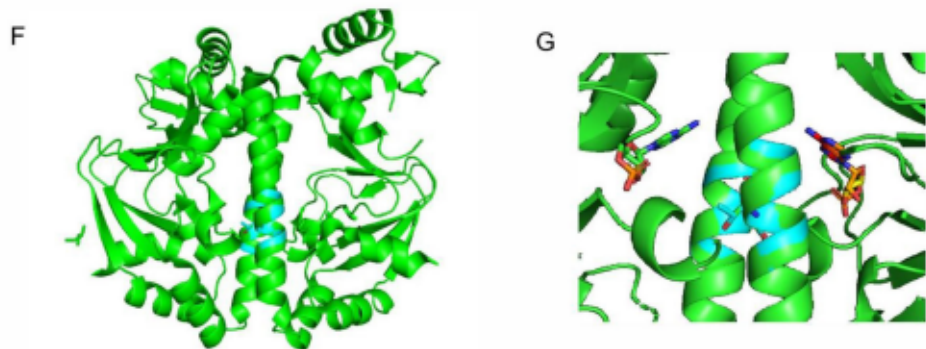
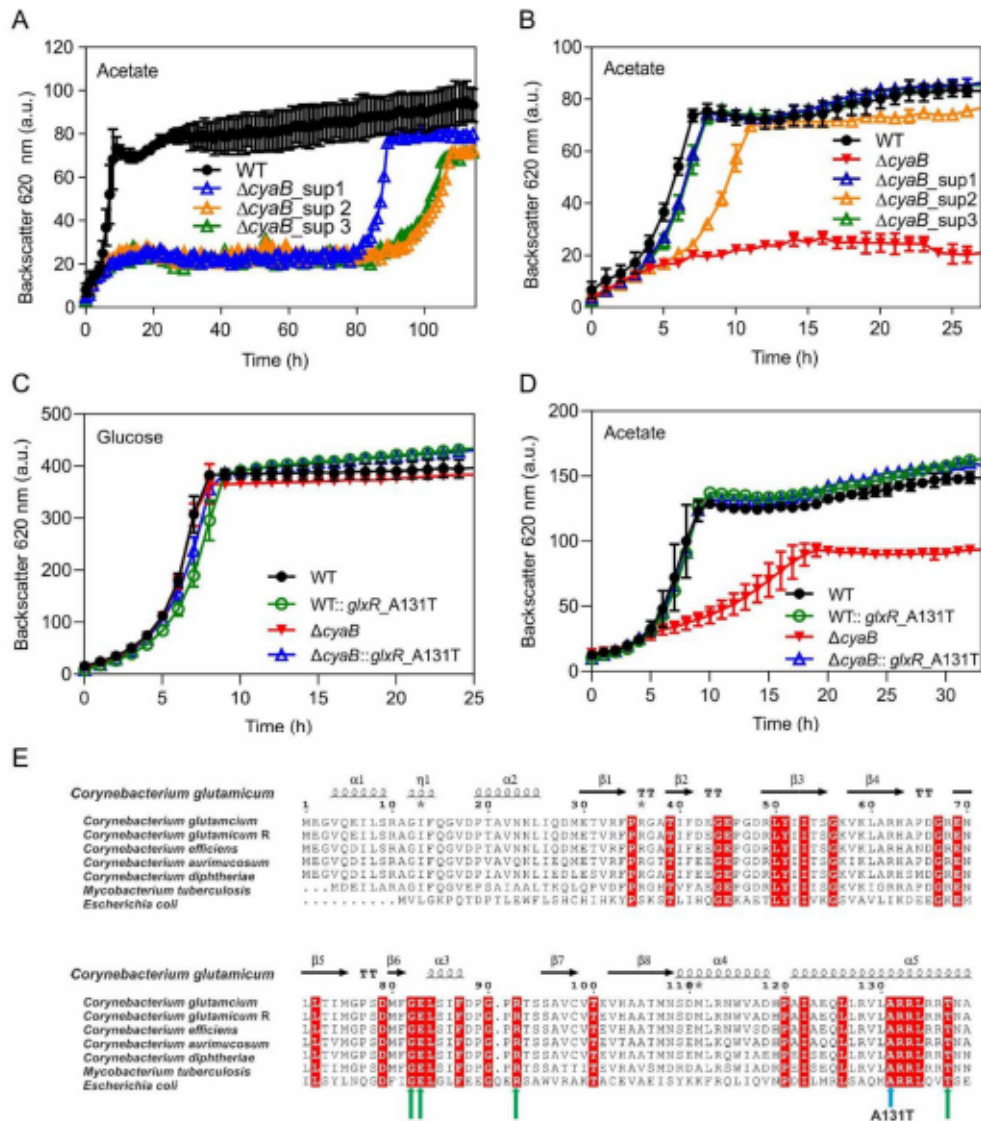


FIGURE S3. Growth of *C. glutamicum* WT and mutant strains $\Delta cyaB$ and $\Delta cyaB \Delta cpdA$ in CGXII medium with 100 mM glucose and 50 mM potassium acetate (A) or with 100 mM glucose and 100 mM potassium acetate (B). Mean values and standard deviations of three biological replicates are shown.



Supplementary Material

FIGURE S4. (A) Generation of suppressor mutants of *C. glutamicum* Δ *cyaB* with restored growth on acetate in a long-term cultivation in CGXII medium with 150 mM potassium acetate. **(B)** Growth of single colonies of the Δ *cyaB* suppressor mutant in CGXII medium with 150 mM acetate using *C. glutamicum* WT and the Δ *cyaB* mutant as controls. **(C, D)** Growth of indicated strains in CGXII medium with 100 mM glucose or 100 mM acetate. The *glxR*_A131T mutation identified in the Δ *cyaB* suppressor mutant was introduced by homologous recombination into the genomes of the WT and the Δ *cyaB* mutant. **(E)** Section of an amino acid sequence alignment of GlxR homologs from different bacterial strains. GlxR (Cg0350) of *C. glutamicum* WT and features derived from its crystal structure (PDB 4CYD) were used as reference. Red boxed amino acids are conserved in all selected sequences. Green arrows indicate residues important for cAMP binding in GlxR according to structural analysis (Townsend et al., 2014). The blue arrow shows the position of the A131T exchange in the Δ *cyaB*_sup1 mutant. The alignment was performed with Clustal W (<https://www.genome.jp/tools-bin/clustalw>) and processed with ESPript 3 (Robert and Gouet, 2014). The following sequences were used for the alignment: *C. glutamicum* strain R CgR0377; *Corynebacterium efficiens* YS-314 CE0287; *Corynebacterium aurimucosum* ATCC700975 Cauri0205; *Corynebacterium diphtheriae* NCTTC13129 CDIP0303; *Mycobacterium tuberculosis* H37Rv Rv3676; *Escherichia coli* MG1655 b3357. **(F)** Overlay of apo-GlxR_{WT} (green) (PDB:4BYY) and model of apo-GlxR_{A131T} (light blue). **(G)** Overlay of holo-GlxR_{WT} (green) (PDB:4CYD) and a model of holo-GlxR_{A131T} (light blue) showing an enlargement of the region close to A131T amino acid exchange including bound cAMP. The model of GlxR-A131T and the overlay were generated with PyMOL.

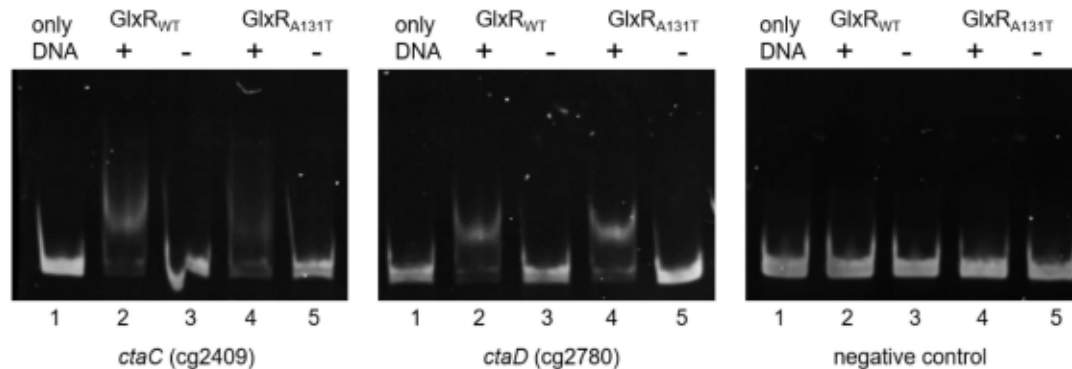


FIGURE S5. Electrophoretic mobility shift assays (EMSAs) with C-terminally Twin-Streptagged GlxR_{WT} or GlxR_{A131T} and DNA fragments covering the known GlxR-binding sites in the promoter regions of *ctaD* (-121 to -261 bp upstream of *ctaD* start codon) and *ctaCF* (-102 to -234 bp upstream of *ctaC* start codon) (Kohl et al., 2008; Toyoda et al., 2011) and an intragenic DNA fragment of cg3153 serving as negative control. 100 ng of the DNA fragments were incubated for 30 min at room temperature with 200 nM purified protein, either with (+) or without (-) 0.2 mM cAMP. After incubation, the reaction mixture was loaded on a 10% native polyacrylamide gel. Lane 1: control sample containing only DNA; lane 2: sample with GlxR_{WT}, the indicated DNA fragment, and cAMP; lane 3: sample with GlxR_{WT} and the indicated DNA fragment, but without cAMP; lane 4: sample of GlxR_{A131T} with the indicated DNA fragment and cAMP; lane 5: sample with GlxR_{A131T} and the indicated DNA fragment, but without cAMP.

3 Supplementary References

- Kohl, T.A., Baumbach, J., Jungwirth, B., Pühler, A., and Tauch, A. (2008). The GlxR regulon of the amino acid producer *Corynebacterium glutamicum*: *In silico* and *in vitro* detection of DNA binding sites of a global transcription regulator. *J. Biotechnol.* 135(4), 340-350. doi: 10.1016/j.jbiotec.2008.05.011.
- Robert, X., and Gouet, P. (2014). Deciphering key features in protein structures with the new ENDscript server. *Nucleic Acids Res.* 42, W320-324. doi: 10.1093/nar/gku316.
- Townsend, P.D., Jungwirth, B., Pojer, F., Bussmann, M., Money, V.A., Cole, S.T., et al. (2014). The crystal structures of apo and cAMP-bound GlxR from *Corynebacterium glutamicum* reveal structural and dynamic changes upon cAMP binding in CRP/FNR family transcription factors. *PLoS One* 9(12), e113265. doi: 10.1371/journal.pone.0113265.
- Toyoda, K., Teramoto, H., Inui, M., and Yukawa, H. (2011). Genome-wide identification of *in vivo* binding sites of GlxR, a cyclic AMP receptor protein-type regulator in *Corynebacterium glutamicum*. *J. Bacteriol.* 193, 4123-4133. doi: 10.1128/JB.00384-11.

2.3 Comparison of *in vivo* GlxR binding in *Corynebacterium glutamicum* ATCC 13032 and the adenylate cyclase deletion mutant Δ *cydB* using ChAP-Seq

Natalie Wolf¹, Lukas Lehmann¹, Andrei Filipchuk¹, Tino Polen¹, Michael Bussmann¹, Meike Baumgart¹ and Michael Bott^{1*}

¹IBG-1: Biotechnology, Institute of Bio- and Geosciences, Forschungszentrum Jülich, Jülich, Germany

*Corresponding author

To be submitted

Author's contributions:

NW constructed mutants, plasmids and performed all experimental work except the one specified below for other authors. LL constructed the strain *C. glutamicum::glxR-TS*, cultivated and generated one of the nine ChAP-Seq samples. MBu performed the microarray experiment. TP supervised the bioinformatics of the microarray analysis and the first evaluation of the ChAP-Seq results. AF normalized the data of the four ChAP-Seq sample conditions and performed comparisons of peak heights and generated the draft version of Fig. 1. NW wrote the first draft of the manuscript and prepared the figures and tables if not mentioned otherwise. MBa coached the experimental work and supported the design of this study. MBo designed the study, supervised the experimental work and was responsible for the final version of the manuscript.

Overall contribution **NW: 80%**

AF: Andrei Filipchuk, LL: Lukas Lehmann, MBa: Meike Baumgart, MBo: Michael Bott, MBu: Michael Bussmann, NW: Natalie Wolf, TP: Tino Polen

Comparison of *in vivo* GlxR binding in *Corynebacterium glutamicum* ATCC 13032 and the adenylate cyclase deletion mutant Δ *cyaB* using ChAP-Seq

Natalie Wolf¹, Lukas Lehmann¹, Andrei Filipchuk¹, Tino Polen¹, Michael Bussmann¹, Meike Baumgart¹, Michael Bott^{1*}

¹IBG-1: Biotechnology, Institute of Bio- and Geosciences, Forschungszentrum Jülich, Jülich, Germany

ABSTRACT

The Crp homolog GlxR is a cyclic adenosine monophosphate (cAMP)-binding global transcriptional regulator of *Corynebacterium glutamicum*, an important production host in industrial biotechnology. *C. glutamicum* contains only a single adenylate cyclase, encoded by *cyaB*. Strains lacking *cyaB* show a strongly reduced or even absent cAMP level. However, in contrast to Δ *glxR* mutants, which show severe growth defects, a Δ *cyaB* mutant grows like the wild type ATCC13032 (WT), except in the presence of acetate, which inhibits growth. To obtain a better understanding of the different growth phenotypes of Δ *glxR* and Δ *cyaB* mutants, we compared *in vivo* DNA-binding of GlxR in the WT and the Δ *cyaB* mutant during growth in minimal medium containing either only glucose or glucose plus acetate as carbon source. Analysis of the four data sets (WT_{GlxR-TS} (glc), Δ *cyaB*_{GlxR-TS} (glc), WT_{GlxR-TS} (glc-ac) and Δ *cyaB*_{GlxR-TS} (glc-ac)) comprising nine individual ChAP-Seq experiments identified 243 GlxR peaks with an enrichment factor (EF) of ≥ 3 in at least one data set. *De novo* motif search identified the consensus sequence TGTGN₈CACA in 242 of the GlxR peaks. 141 of these were also reported in previous studies, whereas 102 represent novel binding sites. Remarkably, the majority of the 243 GlxR binding sites were found to be enriched in all four data sets when using an EF ≥ 1.5 as cutoff. The average EF for the 243 GlxR peaks was 5.23 ± 2.68 for WT_{GlxR-TS} (glc), 3.99 ± 2.53 for Δ *cyaB*_{GlxR-TS} (glc), 4.81 ± 3.34 for WT_{GlxR-TS} (glc-ac), and 2.87 ± 1.40 for Δ *cyaB*_{GlxR-TS} (glc-ac). The results showed that the strongly diminished or completely absent cAMP level in the Δ *cyaB* mutant reduced GlxR binding, particularly in the presence of acetate, but did not prevent it. This suggests that GlxR binding *in vivo* is less dependent on cAMP than GlxR binding *in vitro* and that additional, yet unknown factors might be involved in the control of GlxR binding to DNA within the cell.

Keywords: *Corynebacterium glutamicum*, GlxR, cAMP, transcriptional regulator, adenylate cyclase, acetate, phosphodiesterase, ChAP-Seq

*Correspondence: Michael Bott (m.bott@fz-juelich.de)

INTRODUCTION

Regulation of gene expression at the level of transcription is one of the key steps in the control of metabolism in bacteria. Transcriptional regulators can be classified into global, master, and local regulators, depending on the number of target genes (Schröder & Tauch, 2010). One of the most intensively studied global regulators in bacteria is the cyclic adenosine monophosphate (cAMP) receptor protein (Crp) of *Escherichia coli* (Gosset et al., 2004; Zheng et al., 2004). Crp belongs to the Crp/Fnr-family of transcriptional regulators (Körner et al., 2003) and activates or represses its target genes in response to the internal cAMP concentration. Crp orthologs are widespread in bacteria and have been studied for example in *Mycobacterium*, *Pseudomonas*, and *Corynebacterium* species (Soberón-Chávez et al., 2017).

Corynebacterium glutamicum is a non-pathogenic soil bacterium, which was isolated due to its ability to secrete L-glutamate (Kinoshita et al., 1957). Today this species is widely used in industrial biotechnology for the production of amino acids, mainly L-glutamate and L-lysine (Eggeling & Bott, 2015). Additionally, *C. glutamicum* strains have been developed for the efficient production of organic acids, polyamines, and various other metabolites (Becker & Wittmann, 2012; Wendisch et al., 2018; Wieschalka et al., 2013; Wolf et al., 2021). Also proteins are meanwhile produced industrially with *C. glutamicum* (Freudl, 2017). Due to the importance of *C. glutamicum* in biotechnology and its close phylogenetic relationship to pathogenic bacteria, such as *Corynebacterium diphtheriae* and *Mycobacterium tuberculosis*, it has become a frequently used model organism (Burkovski, 2008; Eggeling & Bott, 2005; Yukawa & Inui, 2013).

C. glutamicum contains a Crp ortholog named GlxR, which has 27% amino acid sequence identity to Crp of *E. coli* and was shown to be a global regulator. More than 200

putative target genes of GlxR were identified, which are involved in central carbon metabolism and a variety of other cellular functions, such as transport processes, respiration, stress responses, or cell division (Jungwirth et al., 2013; Kohl et al., 2008; Letek et al., 2006; Nishimura et al., 2011; Toyoda et al., 2011). *In vitro* binding of purified GlxR to DNA target sites requires the presence of cAMP (Bussmann, 2009; Kim et al., 2004; Townsend et al., 2014). The crystal structures of apo-GlxR and holo-GlxR revealed structural changes upon cAMP binding that lead to the optimization of the orientation of the two DNA-binding helices (Townsend et al., 2014). The affinity of purified GlxR to a double-stranded oligonucleotide containing a GlxR-binding site increased about 100-fold upon cAMP binding (Townsend et al., 2014).

An important issue for understanding the physiological function of GlxR is therefore the control of the cAMP level within the cell. Two enzymes have been identified that are important in this context. One is the membrane-bound adenylate cyclase CyaB, which catalyses the synthesis of cAMP from ATP (Cha et al., 2010; Wolf et al., 2020). The deletion mutant *C. glutamicum* $\Delta cyaB$ lacks cAMP or at least has a strongly reduced cAMP level, depending on the method used for analysis (Wolf et al., 2020). Surprisingly, whereas $\Delta glxR$ mutants have severe growth defects (see below), the $\Delta cyaB$ mutant grew like the wild type in minimal medium with glucose, fructose, gluconate, or ethanol as carbon source (Cha et al., 2010; Wolf et al., 2020). Only in the presence of acetate (alone or in combination with another carbon source), a strong growth defect was observed (Cha et al., 2010; Wolf et al., 2020). This 'acetate effect' was partly explained by a higher uncoupler sensitivity of the $\Delta cyaB$ strain due to a lower transcriptional activation and activity of the cytochrome *bc₁-aa₃* supercomplex in the $\Delta cyaB$ compared to the wild type (Wolf et al., 2020). The same study also described the isolation of a $\Delta cyaB$ strain

that had regained wild type-like acetate tolerance. This suppressor mutant was shown to possess a single point mutation within the coding region of *glxR*, leading to the amino acid exchange Ala131Thr, which emphasizes the connection and importance of GlxR regulation in response to the intracellular cAMP level (Wolf et al., 2020). The second enzyme relevant for the intracellular cAMP level is the phosphodiesterase CpdA, which catalyses the hydrolysis of cAMP (Schulte et al., 2017). The deletion mutant *C. glutamicum* Δ *cpdA* has an increased intracellular cAMP level and shows growth defects in complex medium and in minimal medium with glucose, gluconate, citrate, acetate, or ethanol as carbon sources (Schulte et al., 2017). Many of these growth defects occurred due to stronger repression by GlxR of genes that code for transporters of the respective carbon sources (Schulte et al., 2017).

The search for target genes of transcriptional regulators often involves a transcriptome comparison of a deletion mutant lacking the regulator gene with the wild type. However, a deletion of *glxR* was extremely difficult to obtain and the mutants with only a partly deleted *glxR* showed severe growth defects (Moon et al., 2007; Park et al., 2010). Therefore, current knowledge of the direct target genes of GlxR is based on a variety of alternative approaches, such as (i) bioinformatic identification of GlxR binding sites within the genome combined with electrophoretic mobility shift assays (EMSAs), showing the cAMP-dependent binding of purified GlxR to these motifs (Kohl & Tauch, 2009), (ii) reporter gene assays at varying GlxR levels (Bussmann et al., 2009), (iii) impact of GlxR-binding site mutations on gene expression (Inui et al., 2004), (iv) transcriptome comparisons of strains with an increased (strain Δ *cpdA*) or reduced (strain Δ *cydB*) cAMP level compared with the wild type (Schulte et al., 2017; Wolf et al., 2020) or (v) genome-wide identification of *in vivo* GlxR binding sites. In particular the latter approach is a highly valuable tool and two studies using

it for GlxR were reported. In one study, chromatin immunoprecipitation with an anti-GlxR antibody and subsequent sequencing (ChIP-Seq) was performed with the type strain ATCC13032 grown on either glucose or acetate. Whereas 107 DNA fragments were enriched from glucose-grown cells, only two were also enriched from acetate-grown cells (Jungwirth et al., 2013). In a second study, ChIP-chip analysis was used to determine the GlxR binding sites in *C. glutamicum* strain R and led to the identification of 209 *in vivo* GlxR-binding sites (Toyoda et al., 2011). In the latter study, also a Δ *cydB* mutant of strain R was analysed by ChIP-chip, which revealed that GlxR was still able to interact with its target sites, but with a markedly decreased binding affinity (Toyoda et al., 2011).

Besides ChIP-Seq and ChIP-chip, ChAP-Seq has been established as a variant of ChIP-Seq to detect *in vivo* binding sites of DNA-binding proteins. It involves affinity purification of a tagged DNA-binding protein covalently linked to its genomic target sites followed by sequencing of the enriched DNA fragments. In *C. glutamicum* ATCC13032, the ChAP-Seq method was already successfully applied to study, e.g., the role of the nucleoid-associated protein CgpS or to analyse the influence of intracellular heme concentrations on the binding of response regulator HrrA to target DNA (Keppel et al., 2020; Pfeifer et al., 2016). In the current study, we used ChAP-Seq to analyse *in vivo* GlxR-binding sites in the wild type and the Δ *cydB* mutant of strain ATCC13032 after cultivation in minimal medium with either glucose or a glucose-acetate mixture as carbon sources. The aim was to explore the influence of a decreased or even absent cAMP level and of acetate on *in vivo* GlxR-binding and thus get a better understanding of the function of this global regulator. The results of this study led to the identification of about 100 hitherto unknown GlxR-binding sites and consequently a large expansion of the GlxR regulon. Furthermore, evidence was obtained that, as expected,

cAMP promotes DNA-binding of GlxR, but apparently is not an essential prerequisite for binding.

METHODS

Bacterial strains, plasmids, oligonucleotides and cultivation conditions

All bacterial strains and plasmids used in this study are listed in Table 1. The oligonucleotides used in this study are listed in Table S1. *C. glutamicum* strains were cultivated in brain heart infusion (BHI) medium (Bacto™ BHI, BD, Heidelberg, Germany) or in CGXII minimal medium (adjusted to pH 7.0 with KOH) (Frunzke et al., 2008) containing either 100 mM glucose or a mixture of glucose and acetate (100 mM and 150 mM, respectively) as carbon source. For growth experiments, 5 ml BHI medium was inoculated with a single colony and incubated at 30 °C and 130 rpm for 8 h. The second preculture was inoculated with 400 µl of the first preculture and cultivated for about 16 h at 30 °C and 120 rpm in a 100 ml baffled shake flask containing 20 ml CGXII medium with 2% (w/v) glucose. For the main culture in a microcultivation system, 800 µl CGXII medium in FlowerPlates (m2p-labs, Baesweiler, Germany) was inoculated to an optical density at 600 nm (OD_{600}) of 1 and cultivated at 1200 rpm, 30 °C and 80% humidity in a BioLector microcultivation system (m2p-labs, Baesweiler, Germany). Growth was followed by measuring the backscatter at 620 nm, which reflects the cell density (Kensy et al., 2009). For cultivations in 5 L baffled-shake flasks, 500 ml CGXII medium was inoculated with the second preculture to an OD_{600} of 1. The cultivations in 5 L shake flasks were performed at 30 °C and 90 rpm and growth was followed by measuring OD_{600} . *E. coli* DH5 α was used as host for all cloning purposes and was cultivated at 37 °C in lysogeny broth (LB) medium (Sambrook & Russell, 2001). *E. coli* BL21(DE3) was used for the production of proteins (Studier & Moffatt, 1986). For this

purpose, the strain carrying an overexpression plasmid was cultivated in ZYM-5052 auto-induction medium (Studier, 2005) at 30 °C for 16 h. If required, media were supplemented with kanamycin (25 µg ml⁻¹ for *C. glutamicum* and 50 µg ml⁻¹ for *E. coli*).

Construction of *C. glutamicum* strains with chromosomally encoded GlxR with C-terminal Twin Strep-Tag

C. glutamicum WT and the $\Delta cyaB$ mutant carrying the coding sequence of a Twin Strep-tag at the 3' end of the chromosomal *glxR* gene were constructed by double homologous recombination with the pK19*mobsacB* system as described previously (Niebisch & Bott, 2001; Schäfer et al., 1994). Briefly, *C. glutamicum* WT was transformed with the deletion plasmid pK19*mobsacB-glxR-twinstrep* harbouring a 1143 bp PCR product comprising 540 bp representing the 3' end of *glxR* without the stop codon, followed by the sequence for the Twin Strep-tag (WSHPQFEKGGGSGGGSGGSAWSHPQFEK), a stop codon and 516 bp corresponding to the sequence downstream of *glxR*. After the second homologous recombination event, 25 kanamycin-sensitive and sucrose-resistant clones were analysed by colony PCR; 14 clones harboured the Twin Strep-tag-encoding sequence whereas eleven clones contained the wild-type fragment. The strain *C. glutamicum::glxR-TS* ('WT_{GlxR-TS}') with the chromosomally Twin Strep-tagged was obtained without any difficulties and served as parental strain for construction of *C. glutamicum::glxR-TS* $\Delta cyaB$ (' $\Delta cyaB_{GlxR-TS}$ ') as described (Wolf et al., 2020).

Chromatin affinity purification and sequencing (ChAP-Seq)

The preparation of the samples for the ChAP-Seq runs were performed as described previously (Pfeifer et al., 2016) with the following adaptations: WT_{GlxR-TS} and $\Delta cyaB_{GlxR-TS}$ were cultivated in 500 ml CGXII medium with glucose or glucose-acetate

TABLE 1 | Bacterial strains and plasmids used in this study

Strain or plasmid	Relevant characteristics	Source or Reference
Strains		
<i>E. coli</i> DH5 α	F ⁻ ϕ 80 <i>lacZ</i> Δ M15 Δ (<i>lacZYA-argF</i>)U169 <i>recA1</i> <i>endA1</i> <i>hsdR17</i> (r _K ⁻ , m _K ⁺) <i>phoA</i> <i>supE44</i> λ - <i>thi-1</i> <i>gyrA96</i> <i>relA1</i>	Invitrogen
<i>E. coli</i> BL21(DE3)	B F ⁻ <i>ompT</i> <i>gal</i> <i>dcm</i> <i>lon</i> <i>hsdS_B</i> (r _B ⁻ m _B ⁻) λ (DE3 [<i>lacI</i> <i>lacUV5-T7p07</i> <i>ind1</i> <i>sam7</i> <i>nin5</i>]) [<i>malB</i> ^T] _{K-12} (λ ^S)	(Studier & Moffatt, 1986)
<i>C. glutamicum</i> ATCC13032 (WT)	ATCC13032, biotin-auxotrophic wild-type strain (WT)	(Kinoshita et al., 1957)
<i>C. glutamicum</i> :: <i>glxR</i> -TS (WT _{GlxR-TS})	<i>C. glutamicum</i> ATCC13032 with a Twin Strep-tag encoding sequence at the 3' end of <i>glxR</i> (cg0350). The C-terminal tag has the following amino acid sequence: WSHPQFEKGGGSGGGSSGSAWSHPQFEK.	This study
<i>C. glutamicum</i> Δ <i>cyaB</i>	ATCC13032 with an in frame deletion of the adenylate cyclase gene <i>cyaB</i> (cg0375)	(Wolf et al., 2020)
<i>C. glutamicum</i> :: <i>glxR</i> -TS Δ <i>cyaB</i> (Δ <i>cyaB</i> _{GlxR-TS})	WT _{GlxR-TS} strain with a deletion of <i>cyaB</i> (cg0375)	This study
Plasmids		
pAN6	Kan ^R ; P _{trc} , <i>lacI</i> ^d pBL1 oriV _{Cg} pUC18 oriV _{Eco} , <i>C. glutamicum</i> / <i>E. coli</i> shuttle vector, derivative of pEKEx2	(Frunzke et al., 2008)
pAN6- <i>glxR</i> -twinstrep	Kan ^R ; pAN6 derivative encoding C-terminal Twin Strep-tagged GlxR (Cg0350) under the control of P _{trc}	(Wolf et al., 2020)
pK19 <i>mobsacB</i>	Kan ^R ; oriT oriV _{Eco} <i>sacB</i> <i>lacZ</i> ; vector for allelic exchange in <i>C. glutamicum</i>	(Schäfer et al., 1994)
pK19 <i>mobsacB</i> - Δ <i>cyaB</i>	Kan ^R ; pK19 <i>mobsacB</i> derivative containing an overlap extension PCR product covering the up- and downstream regions of <i>cyaB</i> (cg0375)	(Wolf et al. 2020)
pK19 <i>mobsacB</i> - <i>glxR</i> -twinstrep	Kan ^R ; pK19 <i>mobsacB</i> derivative containing a 1143 bp PCR product covering the 3' terminal 540 bp of <i>glxR</i> (cg0350) without the stop codon but instead the coding sequence of the Twin Strep-tag (WSHPQFEKGGGSGGGSSGSAWSHPQFEK) and 516 bp of the <i>glxR</i> downstream region	This study

mixture, respectively. The cross-linking of GlxR carrying a C-terminal Twin Strep-tag (named GlxR_{TS}) to the bound DNA was performed in the exponential growth phase at an OD₆₀₀ of 6. The GlxR_{TS}-DNA complexes were purified following the Strep-Tactin XT affinity chromatography purification protocol

(IBA Life Sciences, Göttingen, Germany). The elution fractions of the GlxR_{TS}-DNA complexes were incubated overnight at 65 °C, followed by the digestion of GlxR_{TS} with 400 μ g ml⁻¹ proteinase K (AppliChem GmbH, Darmstadt, Germany) for 3 h at 55 °C.

Subsequently, the DNA was purified as described previously (Pfeifer et al., 2016).

The purified DNA fragments of each sample were used for library preparation and indexing with the TrueSeq DNA PCR-free sample preparation kit (Illumina, San Diego, USA) or the NEBNext Ultra II DNA Library Prep kit for Illumina (New England Biolabs GmbH, Frankfurt am Main, Germany) following the manufacturer's instructions, yet omitting the DNA size selection steps. The resulting indexed libraries were quantified using the KAPA Library Quantification kit (Peqlab, Bonn, Germany) and normalized for pooling. Sequencing was performed on a MiSeq instrument (Illumina, San Diego, USA) using paired-end sequencing with a read-length of 2×150 bp. Data analysis and base calling were accomplished with the CLC Genomics workbench (Version 9, Qiagen, Hilden, Germany). The reads were mapped to the genome sequence BA000036.3 of *C. glutamicum* ATCC13032 (Ikeda & Nakagawa, 2003). Evaluation of genomic coverage, peak detection and normalization was essentially performed as described in Keppel et al., 2020. The enrichment factor (EF) was defined as ratio of the sequencing coverage at a certain position divided by the average background coverage of the whole genome. Genome regions with an $EF \geq 3$ in at least one data set were considered as specifically enriched DNA regions and defined as peaks.

ChAP-Seq analysis and motif search

Genome regions with peaks found in at least two independent ChAP-Seq runs of the same strain and the same growth condition (data set) were defined as *in vivo* GlxR-DNA binding regions. For motif search, the DNA sequence of all defined *in vivo* GlxR-DNA binding regions was submitted to MEME-ChIP (Version 5.1.1) (Bailey & Elkan, 1994). The sequences used for MEME-ChIP were generated by taking the highest point of the ChAP-Seq peak and adding 250 bp on each side of the enriched DNA fragment (yielding

sequences of 501 bp). Parameters of the tool were set to search for a palindromic motif with a 16 bp long sequence.

Electrophoretic mobility shift assays (EMSAs) with purified GlxR_{TS}

Protein production of GlxR_{TS} and the subsequent purification was performed as described previously (Wolf et al., 2020). EMSAs with the purified GlxR_{TS} were performed as described previously (Bussmann et al., 2009). The DNA fragments were chosen based on peak detection of the ChAP-Seq analysis and comprised a 100-120 bp fragment with the GlxR-binding site (predicted in our MEME-ChIP analysis) in the centre of the fragment. The respective DNA fragments were generated by PCR using the oligonucleotides listed in Table S1 and purified with the DNA Clean & Concentrator Kit (Zymo Research, Freiburg, Germany).

Transcriptome analysis using DNA microarrays

Preparation of RNA and synthesis of labelled cDNA was prepared from cells in the exponential growth phase. The microarrays were performed according to the description in Wolf et al., 2020. The genome-wide mRNA concentrations of *C. glutamicum* wild type were compared with those of the *C. glutamicum* $\Delta cyaB$ mutant. The strains were cultivated in CGXII medium with 100 mM glucose. Three independent DNA microarray experiments, each starting from independent cultures, were performed.

RESULTS

Experimental setup for the detection of *in vivo* GlxR_{TS}-DNA binding regions

In this study, we wanted to analyse the impact of a lowered cytoplasmic cAMP level and of acetate on the genome-wide GlxR-DNA binding patterns using ChAP-Seq. For this purpose, the ATCC13032 derivatives WT_{GlxR-TS} and $\Delta cyaB$ _{GlxR-TS} were constructed,

which encode GlxR derivatives with a C-terminal Twin Strep-tag. The $\Delta cyaB_{GlxR-TS}$ mutant lacks the *cyaB* gene for adenylyate cyclase and therefore has a low intracellular cAMP level or even no cAMP at all, depending on the method used for cAMP determination (Cha et al., 2010; Wolf et al., 2020). *C. glutamicum* ATCC13032 and $WT_{GlxR-TS}$ showed the same growth behaviour in glucose minimal medium (Fig. S1), indicating that the replacement of native GlxR with a Twin Strep-tagged variant does not disturb the functionality of the protein. Furthermore, GlxR with a C-terminal Strep-tag has previously been used successfully for ChIP-chip analysis with the strain *C. glutamicum* R (Toyoda et al., 2011).

For the ChAP-Seq analysis, three biological replicates were performed for $WT_{GlxR-TS}$ cultivated on glucose and two replicates each for $WT_{GlxR-TS}$ cultivated on glucose and acetate, $\Delta cyaB_{GlxR-TS}$ cultivated on glucose, and $\Delta cyaB_{GlxR-TS}$ cultivated on glucose and acetate. The growth rates of the two strains were comparable during cultivation on glucose ($\mu = 0.36 - 0.38$), but differed during growth on glucose and acetate, where the $\Delta cyaB_{GlxR-TS}$ strain showed a reduced growth rate ($\mu = 0.36$ for $WT_{GlxR-TS}$, $\mu = 0.16$ for $\Delta cyaB_{GlxR-TS}$). The sequencing data of all nine individual ChAP-Seq runs showed good quality and were used for further analysis. The number of reads, the mapping statistics, and the coverages are listed in Table S2. In ChAP-Seq analysis, a low amount of DNA fragments covering the entire genome is always isolated unspecifically, which enables the determination of the background coverage. This background coverage varies between different ChAP-Seq runs, depending, e.g., on the total number of reads. In order to enable a direct comparison of multiple ChAP-Seq runs, the data were normalized as described in (Keppel et al., 2020). This allowed the calculation of average enrichment factors (EF) for a certain genomic position based on the two or three replicate ChAP-Seq runs

performed for each of the four conditions studied in this work. In this way four ChAP-data sets were obtained and used for further analysis: $WT_{GlxR-TS}$ (glc), $\Delta cyaB_{GlxR-TS}$ (glc), $WT_{GlxR-TS}$ (glc-ac), and $\Delta cyaB_{GlxR-TS}$ (glc-ac).

DNA regions bound by $GlxR_{TS}$ and influence of acetate and adenylyate cyclase

In our analysis we focused on those GlxR peaks, which were found to have an $EF \geq 3$ in at least one ChAP-Seq data set. In the four data sets, in total 243 GlxR peaks with an $EF \geq 3$ were identified (Table S3), with the highest number of 229 in $WT_{GlxR-TS}$ (glc) (Table 2). The other 14 GlxR peaks with an $EF \geq 3$ were present in $\Delta cyaB_{GlxR-TS}$ (glc) and/or $WT_{GlxR-TS}$ (glc-ac). The distribution and the EFs of the GlxR peaks throughout the genome are shown for each of the four data sets in Fig. 1. Importantly, this figure and also the summarized data in Table S3 clearly show that for the vast majority of the GlxR peaks an enrichment was detected in all four data sets. When considering all peaks with an $EF \geq 1.5$ as enriched, only two, nine, one, and 37 peaks of the total 243 GlxR peaks were non-enriched in one of the four data sets (Table 2). When looking at the mean EFs of the four data sets as a proxy for the overall effects, it is obvious that the presence of acetate reduced the mean EF in the WT by about 8% from 5.23 in the absence of acetate to 4.81 in its presence. In the $\Delta cyaB$ mutant, the presence of acetate reduced the mean EF by 28%, from 3.99 to 2.87, and thus had a stronger effect than in the WT. The absence of adenylyate cyclase reduced the mean EF during growth on glucose by 24% from 5.23 in the WT to 3.99 in the *cyaB* mutant and during growth on glucose and acetate by even 40% from 4.81 in the WT to 2.87 in the $\Delta cyaB$ mutant. Thus, the absence of adenylyate cyclase clearly reduced GlxR binding *in vivo*, but did not prevent it.

An interesting feature visible in Fig. 1B and D is a missing region of about 34 kb in the background coverage at about 2 Mb in strain $\Delta cyaB_{GlxR-TS}$.

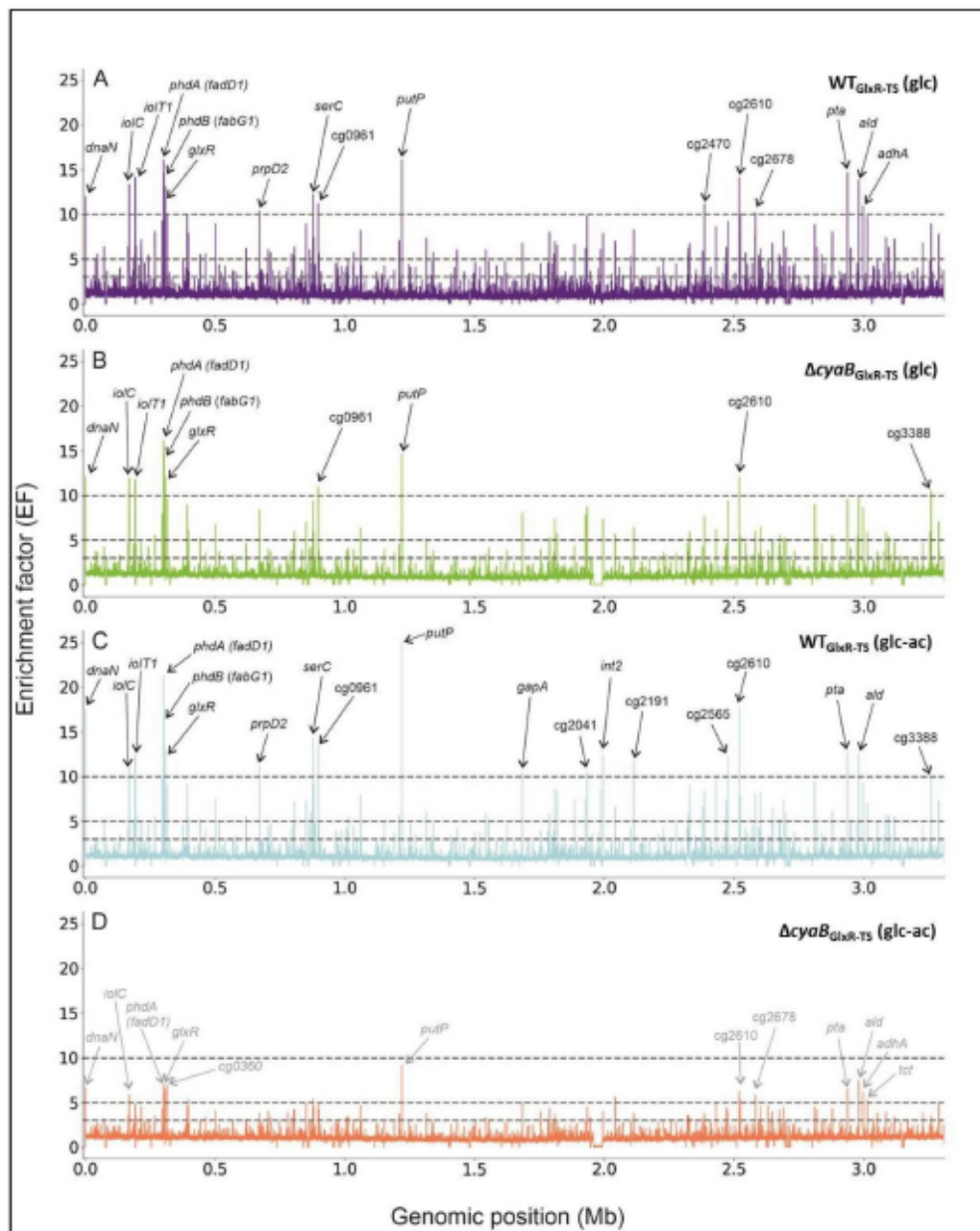


FIGURE 1 | Comparison of the four ChAP-Seq data sets (averaged values from two or three individual ChAP-Seq experiments) produced and analysed in this study. The strains and growth conditions are indicated for each of the four panels **A**, **B**, **C**, and **D**. The DNA sequencing data were normalized as described in (Keppel et al., 2020). The first dashed grey line indicates the EF threshold of 3 used in this work to consider a GlxR peak. When a GlxR-binding site was found to be located -700 bp to +60 bp relative to the TSS or TLS, the respective protein-coding gene was categorized as a neighbouring gene. For GlxR peaks with an EF ≥ 10 and some others, the neighbouring gene is labelled in black. In the case of the data set for $\Delta cyoB_{GlxR-TS}$ (glc-ac), none of the GlxR peaks showed an EF ≥ 10 and in this case the genes next to the GlxR peaks with the highest EFs are labelled in grey.

The missing region corresponds to the CGP4 prophage region (Ikeda & Nakagawa, 2003). As strain $\Delta cyaB_{GlxR-TS}$ was derived from $WT_{GlxR-TS}$, CGP4 must have been lost during the deletion of *cyaB*. We rechecked several $\Delta cyaB$ mutants with different strain backgrounds present in our strain collection, and out of seven tested clones, three had lost CGP4 (data not shown). The CGP3 and CGP4 prophage regions (CGP4 is located within the CGP3 region) share large homologous regions and therefore CGP4 can be excised by homologous recombination. We assume that the excision is favoured upon *cyaB* deletion. This phenomenon was not studied further, but could be interesting for future prophage studies.

DNA sequence motif search and location of GlxR binding sites

Using 501 bp DNA long sequences of the 243 identified GlxR peaks (250 bp on each side of the peak maximum), we performed a *de novo* motif search with MEME-ChIP (Bailey & Elkan, 1994). This resulted in the consensus motif TGTGWBNDNVWCACA (Fig. 2) with highly conserved TGTG and CACA residues at position 1 to 4 and 13 to 16. These conserved bases correspond to the motif previously reported for GlxR (Jungwirth et al., 2013; Kohl et al., 2008; Toyoda et al., 2011). The bases 5 to 12 are hardly conserved in our consensus motif, suggesting that TGTG and CACA are the important residues for binding of GlxR, as also pointed out before (Toyoda et al., 2011). Within the 243 GlxR peaks, the *de novo* motif search found 242 fragments having a binding site with an e-value < 0.03. This result provided strong support for the validity of our ChAP-Seq data. In the case of GlxR peak centred 66 bp upstream of the transcriptional start site (TSS) of *oxyR*, which is a leaderless transcript, no obvious GlxR motif was present and the basis for GlxR binding at this position is not known.

Table S3 shows the distance of the detected GlxR binding motifs to the TSS, or, if this unknown, to the translational start

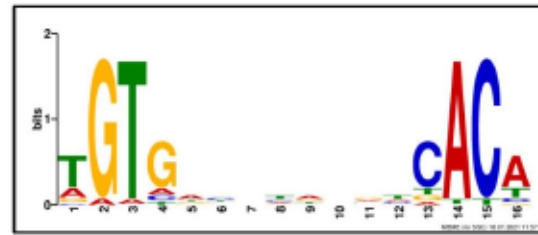


FIGURE 2 | GlxR consensus motif determined by MEME-ChIP analysis (Version 5.1.1) (Bailey & Elkan 1994) using the DNA sequences of the 243 defined GlxR peaks. For motif analysis, a 16 bp palindromic motif was searched in the region of the peak maximum.

site (TLS) of neighbouring genes. The position of the GlxR binding sites was sorted into five groups (Fig. 3): (i) GlxR binding sites (n = 79) located less than 500 bp upstream of a transcriptional start site (TSS), or if TSS is unknown, the translational start site (TLS) of a neighbouring gene or operon. (ii) GlxR binding sites (n = 69) located intergenic of two divergently transcribed genes with less than 500 bp upstream of a transcriptional start site (TSS), or if TSS is unknown, the translational start site (TLS) of a neighbouring gene or operon. (iii) GlxR binding sites (n = 10) located within intergenic regions of two convergently transcribed genes. (iv) GlxR binding sites (n = 40) located intragenically and less than 500 bp upstream of a transcriptional start site (TSS), or if TSS is unknown, the translational start site (TLS) of a neighbouring gene or operon. (v) GlxR binding sites (n = 45) located intragenically and more than 500 bp upstream of a transcriptional start site (TSS), or if TSS is unknown, the translational start site (TLS) of a neighbouring gene or operon. The GlxR binding sites of the latter three groups are summarized in Table S4. Whereas GlxR binding to the sites of groups (i), (ii) and (iv) is known or considered to influence the transcription of the downstream genes, this appears less likely for GlxR binding to the sites of groups (iii), and (v). Due to the lack of a genome-wide comparison of gene expression in a $\Delta GlxR$ mutant and the WT, only selected

TABLE 2 | Overview on GlxR peaks identified in the four ChAP-Seq data sets.

ChAP-Seq data set	WT _{GlxR-TS} (glc)	Δ <i>cydB</i> _{GlxR-TS} (glc)	WT _{GlxR-TS} (glc-ac)	Δ <i>cydB</i> _{GlxR-TS} (glc-ac)
GlxR peaks with EF ≥ 3	229	135	163	90
No. of GlxR peaks with an EF ≥ 1.5 for the 243 total GlxR peaks	241	234	242	205
Mean EF and standard deviation for all 243 GlxR peaks with EF ≥ 3	5.23 \pm 2.68	3.99 \pm 2.53	4.81 \pm 3.34	2.87 \pm 1.40
Max. EF	16.12	16.10	25.00	9.09
No. of GlxR peaks with EF ≥ 10	17	12	12	0

GlxR target genes were experimentally analysed with respect to their activation or repression by GlxR (Bussmann et al., 2009; Nishimura et al., 2011; Park et al., 2010; Toyoda et al., 2011; van Ooyen et al., 2011).

New GlxR peaks and potential GlxR target genes in *C. glutamicum* ATCC13032

In the four ChAP-Seq data sets generated in this study, 243 GlxR peaks were identified based on the criterion that the peak had an EF ≥ 3 in at least one of the data sets. 141 of these GlxR binding sites had also been identified previously by ChIP-Seq or Chip-chip experiments (Jungwirth et al., 2013; Toyoda et al., 2011), or in EMSA studies (Kohl et al., 2008; Kohl & Tauch, 2009; Toyoda et al., 2011). 102 of the GlxR peaks detected in our study were not reported before and provide a large expansion of the GlxR regulon. In Table 3, all 102 new GlxR binding sites and their distance to the TSS or TLS of neighbouring genes are shown, whereas missing peaks that were reported in literature are listed in Table S5. As several of these GlxR binding sites were located within 200 bp upstream of a TSS or TLS, an influence of GlxR on the transcription of the corresponding gene appears likely. Genes that might be repressed by GlxR because its binding site is located downstream of the TSS or TLS are for example *guaA* (GMP synthase) or *siaE*

(periplasmic binding protein of sialic acid ABC transporter).

In order to further confirm the ability of GlxR to bind to some of the newly identified binding sites in strain ATCC13032, DNA fragments covering the GlxR motif upstream of *hemL* (cg0518), *aspA* (cg1657), and the one in the intergenic region of region of *nanR* (cg2936) and *siaE* (cg2937) were amplified and used for EMSAs with purified GlxR. For all three fragments, a cAMP-dependent DNA shift was observed (Fig. S2).

Prediction of transcriptional activation or repression by GlxR in a cAMP-dependent manner

To evaluate whether a transcriptional regulator activates or represses a target gene, transcriptome comparisons of regulator deletion strains with the parental strain are frequently used. Due to the severe growth defects of the *glxR* deletion mutants, meaningful microarray experiments with such a strain were not possible (Moon et al., 2007; Park et al., 2010). Therefore, we performed a transcriptome comparison of the Δ *cydB* mutant with the WT during growth in CGXII medium with glucose. The resulting mRNA ratios were then compared with those obtained in a previously established microarray data set (GEO accession number GSE81004) in which the Δ *cpdA* mutant lacking the cAMP

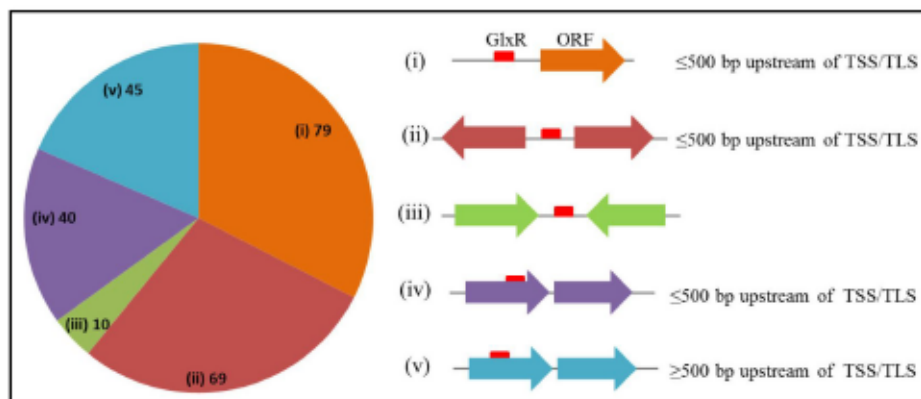


FIGURE 3 | Location of GlxR binding sites with respect to neighbouring TSS or TLS.

phosphodiesterase was compared with the WT (Schulte et al., 2017). Due to the opposing effects of the *cyab* and *cpdA* on the cellular cAMP level (lowered and increased, respectively), a similar effect on the expression on GlxR target genes might be visible, at least in some cases (Table S6). mRNA ratios with a value ≤ 0.6 in the $\Delta cpdA$ mutant and a value ≥ 1.4 in the $\Delta cyab$ mutant, are *here* predicted to be repressed by GlxR in a cAMP-dependent manner. This was found for example for the genes *cysR* (cg0156), *iolT1* (cg0223), *creJ* (cg0645), cg0961, *ptsG* (cg1537), *ptsI* (cg2117), *oppC* (cg2183), *oppD* (cg2184), *vamA* (cg2616), *ptsS* (cg2925), *pta* (cg3048), *cysZ* (cg3112), *tctC* (cg3127) and *gmp* (cg3216). Vice versa, if these mRNA ratios showed a value ≤ 0.6 in the $\Delta cyab$ mutant and a value ≥ 1.4 in the $\Delta cpdA$ mutant, they were *here* predicted to be likely activated by GlxR in a cAMP-dependent manner. This was found for the genes cg2665 and cg2824.

GlxR binding sites upstream of sRNAs, asRNAs, tRNAs, and *rrn*-operons

Many small RNAs (sRNAs), antisense RNAs (asRNA), and intragenic transcripts have been detected in *C. glutamicum* ATCC13032 in the course of comprehensive RNA-Seq studies (Mentz et al., 2013; Pfeifer-Sancar et al., 2013). We identified more than 40 GlxR binding sites that were located closer to the

TSSs of a sRNA, asRNA, or an intragenic transcript than to a TSS of a protein-coding gene (Table S7). For example GlxR binding sites were found that are closely located to the TSS of the asRNAs of cg1052, cg1609, cg1945 and cg3393, respectively (Fig. 4A-D); the sRNAs *cgb_00545* (adjacent genes *cg0054/crgA*) and *cgb_27005* (adjacent genes *phoB/musI*) (Fig. 4E, F), or close to the TSS of an intragenic transcript within the gene cg0706 (Fig. 4G).

GlxR peaks were also found upstream or within the genes of tRNAs, i.e. tRNA^{Leu}, tRNA^{Arg}, tRNA^{Gly} and of tRNA^{Asp} and might influence their transcription (Table S7). In the initial process of peak detection, GlxR peaks containing GlxR binding motifs were found upstream of the 23S rRNA gene (TGTGTGATACCGAACG), within the 23S rRNA gene (TGTGCACTTACTCA), and in four upstream regions of the 5S rRNA gene (TGTGCTGTGTCAGACA), belonging to the *rrn* operon of *rrnA*, *rrnB*, *rrnC* and *rrnF*. In the final version of the peak detection these regions and the peaks were excluded due to fact that the sequences of six *rrn* operons (*rrnA*, *rrnB*, *rrnC*, *rrnD*, *rrnE*, *rrnF*) each coding for 16S, 23S and 5S rRNA are very similar to each other and thus are not unique in the genome. Therefore it could not be shown in which of the six *rrn* regions the *in vivo* interaction of GlxR-DNA was detected.

12

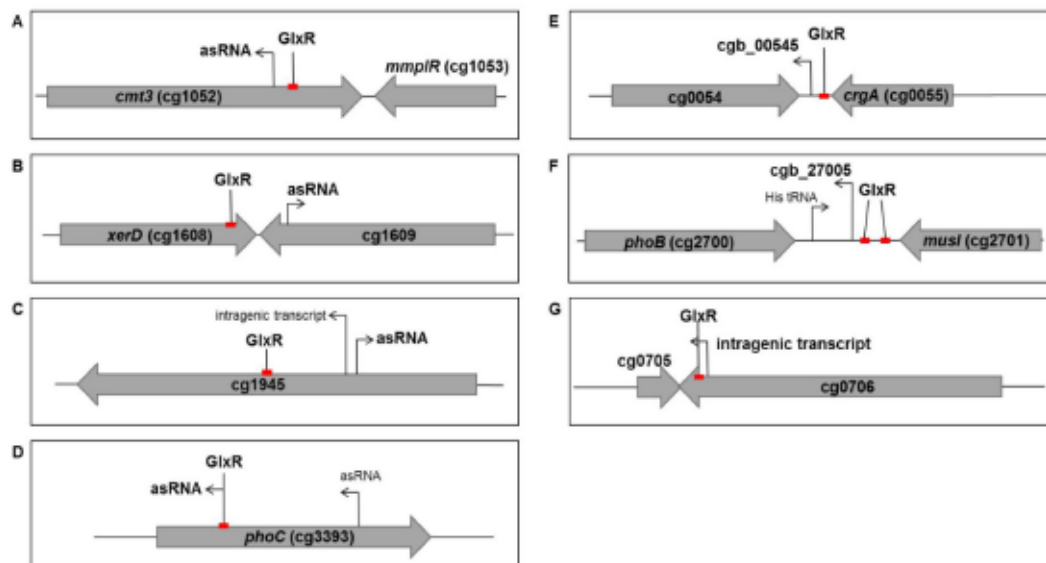


FIGURE 4 | Examples for GlxR binding sites (red boxes) located within coding region or in intergenic regions between convergently transcribed genes with a possible regulatory role for antisense transcripts (asRNA), small RNAs, or intragenic transcripts. GlxR binding site located: (A) -227 bp upstream of the TSS of an asRNA of *cmt3* (cg1052), (B) -114 bp upstream of the TSS of an asRNA of *cg1609*, (C) -618 bp upstream of an asRNA of *cg1945*. (D) on the TSS of an asRNA of *phoC* (cg3393), (E) GlxR binding site in the intergenic region of *cg0054* and *crgA* (cg0055) located -121 bp upstream of the TSS of *cg0054*, (F) in the intergenic region of *phoB* and *musI* located -190 bp and -432 bp upstream of the TSS of the sRNA *cgb_27005* and (G) within the coding region of *cg0706* located +34 bp downstream of an intragenic transcript. Information on sRNA, asRNA and intragenic transcripts was taken from Pfeifer-Sancar et al., 2013 and Mentz et al., 2013. The motifs of the GlxR binding sites are listed in Table S7.

DISCUSSION

In this study we analysed the influence of a missing adenylate cyclase CyaB on *in vivo* DNA binding of the global transcriptional regulator GlxR of *C. glutamicum* in order to better understand the different growth phenotypes of $\Delta cyaB$ and $\Delta glxR$ mutants. Whereas $\Delta glxR$ mutants show severe growth defects, $\Delta cyaB$ mutant grow like the WT except in the presence of acetate (Cha et al., 2010; Moon et al., 2007; Park et al., 2010; Toyoda et al., 2011; Wolf et al., 2020). Numerous *in vitro* studies have been performed with purified GlxR and target DNAs and binding of GlxR was found to be strictly dependent on the presence of cAMP (Bussmann et al., 2009; Jungwirth et al., 2013; Kohl & Tauch, 2009; Nishimura et al., 2011),

except for two cases (*cgR_1596*, *mscL*), where weak binding was observed in the absence of cAMP (Toyoda et al., 2011). CyaB, which is composed of an N-terminal membrane-integral domain with six predicted transmembrane helices that is linked via a HAMP domain to a class IIIc catalytic domain, is the only adenylate cyclase encoded in the genome of *C. glutamicum*. Our recent LC-MS/MS measurements indicated that a $\Delta cyaB$ mutant does not contain cAMP anymore (Wolf et al. 2020). Therefore, if cAMP is also essential for GlxR binding *in vivo*, the $\Delta cyaB$ mutant should show a similarly strong growth defect as a $\Delta glxR$ mutant, which is not the case. Our ChAP-Seq studies provide an explanation for this discrepancy, as they suggest that GlxR

binds *in vivo* to its target sites also in the absence of cAMP.

The four ChAP-Seq data sets generated in this work comparing GlxR binding in the WT and the $\Delta cyaB$ mutant after growth on either glucose or glucose plus acetate identified 243 GlxR peaks, if an EF ≥ 3 in at least one data set was used as initial selection criterion. In the $\Delta cyaB$ mutant, 234 and 205 of these peaks had an EF ≥ 1.5 when cultivated on glucose or on glucose plus acetate, respectively (Table 2). Therefore, GlxR bound to these sites also in the absence of cAMP, but with reduced affinity as shown by the lowered mean EFs in the $\Delta cyaB$ mutant, which was particularly evident in the presence of acetate (Table 2). This result agrees with ChIP-chip data obtained with *C. glutamicum* strain R (Toyoda et al., 2011) and suggests that *in vivo* cAMP is not essential for binding of GlxR to most of its target sites, in contrast to the *in vitro* situation. The difference between the growth phenotypes of $\Delta cyaB$ and $\Delta glxR$ mutants can thus be explained by the fact that GlxR can still exert its functions in the absence of cAMP.

If cAMP has a regulatory, but not an essential function for *in vivo* DNA-binding by GlxR, other, yet unknown factors might also be involved in the control of GlxR binding to DNA target sites within the cell. One possibility could be an interaction of GlxR with another protein, as has been shown, e.g., for CcpA and Hpr in *Bacillus subtilis* (Görke & Stülke, 2008). However, in the currently available literature there is no evidence so far for a protein interacting with GlxR. Another option for influencing the DNA-binding properties of GlxR *in vivo* can be posttranslational modifications. In a study globally analysing protein acetylation and protein succinylation in *C. glutamicum*, three succinylated lysine residues were detected in GlxR, i.e. Lys59, Lys155, and Lys212 (Mizuno et al., 2016). The influence of these modifications could be tested for example by replacing the positively charged lysine

residues with a negatively charged glutamate residue. In the case of the 2-oxoglutarate dehydrogenase inhibitor protein OdhI (Niebisch et al., 2006), succinylation at Lys132 reduced the binding to OdhA and thus inhibition of 2-oxoglutarate dehydrogenase activity (Komine-Abe et al., 2017).

Besides succinylation, also pupylation was detected for the GlxR protein at Lys57 (Küberl et al., 2014). Pupylation is a post-translational modification mainly occurring in Actinobacteria resembling ubiquitination in eukaryotes and was first identified in *Mycobacterium tuberculosis* (Pearce et al., 2008). Selected lysine residues of target proteins are covalently linked by an isopeptide bond with the C-terminal glutamate residue of the small prokaryotic ubiquitin-like protein Pup and this modification typically serves in *Mycobacterium* as a tag for degradation via the proteasome PrcAB (Cerdeira-Maira & Darwin, 2009; Lin et al., 2006; Samanovic et al., 2013). However, *Corynebacterium* species do not contain a proteasome and the only currently known function of pupylation is in the release of iron from ferritin and Dps, as pupylation triggers unfolding of the tagged protein by the ATPase Arc (Küberl et al., 2016). Whether pupylation of GlxR influences its function has not been studied yet. Of the 243 GlxR peaks identified in this study, 242 contained the sequence motif TGTGN₈CACA, which agrees with the previously described motif (Jungwirth et al., 2013; Kohl et al., 2008; Toyoda et al., 2011) and supports the validity of our data. 141 of the GlxR peaks were also found in previous studies, whereas 102 were not reported before (Table 3). Therefore, our analysis further expands the already large GlxR regulon. The reason for the identification of new GlxR targets is probably due to differences in the experimental conditions, such as using a GlxR variant with a Twin Strep-tag. Nevertheless, not all GlxR binding sites reported previously were detected in our study, with at least 24 missing (Table S5).

TABLE 3 | Newly described GlxR peaks identified in the four ChAP-Seq data sets generated in this study with the corresponding GlxR binding sites that were found upstream, intergenic or in the indicated genes. The symbol '<>' denotes divergently and '><' convergently oriented genes with a GlxR binding site in the intergenic region.

Locus tag (cg)	Adjacent gene(s)	Annotation	GlxR binding motif sequence ^a	Distance to next TSS ^b	Distance to next TLS ^b
cg0001	in <i>dnaA</i>	chromosomal replication initiation protein	GGTTCAAATATGCACG	-	+119
cg0054 >< cg0055	(cg0054) >< <i>argA</i>	put. iron-chelator utilization protein >< put. cell division membrane protein	TGACTGCCCGCAGCACA	-	+1188 >< +302
cg0061	<i>rodA</i> (<i>ftsW</i>)	put. FTSW/RODA/SPOVE-family cell cycle protein	AGTATCAGCAGCCACA	-	+48
cg0090	<i>citB</i>	two component response regulator	AGTCTGATTTTGCACA	-642; -807	-950
cg0156	<i>cysR</i>	transcriptional activator, ROK-family	TGTTCCGCAGCAGACT	-310	-310
cg0215	<i>cspA</i>	cold-shock protein A	GGTGTAAAAGCAGACA	-64	-245
cg0235	<i>emb</i> (<i>embC</i>)	arabinoxyltransferase	TGAGTAATTCCTCACC	-73	-73
cg0261	in <i>moeA1</i>	molybdopterin cofactor synthesis protein A1, MoeA-family	CGTGGCGAATCCCACT	-	+132
cg0280	-	hypothetical protein	TGTCTCATTTAACACA	-632	-632
cg0427	<i>tnp17b</i>	transposase fragment	AGTATACTTCCATACA	+16	-281
cg0440	-	hypothetical protein	TATGAGGATGCTCACA	-	-331
cg0576	in <i>rpoB</i>	DNA-directed RNA polymerase β subunit	TGAGTCAAACCAGACA	+1518; +1520	+1308
cg0583	in <i>fusA</i>	elongation factor EF-2/G	TGTAGGCGGTGCCACA	+897; +990	+791
cg0645	<i>creJ</i> (<i>cytP</i>)	cytochrome P450	CGTGATGGCTATCACT	-	-74
cg0646 <> cg0647	<i>creR</i> <> <i>secY</i>	put. transcriptional regulator, IclR-family <> preprotein translocase subunit	TATGATGCGTCTTACA	-71; -115 <> -60; -140	-202 <> -176
cg0658	in <i>rptA</i>	terminal rhamnopyranosyl transferase	TGTCGCCATGTCACT	-	+1393
cg0703	<i>guaA</i>	put. Gmp synthase	TGTCTGAAGGCTCACA	+7	+7
cg0706	in (cg0706)	put. membrane protein, conserved	GGTCTCCAACATCACA	+1070	+1070
cg0755 <> cg0756	<i>metY</i> <> <i>cstA</i>	O-acetylhomoserine sulfhydrylase <> carbon starvation protein A	TATGACTAGCCCCACT	-136 <> -30;-32;- 42; -59	-175 <> -258

Locus tag (cg)	Adjacent gene(s)	Annotation	GlxR binding motif sequence ^a	Distance to next TSS ^b	Distance to next TLS ^b
cg0764	in (cg0764)	put. transcriptional regulator, GntR-family	TGTTCAACCAGCCACA	+126	+126
cg0773	-	put. exodeoxyribonuclease	GGTTCCTCATGCCACA	-667	-667
cg0788	in <i>pmmB</i>	phosphoglucomutase/phosphomannomutase	TGTCTGTCACCCACA	+1423	+1386
cg0845	in (cg0845)	put. superfamily II DNA/RNA helicase, SNF2-family	AGTATGCAGGTTCCACA	+1543	+1543
cg0866	-	purine/pyrimidine phosphoribosyl transferase	CGTGATATTTGTCACG	-	-311
cg0875	in (cg0875)	conserved hypothetical protein	TGTGTCTTCCACCACA	-	+935
cg0904	-	hypothetical protein	TGCTTGATCTCCCACA	-	-328
cg0926	-	put. iron-siderophore transporter	TGTTCTTTACAAGACA	-	-159
cg0933	-	put. DNA or RNA helicase of superfamily II	TGTGGATGAAGCCACA	-87	-115
cg0962	-	put. secreted protein	GGTCAATCAGATCACT	-337	-337
cg0973	<i>pgi</i>	glucose-6-phosphate isomerase	TGTCGTGTTTCCCCT	-59	-87
cg1052	in <i>cmt3</i>	corynomycolyl transferase	GGTGCCAAGGCTCACA	+1374;+1377	+1333
cg1075	in <i>prxA</i>	ribose-phosphate pyrophosphokinase	TGTTCCATGAGCCACT	+377	+225
cg1087	-	put. membrane protein	TGTGAAAGCTATCACA	-3	-29
cg1108	<i>porC</i>	put. secreted protein	AGTCACATAAATCACT	-	-90
cg1111	<i>eno</i>	enolase, phosphopyruvate hydratase	CGTGTCCGATCAGACA	-93	-163
cg1147	in <i>ssul</i>	NADPH-dependent FMN reductase	TGTACCACCGCTCACA	+468	+468
cg1256	<i>dapD</i>	tetrahydrodipicolinate succinylase	AGTTTCAACTGTGACA	-275	-275
cg1432	<i>ilvD</i>	dihydroxy-acid dehydratase	CGTCTGAAACCTCACA	+24; -46	-165
cg1520	in (cg1520)	put. secreted protein CGPI region	TGTACTGCTAATCACA	-	+299
cg1608 > < cg1609	<i>xerD</i> > < (cg1609)	tyrosine recombinase > < put. ATPase component of ABC transporter	TGAGCCCCGCGCCACA	-	+894 > < +1571
cg1697	<i>aspA</i>	aspartate ammonia-lyase aspartase	TGTACTGCCTCTCACA	+33	-8
cg1728 > < cg1730	(cg1728) > < (cg1730)	hypothetical protein, conserved > < put. secreted protease subunit	GGTGAGGTCTGCCACA	-	+727 > < +1486
cg1812	<i>pyrF</i>	orotidine 5-phosphate decarboxylase	TGTTCCGCTGATCACC	-	-119

Locus tag (cg)	Adjacent gene(s)	Annotation	GlxR binding motif sequence ^a	Distance to next TSS ^b	Distance to next TLS ^b
cg1895	in (cg1895)	put. secreted protein, CGP3 region	TGTGGTCTTCAACACT	-	+2116
cg1898	-	hypothetical protein CGP3 region	TGTCGCCACTGCCACA	-	-372
cg1909	-	hypothetical protein CGP3 region	GGTAAGTATTTCAGACA	-	-160
cg1913	-	hypothetical protein CGP3 region	TGTGCAGAATTTCACA	-	+17
cg1924	-	hypothetical protein CGP3 region	AGTAACACAGACCACA	-	-534
cg1927	-	put. molecular chaperone CGP3 region	TGTGCCTCGTAGCACA	-	-362
cg1945	in (cg1945)	hypothetical protein, conserved CGP3 region	TGTTTCATCCCCTCACA	+1175	+1175
cg1972	-	put. translation elongation factor, GTPase CGP3 region	TGTGCATTTCTACACA	-	-31
cg1995	in (cg1995)	hypothetical protein, CGP3 region	TGTATCAGTTGCCACT	-	+4218
cg1999	-	hypothetical protein, CGP3 region	TGTCTACTCTGTTACA	-	-511
cg2035	-	put. methyltransferase, CGP3 region	TGTCTAATATGGTACT	-256	-271
cg2064	-	put. DNA topoisomerase I omega-protein; CGP3 region	CGTGAAATAGGACACA	-	-619
cg2109	<i>oxyR</i>	hydrogen peroxide sensing regulator, Lys-family	no motif	-66	-66
cg2134	-	put. membrane protein	GGTGGCTCCTGCCACA	-60	-99
cg2157	<i>terC</i>	tellurium resistance membrane protein	AGTAACTTAGCCACA	-210; -212	+13
cg2184	<i>oppD</i>	ATPase component of ABC-type transport system	TGTTCCCAGTGCCACA	-	-224
cg2324	-	hypothetical protein	TATGTCTGACAACACT	+10	+7
cg2404	<i>qcrA (qcrA1)</i>	cytochrome bc1 complex, Rieske iron-sulfur protein	TGTCGCCTGCATCACC	-	-650
cg2470	(cg2470)	secreted ABC transporter substrate-binding protein	TGAGACATTTACATA	+7	-81
<>	<>	<>		-202	-205
cg2471	(cg2471)	put. protein			
cg2480	-	hypothetical protein	TGTCGACACCGTCACA	-484; -737	-737
cg2496	(cg2496)	put. secreted protein	GGTCTCTTCGGTCACT	+2090	+2090
><	><	><			
cg2497	(cg2497)	hypothetical protein		-	+1213
cg2497	in (cg2497)	hypothetical protein	AGTGAGATCCCCCACA	-	+250
cg2521	<i>fadD15</i>	long-chain fatty acid CoA ligase	TGTATCTAAATTCACA	-292	-404

Locus tag (cg)	Adjacent gene(s)	Annotation	GlxR binding motif sequence ^a	Distance to next TSS ^b	Distance to next TLS ^b
cg2557	(cg2557)	put. secondary Na ⁺ /bile acid symporter	TATGAAAGTTCGCACA	-	-77
<>	<>	<>		<>	<>
cg2558	(cg2558)	put. protein, related to aldose 1-epimerase		-73	-73
cg2593	(cg2593)	put. secreted or membrane protein	TGACGCTTAAGTCACA	+526	+447
><	><	><		><	><
cg2594	<i>rpmA</i>	50S ribosomal protein L27		-	+265
cg2642	in <i>benK1</i> (<i>benK</i>)	benzoate transport protein, MFS transporter	TGTTCCCTCCTGCCACT	-	+573
cg2651	-	put. protein-fragment	TGTACAATAACACACT	-229	-229
cg2678	-	put. ABC-type transport systems	GGTGACATTATTCACA	-312	-364
cg2692	-	put. thioesterase	CGTCTCTTTGCTCACA	+28	-50
cg2695	in (c2695)	put. ABC-type transport system, ATPase component	TGTCCCTGCCGTCACA	+666; +669	+630
cg2699	<i>ctiP</i>	copper transport and insertion protein	TGTGTGAAGCCCCACA	-108	-108
<>	<>	<>		<>	<>
cg2700	<i>phoB</i>	alkaline phosphatase		-551	-542
cg2700	<i>phoB</i>	alkaline phosphatase	TGTGTTGCAGGTCACA	+1919	-1919
><	><	><		><	><
cg2701	<i>musI</i>	put. membrane protein		+1203	+1203
cg2700	<i>phoB</i>	alkaline phosphatase	TGTGAGCCACGCCACT	+2152	+2161
><	><	><		><	><
cg2701	<i>musI</i>	put. membrane protein		+961	+961
cg2741	-	hypothetical protein	TGCATAGTTTGTCACT	-160; -156	-286
cg2748	-	put. membrane protein, conserved	GGTGCAGTTGGTCACC	-56	-56
cg2785	-	put. membrane protein	TGTCCGTAGACACACA	-	-167
cg2797	-	hypothetical protein	TGTTCAAAGCTTCACA	-	-224
cg2811	in (cg2811)	put. ABC-type transport system	CGTCTGGTTAGTCACA	-	+1840
cg2843	in <i>pstB</i>	ABC-type phosphate transport system	GGTCTGATCGGACACA	-	+640
cg2898	in (cg2898)	put. 3-ketosteroid dehydrogenase	TGTTGATCCCACACC	-	+379
cg2936	<i>nanR</i>	transcriptional regulator, GntR-family	TGAGCATAGCGTCACA	-230	-255
<>	<>	<>		<>	<>
cg2937	<i>siaE</i>	ABC-Transporter for sialic acid		+45	-54
cg3030	-	put. hydrolase or acyltransferase α/β hydrolase superfamily	AGTGCACCACGAGACA	-	-359

Locus tag (cg)	Adjacent gene(s)	Annotation	GlxR binding motif sequence ^a	Distance to next TSS ^b	Distance to next TLS ^b
cg3041	-	put. ABC-type multidrug transport system	AGTCGCATTCAACACA	-	-196
cg3043	-	NTP pyrophosphohydrolase/oxidative damage repair enzyme	TGATGTATACAGCACA	-505	-505
cg3061	<i>cgtR6</i>	two component response regulator	TGTTGCATATGATACA	-179	-233
cg3091	-	hypothetical protein	AGTTTGTGGCTTACA	-	-415
cg3092	in (cg3092)	put. 2-polyprenylphenol hydroxylase or related flavodoxin oxidoreductase	TGTTATTTATTGCACA	+750	+750
cg3112	<i>cysZ</i>	sulfate transporter	AGTTCACACCATACT	-	-474
cg3174	in <i>mmpL1</i>	exporter of the MMPL-family	TGTTTGTTCCTCCACA	-	+909
cg3187	in <i>afbB</i>	arabinofuranosyltransferase	AGTCGCCACCAACACC	+595	+595
cg3203	in (cg3203)	hypothetical protein, conserved	TGCCTCATTACCCT	+227	+223
cg3247	<i>hrrA</i> (<i>cgtR11</i>)	two component response regulator	TGAATGTTTCGCCACA	-352	-434
cg3255	<i>uspA3</i>	universal stress protein no 3	TGAGGCTTTGACACT	-63; -65	-131
cg3313	<i>php1b</i> (<i>mcrB</i>)	membrane carboxypeptidase	TATTCTCTACAGCACA	+6; +202	-51
cg3332	in <i>gor3</i>	put. NADPH:quinone oxidoreductase	GGTACTCTGCGTTACT	+329	+329
cg3393	in <i>phoC</i>	put. secreted phosphoesterase	TGTACCACTCATCACA	-	+1341
cg3417	-	put. NTP pyrophosphohydrolase	GGTGAGCTTTCAGACA	-531	-970
cg3428	<i>gidB</i>	glucose-inhibited division protein B	TGTTCCGGTGCCTCACT	-620; -623	-660
-	-	phage integrase	AATGAATCCACTCACC	-	-254

a: motif sequence was detected by using the program MEME-ChIP with the DNA fragment of the detected GlxR peaks as input sequences; the 16 bp sequence shows the most probable GlxR binding site within this sequences

b: distance counted from the centre of the GlxR binding site to the start of the TSS or TLS (counting includes the first base of TSS or TLS; information of TSS was taken from Pfeifer-Sancar et al. 2013; for some genes several TSS were identified

When checking these sites, we found that 14 of the corresponding DNA regions were enriched in our ChAP-Seq experiments not falling in our definition of a GlxR binding site due to EF < 3 in a data set (e.g. *fumC*, *pabB*, *uspA2*, or *oxiC*). Ten of the 24 missing GlxR binding sites were not enriched in our data at all (e.g. *aceA*, *aceB*, *glnA* or *ldhA*). Reasons

therefore could be DNA regions that were not accessible for GlxR binding under the conditions used.

Table 3 lists newly identified GlxR binding sites and the distances to the neighbouring genes. A prediction of the influence of GlxR on the transcription of the neighbouring gene is possible for the repressed

genes, where GlxR binding is assumed to interfere with binding of RNA polymerase (Browning and Busby 2004). This is likely for binding sites located between 0 and -40 bp upstream of a TSS or TLS and within about 50 bp downstream of a TSS or TLS. According to this assumption, *guaA* (cg0703), cg1087, *aspA* (cg1697), cg1913, cg1972, cg2470, *siaE* (cg2937) and *pbp1b* (cg3313) might represent novel target genes repressed by GlxR. For neighbouring genes with a GlxR binding site located >40 bp upstream of a TSS, an activator function of GlxR might be more likely, but needs to be tested experimentally. Examples for genes that might be activated by GlxR are *pgi* (cg0973, glucose 6-phosphate isomerase), *eno* (cg1111, enolase), or *ctiP* (cg2699, copper transport and insertion protein). The former two genes are involved in glycolysis and several other genes of this pathway were previously shown to be activated by GlxR, such as *pfkA*, *gapA*, or *aceE* (Toyoda et al., 2011). The *ctiP* gene is required for the transport and insertion of copper into the cytochrome *aa₃* oxidase (Morosov et al., 2018), which in *C. glutamicum* forms a supercomplex with the cytochrome *bc₁* complex (Moe et al., 2022; Niebisch & Bott, 2003). Expression of the genes *ctaD* and *ctaC* encoding subunit I and II of cytochrome *aa₃* oxidase was shown to be activated by GlxR (Toyoda et al., 2011) and it seems reasonable that also the *ctiP* gene required for the maturation of cytochrome *aa₃* oxidase is activated by GlxR. In this context, further approaches are required that allow a genome-wide analysis of the influence of GlxR on transcription of its target genes.

GlxR binding sites not clearly linked to the TSS of a protein-coding gene were further manually checked for nearby TSSs of non-protein coding RNAs. Indeed these GlxR binding sites were often found to be close to the TSS of sRNAs (adjacent to the genes cg0054/*crgA*, *metY/cstA*, *cgpS/cg1967*, *phoB/musI*, *cglR6/purA*), asRNAs (e.g. of the gene *cmt3*, cg1609, cg1945, cg2362 or *phoC*) or tRNAs (tRNA^{Leu}, tRNA^{Arg}, tRNA^{Gly} and

tRNA^{Asp}), which suggests that GlxR might influence transcription of these RNAs (Table S7). Therefore, the regulatory influence of GlxR could be even broader than previously assumed (Kohl & Tauch, 2009). In prokaryotes, sRNAs can influence transcription, translation, RNA stability, or protein activity (Storz et al., 2011; Waters & Storz, 2009) and are involved in the regulation of metabolism, transcriptional regulation, transport mechanisms, stress responses, or virulence (Delihias & Forst, 2001; Georg & Hess, 2011; Vogel & Papenfort, 2006). A genome-wide analysis identified over 800 sRNA genes in *C. glutamicum*, which were classified into 316 UTRs of mRNAs, 543 cis-antisense RNAs, and 262 trans-encoded sRNAs (Mentz et al., 2013). Only few of them have been studied experimentally, such as the 6C RNA, which is highly conserved in Actinobacteria and was shown to highly abundant and stable in *C. glutamicum* (Pahlke et al., 2016). A GlxR binding site was identified upstream of the 6C RNA (Jungwirth et al., 2013), which was also found in our analysis. *In vivo* GlxR-DNA binding regions within the *rrn* operons and tRNA^{Glu} of and tRNA^{Asp} were mentioned in literature before, but were excluded from the analysis due to high variation in their read counts (Jungwirth et al., 2013). As our studies also showed *in vivo* GlxR binding upstream of some tRNAs (tRNA^{Leu}, tRNA^{Arg}, tRNA^{Gly} and of tRNA^{Asp}) and within the *rrn* operons (*rrnA*, *rrnB*, *rrnC* and *rrnF*), this should be analysed in further studies.

Several GlxR binding sites were located intragenically far away from neighbouring genes or in intergenic regions of convergently transcribed genes. In these cases, a direct influence of GlxR on transcription appears unlikely. GlxR ortholog, for example Crp of *E. coli* and Crp of *M. tuberculosis*, also revealed a high number of intragenic binding sites in previous studies (Grainger et al., 2005; Knapp et al., 2015). It was suggested that this type of binding influences gene regulation by modifying the chromatin structure, similar to

nucleoid associated proteins (NAPs), instead of direct interaction with RNA polymerase. This NAP-like function of Crp was supported by the observation that Crp is able to bend DNA in *in vitro* studies (Bai et al., 2005; Lin & Lee, 2003). On the other hand, one cannot exclude a regulation of transcription over a long distance, as shown for EspR in *M. tuberculosis* (Hunt et al., 2012). This transcriptional regulator activates the transcription of its target gene by binding to an enhancer-like sequence far upstream of the TSS of the target gene (~800 to 1000 bp), leading to looping of the DNA (Hunt et al., 2012; Rosenberg et al., 2011).

In conclusion, our study provides new potential target genes of GlxR in *C. glutamicum* and shows that *in vivo* DNA-binding by GlxR is enhanced by cAMP, but not strictly dependent on its presence. Therefore, additional factors might be involved in the control of GlxR activity, such as posttranslational modifications (succinylation, pupylation). Regarding a deeper physiological understanding of GlxR, identification of the stimulus sensed by CyaB would be a major breakthrough. If GlxR is considered as a global regulator coordinating catabolism and anabolism with growth and cell division, parameters such as the proton-motive force or the energy charge appear to be suitable for providing key information on the fitness status of the cell.

CONTRIBUTIONS

NW constructed mutants, plasmids and performed all experimental work except the one specified below for other authors, wrote the first draft of the manuscript and generated the figures and tables if not mentioned otherwise. LL constructed the strain *C. glutamicum::glxR-TS* (named WT_{GlxR-TS}), cultivated and generated one of the nine ChAP-Seq samples. MBu performed the microarray experiment with the WT and the Δ *cyaB* mutant on glucose. TP supervised the bioinformatics of the microarray analysis and

the first evaluation of the ChAP-Seq results. AF normalized the data of the four ChAP-Seq sample conditions and performed comparisons of peak heights and generated the draft version of Fig. 1. MBa coached the experimental work and supported the design of this study. MBo designed the study, supervised the experimental work and was responsible for the final version of the manuscript.

REFERENCES

- Bai, G., McCue, L. A., & McDonough, K. A. (2005). Characterization of *Mycobacterium tuberculosis* Rv3676 (CRP_{Mt}), a cyclic AMP receptor protein-like DNA binding protein. *J Bacteriol*, 187(22), 7795-7804.
- Bailey, T. L., & Elkan, C. (1994). Fitting a mixture model by expectation maximization to discover motifs in biopolymers. *Proc Int Conf Intell Syst Mol Biol*, 2, 28-36.
- Becker, J., & Wittmann, C. (2012). Systems and synthetic metabolic engineering for amino acid production - the heartbeat of industrial strain development. *Curr Opin Biotechnol*, 23(5), 718-726.
- Burkovski, A. (2008). *Corynebacteria: Genomics and Molecular Biology* (1 ed.). Caister Academic Press.
- Bussmann, M. (2009). cAMP dependent regulation of the TCA cycle by GlxR and oxidative stress response regulation by RosR in *Corynebacterium glutamicum*. urn:nbn:de:hbz:061-20101104-151101-4.
- Bussmann, M., Emer, D., Hasenbein, S., Degraf, S., Eikmanns, B. J., & Bott, M. (2009). Transcriptional control of the succinate dehydrogenase operon *sdhCAB* of *Corynebacterium glutamicum* by the cAMP-dependent regulator GlxR and the LuxR-type regulator RamA. *J Biotechnol*, 143(3), 173-182.
- Cerda-Maira, F., & Darwin, K. H. (2009). The *Mycobacterium tuberculosis* proteasome: more than just a barrel-shaped protease. *Microbes Infect*, 11(14-15), 1150-1155.
- Cha, P. H., Park, S. Y., Moon, M. W., Subhadra, B., Oh, T. K., Kim, E., Kim, J. F., & Lee, J. K. (2010). Characterization of an adenylate cyclase gene (*cyaB*) deletion mutant of *Corynebacterium glutamicum* ATCC 13032. *Appl Microbiol Biotechnol*, 85(4), 1061-1068.
- Delihias, N., & Forst, S. (2001). MicF: an antisense RNA gene involved in response of *Escherichia coli* to global stress factors. *J Mol Biol*, 313(1), 1-12.
- Eggeling, L., & Bott, M. (2005). *Handbook of Corynebacterium glutamicum* (1 ed.). CRC Press.
- Eggeling, L., & Bott, M. (2015). A giant market and a powerful metabolism: L-lysine provided by *Corynebacterium glutamicum*. *Appl Microbiol Biotechnol*, 99(8), 3387-3394.
- Freudl, R. (2017). Beyond amino acids: Use of the *Corynebacterium glutamicum* cell factory for the secretion of heterologous proteins. *J Biotechnol*, 258, 101-109.
- Frunzke, J., Engels, V., Hasenbein, S., Gatgens, C., & Bott, M. (2008). Coordinated regulation of gluconate catabolism and glucose uptake in *Corynebacterium glutamicum* by two functionally equivalent transcriptional regulators, GntR1 and GntR2. *Mol Microbiol*, 67(2), 305-322.
- Georg, J., & Hess, W. R. (2011). *cis*-antisense RNA, another level of gene regulation in bacteria. *Microbiol Mol Biol Rev*, 75(2), 286-300.
- Görke, B., & Stülke, J. (2008). Carbon catabolite repression in bacteria: many ways to make the most out of nutrients. *Nat Rev Microbiol*, 6(8), 613-624.
- Gosset, G., Zhang, Z., Nayyar, S., Cuevas, W. A., & Saier, M. H., Jr. (2004). Transcriptome analysis of Crp-dependent catabolite control of gene expression in *Escherichia coli*. *J Bacteriol*, 186(11), 3516-3524.
- Grainger, D. C., Hurd, D., Harrison, M., Holdstock, J., & Busby, S. J. W. (2005). Studies of the distribution of *Escherichia coli* cAMP-receptor protein and RNA polymerase along the *E. coli* chromosome. *Proc Natl Acad Sci U S A*, 102(49), 17693-17698.

- Hunt, D. M., Sweeney, N. P., Mori, L., Whalan, R. H., Comas, I., Norman, L., Cortes, T., Arnvig, K. B., Davis, E. O., Stapleton, M. R., Green, J., & Buxton, R. S. (2012). Long-range transcriptional control of an operon necessary for virulence-critical ESX-1 secretion in *Mycobacterium tuberculosis*. *J Bacteriol*, *194*(9), 2307-2320.
- Ikeda, M., & Nakagawa, S. (2003). The *Corynebacterium glutamicum* genome: features and impacts on biotechnological processes. *Appl Microbiol Biotechnol*, *62*(2), 99-109.
- Inui, M., Kawaguchi, H., Murakami, S., Vertès, A. A., & Yukawa, H. (2004). Metabolic engineering of *Corynebacterium glutamicum* for fuel ethanol production under oxygen-deprivation conditions. *J Mol Microbiol Biotechnol*, *8*(4), 243-254.
- Jungwirth, B., Sala, C., Kohl, T. A., Uplekar, S., Baumbach, J., Cole, S. T., Puhler, A., & Tauch, A. (2013). High-resolution detection of DNA binding sites of the global transcriptional regulator GlxR in *Corynebacterium glutamicum*. *Microbiology*, *159*(Pt 1), 12-22.
- Kensy, F., Zang, E., Faulhammer, C., Tan, R. K., & Büchs, J. (2009). Validation of a high-throughput fermentation system based on online monitoring of biomass and fluorescence in continuously shaken microtiter plates. *Microb. Cell Fact.*, *8*, 31.
- Keppel, M., Hünnefeld, M., Filipchuk, A., Viets, U., Davoudi, C. F., Krüger, A., Mack, C., Pfeifer, E., Polen, T., Baumgart, M., Bott, M., & Frunzke, J. (2020). HrrSA orchestrates a systemic response to heme and determines prioritization of terminal cytochrome oxidase expression. *Nucleic Acids Res*, *48*(12), 6547-6562.
- Kim, H. J., Kim, T. H., Kim, Y., & Lee, H. S. (2004). Identification and characterization of *glxR*, a gene involved in regulation of glyoxylate bypass in *Corynebacterium glutamicum*. *J Bacteriol*, *186*(11), 3453-3460.
- Kinoshita, S., Udaka, S., & Shimono, M. (1957). Studies on amino acid fermentation. Part 1. Production of L-glutamic acid by various microorganisms. *J Gen Appl Microbiol*, *3*, 193-205.
- Knapp, G. S., Lyubetskaya, A., Peterson, M. W., Gomes, A. L. C., Ma, Z., Galagan, J. E., & McDonough, K. A. (2015). Role of intragenic binding of cAMP responsive protein (CRP) in regulation of the succinate dehydrogenase genes Rv0249c-Rv0247c in TB complex mycobacteria. *Nucleic Acids Res*, *43*(11), 5377-5393.
- Kohl, T. A., Baumbach, J., Jungwirth, B., Puhler, A., & Tauch, A. (2008). The GlxR regulon of the amino acid producer *Corynebacterium glutamicum*: *in silico* and *in vitro* detection of DNA binding sites of a global transcription regulator. *J Biotechnol*, *135*(4), 340-350.
- Kohl, T. A., & Tauch, A. (2009). The GlxR regulon of the amino acid producer *Corynebacterium glutamicum*: Detection of the corynebacterial core regulon and integration into the transcriptional regulatory network model. *J Biotechnol*, *143*(4), 239-246.
- Komine-Abe, A., Nagano-Shoji, M., Kubo, S., Kawasaki, H., Yoshida, M., Nishiyama, M., & Kosono, S. (2017). Effect of lysine succinylation on the regulation of 2-oxoglutarate dehydrogenase inhibitor, OdhI, involved in glutamate production in *Corynebacterium glutamicum*. *Biosci Biotechnol Biochem*, *81*(11), 2130-2138.
- Körner, H., Sofia, H. J., & Zumft, W. G. (2003). Phylogeny of the bacterial superfamily of Crp-Fnr transcription

- regulators: exploiting the metabolic spectrum by controlling alternative gene programs. *FEMS Microbiol Rev*, 27(5), 559-592.
- Küberl, A., Fränzel, B., Eggeling, L., Polen, T., Wolters, D. A., & Bott, M. (2014). Pupylated proteins in *Corynebacterium glutamicum* revealed by MudPIT analysis. *Proteomics*, 14(12), 1531-1542.
- Küberl, A., Polen, T., & Bott, M. (2016). The pupylation machinery is involved in iron homeostasis by targeting the iron storage protein ferritin. *Proc Natl Acad Sci U S A*, 113(17), 4806-4811.
- Letek, M., Valbuena, N., Ramos, A., Ordonez, E., Gil, J. A., & Mateos, L. M. (2006). Characterization and use of catabolite-repressed promoters from gluconate genes in *Corynebacterium glutamicum*. *J Bacteriol*, 188(2), 409-423.
- Lin, G., Hu, G., Tsu, C., Kunes, Y. Z., Li, H., Dick, L., Parsons, T., Li, P., Chen, Z., Zwickl, P., Weich, N., & Nathan, C. (2006). *Mycobacterium tuberculosis* *prcBA* genes encode a gated proteasome with broad oligopeptide specificity. *Mol Microbiol*, 59(5), 1405-1416.
- Lin, S. H., & Lee, J. C. (2003). Determinants of DNA bending in the DNA-cyclic AMP receptor protein complexes in *Escherichia coli*. *Biochemistry*, 42(17), 4809-4818.
- Mentz, A., Neshat, A., Pfeifer-Sancar, K., Puhler, A., Ruckert, C., & Kalinowski, J. (2013). Comprehensive discovery and characterization of small RNAs in *Corynebacterium glutamicum* ATCC 13032. *BMC Genomics*, 14, 714.
- Mizuno, Y., Nagano-Shoji, M., Kubo, S., Kawamura, Y., Yoshida, A., Kawasaki, H., Nishiyama, M., Yoshida, M., & Kosono, S. (2016). Altered acetylation and succinylation profiles in *Corynebacterium glutamicum* in response to conditions inducing glutamate overproduction. *Microbiologyopen*, 5(1), 152-173.
- Moe, A., Kovalova, T., Król, S., Yanofsky, D. J., Bott, M., Sjöstrand, D., Rubinstein, J. L., Högbom, M., & Brzezinski, P. (2022). The respiratory supercomplex from *C. glutamicum*. *Structure*, 30(3), 338-349, e333.
- Moon, M. W., Park, S. Y., Choi, S. K., & Lee, J. K. (2007). The phosphotransferase system of *Corynebacterium glutamicum*: features of sugar transport and carbon regulation. *J Mol Microbiol Biotechnol*, 12(1-2), 43-50.
- Morosov, X., Davoudi, C. F., Baumgart, M., Brocker, M., & Bott, M. (2018). The copper-deprivation stimulon of *Corynebacterium glutamicum* comprises proteins for biogenesis of the actinobacterial cytochrome *bc₁-aa₃* supercomplex. *J Biol Chem*, 293(40), 15628-15640.
- Niebisch, A., & Bott, M. (2001). Molecular analysis of the cytochrome *bc₁-aa₃* branch of the *Corynebacterium glutamicum* respiratory chain containing an unusual diheme cytochrome *c₁*. *Arch Microbiol*, 175(4), 282-294.
- Niebisch, A., & Bott, M. (2003). Purification of a cytochrome *bc₁-aa₃* supercomplex with quinol oxidase activity from *Corynebacterium glutamicum*. Identification of a fourth subunit of cytochrome *aa₃* oxidase and mutational analysis of diheme cytochrome *c₁*. *J Biol Chem*, 278(6), 4339-4346.
- Niebisch, A., Kabus, A., Schultz, C., Weil, B., & Bott, M. (2006). Corynebacterial protein kinase G controls 2-oxoglutarate dehydrogenase activity via the phosphorylation status of the OdhI protein. *J Biol Chem*, 281(18), 12300-12307.

- Nishimura, T., Teramoto, H., Toyoda, K., Inui, M., & Yukawa, H. (2011). Regulation of the nitrate reductase operon *narKGHJ* by the cAMP-dependent regulator GlxR in *Corynebacterium glutamicum*. *Microbiology*, *157*(Pt 1), 21-28.
- Pahlke, J., Dostálová, H., Holátko, J., Degner, U., Bott, M., Pátek, M., & Polen, T. (2016). The small 6C RNA of *Corynebacterium glutamicum* is involved in the SOS response. *RNA Biol*, *13*(9), 848-860.
- Park, S. Y., Moon, M. W., Subhadra, B., & Lee, J. K. (2010). Functional characterization of the *glxR* deletion mutant of *Corynebacterium glutamicum* ATCC 13032: involvement of GlxR in acetate metabolism and carbon catabolite repression. *FEMS Microbiol Lett*, *304*(2), 107-115.
- Pearce, M. J., Mintseris, J., Ferreyra, J., Gygi, S. P., & Darwin, K. H. (2008). Ubiquitin-like protein involved in the proteasome pathway of *Mycobacterium tuberculosis*. *Science*, *322*(5904), 1104-1107.
- Pfeifer-Sancar, K., Mentz, A., Ruckert, C., & Kalinowski, J. (2013). Comprehensive analysis of the *Corynebacterium glutamicum* transcriptome using an improved RNAseq technique. *BMC Genomics*, *14*, 888.
- Pfeifer, E., Hünnefeld, M., Popa, O., Polen, T., Kohlheyer, D., Baumgart, M., & Frunzke, J. (2016). Silencing of cryptic prophages in *Corynebacterium glutamicum*. *Nucleic Acids Res.*, *44*(21), 10117-10131.
- Rosenberg, O. S., Dovey, C., Tempesta, M., Robbins, R. A., Finer-Moore, J. S., Stroud, R. M., & Cox, J. S. (2011). EspR, a key regulator of *Mycobacterium tuberculosis* virulence, adopts a unique dimeric structure among helix-turn-helix proteins. *Proc Natl Acad Sci U S A*, *108*(33), 13450-13455.
- Samanovic, M. I., Li, H., & Darwin, K. H. (2013). The pup-proteasome system of *Mycobacterium tuberculosis*. *Subcell Biochem*, *66*, 267-295.
- Sambrook, J., & Russell, D. (2001). *Molecular Cloning. A Laboratory Manual* (3rd ed.). Cold Spring Harbor Laboratory Press.
- Schäfer, A., Tauch, A., Jäger, W., Kalinowski, J., Thierbach, G., & Puhler, A. (1994). Small mobilizable multi-purpose cloning vectors derived from the *Escherichia coli* plasmids pK18 and pK19: selection of defined deletions in the chromosome of *Corynebacterium glutamicum*. *Gene*, *145*(1), 69-73.
- Schröder, J., & Tauch, A. (2010). Transcriptional regulation of gene expression in *Corynebacterium glutamicum*: the role of global, master and local regulators in the modular and hierarchical gene regulatory network. *FEMS Microbiol Rev*, *34*(5), 685-737.
- Schulte, J., Baumgart, M., & Bott, M. (2017). Identification of the cAMP phosphodiesterase CpdA as novel key player in cAMP-dependent regulation in *Corynebacterium glutamicum*. *Mol Microbiol*, *103*(3), 534-552.
- Soberón-Chávez, G., Alcaraz, L. D., Morales, E., Ponce-Soto, G. Y., & Servín-González, L. (2017). The transcriptional regulators of the CRP family regulate different essential bacterial functions and can be inherited vertically and horizontally. *Front Microbiol*, *8*(959).
- Storz, G., Vogel, J., & Wassarman, K. M. (2011). Regulation by small RNAs in bacteria: expanding frontiers. *Mol Cell*, *43*(6), 880-891.
- Studier, F. W. (2005). Protein production by auto-induction in high-density shaking cultures. *Protein Expr Pur*, *41*(1), 207-234.

- Studier, F. W., & Moffatt, B. A. (1986). Use of bacteriophage T7 RNA polymerase to direct selective high-level expression of cloned genes. *J Mol Biol*, *189*(1), 113-130.
- Townsend, P. D., Jungwirth, B., Pojer, F., Bussmann, M., Money, V. A., Cole, S. T., Puhler, A., Tauch, A., Bott, M., Cann, M. J., & Pohl, E. (2014). The crystal structures of apo and cAMP-bound GlxR from *Corynebacterium glutamicum* reveal structural and dynamic changes upon cAMP binding in CRP/FNR family transcription factors. *PLoS One*, *9*(12), e113265.
- Toyoda, K., Teramoto, H., Inui, M., & Yukawa, H. (2011). Genome-wide identification of *in vivo* binding sites of GlxR, a cyclic AMP receptor protein-type regulator in *Corynebacterium glutamicum*. *J Bacteriol*, *193*(16), 4123-4133.
- van Ooyen, J., Emer, D., Bussmann, M., Bott, M., Eikmanns, B. J., & Eggeling, L. (2011). Citrate synthase in *Corynebacterium glutamicum* is encoded by two *gltA* transcripts which are controlled by RamA, RamB, and GlxR. *J Biotechnol*, *154*(2-3), 140-148.
- Vogel, J., & Papenfort, K. (2006). Small non-coding RNAs and the bacterial outer membrane. *Curr Opin Microbiol*, *9*(6), 605-611.
- Waters, L. S., & Storz, G. (2009). Regulatory RNAs in bacteria. *Cell*, *136*(4), 615-628.
- Wendisch, V. F., Mindt, M., & Perez-Garcia, F. (2018). Biotechnological production of mono- and diamines using bacteria: recent progress, applications, and perspectives. *Appl Microbiol Biotechnol*, *102*(8), 3583-3594.
- Wieschalka, S., Blombach, B., Bott, M., & Eikmanns, B. J. (2013). Bio-based production of organic acids with *Corynebacterium glutamicum*. *Microb Biotechnol*, *6*(2), 87-102.
- Wolf, N., Bussmann, M., Koch-Koerfges, A., Katcharava, N., Schulte, J., Polen, T., Hartl, J., Vorholt, J. A., Baumgart, M., & Bott, M. (2020). Molecular basis of growth inhibition by acetate of an adenylate cyclase-deficient mutant of *Corynebacterium glutamicum*. *Front Microbiol*, *11*(11:87).
- Wolf, S., Becker, J., Tsuge, Y., Kawaguchi, H., Kondo, A., Marienhagen, J., Bott, M., Wendisch, Volker F., & Wittmann, C. (2021). Advances in metabolic engineering of *Corynebacterium glutamicum* to produce high-value active ingredients for food, feed, human health, and well-being. *Essays Biochem*, *65*(2), 197-212.
- Yukawa, H., & Inui, M. (2013). *Corynebacterium glutamicum: Biology and Biotechnology* (1 ed.). Springer-Verlag.
- Zheng, D., Constantinidou, C., Hobman, J. L., & Minchin, S. D. (2004). Identification of the CRP regulon using *in vitro* and *in vivo* transcriptional profiling. *Nucleic Acids Res*, *32*(19), 5874-5893.

2.4 Supplementary materials ‘Comparison of *in vivo* GlxR binding in *Corynebacterium glutamicum* ATCC 13032 and the adenylate cyclase deletion mutant Δ *cydB* using ChAP-Seq’

Supplementary materials ‘Comparison of *in vivo* GlxR binding in *Corynebacterium glutamicum* ATCC 13032 and the adenylate cyclase deletion mutant Δ *cydB* using ChAP-Seq’

Natalie Wolf¹, Lukas Lehmann¹, Andrei Filipchuk¹, Tino Polen¹, Michael Bussmann¹, Meike Baumgart¹, Michael Bott^{1*}

* Correspondence: Michael Bott (m.bott@fz-juelich.de)

TABLE S1 | Oligonucleotides used in this study

Oligonucleotide	Sequence (5' → 3')
Construction of plasmid pK19<i>mobsacB-glxR-twinstreptag</i> and PCR-analysis of the resulting mutants	
<i>glxR-twinstrept_01-fw</i>	TCACCAAAGCGCTAAAAAGCGCCTG
<i>glxR-twinstrept_02-fw</i>	GGCACGTCGCGCTCGATGGAGTCATCCTCAATTCG
<i>glxR-twinstrept_03-rv</i>	CTTTTGTAGCGCTTTGGTGATTATTTTTTCGAACTGCGGGTG
<i>glxR-twinstrept_04-rv</i>	TCGAGCGCGACGTGCCAAATGC
<i>glxR-twinstrept-control-fw</i>	TCAATTCGAGAAAGGTGGAG
<i>glxR-twinstrept-control-rv</i>	CTTCTCGACGCAAAAACCCATC
EMSA	
<i>hemL</i> (cg0518)_fw	TCACCATAACCGGGTTCGACG
<i>hemL</i> (cg0518)_rv	ACGCGCAGCCGAAACGGTAGC
<i>aspA</i> (cg1697)_fw	CATTCTTTGAGTCTGCTGAAG
<i>aspA</i> (cg1697)_rv	GTACCTAGGATAATCCACAGC
cg2936_cg2937_fw	GACACTACAGCAATTC AATG
cg2936_cg2937_rv	GGAGGAAATTGCGGGCAGT

TABLE S2 | Sequencing, mapping and coverage data from ChAP-Seq experiments

Sample	ChAP-Seq exp. No.	Total reads amount	Mapping		Coverage	
			Mapped uniquely	Mapped uniquely %	Median	Mean
Glucose						
WT _{GlxR-TS}	1	191 299	174.158	91.04%	11	12
	2	285 318	254 654	89.25%	14	16
	3	709 149	672 793	94.87%	50	54
Δ <i>cydB</i> _{GlxR-TS}	4	786 320	737 718	93.82%	63	65
	5	979 464	823 058	84.03%	72	77
Glucose-Acetate						
WT _{GlxR-TS}	6	1 035 286	971 112	93.80%	86	90
	7	1 572 052	1 441 562	91.70%	105	121
Δ <i>cydB</i> _{GlxR-TS}	8	691 265	614 185	88.85%	55	55
	9	1 812 475	1 702 348	93.92%	158	167

TABLE S3 | GlxR peaks and corresponding binding sites identified with ChAP-Seq.

TABLE S4 | GlxR peaks and corresponding binding sites from Table S3. (iii) lists binding sites found intergenic of two covalent transcribed genes (*inter_conv*); (iv) lists binding sites that are found located intragenic but less than 500 bp upstream of a gene start (*intra_up*); (v) lists binding sites that are located intragenic with more than 500 bp upstream from the next gene start (*intragenic*).

TABLE S5 | GlxR bindings sites and corresponding gene targets that are described in the literature but were not defined as GlxR peak in our ChAP-Seq analysis.

TABLE S6 | Microarray data of Δ *cpdA*/WT and Δ *cydB*/WT of (putative) GlxR target genes

TABLE S7 | GlxR peaks and corresponding binding sites found upstream of non-protein coding elements, antisense transcripts or intragenic transcripts (less than 700 bp upstream of its TSS)

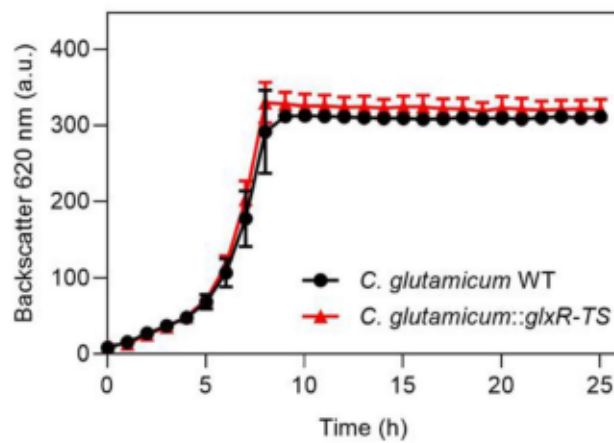


FIGURE S1 | Growth of *C. glutamicum* ATCC13032 wild type (WT) and the mutant *C. glutamicum::glxR-TS* ($WT_{GlxR-TS}$) with a chromosomal Twin Strep-tag encoding sequence at the 3' end of *glxR*. The cells were cultivated in CGXII medium with 2% (w/v) glucose. The first preculture was inoculated in BHI medium and the second preculture in CGXII with 2% (w/v) glucose. Before inoculation of the main culture, cells were washed with saline [0.9% (w/v) NaCl]. The main culture was cultivated in 800 μ l CGXII minimal medium, inoculated to an OD_{600} of 1, and cultivated with the respective amount of carbon sources in a BioLector. Mean values and standard deviation of three biological replicates each.

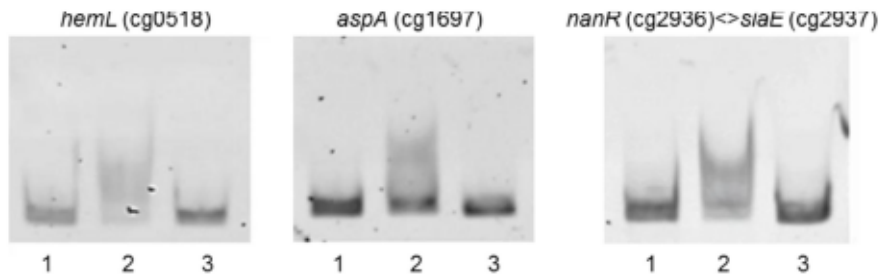


FIGURE S2 | Electrophoretic mobility shift assays (EMSAs) with C-terminally Twin Strep-tagged GlxR ($GlxR_{TS}$) and DNA fragments covering new *in vivo* GlxR binding sites of *C. glutamicum* ATCC13032. DNA fragments are located upstream of depicted genes or in the intergenic region of two divergently transcribed genes (<->) of depicted genes. 100 ng of the 100 bp DNA fragments were incubated for 30 min with 200 nM purified protein at room temperature, either with or without 0.2 mM cAMP. After incubation, the reaction mixture was loaded onto a 10% native polyacrylamide gel. Lane 1: control sample containing only DNA; lane 2: sample with $GlxR_{TS}$, the indicated DNA fragment, and cAMP; lane 3: sample with $GlxR_{TS}$ and the indicated DNA fragment, but without cAMP.

TABLE S1 | Part (A) | GMR peaks and corresponding binding sites identified with ChIP-Seq

locus tag (hg)	locus tag (mgi)	Start position ^a	End position ^a	GMR binding site ^b	k-value	EF ^c WT _{max} n (hg)	EF ^c WT _{max} n (mgi)	log ₂ WT _{max} (hg)	log ₂ WT _{max} (mgi)	Distance to next TSS ^d	Annotations	link peak between new ^e	operator ^f	further transcriptional regulator ^g	No.
g03464	NC021165	2379771	2379771	TGAGGAAAGTTCAGCA	3.34E-05	3.82	4.37	0.57	5.33	-336	hypothetical protein	Topolaz et al. 2013	OP_02144-07	g03464 (hg), g03464 (mgi)	209
g03466	NC021167	2383729	2383729	TGAGGAAAGTTCAGCA	1.34E-05	11.07	7.69	3.31	5.78	-338	hypothetical protein, E1 subunit of proteinase, dehydrogenase, E1 subunit of PDC, increased ABC transporter substrate-binding	NEW	OP_02144-07	g03466 (hg), g03466 (mgi)	217
g03480	NC021180	2393686	2393686	TGTGAAAGTTCAGCA	1.68E-04	3.13	2.02	2.08	2.26	-202	hypothetical protein	NEW	OP_02144-07	g03480 (hg), g03480 (mgi)	218
g03486	NC021195	2408847	2408847	GATGATTCAGTCACT	5.48E-04	2.39	2.48	3.39	2.05	-1059	part. secreted protein	NEW	OP_02144-07	g03486 (hg), g03486 (mgi)	219
g03521	NC021216	2430362	2430362	TGTGAAAGTTCAGCA	5.34E-05	8.57	6.11	3.45	4.33	-484	hypothetical protein, proteinase, dehydrogenase, E1 subunit of PDC, increased ABC transporter substrate-binding	NEW	OP_02144-07	g03521 (hg), g03521 (mgi)	219
g03544	NC022236	2457207	2457207	AUTGATTCAGTCACT	8.01E-06	3.18	2.13	1.77	1.37	-134	part. secreted protein	NEW	OP_02144-07	g03544 (hg), g03544 (mgi)	219
g03557	NC022245	2469221	2469221	TATGAAAGTTCAGCA	7.84E-04	4.47	4.05	3.43	2.58	-77	part. secreted protein, related to alcohol L-epimerase	NEW	OP_02144-07	g03557 (hg), g03557 (mgi)	219
g03558	NC022246	2470303	2470303	GATGATTCAGTCACT	1.17E-04	3.33	3.19	11.04	4.62	-315	hypothetical protein	NEW	OP_02144-07	g03558 (hg), g03558 (mgi)	219
g03561	NC022253	2504093	2504093	TGAGGAAAGTTCAGCA	3.68E-04	3.41	2.25	3.03	2.43	-447	part. secreted protein	NEW	OP_02144-07	g03561 (hg), g03561 (mgi)	219
g03581	NC022294	2533892	2533892	GATGATTCAGTCACT	3.34E-05	13.90	11.80	17.52	6.34	-93	part. secreted protein, related to alcohol L-epimerase	NEW	OP_02144-07	g03581 (hg), g03581 (mgi)	219
g03581	NC022295	2533892	2533892	GATGATTCAGTCACT	3.34E-05	13.90	11.80	17.52	6.34	-93	part. secreted protein, related to alcohol L-epimerase	NEW	OP_02144-07	g03581 (hg), g03581 (mgi)	219
g03615	NC022299	2534846	2534846	TATGAAAGTTCAGCA	4.48E-04	3.75	3.23	7.34	5.39	-125	transcriptional regulator, highly family	NEW	OP_02144-07	g03615 (hg), g03615 (mgi)	219
g03616	NC022300	2534846	2534846	TATGAAAGTTCAGCA	4.48E-04	3.75	3.23	7.34	5.39	-125	transcriptional regulator, highly family	NEW	OP_02144-07	g03616 (hg), g03616 (mgi)	219
g03638	NC022319	2544810	2544810	GATGATTCAGTCACT	6.02E-04	5.66	4.01	4.31	2.32	-108	part. secreted protein	NEW	OP_02144-07	g03638 (hg), g03638 (mgi)	219
g03639	NC022320	2544810	2544810	GATGATTCAGTCACT	6.02E-04	5.66	4.01	4.31	2.32	-108	part. secreted protein	NEW	OP_02144-07	g03639 (hg), g03639 (mgi)	219
g03642	NC022323	2545385	2545385	TGTGAAAGTTCAGCA	3.43E-05	4.15	3.17	3.46	2.53	-46	benzamide 2,2'-dicyanoguanosine substrate	NEW	OP_02144-07	g03642 (hg), g03642 (mgi)	219
g03651	NC022325	2545385	2545385	TGTGAAAGTTCAGCA	3.43E-05	4.15	3.17	3.46	2.53	-46	benzamide 2,2'-dicyanoguanosine substrate	NEW	OP_02144-07	g03651 (hg), g03651 (mgi)	219
g03652	NC022326	2545385	2545385	TGTGAAAGTTCAGCA	3.43E-05	4.15	3.17	3.46	2.53	-46	benzamide 2,2'-dicyanoguanosine substrate	NEW	OP_02144-07	g03652 (hg), g03652 (mgi)	219
g03653	NC022327	2545385	2545385	TGTGAAAGTTCAGCA	3.43E-05	4.15	3.17	3.46	2.53	-46	benzamide 2,2'-dicyanoguanosine substrate	NEW	OP_02144-07	g03653 (hg), g03653 (mgi)	219
g03654	NC022328	2545385	2545385	TGTGAAAGTTCAGCA	3.43E-05	4.15	3.17	3.46	2.53	-46	benzamide 2,2'-dicyanoguanosine substrate	NEW	OP_02144-07	g03654 (hg), g03654 (mgi)	219
g03655	NC022329	2545385	2545385	TGTGAAAGTTCAGCA	3.43E-05	4.15	3.17	3.46	2.53	-46	benzamide 2,2'-dicyanoguanosine substrate	NEW	OP_02144-07	g03655 (hg), g03655 (mgi)	219
g03656	NC022330	2545385	2545385	TGTGAAAGTTCAGCA	3.43E-05	4.15	3.17	3.46	2.53	-46	benzamide 2,2'-dicyanoguanosine substrate	NEW	OP_02144-07	g03656 (hg), g03656 (mgi)	219
g03657	NC022331	2545385	2545385	TGTGAAAGTTCAGCA	3.43E-05	4.15	3.17	3.46	2.53	-46	benzamide 2,2'-dicyanoguanosine substrate	NEW	OP_02144-07	g03657 (hg), g03657 (mgi)	219
g03658	NC022332	2545385	2545385	TGTGAAAGTTCAGCA	3.43E-05	4.15	3.17	3.46	2.53	-46	benzamide 2,2'-dicyanoguanosine substrate	NEW	OP_02144-07	g03658 (hg), g03658 (mgi)	219
g03659	NC022333	2545385	2545385	TGTGAAAGTTCAGCA	3.43E-05	4.15	3.17	3.46	2.53	-46	benzamide 2,2'-dicyanoguanosine substrate	NEW	OP_02144-07	g03659 (hg), g03659 (mgi)	219
g03660	NC022334	2545385	2545385	TGTGAAAGTTCAGCA	3.43E-05	4.15	3.17	3.46	2.53	-46	benzamide 2,2'-dicyanoguanosine substrate	NEW	OP_02144-07	g03660 (hg), g03660 (mgi)	219
g03661	NC022335	2545385	2545385	TGTGAAAGTTCAGCA	3.43E-05	4.15	3.17	3.46	2.53	-46	benzamide 2,2'-dicyanoguanosine substrate	NEW	OP_02144-07	g03661 (hg), g03661 (mgi)	219
g03662	NC022336	2545385	2545385	TGTGAAAGTTCAGCA	3.43E-05	4.15	3.17	3.46	2.53	-46	benzamide 2,2'-dicyanoguanosine substrate	NEW	OP_02144-07	g03662 (hg), g03662 (mgi)	219
g03663	NC022337	2545385	2545385	TGTGAAAGTTCAGCA	3.43E-05	4.15	3.17	3.46	2.53	-46	benzamide 2,2'-dicyanoguanosine substrate	NEW	OP_02144-07	g03663 (hg), g03663 (mgi)	219
g03664	NC022338	2545385	2545385	TGTGAAAGTTCAGCA	3.43E-05	4.15	3.17	3.46	2.53	-46	benzamide 2,2'-dicyanoguanosine substrate	NEW	OP_02144-07	g03664 (hg), g03664 (mgi)	219
g03665	NC022339	2545385	2545385	TGTGAAAGTTCAGCA	3.43E-05	4.15	3.17	3.46	2.53	-46	benzamide 2,2'-dicyanoguanosine substrate	NEW	OP_02144-07	g03665 (hg), g03665 (mgi)	219
g03666	NC022340	2545385	2545385	TGTGAAAGTTCAGCA	3.43E-05	4.15	3.17	3.46	2.53	-46	benzamide 2,2'-dicyanoguanosine substrate	NEW	OP_02144-07	g03666 (hg), g03666 (mgi)	219
g03667	NC022341	2545385	2545385	TGTGAAAGTTCAGCA	3.43E-05	4.15	3.17	3.46	2.53	-46	benzamide 2,2'-dicyanoguanosine substrate	NEW	OP_02144-07	g03667 (hg), g03667 (mgi)	219
g03668	NC022342	2545385	2545385	TGTGAAAGTTCAGCA	3.43E-05	4.15	3.17	3.46	2.53	-46	benzamide 2,2'-dicyanoguanosine substrate	NEW	OP_02144-07	g03668 (hg), g03668 (mgi)	219
g03669	NC022343	2545385	2545385	TGTGAAAGTTCAGCA	3.43E-05	4.15	3.17	3.46	2.53	-46	benzamide 2,2'-dicyanoguanosine substrate	NEW	OP_02144-07	g03669 (hg), g03669 (mgi)	219
g03670	NC022344	2545385	2545385	TGTGAAAGTTCAGCA	3.43E-05	4.15	3.17	3.46	2.53	-46	benzamide 2,2'-dicyanoguanosine substrate	NEW	OP_02144-07	g03670 (hg), g03670 (mgi)	219
g03671	NC022345	2545385	2545385	TGTGAAAGTTCAGCA	3.43E-05	4.15	3.17	3.46	2.53	-46	benzamide 2,2'-dicyanoguanosine substrate	NEW	OP_02144-07	g03671 (hg), g03671 (mgi)	219
g03672	NC022346	2545385	2545385	TGTGAAAGTTCAGCA	3.43E-05	4.15	3.17	3.46	2.53	-46	benzamide 2,2'-dicyanoguanosine substrate	NEW	OP_02144-07	g03672 (hg), g03672 (mgi)	219
g03673	NC022347	2545385	2545385	TGTGAAAGTTCAGCA	3.43E-05	4.15	3.17	3.46	2.53	-46	benzamide 2,2'-dicyanoguanosine substrate	NEW	OP_02144-07	g03673 (hg), g03673 (mgi)	219
g03674	NC022348	2545385	2545385	TGTGAAAGTTCAGCA	3.43E-05	4.15	3.17	3.46	2.53	-46	benzamide 2,2'-dicyanoguanosine substrate	NEW	OP_02144-07	g03674 (hg), g03674 (mgi)	219
g03675	NC022349	2545385	2545385	TGTGAAAGTTCAGCA	3.43E-05	4.15	3.17	3.46	2.53	-46	benzamide 2,2'-dicyanoguanosine substrate	NEW	OP_02144-07	g03675 (hg), g03675 (mgi)	219
g03676	NC022350	2545385	2545385	TGTGAAAGTTCAGCA	3.43E-05	4.15	3.17	3.46	2.53	-46	benzamide 2,2'-dicyanoguanosine substrate	NEW	OP_02144-07	g03676 (hg), g03676 (mgi)	219
g03677	NC022351	2545385	2545385	TGTGAAAGTTCAGCA	3.43E-05	4.15	3.17	3.46	2.53	-46	benzamide 2,2'-dicyanoguanosine substrate	NEW	OP_02144-07	g03677 (hg), g03677 (mgi)	219
g03678	NC022352	2545385	2545385	TGTGAAAGTTCAGCA	3.43E-05	4.15	3.17	3.46	2.53	-46	benzamide 2,2'-dicyanoguanosine substrate	NEW	OP_02144-07	g03678 (hg), g03678 (mgi)	219
g03679	NC022353	2545385	2545385	TGTGAAAGTTCAGCA	3.43E-05	4.15	3.17	3.46	2.53	-46	benzamide 2,2'-dicyanoguanosine substrate	NEW	OP_02144-07	g03679 (hg), g03679 (mgi)	219
g03680	NC022354	2545385	2545385	TGTGAAAGTTCAGCA	3.43E-05	4.15	3.17	3.46	2.53	-46	benzamide 2,2'-dicyanoguanosine substrate	NEW	OP_02144-07	g03680 (hg), g03680 (mgi)	219
g03681	NC022355	2545385	2545385	TGTGAAAGTTCAGCA	3.43E-05	4.15	3.17	3.46	2.53	-46	benzamide 2,2'-dicyanoguanosine substrate	NEW	OP_02144-07	g03681 (hg), g03681 (mgi)	219
g03682	NC022356	2545385	2545385	TGTGAAAGTTCAGCA	3.43E-05	4.15	3.17	3.46	2.53	-46	benzamide 2,2'-dicyanoguanosine substrate	NEW	OP_02144-07	g03682 (hg), g03682 (mgi)	219
g03683	NC022357	2545385	2545385	TGTGAAAGTTCAGCA	3.43E-05	4.15	3.17	3.46	2.53	-46	benzamide 2,2'-dicyanoguanosine substrate	NEW	OP_02144-07	g03683 (hg), g03683 (mgi)	219
g03684	NC022358	2545385	2545385	TGTGAAAGTTCAGCA	3.43E-05	4.15	3.17	3.46	2.53	-46	benzamide 2,2'-dicyanoguanosine substrate	NEW	OP_02144-07	g03684 (hg), g03684 (mgi)	219

TABLE S4 (Part 1/3)

(iii) GkR binding sites (n = 10) located within intergenic regions of two convergently transcribed genes

Gene loci (cg)	Gene name	Gene locus (NCGI)	EF in WT _{Emb 15} (log)	Start position ^a	End position ^b	GkR binding site ^c	E-value	GkR peak known or new ^d	No. ^e
cg0054 > < cg0055	cg0054 > < cnpA	NCGI0038 > < NCGI0039	5.05	40261	40261	TGAGTGGCGGAGGACA	3.10E-03	NEW	232
cg1608 > < cg1609	xerD > < cg1609	NCGI1364 > < NCGI1365	3.34	1496565	1496868	TGAGCCCGCCCGACA	4.49E-04	NEW	180
cg1611 > < cg1612	scpA > < cg1612	NCGI1367 > < NCGI1368	3.19	1500579	1500875	TGTAGCTTAGGTCACT	2.95E-05	Toyoda et al. 2011	43
cg1728 > < cg1730	cg1728 > < cg1730	NCGI1474 > < NCGI1475	4.57	1617934	1618277	GGTGAGGTCGCCACA	4.02E-05	NEW	70
cg2314 > < cg2315	cg2314 > < cg2315	NCGI2030 > < NCGI2031	4.91	2228924	2229203	AGTGTGGTTCGCCACA	2.67E-04	Toyoda et al. 2011	155
cg2460 > < cg2461	cg2460 > < cg2461	NCGI2160 > < NCGI2161	2.91	2376667	2377030	TATGATCTTCGCCACA	6.09E-05	Toyoda et al. 2011	88
cg2496 > < cg2497	cg2496 > < cg2497	NCGI2195 > < NCGI2196	2.59	2408847	2409185	GGTCTCTTCGGTCACT	5.46E-04	NEW	192
cg2593 > < cg2594	cg2593 > < rpsM	- > < NCGI2279	3.41	2503806	2504093	TGAGCGTTAAGTCAACA	3.66E-04	NEW	166
cg2700 > < cg2701	phoB > < mus	NCGI2371 > < NCGI2372	6.02	2603255	2603478	TGTGTTCGACGGTCAACA	5.76E-07	NEW	1
cg2700 > < cg2701	phoB > < mus1	NCGI2371 > < NCGI2372	5.88	2603276	2603715	TGTGAGCCGAGGCCACT	2.48E-06	NEW	7

(iv) GkR binding sites (n=40) located intragenically and less than 500 bp upstream of a transcriptional start site (TSS), or if TSS is unknown, the translational start site (TIS) of a neighbouring gene or operon

Gene locus (cg)	rel. GkR motif location	Gene name	Gene locus (NCGI)	EF in WT _{Emb 15} (log)	Start position ^a	End position ^b	GkR binding site ^c	E-value ^c	GkR peak known or new ^d	No. ^e
cg0002	in	dnaM	NCGI0002	11.52	1622	1949	AGTGGCTTTGTCACA	2.48E-06	Toyoda et al. 2011	5
cg0004	upstream	mosA1	NCGI0209	3.33	228936	229141	CGTGGCAATCCCACT	4.06E-04	Toyoda et al. 2011	177
cg0261	upstream	mosB	NCGI0210	-	-	-	-	-	-	-
cg0262	in	impL7b	NCGI0348	-	-	-	-	-	-	-
cg0436	upstream	impL7b	NCGI0348	5.01	377613	377928	AGTATGCTTCGATGACA	1.71E-03	NEW	224
cg0427	upstream	impL7b	NCGI0348	3.82	387792	388032	TATGGAGTGTTCACG	1.51E-04	NEW	132
cg0440	in	cod	NCGI0355	-	-	-	-	-	-	-
cg0441	in	cod	NCGI0355	-	-	-	-	-	-	-
cg0447	in	srfA8	NCGI0361	7.87	396032	396338	GATGACAGCTGCCACA	8.04E-05	Koeh & Tauch 2009, Han et al. 2008,	96
cg0448	upstream	hemX	NCGI0362	-	-	-	-	-	-	-
cg0517	in	hemY	NCGI0421	-	-	-	-	-	-	-
cg0518	in	hemX	NCGI0422	5.46	462081	462410	TATGGAGTTCGATGACA	2.39E-04	Toyoda et al. 2011	152
cg0766	upstream	cod	NCGI0634	3.75	680094	680413	TGTGTTCCCGCACT	3.47E-05	Toyoda et al. 2011	63
cg0767	in	cod	NCGI0635	-	-	-	-	-	-	-
cg0865	in	cod	NCGI0723	-	-	-	-	-	-	-
cg0866	in	cod	NCGI0724	3.38	794231	794532	CGTGTATTTGTCACG	2.97E-04	NEW	158
cg0867	in	psp-1	NCGI0725	5.45	794899	795164	CGTGTGTGATTCGACG	1.90E-04	Toyoda et al. 2011	144
cg0903	in	psp-1	NCGI0725	-	-	-	-	-	-	-
cg0904	upstream	psp-1	NCGI0725	3.64	835617	835698	TGCTTGACTCCGACA	6.81E-03	NEW	238
cg0933	upstream	psp-1	NCGI0782	5.86	864962	865265	TGTGGATGAGTCACG	3.47E-05	NEW	56
cg0934	in	psp-1	NCGI0783	-	-	-	-	-	-	-
cg0982	upstream	psp-1	NCGI0806	2.74	897324	897585	GATGATGATGATCACT	7.96E-04	NEW	211
cg0983	in	psp-1	NCGI0806	-	-	-	-	-	-	-
cg0967	upstream	cyoQ	NCGI0811	5.59	900194	900525	AGTGTATTTGGGACG	1.12E-05	Toyoda et al. 2011	23
cg0988	in	cyoQ	NCGI0812	-	-	-	-	-	-	-
cg1244	upstream	oxyC4	NCGI1049	3.32	1141185	1141511	TATGCGAGGTCGACG	1.51E-04	Toyoda et al. 2011	134
cg1245	in	oxyC4	NCGI1050	-	-	-	-	-	-	-
cg1256	upstream	arpP	NCGI1061	4.16	1153247	1153654	AGTTTGCATGTCACG	1.01E-03	NEW	216
cg1257	in	arpP	NCGI1062	-	-	-	-	-	-	-
cg1301	in	arpP	NCGI1158	-	-	-	-	-	-	-
cg1362	upstream	arpP	NCGI1159	2.53	1271688	1272121	TGTTATGATGTCACG	1.12E-05	Toyoda et al. 2011	26
cg1432	upstream	invD	NCGI1219	3.04	1335160	1335532	CGTTCGAAATCCCACT	4.96E-04	NEW	186
cg1433	in	invD	NCGI1220	-	-	-	-	-	-	-
cg1812	upstream	pyrF	NCGI1546	3.14	1704186	1704609	TGTTCCGCTGATCACT	6.61E-04	NEW	201
cg1813	in	pyrF	NCGI1547	-	-	-	-	-	-	-
cg1862	upstream	opt	NCGI1591	4.43	1755387	1755884	TGTTGACCTTATGACA	8.01E-06	revised Kohl et al. 2008, Toyoda et al. 2011	1b
cg1864	in	opt	NCGI1592	-	-	-	-	-	-	-

TABLE S4 (Part 2/3)
 (iv) GtXR binding sites (n=40) located intragenically and less than 500 bp upstream of a transcriptional start site (TSS), or if TSS is unknown, the translational start site (TIS) of a neighbouring gene or operon

Gene locus (eg)	rel. GtXR motif location	Gene name	Gene locus (NCBI)	EF in WT _{total} in [pic]	Start position ^a	End position ^b	GtXR binding site ^c	E-value ^c	GtXR peak known or new ^d	No. ^e
cg1597	in	-	NCgl1618	7.79	1788537	1788805	TGTTGGCACTGGCA	1.31E-04	NEW	124
cg1598	upstream	-	NCgl1619	-	-	-	-	-	-	-
cg1526	in	-	NCgl1642	3.52	1807623	1807914	TGTTGGCTGGTAGCA	2.58E-05	NEW	53
cg2034	in	-	NCgl1739	-	-	-	-	-	-	-
cg2034	upstream	-	NCgl1739	6.09	1627741	1628036	TGTTGGCTGGTAGCA	9.29E-04	NEW	213
cg2134	upstream	-	NCgl1873	3.92	2057714	2058023	TGTTGGCTGGTAGCA	1.53E-04	NEW	131
cg2135	in	mob	NCgl1874	-	-	-	-	-	-	-
cg2182	in	oppl	NCgl1916	-	-	-	-	-	-	-
cg2183	upstream	oppl	NCgl1917	3.92	2102610	2102934	TGTTGGCTGGTAGCA	9.14E-05	Toyoda et al. 2011	109
cg2183	in	oppl	NCgl1917	-	-	-	-	-	-	-
cg2184	upstream	oppl	NCgl1918	5.23	2103502	2103846	TGTTGGCTGGTAGCA	1.69E-04	NEW	137
cg2402	upstream	mpc	NCgl2108	3.26	2320901	2321183	TGTTGGCTGGTAGCA	8.01E-06	Kohli & Tauch 2008	18
IGTR_cg2402_cg2403	in	-	-	-	-	-	-	-	-	-
cg2404	upstream	qcrA (trxA1)	NCgl2110	5.45	2324430	2324672	TGTTGGCTGGTAGCA	1.90E-04	Toyoda et al. 2011	143
cg2405	in	qcrC	NCgl2111	-	-	-	-	-	-	-
cg2406	upstream	ctse	NCgl2112	4.90	2325943	2326265	TGTTGGCTGGTAGCA	5.29E-05	Kohli & Tauch 2008	79
cg2407	in	-	-	-	-	-	-	-	-	-
cg2480	upstream	-	NCgl2180	3.13	2393676	2393986	TGTTGGCTGGTAGCA	1.09E-04	NEW	139
cg2482	in	-	NCgl2182	-	-	-	-	-	-	-
cg2521	upstream	foxO15	NCgl2216	8.57	2430262	2430557	TGTTGGCTGGTAGCA	5.29E-05	NEW	77
cg2523	in	moq	NCgl2217	-	-	-	-	-	-	-
cg2546	upstream	-	NCgl2236	3.28	2457005	2457287	AGTGGATTAGTAGCA	8.01E-06	pred. Kohli et al. 2008, Toyoda et al. 2011	17
cg2578	upstream	-	NCgl2353	10.03	2582586	2582892	TGTTGGCTGGTAGCA	1.97E-05	NEW	32
cg2679	in	-	NCgl2354	-	-	-	-	-	-	-
cg2743	upstream	fosA	NCgl3409	6.53	2647825	2648109	TGTTGGCTGGTAGCA	5.29E-05	Kohli & Tauch 2008	78
cg2745	in	-	-	-	-	-	-	-	-	-
cg2796	upstream	-	NCgl3450	-	-	-	-	-	-	-
cg2797	upstream	-	NCgl3451	4.17	2685869	2686208	TGTTGGCTGGTAGCA	4.98E-04	NEW	183
cg2803	in	-	NCgl3456	-	-	-	-	-	-	-
cg2804	upstream	hox27a	NCgl3457	8.11	2691030	2691325	TGTTGGCTGGTAGCA	1.53E-04	Toyoda et al. 2011	173
cg3030	upstream	-	NCgl3639	3.36	2917792	2918090	AGTGGCTGGTAGCA	3.66E-04	NEW	167
cg3031	in	-	NCgl3640	-	-	-	-	-	-	-
cg3041	upstream	-	NCgl3650	3.27	2928359	2928637	AGTGGCTGGTAGCA	1.53E-04	NEW	135
cg3042	in	-	NCgl3651	-	-	-	-	-	-	-
cg3090	in	-	NCgl3692	-	-	-	-	-	-	-
cg3091	upstream	-	NCgl3693	4.50	2974964	2975268	AGTGGCTGGTAGCA	1.34E-03	NEW	218
cg3247	upstream	hoxA (cgrR11)	NCgl3834	3.58	3136728	3137037	TGTTGGCTGGTAGCA	1.34E-03	NEW	220
cg3248	in	hox5	NCgl3835	-	-	-	-	-	-	-
cg3413	upstream	antC	NCgl3977	7.68	3289988	3290261	TGTTGGCTGGTAGCA	8.70E-04	Toyoda et al. 2011	212
cg3414	in	-	NCgl3978	-	-	-	-	-	-	-

TABLE S4 (Part 3/3)
 (v) GxR binding sites (n=15) located intragenically and more than 500 bp upstream of a transcriptional start site (TSS), or if TSS is unknown, the translational start site (TLS) of a neighbouring gene or operon.

In gene locus (cg)	Gene name	Gene locus (NCgl)	EF in WT _{0.8h,3h} (p/c) ^a	Start position ^b	End position ^b	GxR binding site ^c	E-value ^d	GxR peak known or new ^e	No. ^f
GR0001	dnmA	NCgl0001	3.21	0	208	GTTTCAAAATTCACG	1.57E-02	NEW	240
GR0089	glaA	NCgl0067	6.30	71049	71315	AGTCAGATTTTCAGCA	5.46E-04	NEW	187
GR2651	ncsA1	NCgl0209	4.44	228447	228830	CGTGGCGAAATCCGCACT	4.06E-04	NEW	174
GR0576	gypA	NCgl0223	3.81	242137	242468	TGTCGCGATTTTACACCA	2.96E-05	NEW	52
GR0576	gypB	NCgl0471	4.17	514025	514322	TGAGTCAAAACGACCA	9.50E-04	NEW	215
GR0583	gaaA	NCgl0478	3.45	524535	524772	TGTAGCGGGTTCAGCA	2.39E-04	NEW	153
GR0588	rpsA	NCgl0543	2.62	579406	579759	TGTCGCCGATTCGCT	3.06E-04	NEW	169
GR0706	-	NCgl0584	3.60	621894	621894	GGTTCCTCAGACACCA	1.51E-04	NEW	133
GR0764	-	NCgl0632	3.67	676645	676946	TGTTTCAGCGGACCA	7.27E-04	NEW	204
GR0772	-	NCgl0640	3.38	685592	685875	GGTTTCATATTCGACCA	5.46E-04	NEW	190
GR0788	pmrB	NCgl0656	3.32	700413	700712	TGTCGTCGACCCACCA	1.17E-04	NEW	121
GR0845	-	NCgl0707	3.49	775618	775618	AGTATGCGGATTCAGCA	4.96E-04	NEW	184
GR0848	wbbL	NCgl0709	2.63	779163	779514	GGTAGCGTTCGACCA	2.96E-05	Toyoda et al. 2011	54
GR0875	-	NCgl0732	5.29	803117	803421	TGTCGTTCCGACCA	8.01E-06	NEW	15
GR0952	cmr13	NCgl0885	3.13	977403	977763	GGTCCGAGGATTCAGCA	8.04E-05	NEW	101
GR1075	prxA	NCgl0905	3.45	998314	998314	TGTTCCATGATTCGCT	2.97E-04	NEW	157
GR1147	swf	NCgl0968	4.13	1064223	1064532	TGTACCGAGTCAGCA	1.33E-04	NEW	127
GR1520	-	NCgl1294	3.29	1410547	1410841	TGTACTGCTAATTCAGCA	1.33E-04	NEW	179
GR1895	-	NCgl1616	4.45	1783094	1783431	TGTCGTTCCGACCACT	3.47E-05	NEW	57
GR1934	-	NCgl1658	5.62	1806046	1806328	AGTACGAGACCA	9.14E-05	NEW	108
GR1945	-	NCgl1658	3.21	1821008	1821381	TGTTTCATCCGACCA	6.01E-04	NEW	198
GR1995	-	NCgl1702	3.10	1871481	1873791	TGTATCAGTTCGACCT	2.97E-04	NEW	160
GR2000	-	NCgl1707	6.34	1884323	1884613	TGTCATCTGTTAGCA	4.06E-04	NEW	171
GR2042	-	NCgl1747	9.80	1933851	1934130	AGTATCCCGGATTCGCT	7.96E-04	pred. Kohli et al. 2008	205
GR2064	-	NCgl1769	2.55	1955246	1955537	CGTGAATATGAGACCA	3.47E-05	NEW	65
GR2117	psfI	NCgl1858	3.54	2040573	2040845	TGTGGGACTTTCGCT	5.33E-05	Kohli & Touch 2008,	42
GR2405	-	NCgl2111	5.97	2324785	2325080	TGTCGCTTCGACCA	1.90E-04	Jungwirth et al. 2013	142
GR2497	-	NCgl2196	3.92	2409768	2410123	AGTACGATCCGACCA	3.47E-05	NEW	62
GR2642	-	NCgl2325	3.26	2553033	2553385	TGTTCCGTCGACCACT	5.06E-04	NEW	193
GR2695	-	NCgl2368	3.04	2596754	2597196	TGTCGTTCCGACCA	2.13E-04	NEW	150
GR2781	trnAF	NCgl2438	0.80	2673427	2673772	AGTCTCTCCGACCA	6.01E-04	NEW	199
GR2811	-	NCgl2464	6.25	2700486	2700775	CGTCTGTTGATTCAGCA	3.66E-04	Kohli & Touch 2008	164
GR2837	surC	NCgl2477	3.53	2727036	2727790	TGTGGGACTTTCGCT	4.02E-05	Touch 2009	74
GR2843	psfB	NCgl2483	4.45	2731426	2733695	GGTTCGATTCGACCA	4.49E-04	NEW	179
GR2898	-	NCgl2526	3.18	2785006	2785289	TGTTGATTCGACCA	1.85E-03	NEW	227
GR3044	gthX	NCgl2653	3.24	2930206	2930403	TGATGTTAAGACCA	1.71E-03	NEW	225
GR3092	-	NCgl2694	3.62	2977156	2977490	TGTATTTTTCGACCA	9.14E-05	NEW	111
GR3158	nmrA2	NCgl2754	1.85	3041008	3041138	TGTGGGACTTTCGCT	8.04E-05	Toyoda et al. 2011	99
GR3174	nrrM1	NCgl2769	3.77	3058079	3058349	TGTTGTTTCGACCA	1.90E-04	NEW	166
GR3187	gfbB	NCgl2780	4.53	3078011	3078313	AGTCCGCGACGACCA	8.70E-04	NEW	214
GR3203	-	NCgl2795	6.24	3096357	3096690	TGCTCATTTTCGCT	5.31E-03	NEW	237
GR3332	gpr3	NCgl2902	3.91	3205746	3206075	GGTACTGCTTCGCT	2.50E-03	NEW	231
GR3393	phoC	NCgl2959	3.47	3261837	3268141	TGTACCGATTCAGCA	6.09E-05	NEW	86
GR3415	-	NCgl2979	2.56	3191226	3292103	GGTAGGCTTCGACCA	2.97E-04	NEW	161
GR3429	-	NCgl2991	3.63	3306256	3307262	TGTTTCGTCGACCACT	4.06E-04	NEW	176

a: average of enrichment factor (EF) of GxR peak of WT_{0.8h,3h} (p/c) ChIP-Seq samples (n=3)
 b: Reference genome sequence BA000036.3 of *C. glutamicum* ATCC13032 (Ikeda & Nakagawa 2003)
 c: motif was detected by using the program MEME-ChIP with the DNA fragment of the detected GxR peaks as input sequences; the 16 bp sequence shows the most probable GxR binding site within this sequences
 d: distance was counted from the center of the GxR binding site to the first base of TSS or TSS; information of the TSS and TLS was taken from transcriptomes study (Pfeifer-Sancar et al. 2013)
 e: if GxR peak is previously described, the respective literature is mentioned; if the site is only found in our ChIP-Seq results it is described as 'NEW'
 f: No. according to numbering in Table S3

TABLE S6 (Part 1/2) | Microarray data of Δ cpdA/WT and Δ cyoB/WT of (putative) GlxR target genes

locus tag (cg)	Gene name	Annotation	Distance to next T55 ^a	Distance to next T15 ^b	mRNA ratio Δ cpdA/WT ^b	p-value ^c	mRNA ratio Δ cyoB/WT glx ^d	p-value ^e	pred. size of data of microarray ^f	pred. in literature ^g
cg0261	rod4 (rhW)	putative FTSW/RCCA/SPOVE-family cell cycle protein	-	+48	0.63	0.07	1.04	0.01	-	-
cg0268	clbH	citrate transporter, CRMHS-family	-21 ^h , -22 ^h , -24 ^h	-77	0.41	0.00	0.12	n.d.	-	exp. R
cg0305	cmf7	creatine transporter	-	-86	0.88	0.04	0.12	n.d.	-	-
cg0356	cyoB	transcriptional activator, ROR-family	-310	-310	0.52	0.04	1.47	0.03	R	-
cg0396	icbP	repressor of myo-inositol utilization genes, GlnR-family	-263 ⁱ , -264 ⁱ	-400	1.60	0.05	0.50	0.18	-	-
cg0397	icbC	carbohydrate kinase, myo-inositol catabolism	+15	-44	0.67	0.30	1.24	0.02	-	-
cg0710	-	putative transcriptional regulator, LacI-family	-	-85	1.11	0.13	1.23	0.03	-	-
cg0711	owB	putative oxidoreductase dehydrogenase	+25	-56	1.09	0.10	1.40	0.02	-	-
cg0223	icf72	myo-inositol transporter 1	+11 ^j , +39 ^j	-75	0.34	0.01	3.22	0.01	R	-
cg0228	hkm	putative sensor histidine kinase	-25	-58	1.00	0.21	1.17	0.02	-	-
cg0249	-	putative polysaccharide/polyol phosphate export systems	+64	+64	1.25	0.01	1.00	0.13	-	-
cg0250	-	putative aminotransferase class V	+42; -163	-177	0.88	0.43	1.34	0.02	-	-
cg0261	moaA1	molybdopterin cofactor synthesis protein A1, MoaA-family	-	-190	0.73	0.28	1.71	0.04	-	-
cg0303	leuA	2-isopropylmalate synthase	-	-248	0.69	0.07	1.51	0.01	-	-
cg0336	pdp7a	penicillin-binding protein 3A	-579	-579	1.06	0.14	1.29	0.02	-	-
cg0337	whcA (whB4)	putative regulatory protein (whB related protein)	-40; +66	-89	1.43	0.03	0.85	0.48	-	-
cg0341	phdA (phdD1)	acyl-CoA ligase transmembrane protein	-	-22	0.00	0.00	1.95	n.d.	-	-
cg0343	phdF	Repressor of phd operon, MerR-family	-	-163	0.83	0.12	1.51	0.03	-	-
cg0344	phdS (phdG1)	3-hydroxyacyl-CoA dehydrogenase	-	-29	0.48	0.01	1.40	n.d.	-	-
cg0360	-	putative phosphatase	-127	-127	0.76	0.12	1.28	0.00	-	-
cg0444	ramB	transcriptional regulator, MerR-family	-283	-283	3.99	0.00	0.82	0.40	-	exp. R
cg0445	sdhC	succinate menaquinone oxidoreductase, cytochrome b subunit C	-198; -200; -203	-215	0.71	0.22	1.27	0.00	-	exp. R
cg0446	-	putative membrane protein	-61; +88	-100	0.67	0.06	1.62	0.06	-	-
cg0500	glnR	transcriptional activator of glnABCD genes, LysR-family	-	-70	1.33	0.03	1.60	0.09	-	-
cg0501	glnA	putative shikimate permease, MFS-type	-	-207	1.07	0.03	0.08	0.04	-	-
cg0518	hem1	glutamate-1-semialdehyde 2,1-aminomutase	-253	-253	1.10	0.08	1.22	0.02	-	-
cg0505	pwfR/pwfR	putative transcriptional regulator	-65	-124	0.69	0.05	1.32	0.02	-	-
cg0607	-	putative secreted protein	+84; -63	-133	0.79	0.31	1.45	0.00	-	-
cg0645	cro (cypH)	cytochrome P450	-	-74	0.41	0.05	2.99	0.00	R	-
cg0646	croH	putative transcriptional regulator, idR-family	-71; -115	-102	0.88	0.22	0.10	0.00	-	-
cg0703	gpaA	putative Gmp synthase	+7	+7	0.84	0.27	1.06	0.04	-	-
cg0755	metP	O-acetylhomoserine sulfhydrylase	-136	-175	1.30	0.02	1.39	0.00	-	-
cg0756	catA	carbon starvation protein A	-30; -32; -42; -59	-258	5.24	0.00	0.71	0.17	-	-
cg0759	pypD2	2-methylcitrate dehydratase	-4 ⁱ	-41	0.49	0.03	2.79	0.00	R	-
cg0791	pvc	pyruvate carboxylase	+14; +12; +10	-45	0.31	0.02	1.06	0.01	-	pred. R
cg0796	pypD1	2-methylcitrate dehydratase	-32	-68	2.34	0.00	0.97	0.06	-	pred. R
cg0803	otrR	thiosulfate sulfurtransferase	-37	-91	0.69	0.07	1.12	0.00	-	-
cg0806	-	hypothetical protein	61	-238	1.28	0.01	0.96	0.26	-	-
cg0835	tusK (mskK2)	trehalose uptake system	+7	+7	0.76	0.04	0.13	0.00	-	-
cg0836	-	-	-	-94	0.95	0.42	0.02	0.00	-	-
cg0866	-	purine/pyrimidine phosphoribosyl transferase	-	-311	0.74	0.02	n.d.	n.d.	-	-
cg0867	purp-2	putative ribosome-associated protein Y	-162; -300; -303; -306	-384	0.34	0.03	0.85	0.49	-	-
cg0878	whcF (whbB1)	transcriptional regulator	-114	-316	1.03	0.15	0.97	0.02	-	pred. A
cg0934	-	putative putative iron-siderophore transporter	-156	-356	1.14	0.04	0.45	0.03	-	-
cg0936	-	putative putative iron-siderophore transporter	-	-359	0.78	0.23	1.10	0.05	-	-
cg0933	-	putative DNA or RNA helicase of superfamily II	-87	-115	1.12	0.15	1.14	0.01	-	-
cg0936	rgpJ	resuscitation promoting factor	122; 211; 402	-406	1.13	0.24	0.96	0.03	-	pred. A
cg0948	serC	phosphoserine aminotransferase	-258	-318	1.92	0.00	1.08	0.03	-	pred. A
cg0949	gltA	citrate synthase	-288	-409	1.41	0.01	0.99	0.56	-	pred. A
cg0952	mcrB	putative integral membrane protein	-17; +274	-170	1.51	0.05	1.48	0.01	-	pred. R
cg0955	-	putative secreted protein	-84	-328	1.78	0.00	1.16	0.04	-	-
cg0961	-	putative homoserine O-acetyltransferase	-	-26	0.31	0.00	1.85	0.00	R	pred. R
cg0967	lysQ	3-phosphoadenosine 5-phosphosulfate PAPS 3-phosphatase	-405	-405	0.50	0.00	0.94	0.05	-	-
cg0967	lysQ	3-phosphoadenosine 5-phosphosulfate PAPS 3-phosphatase	+41	-42	0.30	0.00	0.94	0.03	-	-
cg0973	rgi	thymine 5-phosphate isomerase	-59	-87	0.40	0.01	1.29	0.04	-	-
cg1037	rgpE	resuscitation promoting factor	-132	-163	1.17	0.02	1.07	0.01	-	exp. A
cg1043	-	putative thiol-disulfide isomerase and thioesterase	-	-30	0.94	0.03	1.16	0.04	-	-
cg1048	-	putative halooxid dehalogenase/epoxide hydrolase-family	-59	-89	0.88	0.41	1.22	0.03	-	-
cg1086	-	putative membrane protein	-126	-126	1.05	0.09	1.28	0.00	-	-
cg1087	-	putative membrane protein	-3	-29	1.63	0.00	1.01	0.07	-	-
cg1090	gltB	L-glutamyltranspeptidase precursor PR	+13	+13	0.64	0.02	1.25	0.00	-	-
cg1091	-	hypothetical protein	-133	-262	4.75	0.00	1.50	0.02	-	-
cg1108	psrC	putative secreted protein	-	-90	2.24	0.02	1.19	0.02	-	-
cg1111	osp	enzyme, phosphopyruvate hydratase	-93	-163	0.62	0.09	1.14	0.02	-	-
cg1142	-	putative Nav/proline, Na+/parithionate symporter	-	-114	0.46	0.03	1.12	0.02	-	pred. R
cg1143	(regulator)	putative transcriptional regulator, GntB-family	-98	-98	1.41	0.01	1.71	0.03	-	pred. R
cg1224	phnB2	PhnB E. coli	-28	-62	1.91	0.00	0.97	0.12	-	-
cg1244	arsC4	arsenate reductase, glutaredoxin-family	-128	-128	1.21	0.00	1.24	0.01	-	-
cg1256	dspD	tetrahydrodipicolinate succinylase	-275	-275	1.28	0.04	0.97	0.11	-	-
cg1290	metE	homocysteine methyltransferase	-252; -254	-494	0.78	0.31	1.32	0.00	-	-
cg1291	-	putative membrane protein	-83	-83	0.41	0.00	0.20	n.d.	-	-
cg1314	putP	proline transport system	-	-68	1.54	0.02	1.34	0.00	-	-
cg1345	nanK	nitrate/nitrite antiporter	-18	-79	0.84	0.39	1.11	0.04	-	exp. A
cg1346	mag	putative molybdopterin biosynthesis MCG protein	-146	-180	0.51	0.01	1.35	0.03	-	exp. A
cg1362	atpB	F1F0-ATP synthase, β -subunit of FO part	-119; -121	-172	1.40	0.10	0.79	0.01	-	exp. A
cg1409	phA	6-phosphofructokinase	-165; -167	-167	0.35	0.02	1.27	0.12	-	exp. A
cg1432	ihcO	dihydroxy-acid dehydratase	+24; -46	-165	1.06	0.00	1.06	0.04	-	-
cg1434	yggB (mscCG)	small-conductance mechanosensitive channel, MscS-family	-137	-137	1.47	0.02	1.37	0.00	-	-
cg1435	ihcE	acetolactate synthase I AHAS	-	-302	1.53	0.02	0.95	0.32	-	-
cg1437	ihcC	ketol-acid reductoisomerase	-43	-139	0.90	0.50	1.47	0.00	-	pred. R
cg1537	phoG	glucose-specific EtAlc component EtAlc of PTS	+31	-255	0.25	0.01	1.64	0.00	R	pred. R
cg1547	uifR	transcriptional regulator, LacI-family	+127	+62	1.99	0.00	1.55	0.02	-	-
cg1577	-	putative secreted hydrolase	-347; -408	-469	1.44	0.03	1.35	0.01	-	-
cg1612	-	putative acetyltransferase	-40	-40	0.26	0.00	3.16	0.00	R	-
cg1613	sovA2	rhodanese-related sulfurtransferase	-200	-200	0.57	0.05	1.35	0.00	-	-
cg1633	-	putative transcriptional regulator, MerR-family	-85; -97	-169	1.00	0.05	1.01	0.03	-	-
cg1656	nah	NADH dehydrogenase type II, NDH-II	-28; -30; -121; -123	-220	0.93	0.44	1.30	0.00	-	pred. A
cg1665	-	putative secreted protein	-54	-80	2.18	0.01	0.29	0.08	-	-
cg1697	aspA	aspartate aminooxylase/aspartase	+33	-8	2.19	0.01	1.03	0.01	-	-

TABLE S6 (Part 2/2) | Microarray data of *ΔcpdA*/WT and *ΔcyoB*/WT of (putative) GltR target genes

Locus tag [cd]	Gene name	Annotation	Distance to next TSS ^a	Distance to next TLS ^b	mRNA ratio <i>ΔcpdA</i> /WT ^c	p-value ^c	mRNA ratio <i>ΔcyoB</i> /WT ^c	p-value ^c	pred. due to data of microarray ^d	pred. in literature ^e
cg1791	<i>cpdA</i> (<i>cpd</i>)	glyceroldehyde-3-phosphate dehydrogenase glycolytic	-245; -300	-429	0.37	0.00	1.13	0.01	-	exp. R
cg1812	<i>pyrF</i>	ornithine 5-phosphate decarboxylase	-	-119	0.53	0.02	1.02	0.02	-	-
cg1837	-	putative holliday junction resolvase-like protein	-	-54	1.44	0.01	0.86	0.49	-	-
cg1862	<i>apt</i>	adenine phosphoribosyltransferase	+91; +126	-90	1.49	0.04	0.93	0.17	-	-
cg1929	<i>rms</i>	resolvase-family recombinase CGPS region	-	-210	0.84	0.36	1.81	0.02	-	-
cg1942	-	putative secreted protein CGPS region	-40	-103	1.10	0.03	0.91	0.25	-	-
cg1967	-	hypothetical protein, CGPS region	-	-78	0.56	0.12	2.52	0.04	-	-
cg2005	-	putative methyltransferase, CGPS region	-256	-271	1.42	0.03	n.d.	n.d.	-	-
cg2005	-	putative phage integrase N-terminal fragment, CGPS region	-	-	-	-	-	-	-	-
cg2071	<i>htz</i>	-	-123	-275	1.43	0.05	1.20	0.02	-	-
cg2109	<i>oxyH</i>	hydrogen peroxide sensing regulator, Lys-family	-66	-66	0.82	0.05	1.08	0.05	-	-
cg2117	<i>ptfH</i>	E1 enzyme, general component of PTS	-197; -132; -130	-225	0.23	0.00	1.66	0.00	R	pred. R
cg2118	<i>fuR</i>	transcriptional regulator, DeoR family	+108	-183	1.01	0.17	1.42	0.01	-	pred. R
cg2134	-	putative membrane protein	-60	-99	0.44	0.01	1.16	0.03	-	-
cg2135	<i>mraB</i>	tRNA methyltransferase	-325	-325	1.15	0.14	1.11	0.02	-	-
cg2136	<i>glnA</i>	glutamate uptake system	+7	+7	0.81	0.25	1.08	0.01	-	-
cg2157	<i>ovC</i>	tellurium resistance membrane protein	-210; -212	+13	1.52	0.08	1.08	0.04	-	-
cg2183	<i>opsC</i>	ABC-type peptide transport system	-	-85	0.02	0.00	1.48	0.00	R	-
cg2184	<i>opsD</i>	ATPase component of peptide ABC-type transport system	-	-224	0.00	0.00	1.55	0.01	R	-
cg2191	-	hypothetical protein, conserved	-104	-104	1.56	0.00	0.80	0.25	-	-
cg2261	<i>amtR</i>	low affinity ammonium uptake protein	-	-201	0.69	0.02	0.73	0.02	-	pred. R
cg2293	-	putative isole-1-glyoxylate synthase	-104	-130	1.37	0.01	0.86	0.47	-	-
cg2361	<i>divIVA</i>	cell division initiation protein	-126; -260; -280	-360	1.41	0.02	0.74	0.27	-	pred. A
cg2402	<i>njC</i>	putative secreted cell wall peptidase	-254; -295	-497	1.04	0.26	1.36	0.02	-	-
cg2409	<i>ctcA</i>	cytochrome aa3 oxidase, subunit 2	-30; -157; -161; -163	-216	1.39	0.00	1.10	0.10	-	exp. A
cg2410	<i>ctcB</i>	glutamine-dependent amidotransferase	-	-304	1.04	0.15	2.24	0.02	-	exp. A
cg2430	-	hypothetical protein	+28	-47	0.85	0.12	1.81	0.02	-	-
cg2437	<i>ihvC</i>	threonine synthase	-101	-101	0.89	0.47	1.30	0.02	-	-
cg2438	-	hypothetical protein	+2	-41	1.33	0.02	1.24	0.00	-	-
cg2464	-	hypothetical protein	-246	-330	0.92	0.96	1.23	0.03	-	-
cg2471	-	putative protein	-202	-205	0.62	0.01	0.97	0.02	-	-
cg2521	<i>fadD25</i>	long-chain fatty acid CoA ligase	-292	-404	0.86	0.41	1.19	0.02	-	-
cg2546	-	putative secondary C4-dicarboxylate transporter	-113	-134	0.35	0.00	0.18	0.15	-	-
cg2557	-	putative secondary Nuv/tile acid symporter	-	-77	2.23	0.00	0.95	0.12	-	-
cg2564	-	hypothetical protein	-207	-265	3.22	0.01	1.20	0.05	-	-
cg2565	-	hypothetical protein	-83	-115	0.84	0.31	1.18	0.02	-	-
cg2610	-	putative ABC-type transport system	-	-91	0.07	0.00	2.70	0.00	R	exp. R
cg2615	<i>vonR</i>	transcriptional regulator, PadR-family	-125	-125	0.72	0.05	n.d.	n.d.	-	-
cg2616	<i>vonA</i>	vanilate demethylase, coenzyme subunit	-	-59	0.54	0.03	4.25	0.01	R	-
cg2636	<i>catA2</i> (<i>catA</i>)	catechol 1,2-dioxygenase	-	-108	0.59	0.00	1.23	0.05	-	pred. R
cg2651	-	putative protein-fragment	-229	-229	3.51	0.01	0.86	0.03	-	-
cg2665	-	hypothetical protein	-	-15	1.71	0.00	0.26	0.04	A	-
cg2666	-	hypothetical protein	-187	-213	1.87	0.01	0.43	0.16	-	-
cg2692	-	putative thioninase	+28	-50	1.04	0.15	0.96	0.00	-	-
cg2700	<i>phoB</i>	alkaline phosphatase	-351	-342	0.00	0.00	n.d.	n.d.	-	-
cg2706	<i>msuA</i> (<i>msuK2</i>)	ABC-type maltose transport system	+27	-64	0.34	0.01	0.96	0.17	-	pred. R
cg2732	<i>gntV</i> (<i>gntK</i>)	putative glucosylase	-	-129	0.34	0.01	n.d.	n.d.	-	-
cg2748	-	putative membrane protein, conserved	-56	-56	0.77	0.28	1.23	0.05	-	-
cg2781	<i>oxyF</i>	ribonucleoside diphosphate sulfotransferase C subunit	-83; -127	-187	1.48	0.01	0.92	0.11	-	pred. R
cg2785	-	putative membrane protein	-	-167	0.00	0.00	n.d.	n.d.	-	-
cg2797	-	hypothetical protein	-	-224	1.22	0.01	n.d.	n.d.	-	-
cg2824	-	putative SAM-dependent methyltransferase	-	-491	1.42	0.04	0.35	0.05	A	exp. A
cg2837	<i>synC</i>	succinyl-CoA synthetase subunit β	-	-94	0.54	0.03	1.02	0.21	-	-
cg2825	<i>ptsS</i>	sucrose-specific EIIABC component EIIIC of PTS	-63	-124	0.27	0.01	2.23	0.00	R	-
cg2936	<i>nanR</i>	transcriptional regulator, GntR-family	-230	-255	0.96	0.20	1.71	0.01	-	-
cg2937	<i>slcA</i>	ABC-transporter for salic acid	+45	-54	1.31	0.08	1.24	0.00	-	-
cg2953	<i>vdh</i>	vanillin dehydrogenase	-18	-46	0.50	0.04	1.09	0.07	-	pred. R
cg2954	<i>hcp</i> (<i>hcyT</i>)	carbonic anhydrase, carbonate dehydratase	-47	-47	1.37	0.00	0.95	0.19	-	-
cg2966	-	putative phenol 2-monooxygenase	-	-74	0.55	0.00	4.26	0.00	R	pred. R
cg2999	-	putative ferredoxin reductase	-77	-137	0.58	0.08	0.16	0.04	-	-
cg3000	-	putative rhodanese-related sulfurtransferase	-75	-119	1.57	0.05	1.03	0.14	-	-
cg3022	-	putative acetyl-CoA acetyltransferase	-35	-254	2.19	0.02	0.90	0.21	-	-
cg3041	-	putative ABC-type multidrug transport system	-	-196	1.23	0.17	0.93	0.00	-	-
cg3046	<i>ptsE</i>	phosphotransacylase	-	-62	0.19	0.00	1.43	0.03	R	pred. R
cg3061	<i>cytR8</i>	two component response regulator	-179	-233	1.25	0.05	1.08	0.02	-	-
cg3096	<i>ald</i>	aldehyde dehydrogenase	+13	-75	0.35	0.00	3.07	0.00	R	exp. R
cg3107	<i>oxyA</i>	Zn-dependent alcohol dehydrogenase	-	-83	0.27	0.00	1.84	0.00	R	-
cg3112	<i>cyoZ</i>	sulfate transporter	-	-474	0.29	0.01	1.91	0.02	R	-
cg3122	<i>pMebE</i>	putative protein	+8	-41	1.41	0.03	0.08	0.06	-	-
cg3124	-	hypothetical protein	-18	-40	1.30	0.17	1.00	0.01	-	-
cg3127	<i>otcC</i>	citrate uptake transporter	-	-296	0.60	0.00	1.58	0.04	R	-
cg3169	<i>gcr</i>	phosphoenolpyruvate carboxykinase-GTP	-24; -55	-92	0.78	0.19	0.54	0.01	-	exp. R
cg3195	-	putative flavin-containing monooxygenase FMO	-	-26	0.07	0.00	3.29	0.00	R	-
cg3216	<i>gntP</i>	glucuronate permease, glucuronate:H ⁺ symporter GntP-family	-	-311	0.52	0.01	2.37	0.00	R	-
cg3226	-	L-lactate permease, operon with <i>hfdD</i> , MFS-type	-17; -21	-90	0.02	0.01	2.10	0.01	R	pred. R
cg3247	<i>AraM</i> (<i>gcpR11</i>)	two component response regulator	-352	-434	1.10	0.03	0.96	0.11	-	-
cg3255	<i>uspA2</i>	universal stress protein no. 3	-63; -65	-131	0.38	0.03	1.00	0.10	-	-
cg3313	<i>phoJb</i> (<i>phoJ</i>)	membrane carboxypeptidase	+6; +202	-51	0.74	0.01	0.98	0.00	-	-
cg3352	<i>nsqR</i> (<i>gntR</i>)	transcriptional regulator, GntR-family	-	-43	1.13	0.05	0.82	0.46	-	exp. R
cg3353	<i>nsqT</i> (<i>gntK</i>)	glutamate transporter, MFS-type	-	-56	0.00	0.00	0.05	n.d.	-	exp. R
cg3387	<i>htz2</i>	myo-inositol transporter 2	-52	-317	1.83	0.04	1.14	0.04	-	-
cg3388	<i>htz1</i>	putative transcriptional regulator, GntR-family	-84	-108	1.27	0.05	1.38	0.00	-	-
cg3413	<i>otcC</i>	branched-chain amino acid permease azalacine resistance	-	-132	0.73	0.29	1.23	0.05	-	-

^a: distance of GltR motif sequence to corresponding TSS or TLS

^b: ratios of mRNA of *ΔcpdA*/WT are taken from Schulte et al. 2017 [GEO database GSE81004]. *ΔcpdA* and WT were cultivated in CGMII minimal medium with 100 mM glucose as carbon source

^c: n.d. means that p-value was not calculated due to only one sample (n=1) instead of standard three samples (n=3). red p-value is highlighted due to p-value >0.05 which makes the result not reliable

^d: ratios of mRNA of *ΔcyoB* and WT cultivated in CGMII minimal medium with 100 mM glucose as carbon source

^e: regulation deduced due to opposite values in the microarray results analysis with the strains *ΔcpdA* (Schulte et al., 2007) and *ΔcyoB*

^f: regulation of the gene by GltR was predicted (pred.) or experimentally verified (exp.) according to Corynebact7.0 (Parsis, 2020)

TABLE S7 (Part 1/2) | G1/R peaks and corresponding binding sites found less than 700 bp upstream of the TSS of antisense transcripts, non-protein coding elements or intragenic transcripts; information of TSS of asRNA, non-protein coding genes and intragenic transcripts was taken from Mentz et al. 2013 and Pfeifer-Sancar et al. 2013

antisense transcript (asRNA)	G1/R motif rel. located to asRNA	Distance to respective TSS	neighbouring genes (< 700 bp of a gene start)	EF in WT _{trans} (log ₂)	Start position ^b	End position ^b	G1/R binding site ^a	E-value	G1/R peak known or new ^d	No. ^c
antisense transcript of <i>cp0236</i>	downstream	+62	<i>emf1</i> (emb3)	4.20	205760	207155	TGAGTAATTCCTCCG	1.34E-03	NEW	219
antisense transcript to <i>cmc3</i> (cg1052)	upstream	-227		3.13	977403	977763	BTGTCCAAAGGCTCCG	8.04E-05	NEW	101
antisense transcripts 1a of <i>cp1509</i>	upstream	-114		3.34	1490505	1490608	TGAGCCCGGCTCCG	4.49E-04	NEW	180
antisense transcripts 3a of <i>cp1508</i>	upstream	-108; -179; -225	<i>cp1309</i>	3.59	1797026	1797319	BTGAGTATTTCGACG	2.32E-03	NEW	230
antisense transcript <i>cp1945</i>	upstream	-618		3.21	1821008	1821181	TGTTCACTCCCTCCG	6.01E-04	NEW	108
antisense transcript of <i>cp2423</i>	upstream	383	<i>cp2011</i>	6.40	1032463	1034380	AGTATGCTCCCTCCG	7.06E-04	pred. Kohli et al. 2008	268
antisense transcript of <i>cp2362</i>	on TSS of asRNA	+3	<i>dmwA</i>	4.31	2276036	2276342	TGTTATCTTTCGACG	3.47E-05	Kohli & Trauch 2009	59
<i>cp1_21615</i>	upstream <i>cp1_23615</i>	-126			2917792	2918090	AGTGCACGACGAGGAC	3.66E-04	NEW	167
antisense transcript of <i>cp0333</i>	upstream	-66	<i>cp0100</i>	3.36	3267837	3268141	TGTAGCACTGATGACG	6.09E-05	NEW	86
antisense transcript to <i>phc1</i> (cg3393)	on TSS of asRNA	+1		3.47						
trans-enclosed sRNA (<i>cpb_xxxx</i>)	motif rel. located to sRNA	Distance to respective TSS	neighbouring genes (< 700 bp of a gene start)	EF in WT _{trans} (log ₂)	Start position ^b	End position ^b	G1/R binding site ^a	E-value	G1/R peak known or new ^d	No. ^c
<i>cpb_00025</i>	upstream	-382	<i>dxn</i>	11.52	1622	1949	AGTGGACTTTTCGACG	2.48E-06	Toyoda et al. 2011	5
<i>cpb_00545</i>	upstream	-123		5.05	39981	40261	TGACTGCCGAGGACG	3.10E-03	NEW	232
<i>cpb_03505</i>	on TSS	+3	<i>glpF</i>	13.19	307411	307714	AGTGGTCTTTCGACG	2.53E-05	Jungwirth et al. 2008, Jungwirth et al. 2013, Siebhahn et al. 2015	44
<i>cpb_03605</i>	in 6' RNA	-89		9.59	314402	314704	AGTGCATTTTCGACG	8.01E-06	Jungwirth et al. 2013	13
<i>cpb_04605</i>	upstream	-60	<i>crp</i> <i>agf46</i> <i>agf47</i>	3.79	569106	569362	TATGATGCTCTTCG	6.61E-04	NEW	200
<i>cpb_07555</i>	upstream	-32	<i>merT</i> <i>cp0755</i>	3.32	607808	608106	TATGACTAGCCGACT	6.01E-04	NEW	106
<i>cpb_08033</i>	upstream	-61	<i>thp</i> <i>cp0803</i>	3.65	721377	721657	AGTAATTAGAGGACG	9.34E-05	pred. Kohli et al. 2008	110
<i>cpb_08785</i>	upstream	-114	<i>wbf</i> (wbf1)	6.37	805907	806235	TTGTTGGTGGAGGACG	8.01E-06	Kohli & Trauch 2008, Jungwirth et al. 2013	14
<i>cpb_09366</i>	upstream	-190	<i>gfp</i> <i>cp0936</i> <i>cp0938</i>	4.45	868599	868896	TTGACATAAATTCGAC	2.48E-06	Kohli & Trauch 2008	8
<i>cpb_09513</i>	upstream	-220	<i>orc03</i> <i>cp0951</i>	7.19	881238	881608	AGTTACTACTACTTCG	4.02E-05	Kohli & Trauch 2008	68
<i>cpb_15755</i>	in <i>cpb_09516</i>	-147	<i>metB</i> <i>cp1577</i>	3.66	1460472	1460771	BTGTGGGAGTTTCGAC	3.47E-05	pred. Kohli et al. 2008	64
<i>cpb_16115</i>	upstream	-12	<i>ssa42</i> <i>cp1612</i> <i>cp1613</i>	3.19	1500579	1500875	AGTCACTAAGCTTCGAC	1.33E-04	Toyoda et al. 2011	43
<i>cpb_16565</i>	upstream	-30	<i>ofw</i> <i>cp1656</i> <i>cp1657</i>	5.59	1544586	1544879	TATGGCAATGTCGCG	2.97E-04	Kohli & Trauch 2008	156
<i>cpb_19606</i>	upstream	-34	<i>cp05</i> <i>cp1966</i> <i>cp1967</i>	3.04	1847031	1847319	AGTGGGTTGCATGCT	9.34E-05	pred. Kohli et al. 2008	113
<i>cpb_20643</i>	upstream	-377	<i>cp2064</i>	2.55	1955246	1955567	GTTGAAATAGGACG	3.47E-05	NEW	65
<i>cpb_20715</i>	upstream	-47	<i>hcz</i> <i>cp2071</i>	7.58	1995412	1995693	AGTCACTACTCTCCG	4.08E-03	pred. Kohli et al. 2008	234
<i>cpb_27005</i>	antisense transcript	-190		6.02	2603255	2603478	TGTTTTGCAAGTTCGAC	5.76E-07	NEW	1
<i>cpb_27025</i>	upstream	-432		5.88	2603276	2603715	TTGTGAGCCAGCCGCT	2.48E-06	NEW	7
<i>cpb_27413</i>	upstream	-556	<i>cp2741</i>	2.80	2637723	2638035	TGCATGTTTTCGACT	4.66E-03	NEW	236
<i>cpb_27803</i>	upstream	-116	<i>crd</i> <i>cp2780</i>	5.42	2072863	2073129	TTGTGACCCCTTCGAC	2.53E-05	Kohli & Trauch 2008	46
<i>cpb_30215</i>	upstream	-15	<i>cp3021</i> <i>cp3022</i>	3.40	2040579	2040641	AGTGGAGGAGGAGGACT	9.44E-05	pred. Kohli et al. 2008	112
<i>cpb_30615</i>	on TSS	-8	<i>cp306</i> <i>cp3061</i>	6.10	2040950	2041060	TGTTTCATATGATGACG	1.51E-04	NEW	130

TABLE S7 (Part 2/2) | GHR peaks and corresponding binding sites found less than 700 bp upstream of the TSS of antisense transcripts, non-protein coding elements or intragenic transcripts; information of TSS of asRNA, non-protein coding genes and intragenic transcripts was taken from Mentz et al. 2013 and Pfeifer-Sancar et al. 2013

intragenic transcript	motif rel. located to intragenic transcript	Distance to respective TSS	neighbouring genes (< 700 bp of a gene start)	EF in WT _{Genes} (p/c) ^a	Start position ^b	End position ^b	GHR binding site ^c	E-value	GHR peak known or new ^d	No. ^e
Intragenic transcript within cg0706	downstream	+34	-	3.60	622394	622684	GCTTCTCAGATTCACA	1.51E-04	NEW	133
Intragenic transcript within cg1044	upstream	-164	cg1043	4.59	916818	970084	AGTTCGCCCCGACACA	4.02E-05	Toyoda et al. 2011	69
Intragenic transcript within cg1111	upstream	-189	emo	5.77	1034624	1034903	CGTTCGCGATTCACA	7.96E-04	NEW	206
Intragenic transcript within cg1313	upstream	-134	pdp1b (mz6)	3.57	3180669	3189109	TATTCTTCAGACACA	1.58E-03	NEW	223
lRNA										
Arg lRNA (cgrNA_3549)	upstream	-179	-	2.74	897324	897585	GCTCAATCGAATCACT	7.96E-04	NEW	211
Arg lRNA (cgrNA_3575)	upstream	-102	phoB	4.89	2400743	2401017	TGTTCGAGGCCACACA	9.65E-06	NEW	20
Asp lRNA (cgrNA_3583)	upstream	-12	stcC	3.53	2727036	2727190	TGTTCCAGCAATTCACCT	4.02E-05	Han et al. 2008, Kohn & Tusch 2009	74
Gly lRNA (cgrRNA_3574)	upstream	-208	-	2.89	2560699	2560992	TGTCAGCATAGCACT	3.66E-04	NEW	168
Leu lRNA (cgrRNA_3579)	upstream	-58	-	5.08	2650120	2650497	CGTTCAGTTCGATCAAC	4.06E-04	NEW	173
new annotated genes										
cg4015	on TSS	+6	levA	7.65	267974	268292	TGTATGCTTCACACA	9.14E-05	Toyoda et al. 2011 Kohl & Tusch 2009, Jungwith et al. 2013	104
cg4016	upstream	-11	lyg8b (musCG)	4.79	1337674	1337967	TGTTTAGCAGTACACA	4.44E-06	NEW	11

a: enrichment factor (EF) of GHR peak of WTGHR-TS (86) ChIP-Seq samples (n=3)

b: nucleotide position refers to genome sequence of B8527147 of *C. glutinosus* ATCC13032 (Malinowski et al. 2005)

c: motif was detected by using the program MEME-ChIP with the DNA fragment of the detected GHR peaks as input sequences; the 16 bp sequence shows the most probable GHR binding site within this sequence

d: if GHR peak is previously described, the respective literature is mentioned; if the site is only found in our ChIP-Seq results it is described as 'NEW'

e: No. according to Table S3

3 Discussion

In order to survive in a changing environment, organisms have to sense the changing conditions and react in an appropriate way. On the molecular level, complex signalling networks exist for this purpose. Signal transduction at the cellular level often involves small molecules that act as second messengers to transduce external stimuli to one or more effectors in the cell. Such second messengers are for example cyclic nucleotides, (p)ppGpp, or Ca^{2+} (Cashel, 1975; Endo, 2006; Valentini & Filloux, 2016). The cyclic nucleotide cAMP is a ubiquitous molecule and plays a central role in numerous signalling processes throughout all kingdoms of life (Gancedo, 2013). In mammalian cells, for example, cAMP activates protein kinases leading to the phosphorylation of several different proteins involved in diverse cellular mechanisms, such as ion transport or transcriptional regulation (Kopperud et al., 2003). In plants, cAMP was found to be involved in sensing and responding to biotic and abiotic environmental stresses (Gehring, 2010; Jha et al., 2016; Maathuis & Sanders, 2001). In prokaryotes, cAMP was first found to play an important role in carbon catabolite repression (Botsford & Harman, 1992) and later also in virulence and pathogenesis of human pathogenic bacteria and in biofilm formation (Liu et al., 2020; McDonough & Rodriguez, 2011). The cAMP receptor protein (CRP), first described in *E. coli*, is a transcriptional regulator that is able to activate or repress the transcription of various gene targets. CRP homologs are found in various other bacterial genera, such as *Mycobacterium*, *Pseudomonas*, *Vibrio* or *Corynebacterium* and the plasticity of this system emphasizes the adaptation to the individual needs of the respective organism (Arce-Rodríguez et al., 2012; Skorupski & Taylor, 1997; Stapleton et al., 2010).

The aim of this thesis was to better understand the cAMP signalling network in *Corynebacterium glutamicum*, a model organism for Actinobacteria and in industrial biotechnology. Therefore, the thesis is focused on two aspects: the characterization of an adenylate cyclase-deficient *C. glutamicum* strain, and the investigation of the consequences of a low intracellular cAMP level for the transcriptional activity of the global regulator GlxR.

3.1 The role of CyaB activity in *C. glutamicum*

Four years after the detection of intracellular cAMP in *C. glutamicum*, two groups reported the identification of a membrane-bound adenylate cyclase, named CyaB, an enzyme that catalyses the synthesis of cAMP (Bussmann, 2009; Cha et al., 2010; Kim et al., 2004). Strains with a partly or entirely deleted *cyaB* gene showed a significant drop in the concentration of intracellular cAMP (Cha et al., 2010; Toyoda et al., 2011; Wolf et al., 2020). Moreover, the $\Delta cyaB$ mutants had a strong growth defect in minimal medium with acetate or glucose plus acetate as carbon source, but not with glucose or ethanol (Bussmann, 2009; Cha et al., 2010; Wolf et al., 2020). As the growth defect in the presence of acetate could be reverted by the addition of cAMP to the medium, the effect was shown to be specific for the deletion of *cyaB* (Bussmann, 2009; Wolf et al., 2020). The reason for the growth defect remained unknown and the theory that it was due to inhibition of acetate uptake by the transporter MctC (Cg0953) could be disproved by the fact that acetate uptake in a *mctC* deletion mutant by passive diffusion across the membrane was sufficient to maintain wild type-like growth (Jolkver et al., 2009). The uptake of acetate was also shown to be transporter-independent in other microorganisms, such as *E. coli* and *Saccharomyces cerevisiae* (Lindahl et al., 2017; Orr et al., 2018).

The 'acetate effect' of the $\Delta cyaB$ mutant was then hypothesized to be due to a higher sensitivity towards acetate compared to the wild-type strain (Wolf et al., 2020). At higher concentrations, acetate is known to have uncoupler-like behaviour causing a net import of protons, which affects the proton-motive force (PMF) (Axe & Bailey, 1995). A strong incidence for the assumption that the growth-defect of the $\Delta cyaB$ mutant was caused by the uncoupling function of acetate was the finding that the acetate sensitivity was concentration- and pH-dependent. The molecular basis for the higher uncoupler sensitivity of the $\Delta cyaB$ mutant was explained by reduced expression of the genes encoding the cytochrome *bc₁-aa₃* supercomplex and the F₁F₀-ATP synthase, as shown in transcriptome array results and RT-qPCR (Wolf et al., 2020). Strong support for this explanation comes from the fact that mutants lacking a functional cytochrome *bc₁-aa₃* supercomplex are unable to grow with acetate as sole carbon source (Wolf et al. 2020). Figure 5 illustrates the features described above.

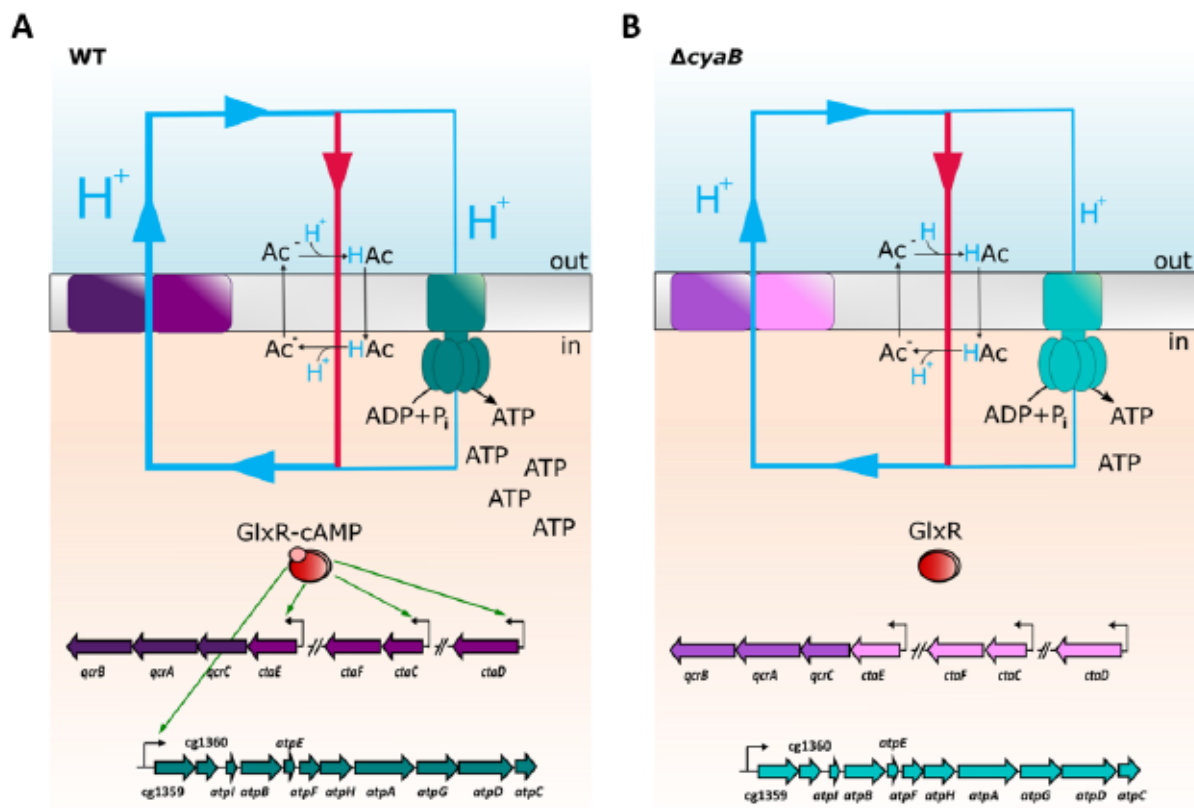


Figure 5: Model of the proton circuit in the presence of acetate in the *C. glutamicum* WT (A) and the $\Delta cyaB$ mutant (B). In this model acetate acts as an uncoupler (red arrow) and disturbs the proton circuit (blue lines) of the respiratory chain (purple) and the ATP synthase (green). In the wild-type strain (WT), the cAMP-GlxR complex (red) activates the transcription of the genes encoding the cytochrome bc_1-aa_3 supercomplex and the F_1F_0 -ATP synthase. In the presence of acetate, the capability of generating pmf is disturbed, but not strong enough to cause a growth defect. In the $\Delta cyaB$ mutant, the reduced or even absent cAMP level causes a lowered expression of the genes for the cytochrome bc_1-aa_3 supercomplex, leading to a reduced capacity to build up pmf and to counteract the uncoupling activity of acetate. Additionally, the growth defect of the $\Delta cyaB$ mutant on acetate is caused by the reduced ATP synthesis via oxidative phosphorylation due to reduced synthesis of the F_1F_0 -ATP synthase.

A $\Delta cyaB$ strain transformed with fluorescence reporters carrying native promoters of genes of the cytochrome bc_1-aa_3 supercomplex (*ctaC*, *ctaE*, or *ctaD*) in front of a gene encoding a fluorescent protein (mVenus) revealed lower fluorescence and thus lower promoter activity compared to the wild type when cultivated in minimal medium with acetate (Figure 6). The reduction of promoter activity can be explained by a reduced activation of transcription by GlxR due the absence of cAMP in the $\Delta cyaB$ mutant.

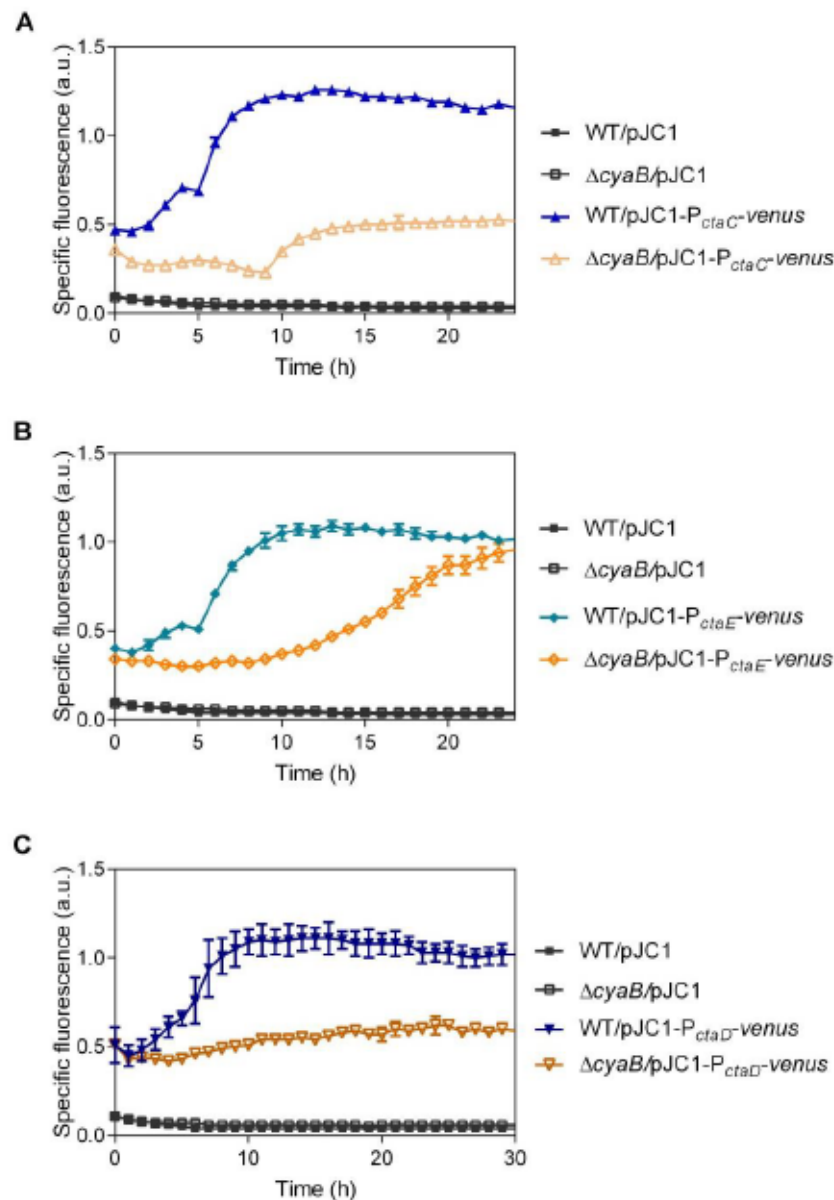


Figure 6: Specific fluorescence of *C. glutamicum* wild type (WT) and the $\Delta cyaB$ mutant carrying fluorescence reporters with the native promoter of *ctaC* (A), *ctaE* (B), or *ctaD* (C). The first preculture was inoculated in BHI medium and the second preculture was grown in CGXII medium with 2% glucose. The cells were washed with saline (0.9% (w/v) NaCl) and used to inoculate the main cultures in 800 μ l CGXII minimal medium with 100 mM potassium acetate as sole carbon sources to an OD_{600} of 1. Cultivation was performed in the BioLector at 30 $^{\circ}$ C and 1200 rpm. Growth was monitored as scattered light at 620 nm and fluorescence was monitored with an eYFP filter (ex. 508 nm/em. 532 nm). The results of three biological replicates with standard deviations are shown.

In the strain SC^+ , the native promoters of *ctaC*, *ctaE*, and *ctaD* have been replaced by the constitutive *tuf* promoter (Platzen, 2013) and therefore their transcription is independent of the cAMP-GlxR complex. However, the inhibitory effect of acetate was also observed in the SC^+ $\Delta cyaB$ strain (Figure 7). A possible explanation for this result was obtained by the ChAP-Seq results of this work, in which *ctiP* (*cg2699*) was identified as an additional GlxR target

gene. CtiP is a large transmembrane protein that was recently shown to be involved in copper transport and insertion into cytochrome *aa₃* oxidase (Morosov et al., 2018). The GlxR binding site is located 108 bp upstream of the TSS of *ctiP* and therefore transcription of *ctiP* is probably activated by GlxR. Insufficient expression of *ctiP* in the SC^+ $\Delta cyaB$ strain could be responsible for the still observed inhibition by acetate, if only insufficient amounts of functional cytochrome *bc₁-aa₃* supercomplex can be formed. In addition, a lower expression of the ATP synthase could also contribute to the inhibition of the SC^+ $\Delta cyaB$ strain by acetate, in particular when acetate serves as sole carbon source, which does not allow net ATP synthesis via substrate level phosphorylation.

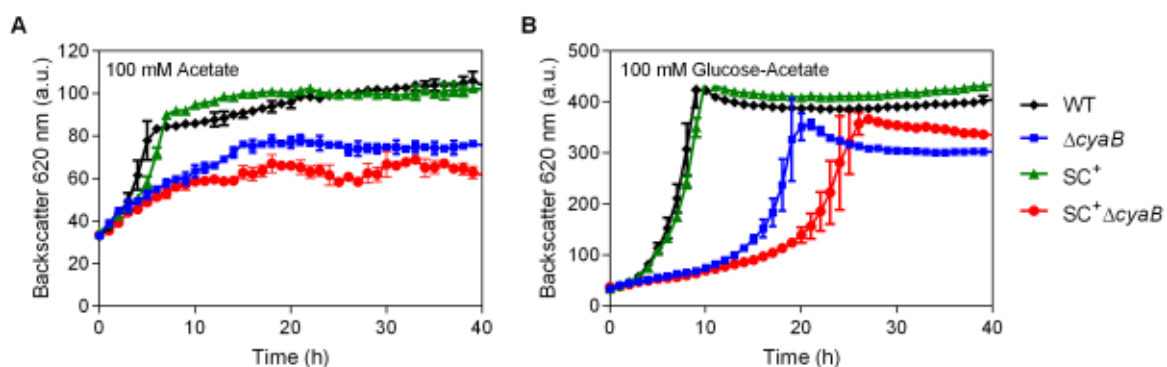


Figure 7: Growth of *C. glutamicum* wild type (WT), the $\Delta cyaB$ mutant, strain SC^+ , and the $SC^+ \Delta cyaB$ strain. Cells were cultivated in CGXII medium with 100 mM potassium acetate (A) or a glucose-acetate mixture, each 100 mM (B). The results of three biological replicates with standard deviations are shown. The first preculture was inoculated in BHI medium and the second preculture was grown in CGXII medium with 2% glucose. The cells were washed with saline (0.9% (w/v) NaCl) and used to inoculate the main cultures in 800 μ l CGXII minimal medium with the indicated carbon sources to an OD_{600} of 1. Cultivation was performed in a BioLector at 30 °C and 1200 rpm and growth was monitored as scattered light at 620 nm.

3.1.1 Further effects contributing to the ‘acetate effect’ of the $\Delta cyaB$ mutant

The uncoupler-like behaviour of acetate in combination with the lower transcription and activity of the respiratory chain and ATP synthase in the *cyaB* deletion strain is believed to be the main reason for the inhibition of growth. However, further effects can contribute to the effect of the acetate sensitivity of the *cyaB* mutant. It can be excluded that the change of the extracellular pH during cultivation with acetate is responsible for the inhibited growth, as the initial pH of 7 was the same as the pH at the end of experiments (data not shown). Furthermore, growth experiments in minimal medium with glucose as sole carbon source and with different initial pH values (pH 6-7) showed that the growth of the *cyaB* deletion strain was comparable, suggesting that the absence of CyaB did not lead to problems in the

pH homeostasis *per se* (Wolf et al., 2020). Only the combination of pH 6 and the presence of acetate in the medium increased the growth inhibition of the $\Delta cyaB$ mutant compared to the growth at pH 7 (Wolf et al., 2020). This could be explained due to the fact that weak acids such as acetic acid act as a proton translocator more effectively if the pH of the medium is closer to its pK_a (acetic acid pK_a 4.76). So the acetate effect was described as pH-dependent. Growth of the *cyaB* deletion strain was tested with other salts such as citrate and L-lactate. Only slightly impaired growth of the *cyaB* deletion strain was observed when cultivated with citrate (100 mM) or L-lactate (100 mM) as carbon source (Figure 8). The growth differences of WT and the *cyaB* deletion strain with citrate and lactate as carbon sources is a further phenotypical characterisation of the *cyaB* deletion strain. However, the growth differences are more likely due to reduced GlxR activity in the $\Delta cyaB$ mutant and are not a pH-effect.

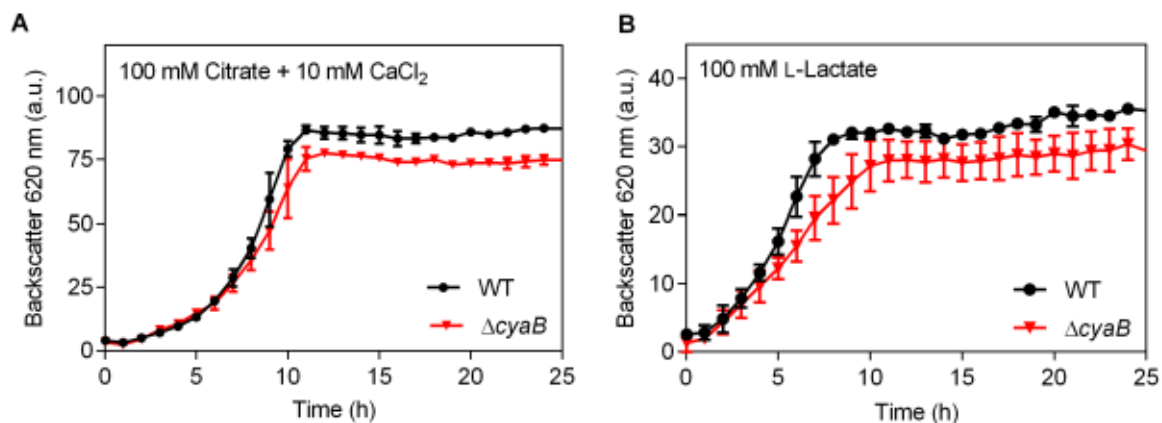


Figure 8: Growth of *C. glutamicum* WT and the $\Delta cyaB$ mutant in CGXII minimal medium with 100 mM citrate (A) or 100 mM L-lactate (B). The first preculture was inoculated in BHI medium and the second preculture was performed in CGXII medium with 2% (w/v) glucose. The cells were washed with saline (0.9% (w/v) NaCl) and used to inoculate the main cultures in 800 μ l CGXII minimal medium with the indicated carbon sources to an OD_{600} of 1. Growth was monitored as scattered light at 620 nm in a BioLector at 30 °C and 1200 rpm. Mean values and standard deviations of three biological replicates are shown.

As GlxR is a global regulator, one cannot exclude further transcriptional changes of genes to be involved in the higher sensitivity towards acetate and the strong sensitivity towards the protonophore CCCP. Due to the absence of cAMP in the $\Delta cyaB$ mutant, genes that would normally be activated by the cAMP-GlxR complex often showed a lower transcription compared to the genes in the wild-type strain (Wolf et al., 2020). As already mentioned, a lower transcription of the newly identified GlxR target gene *ctiP*, a gene coding for a transmembrane protein involved in copper transport and insertion into cytochrome *aa₃*

oxidase (Morosov et al., 2018) probably contributes to the enhanced sensitivity of the Δ *cyaB* mutant towards uncouplers.

Moreover, changes in cell envelope of *C. glutamicum* Δ *cyaB* compared to the wild-type strain could also favour the higher uncoupler-sensitivity. Recent studies on the role of cAMP in *Mycobacterium* revealed that decreased intracellular cAMP level led to a perturbation of the peptidoglycan biosynthesis that probably resulted to increased cell envelope permeability (Thomson et al., 2022). The higher cell envelope permeability was supposed to be the reason for a higher susceptibility towards antimicrobials targeting the cell wall synthesis (e.g. ethambutol or vancomycin).

In the yeast *S. cerevisiae* it was shown that changes in the membrane lipid profile increased the acetic-acid tolerance (Guo et al., 2018; Zheng et al., 2013). For example, the acetic acid-tolerant *S. cerevisiae* YJS329ELO1 (carrying a plasmid, overexpressing a fatty acid desaturase) showed 17.6% higher levels of oleic acids (C18:1n-9) and an improved tolerance to acetic acid compared to the parental strain YJS329 (Guo et al., 2018; Zheng et al., 2013). The increased amount of unsaturated fatty acids in the plasma membrane probably led to a reduction of the diffusion rate of acetic acid, which is in yeast critical because the weak acid was shown to enter the cell mainly in a transporter-independent way by passive diffusion through the membrane lipid bilayer (Lindahl et al., 2017).

Previous studies showed that the *C. glutamicum* wild-type strain is moderately alkali-tolerant and is able to maintain a quite stable intracellular pH around pH 7.5 when cultivated at external pH values between 6.0 and 9.0 (Barriuso-Iglesias et al., 2008; Follmann et al., 2009). To sustain a physiological intracellular pH value, *C. glutamicum* has different cellular mechanisms to resist external acidic or alkaline pH stress. Sigma factors were shown to play a crucial role under pH stress conditions in *C. glutamicum* (Barriuso-Iglesias et al., 2013; Jakob et al., 2007). For example *sigB* (cg2102), which is related to the general stress response, was upregulated under acidic stress conditions and therefore this sigma factor probably contributes to the maintenance of pH homeostasis (Jakob et al., 2007). Experiments with bacteria such as *B. subtilis* and *Listeria monocytogenes* showed that the absence of a functional *sigB* gene led to higher sensitivity towards acidic pH (Hecker & Völker, 2001; Wiedmann et al., 1998). In *C. glutamicum*, the sigma factor H (SigH, Cg0876) is important in the response to heat shock and oxidative stress (Kim et al., 2005) and later experiments suggested that SigH was involved in the transcriptional control of the F_1F_0 -

ATPase operon at alkaline pH of 9 (Barriuso-Iglesias et al., 2013). Not only stress responses, but several cellular processes are involved in sustaining intracellular pH homeostasis. For example, a connection between pH responses, oxidative stress, iron homeostasis, and methionine synthesis was suggested (Follmann et al., 2009). Furthermore, a link between sulphur assimilation and the repression of oxidative stress in the maintenance of pH homeostasis was reported (Xu et al., 2019). It was stated that the repression of genes involved in sulphur metabolism by the transcriptional regulator McbR lead to a reduction of L-cysteine accumulation, which turned out to be advantageous under acidic acid stress conditions (Xu et al., 2019). If the bacterium is not able to react properly to changing pH conditions, a change of the cytoplasmic pH by one unit can lead to changes not only in the PMF, but also in the activity and stability of enzymes, in transcription or translation, in solubility of trace elements, or in the structure of nucleic acids (Follmann et al., 2009; Krulwich et al., 2011; Olson, 1993). The ability to maintain a physiological internal pH could be impaired in the *cydB* deletion strain, which could contribute to the acetate effect.

These effects could add to the effect that the Δ *cydB* mutant has already an impaired energy metabolism due to lower expression of the respiratory chain genes and the genes coding for the F_1F_0 ATP synthase as shown in Toyoda et al., 2011 and in Wolf et al., 2020. In order to prove whether the pH homeostasis is less efficient in Δ *cydB* mutant one could compare the intracellular pH (pH_i) of the wild-type strain and the Δ *cydB* mutant when cultivated with acetate as carbon source. Such measurements were already successfully performed by staining the cells with pH-sensitive fluorochromes and comparison of the cell fluorescence by a flow cytometer (Leyval et al., 1997). Nowadays, pH_i can be monitored online within different *C. glutamicum* strains when they carry a plasmid encoding a pH sensitive variant of GFP, called pHlourin (Kirsch, 2014; Miesenböck et al., 1998). A difference in the pH_i between the *C. glutamicum* wild type and the *cydB* deletion strain cannot be excluded. However, despite many possible reasons for an impaired pH homeostasis (e.g. malfunction of transporters or regulatory proteins), these should contribute only to a lesser extent to the acetate sensitivity in the Δ *cydB* mutant. Still, a functional respiratory chain is obviously the most important factor that contributes to the pH regulation in acidic environments in *C. glutamicum*. All secondary active transporters, such as Mrp1, require the proton motive force (pmf) established by the cytochrome *bc₁-aa₃* supercomplex to be active. In the *C. glutamicum* DOOR strain that is absent of terminal oxidases (Koch-Koerfges et al.,

2013), it was shown that the pH homeostasis was disturbed compared to the wild type strain, especially when the external pH drops below pH 7 (Δ pH 0.51 and 1.09 at pH 6, respectively). Experiments with *E. coli* showed that the direct involvement of terminal oxidases and oxidative phosphorylation plays a crucial role in the pH homeostasis. Acid stress led to an upregulation of the proton-pumping components of the respiratory chain in *E. coli* (Cotter et al., 1990; Maurer et al., 2005; Slonczewski et al., 2009; Sun et al., 2012). These experiments underline that the cytochrome *bc₁-aa₃* supercomplex is the most important factor for the adaptation of *C. glutamicum* to acidic conditions, because it ensures that protons are pumped out of the cell.

3.1.2 CyaB as the main adenylate cyclase in *C. glutamicum*

Because a residual intracellular cAMP concentration was still detected in AC-deficient mutants of *C. glutamicum* (Bussmann, 2009; Cha et al., 2010; Toyoda et al., 2011), the existence of a second AC was expected. However, bioinformatic analyses using a protein-protein basic local alignment search tool (BLASTP) did not reveal hits for another AC besides CyaB (Cg0375) in *C. glutamicum*. A domain-enhanced lookup time accelerated blast (DELTA-BLAST) (Boratyn et al., 2012) with the amino acid sequence of the representative AC of class IV (AC2 or CyaB_{Aer} of *Aeromonas hydrophila*) (Sismeiro et al., 1998) and a proteome database of *C. glutamicum* ATCC13032 as a reference, resulted in one hit (Table 2).

Table 2: Results of DELTA-BLAST (Boratyn et al., 2012). DELTA-BLAST of the amino acid sequence of AC2 (also described as CyaB_{Aer}; UniProt No. O69199/CYAB_AERHY) of *Aeromonas hydrophila* as query sequence and a database comprising non-redundant protein sequences of *C. glutamicum* ATCC13032 as the search set.

Protein Name	Percent Identity	Query Cover	Max Score	Total Score	E-value
Cgl2231* ¹	16.86%	74%	74.3	74.3	9e-17

*¹: The gene encoding for Cgl2231 (Accession: BAB99624.1) has the same coding sequence as cg2450 in the genome of *C. glutamicum* ATCC13032 (BX927147) sequenced by Kalinowski et al., 2003.

The 191 aa long AC2 of *A. hydrophila* showed sequence similarities within the first 240 aa of the protein Cg2450 of *C. glutamicum*. Cg2450 is an uncharacterized protein that is predicted to be putative pyridoxine biosynthesis enzyme (CoryneRegNet 6.0) (Pauling et al., 2012). It contains a CYTH domain and a CHAD domain (PF01928/IPR023577 and PF05235/IPR007899, respectively). The CHAD protein domain stands for ‘conserved histidine α -helical domain’ and is found in all kingdoms of life and putatively involved in binding of inorganic

polyphosphates (Lorenzo-Orts et al., 2019). The CYTH domain is a catalytic domain that is named after the first known members, the AC CyaB of *A. hydrophila* and thiamine triphosphatase of mammalian cells (Bettendorff & Wins, 2013). Both enzymes have in common that they need triphosphorylated substrates and require at least one divalent metal cation for the catalytic reaction (Bettendorff & Wins, 2013). The AC2 (CyaB_{Aer}) of *A. hydrophila* was first described in 1998 and was until 2006 the only bacterial AC member of the class IV AC (Smith et al., 2006). A cAMP-synthesizing activity was only shown under *in vitro* conditions, revealing extraordinary biochemical characteristics, with an optimal activity at 65 °C and a pH of 9.5 (Sismeiro et al., 1998). Under physiological conditions the gene coding for the AC2 was not expressed in *A. hydrophila* and so far no cultivation conditions were found that led to transcription of the AC2 gene (Sismeiro et al., 1998). The presence of a CYTH domain in the protein Cg2450 of *C. glutamicum* suggests that this could be a second AC. Previous studies in our lab by Julia Schulte showed that it was easily possible to obtain a cg2450 deletion mutant and also a double mutant lacking both *cyaB* and the *cg2450* gene. The double deletion mutant $\Delta cg2450\Delta cyaB$ had comparable growth curves with the $\Delta cyaB$ mutant when cultivated in medium containing acetate as carbon source (data not shown). Also, the $\Delta cg2450$ strain showed no growth defect in minimal medium that contained acetate, which argues against the assumption that *cg2450* encodes a second functional AC in *C. glutamicum* (data not shown). Whether Cg2450 catalyses cAMP synthesis *in vitro*, was not tested yet.

3.2 Intracellular cAMP concentration of *C. glutamicum* compared to other bacteria

Intracellular cAMP levels are controlled by the rate of synthesis by adenylate cyclases, the rate of degradation by phosphodiesterases, and possibly by export of cAMP. Because of the various ways of regulation, intracellular cAMP levels are highly variable in different bacterial species. Whereas *M. tuberculosis* and *M. smegmatis* are considered to be species with a high intracellular cAMP concentration, harbouring up to 4 mM cAMP (Dass et al., 2008; Padh & Venkitasubramanian, 1976), *E. coli* is considered as a bacterium with a moderate cAMP level of about 35-40 μM (Bennett et al., 2009; Notley-McRobb et al., 1997) and *Pseudomonas putida* has a cAMP concentration around 0.07-0.12 μM (measured by cAMP radioimmunoassay), whereas no cAMP could be detected applying HPLC methods (Arce-Rodríguez et al., 2012; Arce-Rodríguez et al., 2021; Phillips & Mulfinger, 1981). When comparing the intracellular cAMP levels of the mentioned bacteria with those reported for *C. glutamicum*, one would consider *C. glutamicum* as a species with a low cAMP level. Table 3 gives an overview of the intracellular cAMP concentrations and the binding affinities of CRP-like proteins to cAMP. In all earlier mentioned bacteria, cAMP is a part of a signalling pathway that involves binding of a CRP-like protein which harbours a cAMP-binding domain. And similar to the different intracellular cAMP concentrations, the cAMP-binding affinities for the respective CRP-like proteins are different (Arce-Rodríguez et al., 2012; Ren et al., 1990; Stapleton et al., 2010; Townsend et al., 2014).

Table 3: Comparison of cAMP concentrations and the properties of CRP-like proteins and cAMP phosphodiesterases in *P. putida*, *C. glutamicum*, *E. coli*, and *M. tuberculosis*.

Species	<i>P. putida</i>	<i>C. glutamicum</i>	<i>E. coli</i>	<i>M. tuberculosis</i>
Cytoplasmic cAMP concentration	Low (0.07 μ M-0.12 μ M or below detection limit) (Arce-Rodríguez et al., 2021; Milanesio et al., 2011; Phillips & Mulfinger, 1981)	Low (\sim 1 μ M) (Wolf et al., 2020)	Moderate (35 μ M-40 μ M) (Bennett et al., 2009; Notley-McRobb et al., 1997)	High (up to 4 mM) (Bai et al., 2009; Padh & Venkitasubramanian, 1976)
CRP-like protein: K_d for cAMP	CRP (PP0424): 23 nM–45 nM (Arce-Rodríguez et al., 2012; Arce-Rodríguez et al., 2021)	GlxR (Cg0350): K_{d1} : 17 μ M, K_{d2} : 130 μ M (Townsend et al., 2014)	CRP (ECK3345): 19 μ M–39 μ M (Ren et al., 1990; Takahashi et al., 1980)	Crp (Rv3676): 170 μ M (Stapleton et al., 2010) Cmr (Rv1675c): n.d. (Gazdik et al., 2009; McCue et al., 2000)
Phosphodiesterase (PDE): K_m for cAMP	PDE (PP4917): n.d.	CpdA (Cg2761) K_m : 2.5 mM (Schulte et al., 2017)	CpdA (ECK3032): 500 μ M (Imamura et al., 1996)	CpdA (Rv0805): 200 μ M (Shenoy et al., 2005) Rv1339: n.d. (Thomson et al., 2022)

The highest binding affinity of a CRP-like protein to cAMP shows the CRP protein of *P. putida*. This correlates with the fact that this organism has a very low intracellular cAMP concentration. When comparing the cAMP-binding affinities of the CRP-like proteins of *M. tuberculosis*, *E. coli* and *P. putida* it seems as if there is a link between binding affinities and the intracellular cAMP concentration. *C. glutamicum* would be considered to be an organism with a low intracellular cAMP level, but the cAMP-binding affinity of GlxR seems rather low compared to the intracellular cAMP concentration. *In vivo* GlxR binding studies performed in this work showed that GlxR binding to DNA can occur independent of cAMP and that in most cases the presence of cAMP only enhanced the affinity to DNA binding regions. On the other hand a high intracellular cAMP level seems to be detrimental for *C. glutamicum* as seen in the mutant lacking the phosphodiesterase CpdA (Schulte et al., 2017). The presence and activity of the CpdA plays a key role in the regulation of the intracellular cAMP level. This is surprising considering that the *in vitro* assays with purified CpdA showed a relatively high K_m for cAMP (2.5 mM), far above the measured cytoplasmic concentrations (\sim 1 μ M).

It is noticeable that not only the cAMP levels between different species can vary, but also the level within the same strain can be drastically different (Table 1). Literature references provide data of different intracellular cAMP levels of the same strain, for example due to different cultivation conditions (Bai et al., 2009; Kim et al., 2004). The variation of the cAMP concentration in cells of a particular species can be due to differences in the analytical methods used to determine the cAMP concentrations. However, many other factors can also have an influence on the intracellular cAMP level, such as stress conditions or carbon sources.

3.3 The role of cAMP for the *in vivo* activity of GlxR

In 2004 the protein GlxR (Cg0350) was identified as a CRP-like transcriptional regulator with cAMP- and DNA-binding properties (Kim et al., 2004; Townsend et al., 2014). As an approach to determine the role of intracellular cAMP for the *in vivo* activity of GlxR, transcriptome and ChAP-Seq studies with the wild type and an adenylate cyclase deletion strain were performed. Previous studies assumed that GlxR only binds DNA when cAMP is present, as shown by *in vitro* tests, such as electrophoretic mobility shift assays (EMSAs) (Bussmann et al., 2009; Jungwirth et al., 2013; Kohl et al., 2008). First studies of the *in vivo* GlxR binding activity also in the genome background of a *cydB* deletion mutant of strain R showed that GlxR did still bind to DNA (Toyoda et al., 2011). It was assumed that the reason for that result was residual cAMP that was still measured in the *cydB* mutant. However, in the ChAP-Seq assays that were performed during this work, it was shown that *in vivo* GlxR binds in a Δ *cydB* mutant in which cAMP was under the detection limit of an LC-MS/MS method (Wolf et al., 2020). This suggests that GlxR can bind to many DNA regions also in the absence of its physiological effector cAMP. In the Δ *cydB* mutant the binding of GlxR to DNA was reduced particularly in the presence of acetate. Thus GlxR binding *in vivo* is probably less dependent on cAMP than GlxR binding *in vitro* and additional, yet unknown factors might be involved in the control of GlxR binding to DNA within the cell.

3.3.1 Further CRP-like proteins in *C. glutamicum*

As already mentioned in the introduction of this work, *C. glutamicum* encodes two additional proteins sharing protein domains with GlxR (Figure 2C). The protein Cg1327 is

composed of the same protein domains as GlxR, whereas the protein Cg3291 lacks the cNMP-binding domain but carries the HTH_CRP domain that is found in CRP-like proteins (Figure 2C). Therefore, these proteins, especially Cg1327 might have functions related to GlxR. To find out more about the role of Cg1327 in *C. glutamicum*, the corresponding gene *cg1327* was successfully deleted and first growth experiments of the $\Delta cg1327$ mutant in comparison with the WT were performed in minimal medium containing glucose, gluconate, acetate, citrate, or ethanol as carbon sources (Figure 9A-E).

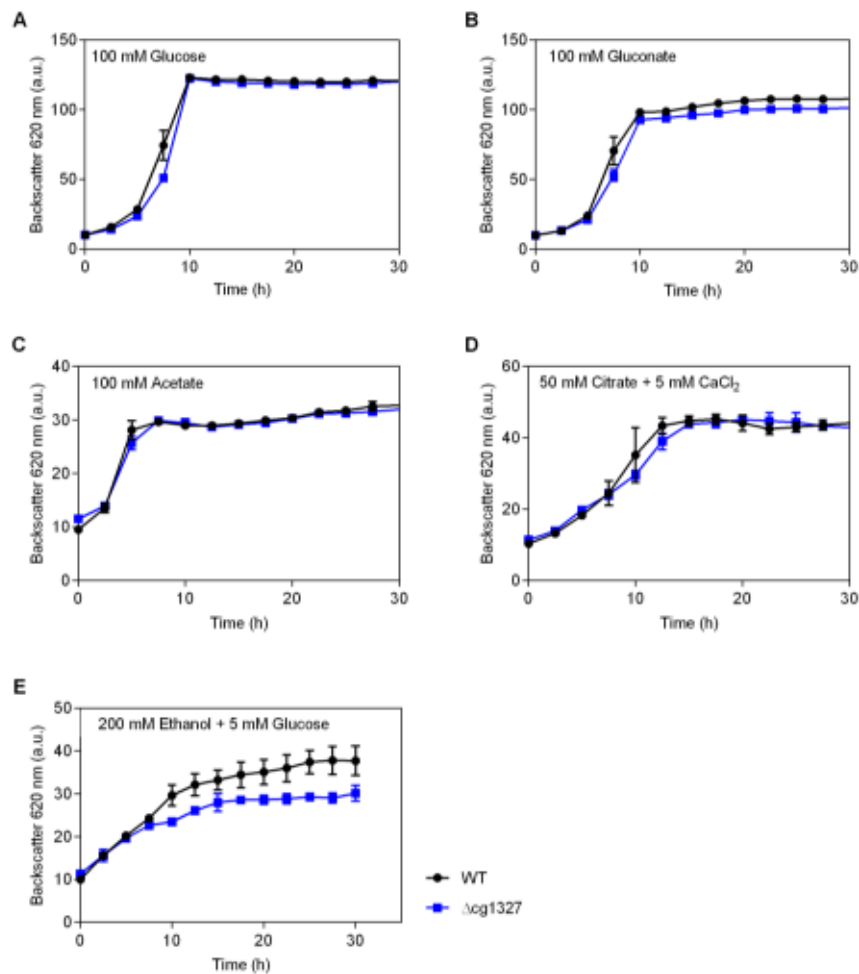


Figure 9: Growth behaviour of *C. glutamicum* wild type (WT) and a $\Delta cg1327$ mutant on different carbon sources. The strains were cultivated in CGXII minimal medium containing 100 mM glucose (A), 100 mM gluconate (B), 100 mM acetate (C), 50 mM citrate supplemented with 5 mM CaCl₂ (D) or 200 mM ethanol supplemented with 5 mM glucose (E). The first preculture was inoculated in BHI medium and the second preculture was grown in CGXII medium with 2% glucose. The cells were washed with saline (0.9% (w/v) NaCl) and used to inoculate the main cultures in 800 μ l CGXII minimal medium with the indicated carbon sources to an OD₆₀₀ of 1. Growth was monitored as scattered light at 620 nm in a Biolector at 30 °C and 1200 rpm. Mean values and standard deviations of three biological replicates are shown.

No differences in growth behaviour were observed on the tested carbon sources except during cultivation with ethanol (Figure 9E), where the initial growth kinetics was comparable, but the Δ cg1327 mutant did not reach the same final backscatter as the WT control. This suggests that Cg1327 is functional in *C. glutamicum* and directly or indirectly involved in ethanol metabolism. Further experiments, such as analysis of DNA-protein interactions (e.g. by fluorescence anisotropy), cAMP-binding studies with purified Cg1327 as well as ChAP-Seq and microarray experiments should be performed to characterize the biochemical properties, target genes, and physiological functions of Cg1327.

Species phylogenetically related to *Corynebacterium*, such as *M. smegmatis*, have two active CRP-like proteins (Msmeg_0539 and Msmeg_6189; 78.48% identity and 99% query cover using BLASTP), which were shown recognize the same consensus sequence, but possess distinct regulons with a small set of overlapping genes, such as the succinate dehydrogenase operon *sdh1* (Aung et al., 2015). EMSAs with the two purified Crp proteins showed that Msmeg_0539 bound to the promoter DNA of the succinate dehydrogenase operon in a cAMP-independent way. BLASTP alignment results of GlxR with Msmeg_0539 and Msmeg_6189 showed 70.59% and 80.36% identity with 97% and 98% query cover, respectively. On the other hand, the results for BLASTP alignment of Cg1327 with Msmeg_0539 and Msmeg_6189 had a low identity (23.65% and 25.87%, respectively) and a lower query cover (both 80%).

3.3.2 cAMP-GlxR system important for energy metabolism in *C. glutamicum*

In this work, for the first time suppressor mutants of *C. glutamicum* Δ *cyaB* were isolated that no longer showed the growth inhibition by acetate. The suppressor mutants were obtained by an at least 80 h cultivation of a Δ *cyaB* mutant in minimal medium with an initial acetate concentration of 150 mM as only carbon source (Wolf et al., 2020). One suppressor mutant showed clear evidence for the correlation of acetate sensitivity and GlxR regulation: Δ *cyaB*_sup1 had only one point mutation in *glxR*, which indicated that the acetate sensitivity of the parental Δ *cyaB* strain is due to a malfunction of GlxR-dependent regulation at low intracellular cAMP levels in the presence of acetate. This suppressor mutant expressed the transcriptional regulator GlxR with an amino acid exchange Ala131Thr. Amino acid residue 131 is located within the central alpha helix 5, which is involved in cAMP-binding (Townsend et al. 2014). When this amino acid exchange was introduced into the original Δ *cyaB* mutant,

it abolished the acetate sensitivity of this strain, confirming that this single amino acid exchange was responsible for phenotype of the suppressor mutant. First experiments with the GlxR_{Ala131Thr} variant revealed that *in vitro* DNA-binding was still dependent on cAMP (Wolf et al., 2020). Further experiments are needed to elucidate why the cell benefits from this mutation when the intracellular cAMP level is low.

3.3.3 Closer look at suppressor mutants *C. glutamicum* Δ *cyaB*_sup2 and Δ *cyaB*_sup3

The suppressor strain Δ *cyaB*_sup3 showed the same Ala131Thr mutation in the coding region of *glxR* as strain Δ *cyaB*_sup1, but carried also an additional silent mutation in the *rpi* gene (cg2658) encoding ribose 5-phosphate isomerase. The mutation is a change from C to A (318 bp) in the open reading frame of *rpi*, leading to a change of the base triplet GGC to GGA coding for the amino acid glycine at amino acid position 106. Tables of the codon usage frequency show that the triplet GGA is less favoured than the triplet GGC (15.2% and 34.1%, respectively) (<https://www.kazusa.or.jp/codon/>) in *C. glutamicum*. It remains unclear if the *rpi* mutation in the suppressor strain Δ *cyaB*_sup3 has additional benefits beside the *glxR*-Ala131Thr mutation.

Another suppressor mutant, strain Δ *cyaB*_sup2, did not show any mutation in the *glxR* coding region, but instead in two intergenic regions. One point mutation was located in the intergenic region of *serC* (cg0948) and *gltA* (cg0949) and second one in the intergenic region of *gpt* (cg1659) and cg1660. The transcription of *gltA* is known to be repressed by GlxR (van Ooyen et al., 2011). However, the mutation in the intergenic region of *serC* and *gltA* is not located within the GlxR binding motif (Figure 10).

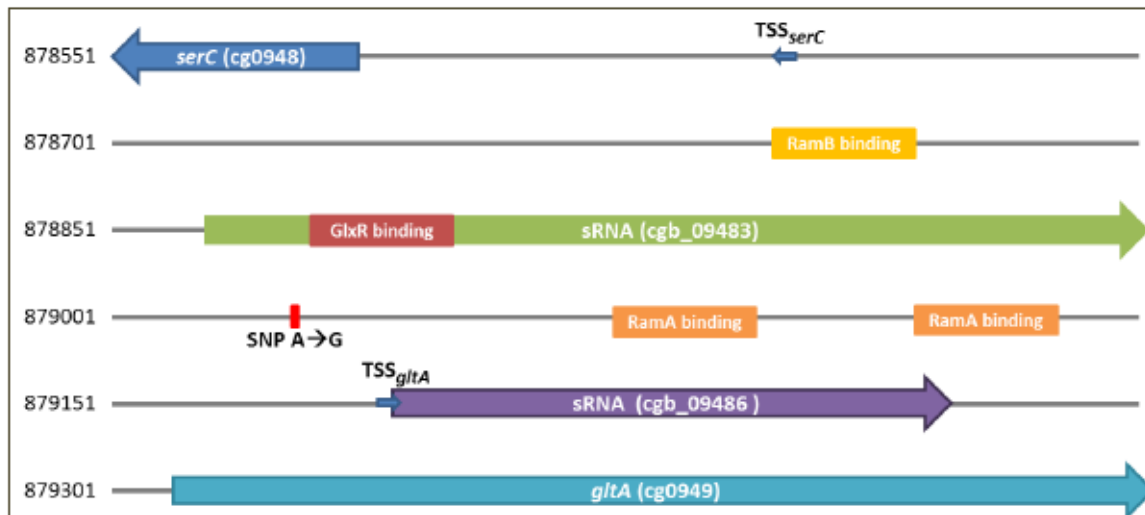


Figure 10: Schematic overview of the genomic region with the single nucleotide polymorphism (SNP) in the *C. glutamicum* $\Delta cyaB_sup2$ suppressor mutant. The mutation is located in the intergenic region of *serC* and *gltA*. The mutation is located upstream of an sRNA (*cgb_09486*). Binding sites of the transcriptional regulators RamB, GlxR, and RamA are highlighted. Information on sRNAs and transcriptional start sites (TSS) were taken from Mentz et al., 2013 and Pfeifer-Sancar et al., 2013.

However, when having a closer look at the location of the mutation in the intergenic region of *serC* and *gltA*, one can see that the mutation is between the sRNA *cgb_09483* and closely located upstream of another sRNA, *cgb_09486*. So far, the biological functions of these two sRNAs are not known, but the mutation could influence the transcription of an sRNA. In general, sRNAs are often located within intergenic regions and can regulate transcription or translation of their target genes or can alter a protein activity upon binding (Georg & Hess, 2011; Storz et al., 2011).

The second mutation in the $\Delta cyaB_sup2$ suppressor strain was located in the intergenic region of *gpt* and *cg1660* and could lead to an altered gene transcription. The genes *gpt* and *cg1660* were not described as GlxR targets so far and other transcriptional regulators involved in the expression of these genes are not known yet. Transcriptome data showed that in the $\Delta cyaB$ mutant, the expression of *gpt* was lower compared to the wild type (mRNA ratio $\Delta cyaB/WT$ 0.56, p-value 0.045), whereas expression of *cg1660* was significantly higher in the $\Delta cyaB$ mutant compared to the wild type (mRNA ratio 3.16, p-value 0.0068) when cultivated in minimal media with a glucose-acetate mixture (Bussmann, 2009; Wolf et al., 2020). This shows that the lack of the adenylate cyclase has an influence on the transcription of *gpt* and *cg1660*. It would be interesting to know if the suppressor mutant $\Delta cyaB_sup2$ has a wild type-like transcription of *gpt* and *cg1660*, which would suggest that Gpt and/or

Cg1660 play a role in the tolerance to high acetate concentrations. Gpt is annotated as a purine phosphoribosyltransferase (PRT) (Kalinowski et al., 2003). In general, purine PRTs are described to catalyse the reversible transfer of a phosphoribosyl group from phosphoribosylpyrophosphate (PRPP) to a purine base (adenine, guanine, hypoxanthine, or xanthine) (Craig III & Eakin, 2000). Bioinformatic analysis of Cg1660 suggests that it might function as a manganese (Mn^{2+}) efflux pump belonging to the MntP family (PF02659/IPR003810) (Waters et al., 2011). In some bacteria Mn^{2+} is important for the protection against oxidative stress (Anjem et al., 2009). It is possible that already one of the mutations found in the suppressor strain $\Delta cyaB_sup2$ is sufficient to rescue the acetate effect. To clarify this point, the mutations have to be introduced separately and together in the $\Delta cyaB$ mutant and tested. Furthermore, the effects of these mutations on the expression of the neighbouring genes need to be analysed.

The suppressor strain $\Delta cyaB_sup2$ shows that there is an alternative way beside the described *glxR* mutation to overcome the 'acetate sensitivity' and thus the lack of cAMP in the *C. glutamicum* $\Delta cyaB$ strain. It would be interesting to test if the mutations in *C. glutamicum* lead to an improved acetate tolerance. This ability could be interesting for biotechnological applications in which strains in fermentation processes are confronted with high acetate concentrations.

3.4 Universal stress protein as putative cAMP binding protein

Recently, a universal stress protein (Usp) of *M. tuberculosis* and *M. smegmatis* was described to be a cAMP-binding protein (Rv1636 and MSMEG_3811, respectively) (Banerjee et al., 2015). These proteins do not have a classical cyclic nucleotide-binding domain, but the binding of Usp to cAMP in *M. smegmatis* was confirmed by cAMP affinity chromatography and verified by isothermal titration calorimetry (ITC) (Banerjee et al., 2015). Proteins that belong to the Usp protein family were described to be involved in stress responses because their synthesis was induced upon different stress conditions, such as starvation for glucose or phosphate, the entry into the stationary phase in rich medium, exposure to heat, or in the presence of uncouplers (Nystrom & Neidhardt, 1992). The biological function of cAMP-binding to Usp in mycobacteria was described to be an additional regulation of the intracellular 'free' cAMP level and therefore a regulation of the downstream effects of cAMP. In another publication, it was shown that Rv1636 of *M. tuberculosis* is in the top

twenty of the most abundant proteins of the organism, which supports the hypothesis that this protein acts as a cAMP reservoir (Schubert et al., 2013).

To find out if *C. glutamicum* harbours orthologues of Rv1636 and MSMEG_3811, a BLASTP search (States and Gish 1994) was performed and revealed that the *C. glutamicum* genome harbours five proteins that belong to the Usp family (Figure 11).

	Protein domain	Gene name	Protein annotation (CoryneRegNet 6.0)
Cg1551		<i>uspA1</i>	Universal stress protein UspA and related nucleotide-binding proteins
Cg1595		<i>uspA2</i>	Universal stress protein UspA or related nucleotide-binding protein, repressed by GlxR
Cg3159		-	Universal stress protein UspA or related nucleotide-binding proteins
Cg3255	 	<i>uspA3</i>	Universal stress protein family
Cg3316	 	-	Universal stress protein UspA or related nucleotide-binding protein

Figure 11: Proteins of *C. glutamicum* that are carrying at least one Usp (universal stress protein) domain (Pfam: PF00582 (El-Gebali et al., 2018); InterPro IPR014729 (Mulder & Apweiler, 2008)).

Cg1551 (UspA1) showed the highest sequence identity (44-50%) to MSMEG_3811 of *M. smegmatis* and Rv1636 of *M. tuberculosis* (Table 4).

Table 4: Results of BLASTP alignment (Altschul et al., 1990) of two sequences using Usp (MSMEG_3811) of *M. smegmatis* as reference protein and depicted protein sequence (Cg1551, Cg1595, Cg3195, Cg3255 or Cg3316) as subject sequence.

Protein name	Percent identity	Query cover	Max score	Total score	E-value
Cg1551/ UspA1	51.75%	97%	105	105	3e-34
Cg1595/ UspA2	28.40%	97%	35	35	8e-08
Cg3159/-	24.31%	95%	30.8	30.8	2e-06
Cg3255/ UspA3	27.81%	97%	36.2	70.8	9e-08
Cg3316/-	29.73%	30%	41.2	41.2	0.013

Therefore, Cg1551 of *C. glutamicum* was further analysed in this work. A crystal structure of MSMEG_3811 with bound cAMP (PDB: 5ahw) revealed the amino acid residues that are most important for binding of cAMP, namely Gly10, Ala40, and Gly114 (Banerjee et al., 2015). These residues are conserved in Cg1551 (Figure 12), as well as the ATP-binding motif (GX₂GX₉G(S/T)) that is found in some Usp family proteins (Mbah, 2014; Sousa & McKay, 2001). If Rv1636 and MSMEG_3811 serve as cAMP reservoirs in mycobacteria, this could also be true for *C. glutamicum*. Similar to the situation in mycobacteria, cg1551 is highly

expressed (top 50 proteins) on the transcriptional level (personal communication Jörn Kalinowski, Bielefeld, Germany) and the protein was found to be highly abundant on 2D gels (Schaffer et al., 2001).

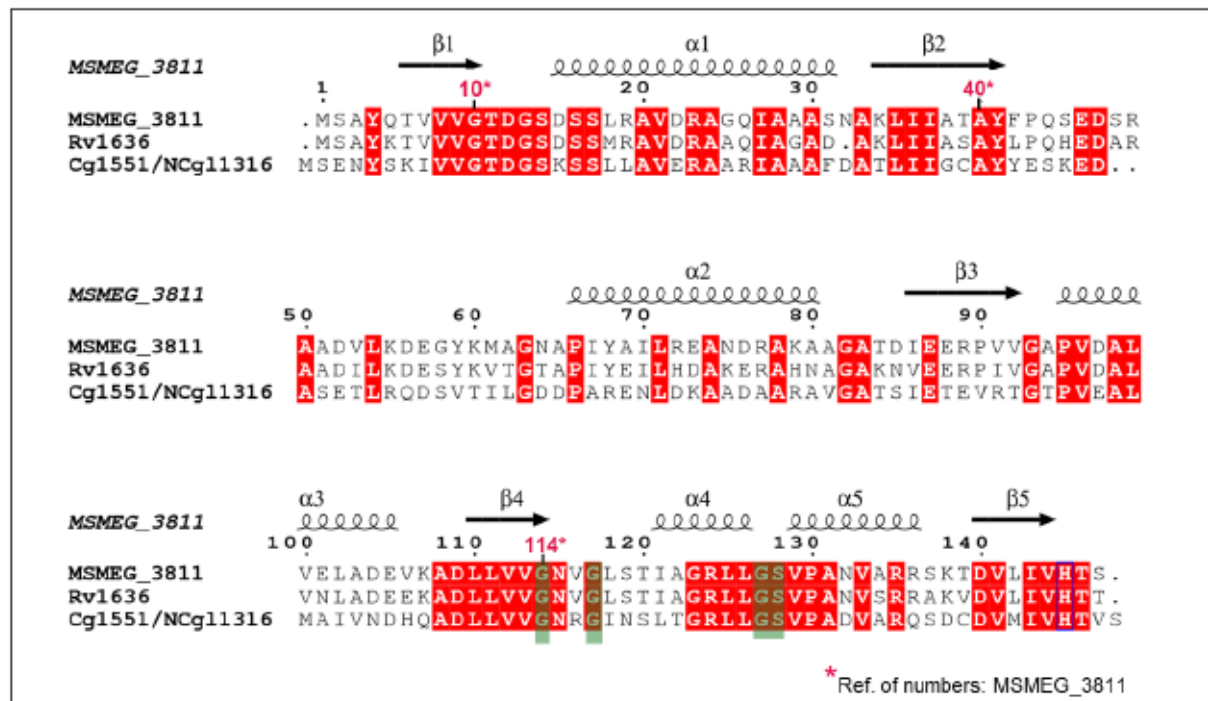


Figure 12: ClustalW alignment of MSMEG_3811, Rv1636 and Cg1551 (UspA1). The amino acid sequence of MSMEG_3811 was used as the query. Identical amino acids of the three proteins are highlighted in red. Red numbers marked with an asterisk designate amino acids (Gly10, Ala40, and Gly114) important for cAMP binding according to Banerjee et al., 2015. Green highlighted are the conserved amino acids of the motif $GX_2GX_9G(S/T)$, an ATP-binding domain found in USPs (Mbah, 2014; Sousa & McKay, 2001). The alignment was performed with ClustalW (Thompson et al., 1994) and further processed with Esprict (Robert & Gouet, 2014).

ITC experiments with purified Cg1551 could be used to determine if the protein binds cAMP. In mycobacteria, the affinity of Usp for cAMP ($K_d \sim 3 \mu M$) was more than 50 times higher compared to the affinity of CRP for cAMP ($K_d \sim 170 \mu M$), which is also a hint for the possible role of UspA as a cAMP reservoir (Banerjee et al., 2015; Stapleton et al., 2010). Previous analysis of *uspA* mutants of *E. coli* showed a growth rate similar to the parental strain, but the growth was delayed, no matter in which medium the mutant was grown (Nystrom & Neidhardt, 1993). In this work, a *C. glutamicum* $\Delta cg1551$ deletion mutant was generated to find out if the lack of this gene has likewise an influence on the cell vitality. The cultivations indeed revealed that the $\Delta cg1551$ mutant has a prolonged lag phase (around 3 h in BHI and 5 h in minimal media) compared to the wild type (Figure 13). Moreover, the $\Delta cg1551$ mutant had a lower final backscatter when cultivated in CGXII minimal medium with glucose.

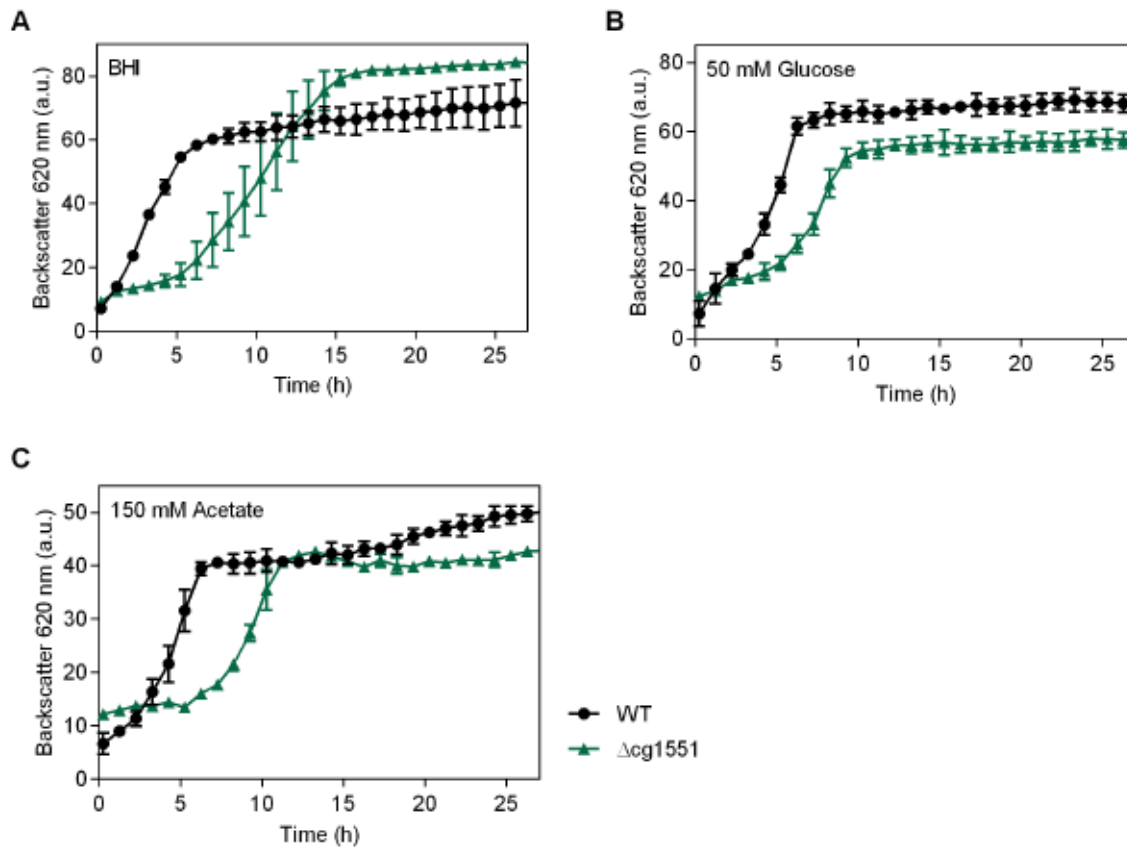


Figure 13: Growth behaviour of *C. glutamicum* wild type (WT) and a $\Delta cg1551$ mutant on different carbon sources. The first preculture was inoculated in BHI medium and the second preculture was performed in BHI (A) in CGXII medium with 50 mM glucose (B) or with 150 mM acetate (C) as carbon source. The cells were washed with saline (0.9% (w/v) NaCl) and used to inoculate the main cultures in 800 μ l CGXII minimal medium to an OD_{600} of 1. Growth was monitored as scattered light at 620 nm in a BioLector at 30°C and 1200 rpm. Mean values and standard deviation of three biological replicates are shown.

A hypothesis for explaining the prolonged lag phase is that the absence of Cg1551 could lead to an elevated cAMP level, which would cause increased DNA-binding of GlxR. As reported previously, a *C. glutamicum* $\Delta cpdA$ strain with a 2-fold higher intracellular cAMP level compared to the wild type had growth defects on all tested carbon sources (Schulte et al., 2017). Further experiments are required to test this idea and the function of Cg1551 in cAMP homeostasis in *C. glutamicum*.

4 Literature

- Agarwal, N., Lamichhane, G., Gupta, R., Nolan, S., & Bishai, W. R. (2009). Cyclic AMP intoxication of macrophages by a *Mycobacterium tuberculosis* adenylate cyclase. *Nature*, *460*(7251), 98-102.
- Altschul, S. F., Gish, W., Miller, W., Myers, E. W., & Lipman, D. J. (1990). Basic local alignment search tool. *J Mol Biol*, *215*(3), 403-410.
- Anjem, A., Varghese, S., & Imlay, J. A. (2009). Manganese import is a key element of the OxyR response to hydrogen peroxide in *Escherichia coli*. *Mol Microbiol*, *72*(4), 844-858.
- Aravind, L., & Ponting, C. P. (1999). The cytoplasmic helical linker domain of receptor histidine kinase and methyl-accepting proteins is common to many prokaryotic signalling proteins. *FEMS Microbiol Lett*, *176*(1), 111-116.
- Arce-Rodríguez, A., Durante-Rodríguez, G., Platero, R., Krell, T., Calles, B., & de Lorenzo, V. (2012). The Crp regulator of *Pseudomonas putida*: evidence of an unusually high affinity for its physiological effector, cAMP. *Environ Microbiol*, *14*(3), 702-713.
- Arce-Rodríguez, A., Nikel, P. I., Calles, B., Chavarría, M., Platero, R., Krell, T., & de Lorenzo, V. (2021). Low CyaA expression and anti-cooperative binding of cAMP to CRP frames the scope of the cognate regulon of *Pseudomonas putida*. *Environ Microbiol*, *23*(3), 1732-1749.
- Arumugham, V. B., Ulivieri, C., Onnis, A., Finetti, F., Tonello, F., Ladant, D., & Baldari, C. T. (2018). Compartmentalized cyclic AMP production by the *Bordetella pertussis* and *Bacillus anthracis* adenylate cyclase toxins differentially affects the immune synapse in T lymphocytes. *Front Immunol*, *9*, 919.
- Attey, A., Belyaeva, T., Savery, N., Hoggett, J., Fujita, N., Ishihama, A., & Busby, S. (1994). Interactions between the cyclic AMP receptor protein and the alpha subunit of RNA polymerase at the *Escherichia coli* galactose operon P1 promoter. *Nucleic Acids Res*, *22*(21), 4375-4380.
- Aung, H. L., Berney, M., & Cook, G. M. (2014). Hypoxia-activated cytochrome *bd* expression in *Mycobacterium smegmatis* is cyclic AMP receptor protein dependent. *J Bacteriol*, *196*(17), 3091-3097.
- Aung, H. L., Dixon, L. L., Smith, L. J., Sweeney, N. P., Robson, J. R., Berney, M., Buxton, R. S., Green, J., & Cook, G. M. (2015). Novel regulatory roles of cAMP receptor proteins in fast-growing environmental mycobacteria. *Microbiology*, *161*(Pt 3), 648-661.
- Axe, D. D., & Bailey, J. E. (1995). Transport of lactate and acetate through the energized cytoplasmic membrane of *Escherichia coli*. *Biotechnol Bioeng*, *47*(1), 8-19.
- Bai, G., Schaak, D. D., & McDonough, K. A. (2009). cAMP levels within *Mycobacterium tuberculosis* and *Mycobacterium bovis* BCG increase upon infection of macrophages. *FEMS Immun Med Microbiol*, *55*(1), 68-73.
- Bai, G., Schaak, D. D., Smith, E. A., & McDonough, K. A. (2011). Dysregulation of serine biosynthesis contributes to the growth defect of a *Mycobacterium tuberculosis* *crp* mutant. *Mol Microbiol*, *82*(1), 180-198.
- Banerjee, A., Adolph, R. S., Gopalakrishnapai, J., Kleinboelting, S., Emmerich, C., Steegborn, C., & Visweswariah, S. S. (2015). A universal stress protein (USP) in mycobacteria binds cAMP. *J Biol Chem*, *290*(20), 12731-12743.
- Barriuso-Iglesias, M., Barreiro, C., Sola-Landa, A., & Martín, J. F. (2013). Transcriptional control of the F₀F₁-ATP synthase operon of *Corynebacterium glutamicum*: SigmaH factor binds to its promoter and regulates its expression at different pH values. *Microb Biotechnol*, *6*(2), 178-188.

- Barriuso-Iglesias, M., Schluesener, D., Barreiro, C., Poetsch, A., & Martín, J. F. (2008). Response of the cytoplasmic and membrane proteome of *Corynebacterium glutamicum* ATCC 13032 to pH changes. *BMC Microbiol*, *8*, 225.
- Bârzu, O., & Danchin, A. (1994). Adenylyl cyclases: a heterogeneous class of ATP-utilizing enzymes. *Prog Nucleic Acid Res Mol Biol*, *49*, 241-283.
- Bassler, J., Schultz, J. E., & Lupas, A. N. (2018). Adenylate cyclases: Receivers, transducers, and generators of signals. *Cell Signal*, *46*, 135-144.
- Becker, J., & Wittmann, C. (2012). Systems and synthetic metabolic engineering for amino acid production - the heartbeat of industrial strain development. *Curr Opin Biotechnol*, *23*(5), 718-726.
- Bennett, B. D., Kimball, E. H., Gao, M., Osterhout, R., Van Dien, S. J., & Rabinowitz, J. D. (2009). Absolute metabolite concentrations and implied enzyme active site occupancy in *Escherichia coli*. *Nat Chem Biol*, *5*(8), 593-599.
- Benoff, B., Yang, H., Lawson, C. L., Parkinson, G., Liu, J., Blatter, E., Ebright, Y. W., Berman, H. M., & Ebright, R. H. (2002). Structural basis of transcription activation: the CAP-alpha CTD-DNA complex. *Science*, *297*(5586), 1562-1566.
- Berthet, J., Rall, T. W., & Sutherland, E. W. (1957). The relationship of epinephrine and glucagon to liver phosphorylase. IV. Effect of epinephrine and glucagon on the reactivation of phosphorylase in liver homogenates. *J Biol Chem*, *224*(1), 463-475.
- Bettenbrock, K., Sauter, T., Jahreis, K., Kremling, A., Lengeler, J. W., & Gilles, E. D. (2007). Correlation between growth rates, EIIA^{GTP} phosphorylation, and intracellular cyclic AMP levels in *Escherichia coli* K-12. *J Bacteriol*, *189*(19), 6891-6900.
- Bettendorff, L., & Wins, P. (2013). Thiamine triphosphatase and the CYTH superfamily of proteins. *FEBS J*, *280*(24), 6443-6455.
- Binder, S., Schendzielorz, G., Stabler, N., Krumbach, K., Hoffmann, K., Bott, M., & Eggeling, L. (2012). A high-throughput approach to identify genomic variants of bacterial metabolite producers at the single-cell level. *Genome Biol*, *13*(5), R40.
- Blanco, E., Fortunato, S., Viggiano, L., & de Pinto, M. C. (2020). Cyclic AMP: A polyhedral signalling molecule in plants. *Int J Mol Sci*, *21*(14).
- Blombach, B., Riester, T., Wieschalka, S., Ziert, C., Youn, J., Wendisch, V. F., & Eikmanns, B. J. (2011). *Corynebacterium glutamicum* tailored for efficient isobutanol production. *Appl Environ Microbiol*, *77*(10), 3300-3310.
- Boratyn, G. M., Schäffer, A. A., Agarwala, R., Altschul, S. F., Lipman, D. J., & Madden, T. L. (2012). Domain enhanced lookup time accelerated BLAST. *Biol Direct*, *7*(1), 12.
- Botsford, J. L., & Harman, J. G. (1992). Cyclic AMP in prokaryotes. *Microbiol Rev*, *56*(1), 100-122.
- Busby, S., & Ebright, R. H. (1997). Transcription activation at class II CAP-dependent promoters. *Mol Microbiol*, *23*(5), 853-859.
- Busby, S., & Ebright, R. H. (1999). Transcription activation by catabolite activator protein (CAP). *J Mol Biol*, *293*(2), 199-213.
- Bussmann, M. (2009). cAMP dependent regulation of the TCA cycle by GlxR and oxidative stress response regulation by RosR in *Corynebacterium glutamicum*. urn:nbn:de:hbz:061-20101104-151101-4.

- Bussmann, M., Emer, D., Hasenbein, S., Degraf, S., Eikmanns, B. J., & Bott, M. (2009). Transcriptional control of the succinate dehydrogenase operon *sdhCAB* of *Corynebacterium glutamicum* by the cAMP-dependent regulator GlxR and the LuxR-type regulator RamA. *J Biotechnol*, *143*(3), 173-182.
- Callahan, S. M., Cornell, N. W., & Dunlap, P. V. (1995). Purification and properties of periplasmic 3':5'-cyclic nucleotide phosphodiesterase. A novel zinc-containing enzyme from the marine symbiotic bacterium *Vibrio fischeri*. *J Biol Chem*, *270*(29), 17627-17632.
- Cashel, M. (1975). Regulation of bacterial ppGpp and pppGpp. *Ann Rev Microbiol*, *29*(1), 301-318.
- Cha, P. H., Park, S. Y., Moon, M. W., Subhadra, B., Oh, T. K., Kim, E., Kim, J. F., & Lee, J. K. (2010). Characterization of an adenylate cyclase gene (*cydB*) deletion mutant of *Corynebacterium glutamicum* ATCC 13032. *Appl Microbiol Biotechnol*, *85*(4), 1061-1068.
- Conti, M., & Beavo, J. (2007). Biochemistry and physiology of cyclic nucleotide phosphodiesterases: essential components in cyclic nucleotide signaling. *Annu Rev Biochem*, *76*, 481-511.
- Cook, W. H., Lipkin, D., & Markham, R. (1957). The formation of a cyclic dianhydro cyclic dianhydrodiadenylic acid (I) by the alkaline degradation of adenosine-5'-triphosphoric acid (II)1. *J Am Chem Soc*, *79*(13), 3607-3608.
- Cotta, M. A., Whitehead, T. R., & Wheeler, M. B. (1998). Identification of a novel adenylate cyclase in the ruminal anaerobe, *Prevotella ruminicola* D31d. *FEMS Microbiol Lett*, *164*(2), 257-260.
- Cotter, P. A., Chepuri, V., Gennis, R. B., & Gunsalus, R. P. (1990). Cytochrome *o* (*cyoABCDE*) and *d* (*cydAB*) oxidase gene expression in *Escherichia coli* is regulated by oxygen, pH, and the *fnr* gene product. *J Bacteriol*, *172*(11), 6333-6338.
- Craig III, S. P., & Eakin, A. E. (2000). Purine phosphoribosyltransferases. *J Biol Chem*, *275*(27), 20231-20234.
- D'Souza, C. A., & Heitman, J. (2001). Conserved cAMP signaling cascades regulate fungal development and virulence. *FEMS Microbiol Rev*, *25*(3), 349-364.
- da Luz, J. A., Hans, E., Frank, D., & Zeng, A. P. (2017). Analysis of intracellular metabolites of *Corynebacterium glutamicum* at high cell density with automated sampling and filtration and assessment of engineered enzymes for effective L-lysine production. *Eng Life Sci*, *17*(5), 512-522.
- Danchin, A. (1993). Phylogeny of adenylate cyclases. *Adv Second Messenger Phosphoprotein Res*, *27*, 109-162.
- Dass, B. K., Sharma, R., Shenoy, A. R., Mattoo, R., & Visweswariah, S. S. (2008). Cyclic AMP in mycobacteria: characterization and functional role of the Rv1647 ortholog in *Mycobacterium smegmatis*. *J Bacteriol*, *190*(11), 3824-3834.
- Dautin, N., Karimova, G., & Ladant, D. (2002). *Bordetella pertussis* adenylate cyclase toxin: a versatile screening tool. *Toxicon*, *40*(10), 1383-1387.
- de Crombrughe, B., Busby, S., & Buc, H. (1984). Cyclic AMP receptor protein: role in transcription activation. *Science*, *224*(4651), 831-838.
- Dessauer, C. W., Watts, V. J., Ostrom, R. S., Conti, M., Dove, S., & Seifert, R. (2017). International union of basic and clinical pharmacology. CI. structures and small molecule modulators of mammalian adenylate cyclases. *Pharmacol Rev*, *69*(2), 93-139.
- Eggeling, L., & Bott, M. (2015). A giant market and a powerful metabolism: L-lysine provided by *Corynebacterium glutamicum*. *Appl Microbiol Biotechnol*, *99*(8), 3387-3394.
- Eggeling, L., Bott, M., & Marienhagen, J. (2015). Novel screening methods—biosensors. *Curr Opin Biotechnol*, *35*, 30-36.

- El-Gebali, S., Mistry, J., Bateman, A., Eddy, S. R., Luciani, A., Potter, S. C., Qureshi, M., Richardson, L. J., Salazar, G. A., Smart, A., Sonnhammer, E. L. L., Hirsh, L., Paladin, L., Piovesan, D., Tosatto, S. C. E., & Finn, R. D. (2018). The Pfam protein families database in 2019. *Nucleic Acids Res*, *47*(D1), D427-D432.
- Emmer, M., deCrombrughe, B., Pastan, I., & Perlman, R. (1970). Cyclic AMP receptor protein of *E. coli*: its role in the synthesis of inducible enzymes. *Proc Natl Acad Sci U S A*, *66*(2), 480-487.
- Endo, M. (2006). Calcium ion as a second messenger with special reference to excitation-contraction coupling. *J Pharmacol Sci*, *100*(5), 519-524.
- Follmann, M., Ochrombel, I., Krämer, R., Trötschel, C., Poetsch, A., Rückert, C., Hüser, A., Persicke, M., Seiferling, D., Kalinowski, J., & Marin, K. (2009). Functional genomics of pH homeostasis in *Corynebacterium glutamicum* revealed novel links between pH response, oxidative stress, iron homeostasis and methionine synthesis. *BMC Genomics*, *10*, 621-621.
- Francis, S. H., Blount, M. A., & Corbin, J. D. (2011). Mammalian cyclic nucleotide phosphodiesterases: molecular mechanisms and physiological functions. *Physiol Rev*, *91*(2), 651-690.
- Francis, S. H., Turko, I. V., & Corbin, J. D. (2001). Cyclic nucleotide phosphodiesterases: relating structure and function. *Prog Nucleic Acid Res Mol Biol*, *65*, 1-52.
- Gallagher, D. T., Smith, N. N., Kim, S. K., Heroux, A., Robinson, H., & Reddy, P. T. (2006). Structure of the class IV adenylyl cyclase reveals a novel fold. *J Mol Biol*, *362*(1), 114-122.
- Gancedo, J. M. (2013). Biological roles of cAMP: variations on a theme in the different kingdoms of life. *Biol Rev Camb Philos Soc*, *88*(3), 645-668.
- Gao, B., & Gupta, R. S. (2012). Phylogenetic framework and molecular signatures for the main clades of the phylum *Actinobacteria*. *Microbiol Mol Biol Rev*, *76*(1), 66-112.
- Gazdik, M. A., Bai, G., Wu, Y., & McDonough, K. A. (2009). Rv1675c (*cmr*) regulates intramacrophage and cyclic AMP-induced gene expression in *Mycobacterium tuberculosis*-complex mycobacteria. *Mol Microbiol*, *71*(2), 434-448.
- Gehring, C. (2010). Adenyl cyclases and cAMP in plant signaling - past and present. *Cell Commun Signal*, *8*, 15.
- Georg, J., & Hess, W. R. (2011). *cis*-antisense RNA, another level of gene regulation in bacteria. *Microbiol Mol Biol Rev*, *75*(2), 286-300.
- Goldenbaum, P. E., & Hall, G. A. (1979). Transport of cyclic adenosine 3',5'-monophosphate across *Escherichia coli* vesicle membranes. *J Bacteriol*, *140*(2), 459-467.
- Görke, B., & Stülke, J. (2008). Carbon catabolite repression in bacteria: many ways to make the most out of nutrients. *Nat Rev Microbiol*, *6*(8), 613-624.
- Gosset, G., Zhang, Z., Nayyar, S., Cuevas, W. A., & Saier, M. H., Jr. (2004). Transcriptome analysis of Crp-dependent catabolite control of gene expression in *Escherichia coli*. *J Bacteriol*, *186*(11), 3516-3524.
- Guo, Z. P., Khoomrung, S., Nielsen, J., & Olsson, L. (2018). Changes in lipid metabolism convey acid tolerance in *Saccharomyces cerevisiae*. *Biotechnol Biofuels*, *11*, 297.
- Hecker, M., & Völker, U. (2001). General stress response of *Bacillus subtilis* and other bacteria. *Adv Microb Physiol*, *44*, 35-91.
- Heider, S. A., Wolf, N., Hofemeier, A., Peters-Wendisch, P., & Wendisch, V. F. (2014). Optimization of the IPP precursor supply for the production of lycopene, decaprenoxanthin and astaxanthin by *Corynebacterium glutamicum*. *Front Bioeng Biotechnol*, *20*, 2-28.
- Henderson, P. J. (1993). The 12-transmembrane helix transporters. *Curr Opin Cell Biol*, *5*(4), 708-721.

- Henke, N. A., Heider, S. A., Peters-Wendisch, P., & Wendisch, V. F. (2016). Production of the marine carotenoid astaxanthin by metabolically engineered *Corynebacterium glutamicum*. *Mar Drugs*, *14*(7), 124.
- Hong, E. J., Park, J. S., Kim, Y., & Lee, H. S. (2014). Role of *Corynebacterium glutamicum sprA* encoding a serine protease in *glxR*-mediated global gene regulation. *PLoS One*, *9*(4), e93587.
- Ikeda, M., & Nakagawa, S. (2003). The *Corynebacterium glutamicum* genome: features and impacts on biotechnological processes. *Appl Microbiol Biotechnol*, *62*(2), 99-109.
- Imamura, R., Yamanaka, K., Ogura, T., Hiraga, S., Fujita, N., Ishihama, A., & Niki, H. (1996). Identification of the *cpdA* gene encoding cyclic 3',5'-adenosine monophosphate phosphodiesterase in *Escherichia coli*. *J Biol Chem*, *271*(41), 25423-25429.
- Inui, M., Kawaguchi, H., Murakami, S., Vertès, A. A., & Yukawa, H. (2004). Metabolic engineering of *Corynebacterium glutamicum* for fuel ethanol production under oxygen-deprivation conditions. *J Mol Microbiol Biotechnol*, *8*(4), 243-254.
- Jakob, K., Satorhelyi, P., Lange, C., Wendisch, V. F., Silakowski, B., Scherer, S., & Neuhaus, K. (2007). Gene expression analysis of *Corynebacterium glutamicum* subjected to long-term lactic acid adaptation. *J Bacteriol*, *189*(15), 5582-5590.
- Jha, S. K., Sharma, M., & Pandey, G. K. (2016). Role of cyclic nucleotide gated channels in stress management in plants. *Curr Genomics*, *17*(4), 315-329.
- Jolkver, E., Emer, D., Ballan, S., Kramer, R., Eikmanns, B. J., & Marin, K. (2009). Identification and characterization of a bacterial transport system for the uptake of pyruvate, propionate, and acetate in *Corynebacterium glutamicum*. *J Bacteriol*, *191*(3), 940-948.
- Jungwirth, B., Emer, D., Brune, I., Hansmeier, N., Puhler, A., Eikmanns, B. J., & Tauch, A. (2008). Triple transcriptional control of the resuscitation promoting factor 2 (*rpf2*) gene of *Corynebacterium glutamicum* by the regulators of acetate metabolism RamA and RamB and the cAMP-dependent regulator GlxR. *FEMS Microbiol Lett*, *281*(2), 190-197.
- Jungwirth, B., Sala, C., Kohl, T. A., Uplekar, S., Baumbach, J., Cole, S. T., Puhler, A., & Tauch, A. (2013). High-resolution detection of DNA binding sites of the global transcriptional regulator GlxR in *Corynebacterium glutamicum*. *Microbiology*, *159*(Pt 1), 12-22.
- Kabus, A., Niebisch, A., & Bott, M. (2007). Role of cytochrome *bd* oxidase from *Corynebacterium glutamicum* in growth and lysine production. *Appl Environ Microbiol*, *73*(3), 861-868.
- Kalinowski, J., Bathe, B., Bartels, D., Bischoff, N., Bott, M., Burkovski, A., Dusch, N., Eggeling, L., Eikmanns, B. J., Gaigalat, L., Goesmann, A., Hartmann, M., Huthmacher, K., Kramer, R., Linke, B., McHardy, A. C., Meyer, F., Mockel, B., Pfefferle, W., Puhler, A., Rey, D. A., Ruckert, C., Rupp, O., Sahm, H., Wendisch, V. F., Wiegrabe, I., & Tauch, A. (2003). The complete *Corynebacterium glutamicum* ATCC 13032 genome sequence and its impact on the production of L-aspartate-derived amino acids and vitamins. *J Biotechnol*, *104*, 5-25.
- Kallscheuer, N., Vogt, M., Stenzel, A., Gatgens, J., Bott, M., & Marienhagen, J. (2016). Construction of a *Corynebacterium glutamicum* platform strain for the production of stilbenes and (2S)-flavanones. *Metab Eng*, *38*, 47-55.
- Kamenetsky, M., Middelhaufe, S., Bank, E. M., Levin, L. R., Buck, J., & Steegborn, C. (2006). Molecular details of cAMP generation in mammalian cells: a tale of two systems. *J Mol Biol*, *362*(4), 623-639.
- Kana, B. D., Weinstein, E. A., Avarbock, D., Dawes, S. S., Rubin, H., & Mizrahi, V. (2001). Characterization of the *cydAB*-encoded cytochrome *bd* oxidase from *Mycobacterium smegmatis*. *J Bacteriol*, *183*(24), 7076-7086.

- Kasahara, M., Unno, T., Yashiro, K., & Ohmori, M. (2001). CyaG, a novel cyanobacterial adenylyl cyclase and a possible ancestor of mammalian guanylyl cyclases. *J Biol Chem*, 276(13), 10564-10569.
- Katcharava, N. (2015). Untersuchung einer *Corynebacterium glutamicum* *cyaB*-Deletionsmutante [Bachelor Thesis, Fachhochschule Aachen].
- Kim, H. J., Kim, T. H., Kim, Y., & Lee, H. S. (2004). Identification and characterization of *glxR*, a gene involved in regulation of glyoxylate bypass in *Corynebacterium glutamicum*. *J Bacteriol*, 186(11), 3453-3460.
- Kim, T. H., Kim, H. J., Park, J. S., Kim, Y., Kim, P., & Lee, H. S. (2005). Functional analysis of *sigH* expression in *Corynebacterium glutamicum*. *Biochem Biophys Res Commun*, 331(4), 1542-1547.
- Kimura, Y., Yoshimi, M., & Takata, G. (2011). Enzymatic and mutational analyses of a class II 3',5'-cyclic nucleotide phosphodiesterase, PdeE, from *Myxococcus xanthus*. *J Bacteriol*, 193(8), 2053-2057.
- Kinoshita, S., Udaka, S., & Shimono, M. (1957). Studies on amino acid fermentation. Part 1. Production of L-glutamic acid by various microorganisms. *J Gen Appl Microbiol*, 3, 193-205.
- Kirsch, K. M. (2014). The impact of CO₂ on inorganic carbon supply and pH homeostasis in *Corynebacterium glutamicum*. urn:nbn:de:hbz:38-55451
- Kishii, R., Falzon, L., Yoshida, T., Kobayashi, H., & Inouye, M. (2007). Structural and functional studies of the HAMP domain of EnvZ, an osmosensing transmembrane histidine kinase in *Escherichia coli*. *J Biol Chem*, 282(36), 26401-26408.
- Ko, E. M., & Oh, J. I. (2020). Induction of the *cydAB* operon encoding the *bd* quinol oxidase under respiration-inhibitory conditions by the major cAMP receptor protein MSMEG_6189 in *Mycobacterium smegmatis*. *Front Microbiol*, 11, 608624.
- Koch-Koerfges, A., Pflzer, N., Platzen, L., Oldiges, M., & Bott, M. (2013). Conversion of *Corynebacterium glutamicum* from an aerobic respiring to an aerobic fermenting bacterium by inactivation of the respiratory chain. *Biochim Biophys Acta Bioenerg*, 1827(6), 699-708.
- Kohl, T. A., Baumbach, J., Jungwirth, B., Puhler, A., & Tauch, A. (2008). The GlxR regulon of the amino acid producer *Corynebacterium glutamicum*: *in silico* and *in vitro* detection of DNA binding sites of a global transcription regulator. *J Biotechnol*, 135(4), 340-350.
- Kohl, T. A., & Tauch, A. (2009). The GlxR regulon of the amino acid producer *Corynebacterium glutamicum*: Detection of the corynebacterial core regulon and integration into the transcriptional regulatory network model. *J Biotechnol*, 143(4), 239-246.
- Kolb, A., Busby, S., Buc, H., Garges, S., & Adhya, S. (1993). Transcriptional regulation by cAMP and its receptor protein. *Annu Rev Biochem*, 62, 749-795.
- Kopperud, R., Krakstad, C., Selheim, F., & Døskeland, S. O. (2003). cAMP effector mechanisms. Novel twists for an 'old' signaling system. *FEBS Lett*, 546(1), 121-126.
- Krulwich, T. A., Sachs, G., & Padan, E. (2011). Molecular aspects of bacterial pH sensing and homeostasis. *Nat Rev Microbiol*, 9(5), 330-343.
- Küberl, A., Fränzel, B., Eggeling, L., Polen, T., Wolters, D. A., & Bott, M. (2014). Pupylated proteins in *Corynebacterium glutamicum* revealed by MudPIT analysis. *Proteomics*, 14(12), 1531-1542.
- Laslo, T., von Zalusowski, P., Gabris, C., Lodd, E., Rückert, C., Dangel, P., Kalinowski, J., Auchter, M., Seibold, G., & Eikmanns, B. J. (2012). Arabitol metabolism of *Corynebacterium glutamicum* and its regulation by AtIR. *J Bacteriol*, 194(5), 941-955.

- Lee, D. J., Minchin, S. D., & Busby, S. J. (2012). Activating transcription in bacteria. *Annu Rev Microbiol*, 66, 125-152.
- Letek, M., Valbuena, N., Ramos, A., Ordonez, E., Gil, J. A., & Mateos, L. M. (2006). Characterization and use of catabolite-repressed promoters from gluconate genes in *Corynebacterium glutamicum*. *J Bacteriol*, 188(2), 409-423.
- Leuchtenberger, W., Huthmacher, K., & Drauz, K. (2005). Biotechnological production of amino acids and derivatives: current status and prospects. *Appl Microbiol Biotechnol*, 69(1), 1-8.
- Leyval, D., Debay, F., Engasser, J., & Goergen, J. (1997). Flow cytometry for the intracellular pH measurement of glutamate producing *Corynebacterium glutamicum*. *J Microbiol Methods*, 29(2), 121-127.
- Lindahl, L., Genheden, S., Faria-Oliveira, F., Allard, S., Eriksson, L. A., Olsson, L., & Bettiga, M. (2017). Alcohols enhance the rate of acetic acid diffusion in *S. cerevisiae*: biophysical mechanisms and implications for acetic acid tolerance. *Microbial Cell*, 5(1), 42-55.
- Linder, J. U., Hammer, A., & Schultz, J. E. (2004). The effect of HAMP domains on class IIIb adenylyl cyclases from *Mycobacterium tuberculosis*. *Eur J Biochem*, 271(12), 2446-2451.
- Linder, J. U., & Schultz, J. E. (2003). The class III adenylyl cyclases: multi-purpose signalling modules. *Cell Signal*, 15(12), 1081-1089.
- Litsanov, B., Brocker, M., & Bott, M. (2012). Toward homosuccinate fermentation: metabolic engineering of *Corynebacterium glutamicum* for anaerobic production of succinate from glucose and formate. *Appl Environ Microbiol*, 78(9), 3325-3337.
- Litsanov, B., Kabus, A., Brocker, M., & Bott, M. (2012). Efficient aerobic succinate production from glucose in minimal medium with *Corynebacterium glutamicum*. *Microb Biotechnol*, 5(1), 116-128.
- Liu, C., Sun, D., Zhu, J., Liu, J., & Liu, W. (2020). The regulation of bacterial biofilm formation by cAMP-CRP: A Mini-Review. *Front Microbiol*, 11, 802.
- Lorenzo-Orts, L., Hohmann, U., Zhu, J., & Hothorn, M. (2019). Molecular characterization of CHAD domains as inorganic polyphosphate-binding modules. *Life Sci Alliance*, 2(3), e201900385.
- Lowrie, D. B., Aber, V. R., & Jackett, P. S. (1979). Phagosome-lysosome fusion and cyclic adenosine 3':5'-monophosphate in macrophages infected with *Mycobacterium microti*, *Mycobacterium bovis* BCG or *Mycobacterium lepraemurium*. *J Gen Microbiol*, 110(2), 431-441.
- Maathuis, F. J., & Sanders, D. (2001). Sodium uptake in Arabidopsis roots is regulated by cyclic nucleotides. *Plant Physiol*, 127(4), 1617-1625.
- Majors, J. (1975). Specific binding of CAP factor to lac promoter DNA. *Nature*, 256(5519), 672-674.
- Maurer, L. M., Yohannes, E., Bondurant, S. S., Radmacher, M., & Slonczewski, J. L. (2005). pH regulates genes for flagellar motility, catabolism, and oxidative stress in *Escherichia coli* K-12. *J Bacteriol*, 187(1), 304-319.
- Mbah, A. N. (2014). Application of hybrid functional groups to predict ATP binding proteins. *ISRN Comput Biol*, 2014, 581245.
- McCue, L. A., McDonough, K. A., & Lawrence, C. E. (2000). Functional classification of cNMP-binding proteins and nucleotide cyclases with implications for novel regulatory pathways in *Mycobacterium tuberculosis*. *Genome Res*, 10(2), 204-219.
- McDonough, K. A., & Rodriguez, A. (2011). The myriad roles of cyclic AMP in microbial pathogens: from signal to sword. *Nat Rev Microbiol*, 10(1), 27-38.
- McKnight, G. S. (1991). Cyclic AMP second messenger systems. *Curr Opin Cell Biol*, 3(2), 213-217.

- Mendoza-Vargas, A., Olvera, L., Olvera, M., Grande, R., Vega-Alvarado, L., Taboada, B., Jimenez-Jacinto, V., Salgado, H., Juárez, K., Contreras-Moreira, B., Huerta, A. M., Collado-Vides, J., & Morett, E. (2009). Genome-wide identification of transcription start sites, promoters and transcription factor binding sites in *E. coli*. *PLoS One*, *4*(10), e7526.
- Miesenböck, G., De Angelis, D. A., & Rothman, J. E. (1998). Visualizing secretion and synaptic transmission with pH-sensitive green fluorescent proteins. *Nature*, *394*(6689), 192-195.
- Milanesio, P., Arce-Rodríguez, A., Muñoz, A., Calles, B., & de Lorenzo, V. (2011). Regulatory exaptation of the catabolite repression protein (Crp)-cAMP system in *Pseudomonas putida*. *Environ Microbiol*, *13*(2), 324-339.
- Mistry, J., Chuguransky, S., Williams, L., Qureshi, M., Salazar, G. A., Sonnhammer, E. L. L., Tosatto, S. C. E., Paladin, L., Raj, S., Richardson, L. J., Finn, R. D., & Bateman, A. (2020). Pfam: The protein families database in 2021. *Nucleic Acids Res*, *49*(D1), D412-D419.
- Mizuno, Y., Nagano-Shoji, M., Kubo, S., Kawamura, Y., Yoshida, A., Kawasaki, H., Nishiyama, M., Yoshida, M., & Kosono, S. (2016). Altered acetylation and succinylation profiles in *Corynebacterium glutamicum* in response to conditions inducing glutamate overproduction. *Microbiologyopen*, *5*(1), 152-173.
- Morosov, X., Davoudi, C. F., Baumgart, M., Brocker, M., & Bott, M. (2018). The copper-deprivation stimulon of *Corynebacterium glutamicum* comprises proteins for biogenesis of the actinobacterial cytochrome *bc₁-aa₃* supercomplex. *J Biol Chem*, *293*(40), 15628-15640.
- Mulder, N. J., & Apweiler, R. (2008). The InterPro database and tools for protein domain analysis. *Curr Protoc Bioinformatics*, *21*(1), 2.7.1-2.7.18.
- Mustafi, N., Grünberger, A., Kohlheyer, D., Bott, M., & Frunzke, J. (2012). The development and application of a single-cell biosensor for the detection of L-methionine and branched-chain amino acids. *Metab Eng*, *14*(4), 449-457.
- Nambi, S., Basu, N., & Visweswariah, S. S. (2010). cAMP-regulated protein lysine acetylases in mycobacteria. *J Biol Chem*, *285*(32), 24313-24323.
- Nambi, S., Gupta, K., Bhattacharyya, M., Ramakrishnan, P., Ravikumar, V., Siddiqui, N., Thomas, A. T., & Visweswariah, S. S. (2013). Cyclic AMP-dependent protein lysine acylation in mycobacteria regulates fatty acid and propionate metabolism. *J Biol Chem*, *288*(20), 14114-14124.
- Nambi, S., Gupta, K., Bhattacharyya, M., Ramakrishnan, P., Ravikumar, V., Siddiqui, N., Thomas, A. T., & Visweswariah, S. S. (2019). Correction: Cyclic AMP-dependent protein lysine acylation in mycobacteria regulates fatty acid and propionate metabolism. *J Biol Chem*, *294*(28), 11046.
- Nishimura, T., Teramoto, H., Toyoda, K., Inui, M., & Yukawa, H. (2011). Regulation of the nitrate reductase operon *narKGHIJ* by the cAMP-dependent regulator GlxR in *Corynebacterium glutamicum*. *Microbiology*, *157*(Pt 1), 21-28.
- Notley-McRobb, L., Death, A., & Ferenci, T. (1997). The relationship between external glucose concentration and cAMP levels inside *Escherichia coli*: implications for models of phosphotransferase-mediated regulation of adenylate cyclase. *Microbiology*, *143*(6), 1909-1918.
- Nystrom, T., & Neidhardt, F. C. (1992). Cloning, mapping and nucleotide sequencing of a gene encoding a universal stress protein in *Escherichia coli*. *Mol Microbiol*, *6*(21), 3187-3198.
- Nystrom, T., & Neidhardt, F. C. (1993). Isolation and properties of a mutant of *Escherichia coli* with an insertional inactivation of the *uspA* gene, which encodes a universal stress protein. *J Bacteriol*, *175*(13), 3949-3956.

- Okino, S., Noburyu, R., Suda, M., Jojima, T., Inui, M., & Yukawa, H. (2008). An efficient succinic acid production process in a metabolically engineered *Corynebacterium glutamicum* strain. *Appl Microbiol Biotechnol*, *81*(3), 459-464.
- Okino, S., Suda, M., Fujikura, K., Inui, M., & Yukawa, H. (2008). Production of D-lactic acid by *Corynebacterium glutamicum* under oxygen deprivation. *Appl Microbiol Biotechnol*, *78*(3), 449-454.
- Olson, E. R. (1993). Influence of pH on bacterial gene expression. *Mol Microbiol*, *8*(1), 5-14.
- Omori, K., & Kotera, J. (2007). Overview of PDEs and their regulation. *Circ Res*, *100*(3), 309-327.
- Oren, A., & Garrity, G. M. (2021). Valid publication of the names of forty-two phyla of prokaryotes. *Int J Syst Evol Microbiol*, *71*(10).
- Orr, J. S., Christensen, D. G., Wolfe, A. J., & Rao, C. V. (2018). Extracellular acidic pH inhibits acetate consumption by decreasing gene transcription of the tricarboxylic acid cycle and the glyoxylate shunt. *J Bacteriol*, *201*(2), e00410-00418.
- Padh, H., & Venkitasubramanian, T. A. (1976). Cyclic adenosine 3', 5'-monophosphate in mycobacteria. *Indian J Biochem Biophys*, *13*(4), 413-414.
- Panhorst, M., Sorger-Herrmann, U., & Wendisch, V. F. (2011). The *pstSCAB* operon for phosphate uptake is regulated by the global regulator GlxR in *Corynebacterium glutamicum*. *J Biotechnol*, *154*(2-3), 149-155.
- Park, S. Y., Moon, M. W., Subhadra, B., & Lee, J. K. (2010). Functional characterization of the *glxR* deletion mutant of *Corynebacterium glutamicum* ATCC 13032: involvement of GlxR in acetate metabolism and carbon catabolite repression. *FEMS Microbiol Lett*, *304*(2), 107-115.
- Park, Y. H., Lee, B. R., Seok, Y. J., & Peterkofsky, A. (2006). *In vitro* reconstitution of catabolite repression in *Escherichia coli*. *J Biol Chem*, *281*(10), 6448-6454.
- Passner, J. M., Schultz, S. C., & Steitz, T. A. (2000). Modeling the cAMP-induced allosteric transition using the crystal structure of CAP-cAMP at 2.1 Å resolution. *J Mol Biol*, *304*(5), 847-859.
- Pauling, J., Röttger, R., Tauch, A., Azevedo, V., & Baumbach, J. (2012). CoryneRegNet 6.0-Updated database content, new analysis methods and novel features focusing on community demands. *Nucleic Acids Res*, *40*(D1), D610-D614.
- Peng, X., Okai, N., Vertès, A. A., Inatomi, K.-I., Inui, M., & Yukawa, H. (2011). Characterization of the mannitol catabolic operon of *Corynebacterium glutamicum*. *Appl Microbiol Biotechnol*, *91*(5), 1375-1387.
- Pfeifer-Sancar, K., Mentz, A., Ruckert, C., & Kalinowski, J. (2013). Comprehensive analysis of the *Corynebacterium glutamicum* transcriptome using an improved RNAseq technique. *BMC Genomics*, *14*, 888.
- Phillips, A. T., & Mulfinger, L. M. (1981). Cyclic adenosine 3',5'-monophosphate levels in *Pseudomonas putida* and *Pseudomonas aeruginosa* during induction and carbon catabolite repression of histidase synthesis. *J Bacteriol*, *145*(3), 1286-1292.
- Platzen, L. (2013). Modifikation der Atmungskette in *Corynebacterium glutamicum* und Rolle des Flävohämoproteins Hmp. ISBN 978-3-89336-931-7
- Polen, T., Schluesener, D., Poetsch, A., Bott, M., & Wendisch, V. F. (2007). Characterization of citrate utilization in *Corynebacterium glutamicum* by transcriptome and proteome analysis. *FEMS Microbiol Lett*, *273*(1), 109-119.
- Popovych, N., Tzeng, S. R., Tonelli, M., Ebright, R. H., & Kalodimos, C. G. (2009). Structural basis for cAMP-mediated allosteric control of the catabolite activator protein. *Proc Natl Acad Sci U S A*, *106*(17), 6927-6932.

- Powell, S., Forslund, K., Szklarczyk, D., Trachana, K., Roth, A., Huerta-Cepas, J., Gabaldón, T., Rattei, T., Creevey, C., Kuhn, M., Jensen, L. J., von Mering, C., & Bork, P. (2014). eggNOG v4.0: nested orthology inference across 3686 organisms. *Nucleic Acids Res*, *42*(D1), D231-239.
- Ren, Y. L., Garges, S., Adhya, S., & Krakow, J. S. (1990). Characterization of the binding of cAMP and cGMP to the CRP*598 mutant of the *E. coli* cAMP receptor protein. *Nucleic Acids Res*, *18*(17), 5127-5132.
- Richet, E., Vidal-Ingigliardi, D., & Raibaud, O. (1991). A new mechanism for coactivation of transcription initiation: repositioning of an activator triggered by the binding of a second activator. *Cell*, *66*(6), 1185-1195.
- Richter, W. (2002). 3',5' Cyclic nucleotide phosphodiesterases class III: members, structure, and catalytic mechanism. *Proteins*, *46*(3), 278-286.
- Robert, X., & Gouet, P. (2014). Deciphering key features in protein structures with the new ENDscript server. *Nucleic Acids Res*, *42*(W1), W320-W324.
- Robison, K., McGuire, A. M., & Church, G. M. (1998). A comprehensive library of DNA-binding site matrices for 55 proteins applied to the complete *Escherichia coli* K-12 genome. *J Mol Biol*, *284*(2), 241-254.
- Saier, M. H., Jr., Feucht, B. U., & McCaman, M. T. (1975). Regulation of intracellular adenosine cyclic 3':5'-monophosphate levels in *Escherichia coli* and *Salmonella typhimurium*. Evidence for energy-dependent excretion of the cyclic nucleotide. *J Biol Chem*, *250*(19), 7593-7601.
- Sass, P., Field, J., Nikawa, J., Toda, T., & Wigler, M. (1986). Cloning and characterization of the high-affinity cAMP phosphodiesterase of *Saccharomyces cerevisiae*. *Proc Natl Acad Sci U S A*, *83*(24), 9303-9307.
- Sassone-Corsi, P. (2012). The cyclic AMP pathway. *Cold Spring Harb Perspect Biol*, *4*(12), a011148.
- Savery, N. J., Lloyd, G. S., Kainz, M., Gaal, T., Ross, W., Ebricht, R. H., Gourse, R. L., & Busby, S. J. (1998). Transcription activation at Class II CRP-dependent promoters: identification of determinants in the C-terminal domain of the RNA polymerase alpha subunit. *EMBO J*, *17*(12), 3439-3447.
- Schaffer, S., Weil, B., Nguyen, V. D., Dongmann, G., Günther, K., Nickolaus, M., Hermann, T., & Bott, M. (2001). A high-resolution reference map for cytoplasmic and membrane-associated proteins of *Corynebacterium glutamicum*. *Electrophoresis*, *22*(20), 4404-4422.
- Schendzielorz, G., Dippong, M., Grünberger, A., Kohlheyer, D., Yoshida, A., Binder, S., Nishiyama, C., Nishiyama, M., Bott, M., & Eggeling, L. (2014). Taking control over control: use of product sensing in single cells to remove flux control at key enzymes in biosynthesis pathways. *ACS Synth Biol*, *3*(1), 21-29.
- Schubert, O. T., Mouritsen, J., Ludwig, C., Rost, H. L., Rosenberger, G., Arthur, P. K., Claassen, M., Campbell, D. S., Sun, Z., Farrah, T., Gengenbacher, M., Maiolica, A., Kaufmann, S. H. E., Moritz, R. L., & Aebbersold, R. (2013). The Mtb proteome library: a resource of assays to quantify the complete proteome of *Mycobacterium tuberculosis*. *Cell Host Microbe*, *13*(5), 602-612.
- Schulte, J., Baumgart, M., & Bott, M. (2017). Identification of the cAMP phosphodiesterase CpdA as novel key player in cAMP-dependent regulation in *Corynebacterium glutamicum*. *Mol Microbiol*, *103*(3), 534-552.
- Sharma, R., Zaveri, A., Gopalakrishnapai, J., Srinath, T., Varshney, U., & Visweswariah, S. S. (2014). Paralogous cAMP receptor proteins in *Mycobacterium smegmatis* show biochemical and functional divergence. *Biochemistry*, *53*(49), 7765-7776.

- Shenoy, A. R., Sivakumar, K., Krupa, A., Srinivasan, N., & Visweswariah, S. S. (2004). A survey of nucleotide cyclases in actinobacteria: unique domain organization and expansion of the class III cyclase family in *Mycobacterium tuberculosis*. *Comp Funct Genomics*, 5(1), 17-38.
- Shenoy, A. R., Sreenath, N., Podobnik, M., Kovacevic, M., & Visweswariah, S. S. (2005). The Rv0805 gene from *Mycobacterium tuberculosis* encodes a 3',5'-cyclic nucleotide phosphodiesterase: biochemical and mutational analysis. *Biochemistry*, 44(48), 15695-15704.
- Shenoy, A. R., & Visweswariah, S. S. (2006). Mycobacterial adenyl cyclases: biochemical diversity and structural plasticity. *FEBS Lett*, 580(14), 3344-3352.
- Sismeiro, O., Trotot, P., Biville, F., Vivares, C., & Danchin, A. (1998). *Aeromonas hydrophila* adenyl cyclase 2: a new class of adenyl cyclases with thermophilic properties and sequence similarities to proteins from hyperthermophilic archaeobacteria. *J Bacteriol*, 180(13), 3339-3344.
- Skorupski, K., & Taylor, R. K. (1997). Cyclic AMP and its receptor protein negatively regulate the coordinate expression of cholera toxin and toxin-coregulated pilus in *Vibrio cholerae*. *Proc Natl Acad Sci U S A*, 94(1), 265-270.
- Slonczewski, J. L., Fujisawa, M., Dopson, M., & Krulwich, T. A. (2009). Cytoplasmic pH measurement and homeostasis in bacteria and archaea. *Adv Microb Physiol*, 55, 1-79, 317.
- Smith, N. N., Kim, S. K., Reddy, P. T., & Gallagher, D. T. (2006). Crystallization of the class IV adenyl cyclase from *Yersinia pestis*. *Acta Cryst*, F62, 200-204.
- Sousa, M. C., & McKay, D. B. (2001). Structure of the universal stress protein of *Haemophilus influenzae*. *Structure*, 9(12), 1135-1141.
- Stapleton, M., Haq, I., Hunt, D. M., Arnvig, K. B., Artymiuk, P. J., Buxton, R. S., & Green, J. (2010). *Mycobacterium tuberculosis* cAMP receptor protein (Rv3676) differs from the *Escherichia coli* paradigm in its cAMP binding and DNA binding properties and transcription activation properties. *J Biol Chem*, 285(10), 7016-7027.
- Stolz, M., Peters-Wendisch, P., Etterich, H., Gerharz, T., Faurie, R., Sahm, H., Fersterra, H., & Eggeling, L. (2007). Reduced folate supply as a key to enhanced L-serine production by *Corynebacterium glutamicum*. *Appl Environ Microbiol*, 73(3), 750-755.
- Storz, G., Vogel, J., & Wassarman, K. M. (2011). Regulation by small RNAs in bacteria: expanding frontiers. *Mol Cell*, 43(6), 880-891.
- Subhadra, B., & Lee, J. K. (2013). Elucidation of the regulation of ethanol catabolic genes and *ptsG* using a *glxR* and adenylate cyclase gene (*cydB*) deletion mutants of *Corynebacterium glutamicum* ATCC 13032. *J Microbiol Biotechnol*, 23(12), 1683-1690.
- Subhadra, B., Ray, D., Han, J. Y., Bae, K. H., & Lee, J. K. (2015). Identification of the regulators binding to the upstream region of *glxR* in *Corynebacterium glutamicum*. *J Microbiol Biotechnol*, 25(8), 1216-1226.
- Sun, Y., Fukamachi, T., Saito, H., & Kobayashi, H. (2012). Respiration and the F₁F_o-ATPase enhance survival under acidic conditions in *Escherichia coli*. *PLoS One*, 7(12), e52577.
- Sutherland, E. W., & Rall, T. W. (1958). Fractionation and characterization of a cyclic adenine ribonucleotide formed by tissue particles. *J Biol Chem*, 232(2), 1077-1091.
- Takahashi, M., Blazy, B., & Baudras, A. (1980). An equilibrium study of the cooperative binding of adenosine cyclic 3',5'-monophosphate and guanosine cyclic 3',5'-monophosphate to the adenosine cyclic 3',5'-monophosphate receptor protein from *Escherichia coli*. *Biochemistry*, 19(22), 5124-5130.

- Télliez-Sosa, J., Soberón, N., Vega-Segura, A., Torres-Márquez, M. E., & Cevallos, M. A. (2002). The *Rhizobium etli cyaC* product: characterization of a novel adenylate cyclase class. *J Bacteriol*, *184*(13), 3560-3568.
- Tews, I., Findeisen, F., Sinning, I., Schultz, A., Schultz, J. E., & Linder, J. U. (2005). The structure of a pH-sensing mycobacterial adenyl cyclase holoenzyme. *Science*, *308*(5724), 1020-1023.
- Thomason, P. A., Traynor, D., Stock, J. B., & Kay, R. R. (1999). The RdeA-RegA system, a eukaryotic phospho-relay controlling cAMP breakdown. *J Biol Chem*, *274*(39), 27379-27384.
- Thompson, J. D., Higgins, D. G., & Gibson, T. J. (1994). CLUSTAL W: improving the sensitivity of progressive multiple sequence alignment through sequence weighting, position-specific gap penalties and weight matrix choice. *Nucleic Acids Res*, *22*(22), 4673-4680.
- Thomson, M., Nunta, K., Cheyne, A., Liu, Y., Garza-Garcia, A., & Larrouy-Maumus, G. (2020). Modulation of the cAMP levels with a conserved actinobacteria phosphodiesterase enzyme reduces antimicrobial tolerance in mycobacteria. *bioRxiv*, 2020.2008.2026.267864.
- Thomson, M., Liu, Y., Nunta, K., Cheyne, A., Fernandes, N., Williams, R., Garza-Garcia, A., & Larrouy-Maumus, G. (2022). Expression of a novel mycobacterial phosphodiesterase successfully lowers cAMP levels resulting in reduced tolerance to cell wall-targeting antimicrobials. *J Biol Chem*, *298*(8), 102151.
- Townsend, P. D., Jungwirth, B., Pojer, F., Bussmann, M., Money, V. A., Cole, S. T., Puhler, A., Tauch, A., Bott, M., Cann, M. J., & Pohl, E. (2014). The crystal structures of apo and cAMP-bound GlxR from *Corynebacterium glutamicum* reveal structural and dynamic changes upon cAMP binding in CRP/FNR family transcription factors. *PLoS One*, *9*(12), e113265.
- Toyoda, K., & Inui, M. (2016). Regulons of global transcription factors in *Corynebacterium glutamicum*. *Appl Microbiol Biotechnol*, *100*(1), 45-60.
- Toyoda, K., Teramoto, H., Gunji, W., Inui, M., & Yukawa, H. (2013). Involvement of regulatory interactions among global regulators GlxR, SugR, and RamA in expression of *ramA* in *Corynebacterium glutamicum*. *J Bacteriol*, *195*(8), 1718-1726.
- Toyoda, K., Teramoto, H., Inui, M., & Yukawa, H. (2009). Involvement of the LuxR-type transcriptional regulator RamA in regulation of expression of the *gapA* gene, encoding glyceraldehyde-3-phosphate dehydrogenase of *Corynebacterium glutamicum*. *J Bacteriol*, *191*(3), 968-977.
- Toyoda, K., Teramoto, H., Inui, M., & Yukawa, H. (2011). Genome-wide identification of *in vivo* binding sites of GlxR, a cyclic AMP receptor protein-type regulator in *Corynebacterium glutamicum*. *J Bacteriol*, *193*(16), 4123-4133.
- Tsirigos, K. D., Peters, C., Shu, N., Käll, L., & Elofsson, A. (2015). The TOPCONS web server for consensus prediction of membrane protein topology and signal peptides. *Nucleic Acids Res*, *43*(W1), W401-W407.
- Udaka, S. (1960). Screening method for microorganisms accumulating metabolites and its use in the isolation of *Micrococcus glutamicus*. *J Bacteriol*, *79*, 754-755.
- Valentini, M., & Filloux, A. (2016). Biofilms and cyclic di-GMP (c-di-GMP) signaling: Lessons from *Pseudomonas aeruginosa* and other bacteria. *J Biol Chem*, *291*(24), 12547-12555.
- van Ooyen, J., Emer, D., Bussmann, M., Bott, M., Eikmanns, B. J., & Eggeling, L. (2011). Citrate synthase in *Corynebacterium glutamicum* is encoded by two *gltA* transcripts which are controlled by RamA, RamB, and GlxR. *J Biotechnol*, *154*(2-3), 140-148.
- Vogt, M., Haas, S., Klaffl, S., Polen, T., Eggeling, L., van Ooyen, J., & Bott, M. (2014). Pushing product formation to its limit: metabolic engineering of *Corynebacterium glutamicum* for L-leucine overproduction. *Metab Eng*, *22*, 40-52.

- Vogt, M., Krumbach, K., Bang, W. G., van Ooyen, J., Noack, S., Klein, B., Bott, M., & Eggeling, L. (2015). The contest for precursors: channelling L-isoleucine synthesis in *Corynebacterium glutamicum* without byproduct formation. *Appl Microbiol Biotechnol*, *99*(2), 791-800.
- Vollmer, A. C., & Bark, S. J. (2018). Twenty-five years of investigating the universal stress protein: function, structure, and applications. *Adv Appl Microbiol*, *102*, 1-36.
- Waters, L. S., Sandoval, M., & Storz, G. (2011). The *Escherichia coli* MntR miniregulon includes genes encoding a small protein and an efflux pump required for manganese homeostasis. *J Bacteriol*, *193*(21), 5887-5897.
- Weber, I. T., & Steitz, T. A. (1987). Structure of a complex of catabolite gene activator protein and cyclic AMP refined at 2.5 Å resolution. *J Mol Biol*, *198*(2), 311-326.
- Weiss, A. A., Hewlett, E. L., Myers, G. A., & Falkow, S. (1984). Pertussis toxin and extracytoplasmic adenylate cyclase as virulence factors of *Bordetella pertussis*. *J Infect Dis*, *150*(2), 219-222.
- Wendisch, V. F., Jorge, J. M. P., Pérez-García, F., & Sgobba, E. (2016). Updates on industrial production of amino acids using *Corynebacterium glutamicum*. *World J Microbiol Biotechnol*, *32*(6), 105.
- Wiedmann, M., Arvik, T. J., Hurley, R. J., & Boor, K. J. (1998). General stress transcription factor SigmaB and its role in acid tolerance and virulence of *Listeria monocytogenes*. *J Bacteriol*, *180*(14), 3650-3656.
- Wieschalka, S., Blombach, B., Bott, M., & Eikmanns, B. J. (2013). Bio-based production of organic acids with *Corynebacterium glutamicum*. *Microb Biotechnol*, *6*(2), 87-102.
- Williams, S. B., & Stewart, V. (1999). Functional similarities among two-component sensors and methyl-accepting chemotaxis proteins suggest a role for linker region amphipathic helices in transmembrane signal transduction. *Mol Microbiol*, *33*(6), 1093-1102.
- Wolf, N., Bussmann, M., Koch-Koerfges, A., Katcharava, N., Schulte, J., Polen, T., Hartl, J., Vorholt, J. A., Baumgart, M., & Bott, M. (2020). Molecular basis of growth inhibition by acetate of an adenylate cyclase-deficient mutant of *Corynebacterium glutamicum*. *Front Microbiol*, *11*(87).
- Xu, N., Lv, H., Wei, L., Liang, Y., Ju, J., Liu, J., & Ma, Y. (2019). Impaired oxidative stress and sulfur assimilation contribute to acid tolerance of *Corynebacterium glutamicum*. *Appl Microbiol Biotechnol*, *103*(4), 1877-1891.
- You, C., Okano, H., Hui, S., Zhang, Z., Kim, M., Gunderson, C. W., Wang, Y. P., Lenz, P., Yan, D., & Hwa, T. (2013). Coordination of bacterial proteome with metabolism by cyclic AMP signalling. *Nature*, *500*(7462), 301-306.
- Zhang, G., Liu, Y., Ruoho, A. E., & Hurley, J. H. (1997). Structure of the adenylyl cyclase catalytic core. *Nature*, *386*(6622), 247-253.
- Zhang, X., & Schleif, R. (1998). Catabolite gene activator protein mutations affecting activity of the *araBAD* promoter. *J Bacteriol*, *180*(2), 195-200.
- Zheng, D., Constantinidou, C., Hobman, J. L., & Minchin, S. D. (2004). Identification of the CRP regulon using *in vitro* and *in vivo* transcriptional profiling. *Nucleic Acids Res*, *32*(19), 5874-5893.
- Zheng, D. Q., Liu, T. Z., Chen, J., Zhang, K., Li, O., Zhu, L., Zhao, Y. H., Wu, X. C., & Wang, P. M. (2013). Comparative functional genomics to reveal the molecular basis of phenotypic diversities and guide the genetic breeding of industrial yeast strains. *Appl Microbiol Biotechnol*, *97*(5), 2067-2076.
- Zheng, Z., Zhu, M., He, Y., Li, N., Guo, T., Chen, Y., Wu, J., Ying, H., & Xie, J. (2013). Gene cloning, expression, and characterization of a cyclic nucleotide phosphodiesterase from *Arthrobacter* sp. CGMCC 3584. *Appl Biochem Biotechnol*, *169*(8), 2442-2456.

Danksagung

Ein besonderer Dank gilt Prof. Dr. Michael Bott für die Überlassung des spannenden Themas, die Ratschläge und die vielen hilfreichen Diskussionen, die den stetigen Fortschritt des Projekts ermöglicht haben.

Prof. Dr. Georg Groth danke ich für die freundliche Übernahme des Zweitgutachtens.

Dr. Meike Baumgart danke ich sehr herzlich für ihre Betreuung und Ihr Interesse am Fortlauf dieser Arbeit. Für die tolle Unterstützung der bioinformatische Analysen für dieses Projekt bedanke ich mich bei Dr. Andrei Filipchuk, Dr. Angela Kranz und Dr. Tino Polen.

Vielen Dank an Dr. Johannes Hartl und Prof. Dr. Julia Vorholt-Zambelli für die cAMP Messungen mittels LC-MS/MS und für die gelungene Zusammenarbeit an dem *cydB*-Paper.

Mein Dank geht auch an alle Mitarbeitende des IBG-1 Instituts, insbesondere der Infrastruktur, die stets freundlich und hilfsbereit waren.

Der Arbeitsgruppe „Stoffwechselregulation und Metabolic Engineering“ danke ich für die stets sehr gute Arbeitsatmosphäre. Insbesondere meinen ehemaligen Kollegen Andy, Alina, Angela, Alexander, Brita, Cedric, Helga, Johanna, Kai, Karen, Kim, Lea, Lingfeng, Maïke, Paul, Susana, und Yannik für ihre tolle Unterstützung im Labor und für die vielen spannenden Gespräche wissenschaftlicher und nicht-wissenschaftlicher Art. Ein besonderer Dank geht dabei an meine Labor- und Bürokollegin Tina. Bei Lukas bedanke ich mich für die Mitarbeit am Projekt in Form seiner Masterarbeit.

Darüber hinaus bedanke ich mich bei meinen Eltern, Geschwistern und Freunden für ihre Unterstützung in der gesamten Studien- und Doktorzeit. Ein besonderer Dank geht an meinen Mann, der mich in allem unterstützt hat.

Erklärung

Ich versichere an Eides Statt, dass die vorgelegte Dissertation von mir selbständig und ohne unzulässige fremde Hilfe unter Beachtung der „Grundsätze zur Sicherung guter wissenschaftlicher Praxis an der Heinrich-Heine-Universität Düsseldorf“ erstellt worden ist. Die Dissertation wurde in der vorgelegten oder in ähnlicher Form noch bei keiner anderen Institution eingereicht. Ich habe bisher keine erfolglosen Promotionsversuche unternommen.

Düsseldorf, 15.04.2023